

**DESIGN AND TESTING OF A NOVEL EXHAUST AIR  
ENERGY RECOVERY WIND TURBINE GENERATOR**

**AHMAD FAZLIZAN BIN ABDULLAH**

**FACULTY OF ENGINEERING  
UNIVERSITY OF MALAYA  
KUALA LUMPUR**

**2016**

**DESIGN AND TESTING OF A NOVEL EXHAUST AIR  
ENERGY RECOVERY WIND TURBINE GENERATOR**

**AHMAD FAZLIZAN BIN ABDULLAH**

**THESIS SUBMITTED IN FULFILMENT OF THE  
REQUIREMENTS FOR THE DEGREE OF DOCTOR OF  
PHILOSOPHY**

**FACULTY OF ENGINEERING  
UNIVERSITY OF MALAYA  
KUALA LUMPUR**

**2016**

**UNIVERSITY OF MALAYA**  
**ORIGINAL LITERARY WORK DECLARATION**

Name of Candidate: **Ahmad Fazlizan bin Abdullah**

(I.C/Passport No:

Registration/Matric No: **KHA120035**

Name of Degree: **Doctor of Philosophy**

Title of ~~Project Paper/Research Report/Dissertation/Thesis~~ (“this Work”):

**Design, Testing of a Novel Exhaust Air Energy Recovery Wind Turbine Generator**

Field of Study: **Energy**

I do solemnly and sincerely declare that:

- (1) I am the sole author/writer of this Work;
- (2) This Work is original;
- (3) Any use of any work in which copyright exists was done by way of fair dealing and for permitted purposes and any excerpt or extract from, or reference to or reproduction of any copyright work has been disclosed expressly and sufficiently and the title of the Work and its authorship have been acknowledged in this Work;
- (4) I do not have any actual knowledge nor do I ought reasonably to know that the making of this work constitutes an infringement of any copyright work;
- (5) I hereby assign all and every rights in the copyright to this Work to the University of Malaya (“UM”), who henceforth shall be owner of the copyright in this Work and that any reproduction or use in any form or by any means whatsoever is prohibited without the written consent of UM having been first had and obtained;
- (6) I am fully aware that if in the course of making this Work I have infringed any copyright whether intentionally or otherwise, I may be subject to legal action or any other action as may be determined by UM.

Candidate’s Signature

Date:

Subscribed and solemnly declared before,

Witness’s Signature

Date:

Name:

Designation:

## ABSTRACT

An innovative system to recover part of the energy from man-made wind resources (exhaust air systems) is introduced. A vertical axis wind turbine (VAWT) in cross-wind orientation, with diffuser-plates is mounted above a cooling tower's exhaust fan to harness the wind energy for producing electricity. The diffuser-plates are designed as a power-augmentation device to improve the performance of the VAWT as well as the cooling tower airflow performance. The performance of the VAWT and its effects on the cooling tower were investigated by experiment. A small scale of cooling tower is fabricated to mimic the actual counter-flow induced draft cooling tower. The supporting structure to hold the VAWT and dynamometer where turbine the position can be moved vertically and horizontally to study the performance in various configurations. The wind from the discharge outlet is generated by fan which is not in uniform profile. From the experiment, it is determined that the best horizontal position of the VAWT with a diameter of 300 mm at the outlet of the cooling tower with the outlet diameter of 730 mm is when the center of the turbine is at a distance of 250 mm to the center of the outlet. The distance is about  $\frac{2}{3}$  of the outlet radius. However, the vertical distance of the VAWT to the outlet is different depending on the fan speed. Based on the evaluation on the VAWT performance as well as the cooling tower performance, the best configuration of the system at fan speed of 708 rpm is when the VAWT is at horizontal position of 250 mm and vertical position of 350 mm. At this configuration, the cooling tower's flow rate improved by 9.55%, the fan motor power consumption reduced by 2.07% while the turbine generating energy. For the fan speed of 910 rpm, the best VAWT position at the outlet of the cooling tower is at horizontal position of 250 mm and vertical position of 400 mm with the air flow rate of the cooling tower and fan motor consumption showed a 9.09% increase and 3.92% decrease respectively. The double multiple stream tube analysis produced similar pattern of graphs to the experimental result which indicates an

agreement between these two analyses. Theoretical analysis explains the wind turbine behavior in the not uniform wind stream as acquired from the experiment. For the selected wind turbine, it is the best to match the highest wind velocity region to the wind turbine at the range of  $45^\circ$  to  $115^\circ$  azimuth angle. This is as shown by the wind turbine at the positions of  $X = 250$  mm and  $-250$  mm. At this range of azimuth angle, the turbine produces higher instantaneous torque and better angle of attack compared to the other azimuth angle. The dual rotor exhaust air energy recovery turbine generator experiments found that the system produced the best performance at the VAWT vertical distance of 300 mm to the outlet plane. The integration of diffuser-plates further improved the VAWT performance with 20% and 27% for the fan speed of 708 rpm and 910 rpm respectively. At 910 rpm, with the diffuser-plates, the cooling tower air flow rate improved by 10.05% and the fan consumption decreased by 2.68% compared to the bare cooling tower. It also improved the energy recovery by 27.03% compare to the VAWT without diffuser-plates. For the actual size of cooling tower, it is estimated that 13% of the energy from the common cooling tower with the outlet size of 2.4 m and rated motor consumption of 7.5 kW is recovered. For the cooling tower that operates for 20 hours per day, every day throughout the year, a sum of 7,300 kWh/year is expected to be recovered. The payback period for the system of this size is 7 years while the net present value of the system at the end of the life cycle of the analysis is RM 25,437. The cumulative recovered energy value at the end of the life cycle of the system is RM 179,786. This system is retrofit-able to the existing cooling towers and has very high market potential due to abundant cooling towers and other unnatural exhaust air resources globally. In addition, the energy output is predictable and consistent, allowing simpler design of the downstream system.

## ABSTRAK

Satu sistem inovatif diperkenalkan untuk menjana semula sebahagian daripada sumber angin buatan manusia (sistem ekzos udara). Kincir angin berpaksi menegak (VAWT) dalam orientasi merentas angin, dengan plat peresap dipasang di atas laluan keluar ekzos menara penyejuk untuk mengumpul tenaga angin bagi menghasilkan elektrik. Plat peresap direkabentuk sebagai alat untuk menggandakan kuasa bagi meningkatkan prestasi VAWT dan aliran udara menara penyejuk. Prestasi VAWT dan kesan keatas menara penyejuk dikaji melalui eksperimen. Model menara penyejuk berskala kecil di fabrikasi berdasarkan menara penyejuk jenis berlawanan aliran sebenar. Struktur untuk menyokong VAWT dan dinamometer dibina supaya posisi kincir boleh diubah secara menegak dan mendatar untuk mengkaji prestasi dalam berbagai keadaan. Angin dari aliran keluar menara penyejuk dijanakan melalui kipas yang menghasilkan taburan angin yang tidak sekata. Dari eksperimen, kedudukan mendatar yang terbaik untuk VAWT dengan diameter 300 mm di laluan keluar menara penyejuk berdiameter 730 mm adalah apabila pusat VAWT pada kedudukan 250 mm ke pusat laluan keluar tersebut. Kedudukan tersebut adalah kira-kira  $\frac{2}{3}$  daripada jejari laluan tersebut. Walaubagaimanapun, kedudukan menegak VAWT ke laluan keluar angin bergantung kepada kelajuan kipas. Berdasarkan penilaian keatas VAWT dan prestasi menara penyejuk, konfigurasi terbaik sistem pada 708 rpm ialah apabila VAWT pada kedudukan mendatar 250 mm dan kedudukan menegak 350 mm. Pada kedudukan ini, kadar aliran menara penyejuk meningkat sebanyak 9.55%, kuasa motor menurun sebanyak 2.07% manakala VAWT menjana tenaga. Untuk kipas berkelajuan 910 rpm, kedudukan VAWT terbaik adalah ialah pada kedudukan mendatar 250 mm dan kedudukan menegak 400 mm dengan kadar alir dan kuasa motor menara penyejuk masing-masing menunjukkan 9.09% peningkatan dan 3.92% penurunan. Analisis melalui teori tiub aliran berkembar berganda (DMST) menghasilkan graf yang hampir sama dengan keputusan eksperimen seterusnya

menunjukkan persetujuan antara kedua-dua analisis ini. Analisis secara teoritikal menerangkan sifat VAWT dalam aliran angin tidak sekata seperti yang diperoleh dari eksperimen. Untuk VAWT ini, adalah terbaik untuk menyamakan kawasan angin paling tinggi kepada azimuth VAWT dari  $45^\circ$  ke  $115^\circ$ . Ini adalah seperti yang ditunjukkan oleh VAWT dalam kedudukan  $X = 250$  mm dan  $-250$  mm. Pada julat azimuth ini, VAWT menghasilkan daya kilas setempat lebih tinggi dan sudut serangan yang lebih baik berbanding pada azimuth yang lain. Eksperimen bagi sistem dengan rotor berkembar menunjukkan sistem ini menghasilkan prestasi terbaik pada kedudukan VAWT 300 mm secara menegak ke aras laluan keluar angin. Penambahan plat peresap meningkatkan lagi prestasi VAWT sebanyak 20% dan 27% masing-masing untuk kipas berkelajuan 708 rpm dan 910 rpm. Pada 910 rpm, dengan plat peresap, kadar alir menara penyejuk meningkat sebanyak 10.05% dan kuasa kipas menurun sebanyak 2.68% berbanding menara penyejuk biasa. Penggunaan semula tenaga juga meningkat sebanyak 27.03% berbanding VAWT tanpa plat peresap. Untuk menara penyejuk bersaiz sebenar, dianggarkan sebanyak 13% daripada tenaga menara penyejuk yang bersaiz 2.4 m dan motor berkuasa 7.5 kW dapat dijana semula. Untuk menara penyejuk yang beroperasi selama 20 jam sehari, setiap hari dalam setahun, sejumlah 7,300 kWh/tahun dijangka dapat diguna semula. Tempoh balik modal untuk sistem dengan saiz ini ialah 7 tahun manakala nilai semasa sekarang pada penghujung hayat analisis ialah RM 25,347. Jumlah keseluruhan penjanaan semula tenaga pada penghujung kitaran hayat ialah bernilai RM 179,786. Sistem ini boleh diintegrasikan dengan menara penyejuk sedia ada dan mempunyai potensi pasaran yang tinggi berdasarkan kuantiti menara penyejuk dan ekzos sistem lain yang banyak di dunia. Selain itu, tenaga yang dihasilkan adalah boleh dijangka dan konsisten membolehkan rekabentuk hiliran yang lebih ringkas.

## ACKNOWLEDGEMENTS

All praises be to Allah SWT the Cherisher and Sustainer of the worlds.

Most Gracious, Most Merciful.

Greatest gratitude to my supervisor, Assoc. Prof. Dr. Chong Wen Tong and Prof. Ir. Dr. Hew Wooi Ping for their patience in supervising, critics and giving thoughtful guidance with knowledge towards the completion of this research.

I would like to thank the Ministry of Education Malaysia for the Ph.D. scholarship (under the MyPHD programme) and University of Malaya through High Impact Research Grant (Project No. 22) for providing financial support to me. I would like to seize this opportunity to express my gratitude to the University Malaya for the PPP research grant (Project No. PG047-2012B). I also would like to express my sincere appreciation to all researchers in the Renewable Energy & Green Technology Laboratory, Department of Mechanical Engineering who have given me advice and fruitful discussions for conducting this research.

I would like to acknowledge and extend my heartfelt to my family and in-laws for always giving me their great support.

My wife, Dr. Noorashikin for always being by my side during the ups and downs. My charming sons, Ahmad Akif Fahim & Ahmad Hail Fahim for always make me smile.

Thank you...



## TABLE OF CONTENTS

Abstract .....	iv
Abstrak .....	vi
Acknowledgements .....	viii
Table of Contents .....	ix
List of Figures .....	xiv
List of Tables.....	xix
List of Symbols and Abbreviations.....	xx
List of Appendices .....	xxii
<b>CHAPTER 1: INTRODUCTION.....</b>	<b>1</b>
1.1 Overview.....	1
1.2 Problem statement .....	3
1.3 Objectives of research.....	4
1.4 Thesis outline.....	5
<b>CHAPTER 2: LITERATURE REVIEW.....</b>	<b>7</b>
2.1 Wind energy.....	7
2.1.1 Aerodynamic analysis of wind turbine.....	11
2.1.1.1 General mathematical expressions for aerodynamic analysis of straight bladed Darrieus vertical axis wind turbine.....	14
2.1.1.2 Aerodynamic prediction models for vertical axis wind turbine	17
2.1.2 Research development on wind energy.....	24
2.1.2.1 Recent design of vertical axis wind turbine .....	26
2.1.2.2 Wind turbine power-augmentation system .....	27
2.1.2.3 Urban wind energy generation system .....	28

2.1.3	Wind energy generation system implementation in Malaysia .....	34
2.2	Exhaust air system .....	36
2.2.1	Basics of cooling tower .....	36
2.2.2	Cooling tower behavior and factors affecting its performance .....	37
2.2.2.1	Interference .....	37
2.2.2.2	Re-entrainment .....	38
2.3	Existing energy recovery system .....	38
<b>CHAPTER 3: DESIGN DESCRIPTION AND METHODOLOGY .....</b>		<b>40</b>
3.1	Design description of the exhaust air energy recovery turbine generator .....	40
3.1.1	General arrangement and working principles of the system .....	40
3.1.2	Benefits of the energy recovery wind turbine generator .....	42
3.1.3	Variations of exhaust air energy recovery wind turbine .....	43
3.2	Cooling tower model and exhaust air energy recovery turbine generator test rig fabrication .....	44
3.2.1	Cooling tower model fabrication .....	44
3.2.2	Exhaust air energy recovery turbine generator test rig fabrication .....	47
3.3	Experimental methodology .....	49
3.3.1	Cooling tower model performance evaluation .....	49
3.3.2	Cooling tower model with exhaust air energy recovery turbine generator	
50		
3.4	Double multiple stream tube analysis for the exhaust air energy recovery turbine generator .....	51
3.4.1	Stream tube .....	52
3.4.2	Assumptions .....	53
3.4.3	Calculation procedure .....	54

3.5	Dual rotor exhaust air energy recovery turbine generator with and without the integration of diffuser-plates.....	57
3.5.1	Dual rotor exhaust air energy recovery setup.....	57
3.5.2	Integration of diffuser-plates onto the exhaust air energy recovery turbine generator.....	58
<b>CHAPTER 4: RESULTS AND DISCUSSION .....</b>		<b>61</b>
4.1	Performance of bare cooling tower.....	61
4.1.1	Blockage effect assessment .....	62
4.1.2	Wind velocity profile.....	63
4.2	Cooling tower with exhaust air energy recovery wind turbine generator .....	64
4.2.1	Wind turbine performance.....	64
4.2.1.1	Wind turbine rotational speed .....	64
4.2.1.2	Wind turbine power generation.....	66
4.2.1.3	Coefficient of power of wind turbine.....	68
4.2.2	Cooling tower performance .....	75
4.2.2.1	Air flow rate of the cooling tower model.....	75
4.2.2.2	Cooling tower fan motor power consumption.....	76
4.2.3	Overall performance comparison .....	78
4.3	Double multiple stream tube analysis for the exhaust air energy recovery turbine generator .....	82
4.3.1	Comparison between the experimental result and the calculated result... 82	
4.3.2	Wind turbine power generation against non-uniform wind velocity profile	
		85
4.4	Dual rotor exhaust air energy recovery turbine generator with and without the diffuser-plates .....	95
4.4.1	Cooling tower performance.....	97

4.4.2 Overall performance comparison .....	99
--	----

**CHAPTER 5: ENERGY RECOVERY ESTIMATION AND TECHNO-ECONOMIC ANALYSIS OF THE EXHAUST AIR ENERGY RECOVERY TURBINE GENERATOR ON AN ACTUAL COOLING TOWER .....105**

5.1 Introduction.....	105
5.2 Methodology.....	106
5.2.1 Cooling tower and wind turbine matching .....	106
5.2.2 Economic assessment .....	109
5.3 Results and discussion .....	111
5.3.1 Energy recovery estimation.....	111
5.3.2 Economic assessment .....	112
5.4 Summary.....	113

**CHAPTER 6: CONCLUSIONS AND RECOMMENDATIONS.....115**

6.1 Conclusions .....	115
6.2 Contributions .....	117
6.3 Limitations.....	118
6.4 Recommendations.....	118
References .....	119
Appendix A.....	130
Appendix B .....	134
Appendix C .....	136
Appendix D.....	142
Appendix E .....	172
List of Publications: Journal Papers .....	175
List of Publications: Conference papers .....	181

Patent Filing .....	187
List of Awards.....	188

University of Malaya

## LIST OF FIGURES

Figure 2.1 Components of a HAWT (Hau, 2006).....	9
Figure 2.2 Illustrations of the VAWTs. From left, Savonius rotor, Darrieus turbine and H-rotor (Islam et al., 2008). .....	10
Figure 2.3 The power coefficient as a function of the tip speed ratio for different wind machine designs (Patel, 2006).....	11
Figure 2.4 Actuator disk model of a wind turbine (Beri & Yao, 2011).....	12
Figure 2.5 Airfoil velocity and force diagram (Beri & Yao, 2011). .....	15
Figure 2.6 Force diagram of an airfoil blade (Islam et al., 2008). .....	17
Figure 2.7 Schematic of single stream tube model (Islam et al., 2008).....	19
Figure 2.8 Principle of multiple stream tube model with 6 stream tubes divided by uniform $\Delta\theta$ (Beri & Yao, 2011). .....	21
Figure 2.9 DMST with actuator discs and velocity vectors $V_{au}$ is induced velocity at upstream actuator disc, $V_e$ is equilibrium value, and $V_{ad}$ induced velocity at downstream actuator disc (Beri & Yao, 2011). .....	23
Figure 2.10 Double-blade vertical axis wind turbine (left) and butterfly wind turbine (right) (Hara et al., 2014). .....	27
Figure 2.11 Stand-alone wind turbine at McGlynn Elementary School, Boston (left) and Great Lakes Science Center, Cleveland. ....	30
Figure 2.12 A fleet of micro wind turbines at Boston Logan International Airport (Yu, 2008). .....	32
Figure 2.13 Top: Bahrain World Trade Centre ("Bahrain world trade centre (BWTC)," 2015); Bottom left: Strata Tower ; Bottom right: Pearl River Tower ("Pearl River Tower,") .....	33
Figure 2.14 Interference phenomenon on cooling towers (Hensley, 2009).....	37
Figure 2.15 Recirculation phenomenon on cooling towers (Hensley, 2009).....	38
Figure 3.1 General arrangement of the exhaust air energy recovery wind turbine generator.....	40
Figure 3.2 Artist's impression of the energy recovery wind turbine generator mounted above an exhaust air system.....	43

Figure 3.3 (a) Single rotor exhaust air energy recovery turbine generator; (b) Twin-rotor exhaust air energy recovery turbine generator .....	44
Figure 3.4 FRP square channel. ....	44
Figure 3.5 Internal structure of the cooling tower model.....	45
Figure 3.6 FRP plane for top cover, FRP corrugated plane for side cover and L channel for corner.....	45
Figure 3.7 Discharged air outlet duct.....	46
Figure 3.8 Assembly and exploded view of the cooling tower box.....	46
Figure 3.9 Fan mechanism assembly .....	47
Figure 3.10 Break out view and isometric view of the cooling tower model assembly with fan mechanism. ....	47
Figure 3.11 Extruded aluminum modular profile. ....	48
Figure 3.12 Assembled aluminium profile as the supporting structure for wind turbine and dynamometer. ....	48
Figure 3.13 Measuring points for each band at the discharge outlet. ....	49
Figure 3.14 Test rig, consisting of cooling tower model, wind turbine, dynamometer and supporting frame. ....	50
Figure 3.15 Horizontal and vertical range for turbine positioning experiment.....	51
Figure 3.16 Cross section of MH114 air foil. ....	52
Figure 3.17 Double multiple stream tube model with 18 stream tubes divided by uniform $\Delta\theta$ ( $10^\circ$ ) .....	53
Figure 3.18 Calculation flow chart of the DMST theory.....	55
Figure 3.19 Velocity contour of non-uniform wind (not to scale) from exhaust air outlet and wind turbine position.....	56
Figure 3.20 The wind turbine blade is equally divided to 5 sections for analysis. ....	56
Figure 3.21 VAWT position at the cooling tower outlet. ....	57
Figure 3.22 Assembly of cooling tower model with dual rotor exhaust air energy recovery turbine generator. ....	58

Figure 3.23 Isometric view and side view of the assembly of the diffuser, energy recovery turbine generator and the cooling tower model.....	59
Figure 3.24 Position of dual rotor VAWT for the diffuser-augmented exhaust air energy recovery turbine generator. ....	59
Figure 4.1 The effect of blockage to the cooling tower flow rate.....	62
Figure 4.2 The effect of blockage to the cooling tower fan power consumption. ....	62
Figure 4.3 Mean wind velocity at the outlet of the cooling tower model. ....	64
Figure 4.4 Rotational speed of wind turbine at various positions for fan speed of 708 rpm (VAWT rotates in clockwise direction). ....	65
Figure 4.5 Rotational speed of wind turbine at various positions for fan speed of 910 rpm (VAWT rotates in clockwise direction). ....	65
Figure 4.6 Energy generated by the wind turbine at various positions for the fan speed of 708 rpm. ....	67
Figure 4.7 Energy generated by the wind turbine at various positions for the fan speed of 910 rpm. ....	67
Figure 4.8 Coefficient of power against tip speed ratio wind turbine at the considered horizontal position and vertical position of $Y = 200$ mm. ....	70
Figure 4.9 Coefficient of power against tip speed ratio wind turbine at the considered horizontal position and vertical position of $Y = 250$ mm. ....	71
Figure 4.10 Coefficient of power against tip speed ratio wind turbine at the considered horizontal position and vertical position of $Y = 300$ mm. ....	72
Figure 4.11 Coefficient of power against tip speed ratio wind turbine at the considered horizontal position and vertical position of $Y = 350$ mm. ....	73
Figure 4.12 Coefficient of power against tip speed ratio wind turbine at the considered horizontal position and vertical position of $Y = 400$ mm. ....	74
Figure 4.13 Average flow rate of the cooling tower model with various configurations for the fan speed of 708 rpm. ....	76
Figure 4.14 Average flow rate of the cooling tower model with various configurations for the fan speed of 910 rpm. ....	76
Figure 4.15 Average fan motor power consumption of the cooling tower model with various configurations for the fan speed of 708 rpm. ....	77



Figure 4.16 Average fan motor power consumption of the cooling tower model with various configurations for the fan speed of 910 rpm. ....	78
Figure 4.17 Comparison between the power obtained from the experiments and obtained from the DMST calculations for the fan speed of 708 rpm. (a) For the wind turbine at 200 mm distance, (b) for the wind turbine at 250 mm distance, (c) for the wind turbine at 300 mm distance, and (d) for the wind turbine at 400 mm distance. ....	83
Figure 4.18 Comparison between the power obtained from the experiments and obtained from the DMST calculations for the fan speed of 910 rpm. (a) For the wind turbine at 200 mm distance, (b) for the wind turbine at 250 mm distance, (c) for the wind turbine at 300 mm distance, and (d) for the wind turbine at 400 mm distance. ....	84
Figure 4.19 (a) Plan view of wind turbine position against circular bands of exhaust air outlet; (b) Side view of wind turbine against the wind stream; (c) Instantaneous torque against azimuth angle and angle of attack versus azimuth angle at horizontal position of $X = 300$ mm and vertical position of $Y = 300$ mm for the fan speed of 910 rpm. ....	86
Figure 4.20 (a) Plan view of wind turbine position against circular bands of exhaust air outlet; (b) Side view of wind turbine against the wind stream; (c) Instantaneous torque against azimuth angle and angle of attack versus azimuth angle at horizontal position of $X = 250$ mm and vertical position of $Y = 300$ mm for the fan speed of 910 rpm. ....	88
Figure 4.21 (a) Plan view of wind turbine position against circular bands of exhaust air outlet; (b) Side view of wind turbine against the wind stream; (c) Instantaneous torque against azimuth angle and angle of attack versus azimuth angle at horizontal position of $X = 150$ mm and vertical position of $Y = 300$ mm for the fan speed of 910 rpm. ....	89
Figure 4.22 (a) Plan view of wind turbine position against circular bands of exhaust air outlet; (b) Side view of wind turbine against the wind stream; (c) Instantaneous torque against azimuth angle and angle of attack versus azimuth angle at horizontal position of $X = -150$ mm and vertical position of $Y = 300$ mm for the fan speed of 910 rpm. ....	91
Figure 4.23 Plan view of wind turbine position against circular bands of exhaust air outlet; (b) Side view of wind turbine against the wind stream; (c) Instantaneous torque against azimuth angle and angle of attack versus azimuth angle at horizontal position of $X = -250$ mm and vertical position of $Y = 300$ mm for the fan speed of 910 rpm. ....	92
Figure 4.24 Plan view of wind turbine position against circular bands of exhaust air outlet; (b) Side view of wind turbine against the wind stream; (c) Instantaneous torque against azimuth angle and angle of attack versus azimuth angle at horizontal position of $X = -300$ mm and vertical position of $Y = 300$ mm for the fan speed of 910 rpm. ....	94
Figure 4.25 Comparison of free running rotational speed of VAWT for the condition with and without the integration of diffuser-plates. The rotational speed values are the average from 2 VAWTs. ....	96

Figure 4.26 Comparison the average power generation by the VAWT for the condition with and without the integration of diffuser-plates .....	97
Figure 4.27 Comparison of the fan motor power consumption for the bare cooling tower, cooling tower with the VAWT and the cooling tower with the VAWT integrated with diffuser-plates at various vertical VAWT positions.....	98
Figure 4.28 Comparison of the cooling tower intake flow rate for the bare cooling tower, cooling tower with the VAWT and the cooling tower with the VAWT integrated with diffuser-plates at various vertical VAWT positions.....	99
Figure 5.1 Modified screenshot of the cooling tower model TCS 300-1B from Truwater (Truwater, 2011). .....	107
Figure 5.2 Mean wind velocity at the outlet of the cooling tower. ....	108
Figure 5.3 Front view and top view of the installation setup.....	109
Figure 5.4 Cost analysis of the exhaust air energy recovery generator (20 years life cycle). .....	113
Figure 5.5 Cumulative value of recovered energy .....	113

## LIST OF TABLES

Table 3.1 Wind outlet velocity measuring points. ....	50
Table 4.1 Performance of bare cooling tower. ....	61
Table 4.2 Average free-stream wind velocity on each wind turbine configuration. ....	68
Table 4.3 Comparative performance of cooling tower and wind turbine compared to bare cooling tower at positive side of horizontal position and fan speed of 708 rpm. ....	80
Table 4.4 Comparative performance of cooling tower and wind turbine compared to bare cooling tower at positive side of horizontal position and fan speed of 910 rpm. ....	81
Table 4.5 Summary of cooling tower performance and wind turbine performance for the bare cooling tower, cooling tower with diffuser-plates integrated VAWT and cooling tower with VAWT only for the fan speed of 708 rpm. ....	101
Table 4.6 Summary of cooling tower performance and wind turbine performance for the bare cooling tower, cooling tower with diffuser-plates integrated VAWT and cooling tower with VAWT only for the fan speed of 910 rpm. ....	102
Table 4.7 Test results of different configurations of cooling tower model. ....	103
Table 5.1 Estimated system components price and operating cost. ....	110
Table 5.2 Economic parameters. ....	111
Table 5.3 Projection of power recovered by an exhaust air energy recovery turbine generator with twin-rotor installed on a single unit of cooling tower. ....	112

## LIST OF SYMBOLS AND ABBREVIATIONS

$A$	:	Swept area	[ m <sup>2</sup> ]
$a$	:	Axial induction factor	[ - ]
$c$	:	Chord length	[ m ]
$C_D$	:	Drag coefficient	[ - ]
$C_L$	:	Lift coefficient	[ - ]
$C_n$	:	Normal coefficient	[ - ]
$C_p$	:	Power coefficient	[ - ]
$C_Q$	:	Torque coefficient	[ - ]
$C_T$	:	Thrust coefficient	[ - ]
$C_t$	:	Tangential coefficient	[ - ]
$D$	:	Rotor diameter	[ m ]
$F_D$	:	Drag force	[ N ]
$F_L$	:	Lift force	[ N ]
$h$	:	Blade height	[ m ]
$\dot{m}$	:	Mass flow rate	[ m <sup>3</sup> /s ]
$N$	:	Blade number	[ - ]
$P$	:	Power	[ W ]
$p$	:	Pressure	[ Pa ]
$Q$	:	Torque	[ Nm ]
$R$	:	Rotor radius	[ m ]
$T$	:	Thrust force	[ N ]
$V$	:	Wind velocity	[ m/s ]

Greek letters

$\rho$	:	Density	[ kg/m <sup>3</sup> ]
$\lambda$ or <i>TSR</i>	:	Tip speed ratio	[ - ]
$\theta$	:	Azimuth angle	[ ° ]
$\alpha$	:	Angle of attack	[ ° ]
$\omega$	:	Angular velocity	[ ° ]

Subscripts

$\infty$	:	free stream	[ - ]
$a$	:	induce velocity	[ - ]
$e$	:	equilibrium	[ - ]
$i$	:	instantaneous	[ - ]
$R$	:	relative velocity	[ - ]

## LIST OF APPENDICES

### Appendix A:

Appendix A1: Sample of data collected by the dynamometer system 130

Appendix A2: Sample of uncertainty analysis 131

### Appendix B:

Appendix B1: Lift coefficient against drag coefficient and lift coefficient against angle of attack of the MH 114 airfoil (Airfoil Investigation Database). 134

Appendix B2: Extrapolated aerodynamic data of MH114 airfoil (angle of attack,  $\alpha$  against lift coefficient,  $C_L$  and drag coefficient,  $C_D$ ) 135

### Appendix C:

Appendix C1: Plan view of the wind turbine position against the circular band of the cooling tower model outlet. X indicates the distance of the wind turbine center from the center of the outlet. 136

Appendix C2: Sample of double multiple stream tube calculation 137

### Appendix D:

Appendix D1: Instantaneous torque against azimuth angle and angle of attack versus azimuth angle at vertical position of  $Y = 200$  mm for the fan speed of 708 rpm 142

Appendix D2: Instantaneous torque against azimuth angle and angle of attack versus azimuth angle at vertical position of  $Y = 250$  mm for the fan speed of 708 rpm 145

Appendix D3: Instantaneous torque against azimuth angle and angle of attack versus azimuth angle at vertical position of  $Y = 300$  mm for the fan speed of 708 rpm 158

Appendix D4: Instantaneous torque against azimuth angle and angle of attack versus azimuth angle at vertical position of  $Y = 350$  mm for the fan speed of 708 rpm 151

Appendix D5: Instantaneous torque against azimuth angle and angle of attack versus azimuth angle at vertical position of  $Y = 400$  mm for the fan speed of 708 rpm 154

Appendix D6: Instantaneous torque against azimuth angle and angle of attack versus azimuth angle at vertical position of  $Y = 200$  mm for the fan speed of 910 rpm 157

Appendix D7: Instantaneous torque against azimuth angle and angle of attack versus azimuth angle at vertical position of $Y = 250$ mm for the fan speed of 910 rpm	160
Appendix D8: Instantaneous torque against azimuth angle and angle of attack versus azimuth angle at vertical position of $Y = 300$ mm for the fan speed of 910 rpm	163
Appendix D9: Instantaneous torque against azimuth angle and angle of attack versus azimuth angle at vertical position of $Y = 350$ mm for the fan speed of 910 rpm	166
Appendix D10: Instantaneous torque against azimuth angle and angle of attack versus azimuth angle at vertical position of $Y = 400$ mm for the fan speed of 910 rpm	169
Appendix E:	
Appendix E1: Wind turbine manufacturer's price (Source: <a href="http://ww.hi-vawt.com.tw">ww.hi-vawt.com.tw</a> , <a href="mailto:sales@hi-vawt.com.tw">sales@hi-vawt.com.tw</a> , October 2015)	172
Appendix E2: Maintenance free battery price from supplier (Source: Prodigy Integration, September 2015)	173
Appendix E3: Controller price from supplier (Source: Prodigy Integration, January 2016)	174

## CHAPTER 1: INTRODUCTION

### 1.1 Overview

Economic growth and energy demand are intertwined. Developed countries are known as the major users of energy globally, however, most of the increasing demand will occur in developing countries, where populations, economic activities and improvements in quality of life are growing most rapidly. Global energy consumption in both developed and developing countries is expected to double or more by the year 2040 ("The Outlook for Energy: A view to 2040," 2012). Currently, the world relies on coal, crude oil and natural gas for energy generation. However, energy crisis such as climate change and depletion of oil (which leads to the oil price inflation) becomes one of the main problems to all countries.

In Malaysia, the total primary energy supply had increased steadily over the past few decades. In 2013, the energy supply reached 97 Mtoe, which is a 62% increase from 1993 ("Malaysia Energy Statistics 2015," 2015). Total energy demand is growing at 5.4% per annum with 1.8% average annual population growth rate and in the year 2020 the energy demand will be approximately 971 TWh with 33.4 million population (Ali, Daut, & Taib, 2012). Most of the power plants in Malaysia are using fossil fuel for electricity generation while only 10.7% of the electricity generation comes from renewable sources such as hydropower, mini-hydro and biomass from palm oil waste (Shekarchian, Moghavvemi, Mahlia, & Mazandarani, 2011). In order to meet the increasing demand for energy, the country has extensively implemented energy conservation in order to reduce the consumption growth rate. Researchers have deeply discussed and proposed possible initiatives in order to promote the energy conservation programs such as fuel economy standard for motor vehicles (Mahlia, Saidur, Memon, Zulkifli, & Masjuki, 2010), energy



efficiency standards and energy labels for room air conditioners and refrigerator–freezers (Mahlia & Saidur, 2010) and energy efficiency award system (Manan et al., 2010).

By the end of year 2014, one of the primary sources of energy, i.e. crude oil has been showing a reduction trend in price which might lead to the reduction of electricity price (Chen, Gong, Raju Huidrom, Vashakmadze, & Zhao, 2015) ("World Economic Situation and Prospects 2015 ", 2015). According to the Organization of the Petroleum Exporting Countries (OPEC), the declining trends will continue throughout 2015 (OPEC, 2014). At the moment, energy security is not only evaluated in economic perspective, but it becomes more complex which covers the emerging global challenges, such as energy resource depletion, climate change, and geopolitical tension (Mirchi, Hadian, Madani, Rouhani, & Rouhani, 2012; Prambudia & Nakano, 2012). Limited capacity of the world to cope with the pollution caused by fossil fuels is one of the major considerations that have forced the world to seek an alternative energy system (Chauhan & Singh, 2014). More than 90% of the energy related greenhouse gases emission is a result of the CO<sub>2</sub> emissions from fuel combustion globally (Ahmad, Kadir, & Shafie, 2011). Currently, the increase in the concentration of greenhouse gases emission has caused a notable rise of temperature in the earth's atmosphere (global warming) and thus widespread melting of snow and ice at the polar ice caps (Solomon et al., 2007). Due to concerns for environmental issues, the development and application of renewable and clean new energy are strongly expected (Ohya & Karasudani, 2010).

For that reason, generating energy from renewable sources remain relevant to be implemented and explored. To meet the energy demand without damaging the planet, the energy generation from renewable sources becomes more widespread. It is proven that the renewable energy sources available can meet many times the present world energy demand, thus their potentials are enormous (Naghavi, 2010). However, most of the

current technologies on renewable energy generation are still at an early stage of development and not technically mature. Thus, there is an urgent call for researchers and innovators to come out with the best possible solution for clean energy.

## **1.2 Problem statement**

In order to reduce the dependence on fossil fuels for energy generation, renewable energy plays a critical role in reducing the greenhouse gases emission leading the world toward fossil fuel independence. Wind energy is the second biggest source of renewable energy after solar energy. It is the fastest growing RE source in the world with an annual growth rate of 30% (Kalantar & Mousavi G, 2010) (Ponta, Seminara, & Otero, 2007). The share of wind energy is 14% at the global scale on the total mid-term renewable energy resources potential and this value reflects its maturity in technology (Resch et al., 2008). Many researchers have proposed the ideas of wind energy systems that can possibly be installed in urban settings for local energy generation (W. T. Chong, Pan, et al., 2013; Müller, Jentsch, & Stoddart, 2009; Sharpe & Proven, 2010; Wang et al., 2015). These systems feature additional augmentation systems, either utilizing the building geometry or retrofitted onto the building or a combination of these. However, the uncertainty in wind energy is the main problem in matching the increasing demand for renewable energy. The operation of wind power systems is susceptible to changing wind patterns resulting from climate change (Schaeffer et al., 2012). Thus, an efficient method is strongly demanded to harness the uncertain wind energy.

Besides turning to available alternative resources for generating clean energy, energy recovery from wastes such as heat sink, exhaust air, etc. also have a great potential in helping to address the global energy issue. Energy saving and emission reducing technologies consist of three types, i.e. resource conservation, energy economizing and environment-friendly (Shan, Qin, Liu, & Liu, 2012). The available wind source can be

divided into natural wind and man-made wind. The man-made wind is considered as unnatural that is available from man-made systems or operations such as cooling tower, exhaust air, etc. The high-speed, consistent and predictable wind produced by the system is good to be recovered into a useful form of energy. Thus, this research investigates the concept of energy recovery systems on cooling towers by using commercially available wind turbines. It is an energy recovery system which may reduce the energy demand by generating energy from waste. This system enables the low wind speed countries especially in urban areas to harness wind energy from exhaust air resources which are consistent and predictable.

### **1.3 Objectives of research**

This report presents the design and testing of an exhaust air energy recovery wind turbine generator in order to propose a new system on clean energy generation. The system uses a commercially available wind turbine mounted on a predefined configuration facing the outlet of an exhaust air system. The objectives of this research are as listed below:

- i) Determination of exhaust air energy recovery turbine generator configuration by experimental analysis on wind turbine and exhaust air system performance with various configurations
- ii) Analysis of wind turbine behavior using the double multiple stream tube theory of the various configurations of exhaust air energy recovery turbine generator
- iii) Experimental analysis of the diffuser as a power-augmentation device for the exhaust air energy recovery turbine generator
- iv) Energy estimation and techno-economic analysis of the integration of exhaust air energy recovery turbine generator onto actual cooling tower

The main aim of the research is to prove that the wind from an exhaust air system can be utilized into useful forms of energy. Moreover, the utilization of this man-made wind energy by the energy recovery wind turbine generator is aimed to give no negative effect on the performance of the exhaust air system.

#### **1.4 Thesis outline**

In this thesis, the design and testing of an exhaust air energy recovery wind turbine generator for clean energy generation is presented. The system is targeted to generate clean energy from the wind that is blown from an exhaust air system without causing any negative effect on the performance of the exhaust air system which in this case is represented by a cooling tower. The study intends to prove the concept of a recovery system from exhaust air sources. The thesis is divided into six chapters and the organization of the thesis is as explained below.

Chapter 1 is the introduction to this research which covers the overview and background of this research. It is followed by the problem statement, objective of research and the thesis outline.

Chapter 2 is the literature review which consists of the overview of the related studies regarding wind energy systems. The review also covers the area of exhaust air system which refers particularly to cooling towers and the design of the existing energy recovery system. A comprehensive review is done to examine its relationship to this study.

Chapter 3 is the design description and methodology. The first part of this chapter covers the design description of the exhaust air energy recovery turbine generator and its benefits as well as the design variations. The fabrication of the test rig, i.e. cooling tower model, wind turbine supports and diffuser is also presented. The methodologies, i.e.

experimental procedures and double multiple stream tubes analysis procedure are then explained in this chapter.

Chapter 4 covers the results and discussions from the research methodology done. The result and discussion include the performance cooling tower with and without the energy recovery turbine generator, double multiple stream tube analysis and the evaluation of the diffuser-plates as a power augmentation device for the system.

Chapter 5 is the energy estimation and techno-economic analysis of the exhaust air energy recovery turbine generator. Literature review, methodology and results and discussion is presented independently (from Chapter 2 – 4) in this chapter.

Chapter 6 is the conclusion of the study which consists of the conclusion of the present work and recommendations for future work. In addition, the conclusion achieved in this study is summarized in this section.

## CHAPTER 2: LITERATURE REVIEW

### 2.1 Wind energy

Wind is a natural phenomenon that is caused by the uneven heating of the atmosphere by the sun, the irregularities of the earth's surface, and rotation of the earth (Bhatia, 2014). Energy available in wind is basically the energy of large masses of air moving over the earth's surface. Blades of wind turbine receive this kinetic energy, which is then transformed to mechanical or electrical forms, depending on the end use. The efficiency of converting wind to other useful forms of energy greatly depends on the efficiency with which the rotor interacts with the wind stream (Mathew, 2006). Nowadays the utilization of wind energy for electricity generation has become very popular where the global installed wind power capacity is approximately 370 GW at the end of 2014, a 16% increase from the previous year ("Global Wind Energy Report: Annual Market Update 2014," 2015). Wind energy is one of the earliest sources of energy when it was utilized to propel ships and boats during ancient times. The first documented design of a wind mill dates back to 200 B.C. where the Persians used wind mills for grinding grains. At the end of the 18<sup>th</sup> century, experiments began in which windmills were used to generate electricity in the United States and Denmark. The research continues until today and wind power generation has become an icon for clean and sustainable energy generation.

Wind power is the kinetic energy of air in motion. The kinetic power (kinetic energy per unit time) can be expressed as:

$$P = \frac{1}{2} \dot{m} V^2 \quad (2.1)$$

where  $P$  is the kinetic power,  $v$  is the air velocity and  $\dot{m}$  is the air mass flow rate which can be expressed as:

$$\dot{m} = \rho AV \quad (2.2)$$

where  $\rho$  is the air density and  $A$  is the swept area perpendicular to the flow direction. The combination of Equations 2.1 and 2.2 can be expressed as:

$$P = \frac{1}{2} \rho AV^3 \quad (2.3)$$

From the equation, the power available in wind is a function of air density ( $\rho$ ), swept area of the wind rotor ( $A$ ) and the wind velocity ( $V$ ). The power in the wind is proportional to the cubic power of the velocity approaching the wind turbine, which means that even a small increment in wind speed gives a large increase in energy generation.

Today, most wind turbines are used to generate electricity. As electrical power generators, wind turbines are connected to the electrical network, including battery charging circuits, residential power systems, isolated networks and large utility grids (Manwell, McGowan, & Rogers, 2002). Large utility grids normally use larger turbines in wind farms to generate electricity. The wind farms are mostly available in Europe and the United States which experience strong winds throughout the year. The largest wind farm is the Alta Wind Energy Center in California, USA with an operational capacity of 1,020MW (Chauhan & Singh, 2014).

Wind energy conversion systems are classified into two types according to the aerodynamic force characteristic, i.e. drag-based and lift-based. The drag-based wind turbine is the earliest type of wind turbine that was used during ancient times. The wind turbine called the Sistan turbine was used in Afghanistan from the year 644 A.D. up to the present time (Hau, 2006). Old structures of drag devices, however, had a very low power coefficient,  $C_p$  with a maximum value of around 0.16 (Gasch, 1982) (Ackermann, 2005). Aerodynamic lift is the main base for modern wind turbines, where airfoil blades

are used. The lift force supplies more than the drag force and thus, the relevant driving power of the rotor is much more for lift power rather than the drag power.

Wind turbines also have been described by the axis of rotation. Therefore, modern wind turbines, i.e. aerodynamic lift-based wind turbines can be further divided into horizontal-axis and vertical-axis type turbines. The horizontal-axis wind turbine (HAWT) currently dominates the wind turbine applications where the axis of rotation is parallel to the ground. Figure 2.1 shows the schematic arrangement of a HAWT. The number of blades of a HAWT depends on the purpose of the wind turbine. For example, two or three bladed turbines are usually used for electricity power generation. Turbines with 20 or more blades are suitable for mechanical power, e.g. water pumping.

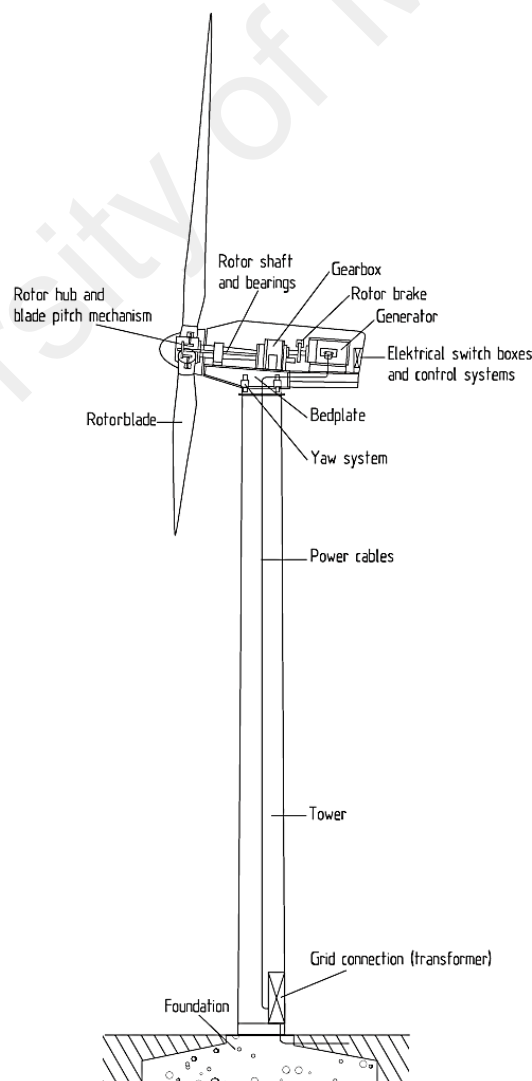


**Figure 2.1 Components of a HAWT (Hau, 2006).**



Another type of turbine according to the axis of rotation is the vertical axis wind turbine (VAWT). There have been many designs of vertical axis windmills over the centuries and currently the VAWT can be broadly divided into three basic types, namely the Savonius type, Darrieus type and H-rotor type as shown in Figure 2.2 (Islam, Ting, & Fartaj, 2008). The Savonius-type VAWT was invented by a Finnish engineer S.J. Savonius in 1929, and it is basically a drag force driven wind turbine with two cups or half drums fixed to a central shaft in opposing directions (Savonius, 1931). However, the Savonius turbine unfortunately has a rather poor efficiency when considering the standard design; theoretically,  $C_p = 0.18$  at best (Mohamed, Janiga, Pap, & Thévenin, 2010). The Darrieus wind turbine is another type of VAWT. Consisting of a number of airfoil blades, the Darrieus turbine is a lift-based VAWT that uses lift forces generated by the wind hitting airfoil blades to create rotation. Compared to a drag-type VAWT, e.g. Savonius turbine, a Darrieus generates less torque, but it rotates much faster. Thus, Darrieus wind turbines are much better suited to electricity generation rather than water pumping and similar activities (REUK.co.uk, 2007). A variation of the Darrieus turbine is the so-called H-rotor turbine. Instead of the curved rotor blades, straight airfoil blades connected to the rotor shaft are used. However, there are substantial drawbacks of the H-rotor VAWT, that is lower power coefficient and it has a poor self-starting characteristic compared to the HAWT (Takao, Maeda, Kamada, Oki, & Kuma, 2008).

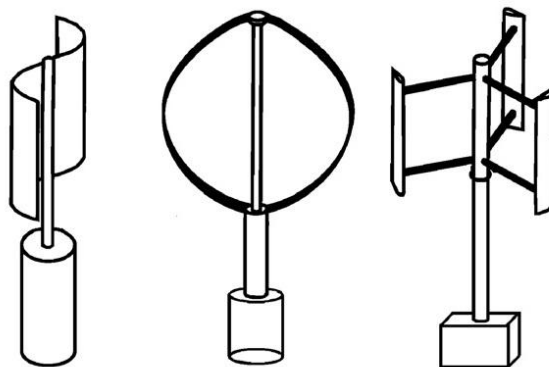


**Figure 2.2 Illustrations of the VAWTs. From left, Savonius rotor, Darrieus turbine and H-rotor (Islam et al., 2008).**

The maximum theoretical efficiency of a wind turbine is given by the Betz Limit, and is around 59 percent (Ragheb & Ragheb, 2011). Practically, wind turbines operate below the Betz Limit. In order to achieve the maximum power coefficient, a wind turbine need to operate at its optimum tip speed ratio (TSR). TSR refers to the ratio between the wind speed and the speed of the tips of the wind turbine blades. The relationship between the rotor power coefficient and the TSR is shown in Figure 2.3 for different types of wind machines. It can be noticed that it reaches a maximum at different positions for different machine designs.

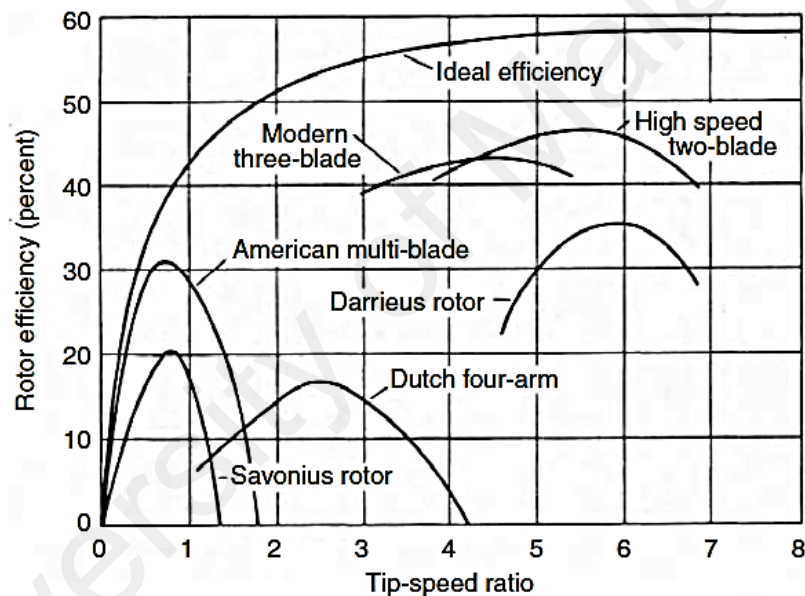


**Figure 2.3 The power coefficient as a function of the tip speed ratio for different wind machine designs (Patel, 2006).**

### 2.1.1 Aerodynamic analysis of wind turbine

Betz (1926) attributed a simple model that can be used to determine the power from an ideal turbine rotor (Duran, 2005; Manwell et al., 2002). The model is based on the linear momentum theory. The analysis assumes the flow in a stream tube as shown in Figure 2.4. The turbine is represented by a uniform actuator disk which creates discontinuity of pressure in the stream tube of air flowing through it. The analysis applies the following assumptions (Biadgo, Simonovic, Komarov, & Stupar, 2013):

- i. The analysis assumes a control volume where the boundaries are the surface and two cross-sections of the stream tube;
- ii. Homogenous, incompressible, steady state fluid flow;
- iii. No frictional drag;
- iv. An infinite number of blades;
- v. Uniform thrust over the disk and rotor area;
- vi. There is continuity of velocity through the disk;
- vii. A non-rotating wake;
- viii. The static pressure far upstream and far downstream of the rotor is equal to the undisturbed ambient static pressure.

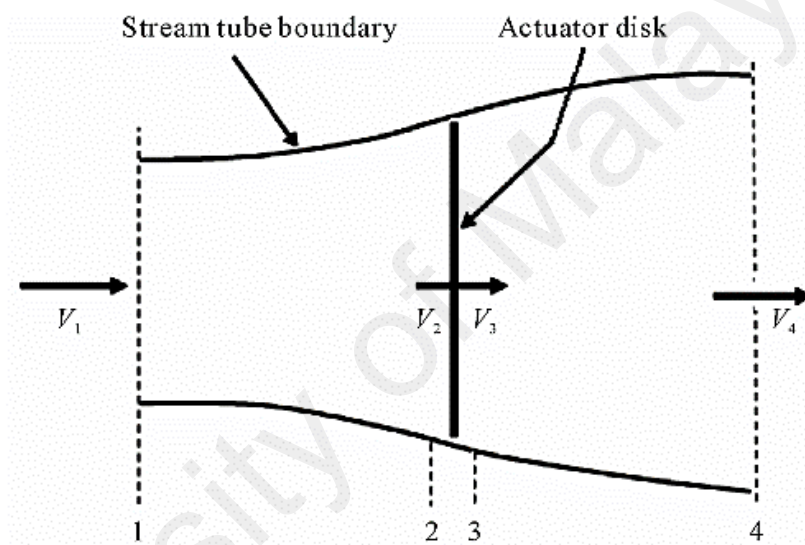


**Figure 2.4 Actuator disk model of a wind turbine (Beri & Yao, 2011).**

Referring to Figure 2.4, applying the conservation of linear momentum to the control volume enclosing the whole system, it is possible to find the net force on the contents of the control volume. According to the law of conservation of mass, the mass of air flowing through the sections of the stream tube is equal (Mathew, 2006). Thus, the mass flow rate,  $\dot{m}$  is expressed as below:

$$\dot{m} = (\rho AV)_1 = (\rho AV)_2 = (\rho AV)_3 = (\rho AV)_4 \quad (2.4)$$

where  $\rho$  is the density,  $A$  is the cross sectional area,  $V$  is the air velocity and the subscripts indicate values at numbered cross sections in Figure 2.4.

The thrust force,  $T$  experienced by the rotor is due to the difference in momentum of the incoming and outgoing wind, which is given by:

$$T = V_1(\rho AV)_1 - V_4(\rho AV)_4 \quad (2.5)$$

Substituting Equation 2.4 into Equation 2.5, the expression becomes:

$$T = \dot{m}(V_1 - V_4) \quad (2.6)$$

The positive thrust value indicates the velocity behind the rotor,  $V_4$ , is less than the free stream velocity,  $V_1$ . No work is done on either side of the turbine rotor. Thus, the Bernoulli function can be used in the two control volumes on either side of the actuator disk. The Bernoulli function at the stream tube, upstream of the disk is expressed as below:

$$p_1 + \frac{1}{2}\rho V_1^2 = p_2 + \frac{1}{2}\rho V_2^2 \quad (2.7)$$

While at the downstream of the disk, the function is:

$$p_3 + \frac{1}{2}\rho V_3^2 = p_4 + \frac{1}{2}\rho V_4^2 \quad (2.8)$$

where  $p$  is the pressure. Pressure at the far upstream and far downstream are assumed as equal ( $p_1 = p_4$ ), while the velocity across the disk is assumed as the same ( $V_2 = V_3$ ). With these assumptions, the thrust can also be expressed as the net sum of the forces on each side of the actuator disk as shown below:

$$T = A_2(p_2 - p_3) \quad (2.9)$$

Solving the Equations 2.4, 2.5 and 2.6, it is possible to obtain:

$$T = \frac{1}{2}\rho A_2(V_1^2 - V_4^2) \quad (2.10)$$

Comparing Equations 2.9 and 2.10, yield:

$$V_2 = \frac{V_1 + V_4}{2} \quad (2.11)$$

Thus the velocity of the wind stream at the rotor section is the average of the velocities at its upstream and downstream sides. At this stage, a parameter is introduced, termed as the axial induction factor into the analysis. The axial induction factor,  $a$ , indicates the degree with which the wind velocity at the upstream of the rotor is slowed down by the turbine. Thus,

$$a = \frac{V_1 - V_2}{V_2} \quad (2.12)$$

$$V_2 = V_1(1 - a) \quad (2.13)$$

$$V_4 = V_1(1 - 2a) \quad (2.14)$$

From Equations 2.7, 2.10 and 2.11, the axial thrust on the disk is expressed as:

$$T = \frac{1}{2} \rho A V_1^2 [4a(1 - a)] \quad (2.15)$$

The thrust on a wind turbine can be characterized by a non-dimensional thrust coefficient,  $C_T$  as:

$$C_T = \frac{\text{Thrust force}}{\text{Dynamic Force}} = \frac{T}{\frac{1}{2} \rho A V^2} \quad (2.16)$$

The equation can be simplified for an ideal wind turbine as:

$$C_T = 4a(1 - a) \quad (2.17)$$

### 2.1.1.1 General mathematical expressions for aerodynamic analysis of straight bladed Darrieus vertical axis wind turbine

Straight bladed Darrieus vertical axis wind turbine is the simplest wind turbine in the structural aspect (Beri & Yao, 2011; Islam et al., 2008). However, the aerodynamic analysis for this type of wind turbine is quite complex since the magnitude and vector

components keep on changing with the azimuth angle. Before proceeding with the main aerodynamic models, the general mathematical expressions, which are common to most of the aerodynamic models, are described in this section. Figure 2.5 illustrates the diagram of forces and velocities of an airfoil blade at a specific location.

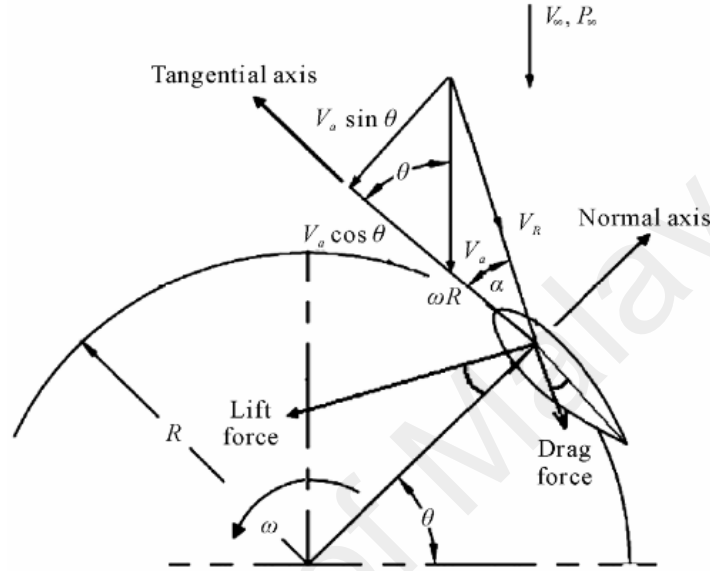


**Figure 2.5 Airfoil velocity and force diagram (Beri & Yao, 2011).**

From the figure,  $\theta$  represents the azimuth angle,  $\omega$  is the rotational velocity in rad/s,  $\alpha$  is the angle of attack,  $V_a$  is the induced velocity,  $V_R$  is the relative velocity components and  $R$  is the radius of the turbine. Subscript  $\infty$  represents the free stream condition.

Referring to Figure 2.5, based on vector velocity triangle,  $V_R$  can be expressed as below:

$$V_R = \sqrt{(V_a \sin \theta)^2 + (\omega R + V_a \cos \theta)^2} \quad (2.18)$$

Normalizing the relative velocity using free stream wind velocity one can obtain:

$$\frac{V_R}{V_\infty} = \sqrt{\left(\frac{V_a}{V_\infty} \sin \theta\right)^2 + \left(\frac{\omega R}{V_\infty} + \frac{V_a}{V_\infty} \cos \theta\right)^2} \quad (2.19)$$

Substituting  $V_2$  with  $V_a$  and  $V_I$  with  $V_\infty$ , and referring back to Equation 2.10, Equation 2.19 can be rewritten as:

$$\frac{V_R}{V_\infty} = \sqrt{[(1-a)\sin\theta]^2 + [(1-a)\cos\theta + \lambda]^2} \quad (2.20)$$

where  $\lambda$  is the tip speed ratio as expressed below:

$$\lambda = \frac{\omega R}{V_\infty} \quad (2.21)$$

Referring Figure 2.5, the angle of attack,  $\alpha$  can be expressed as:

$$\tan\alpha = \frac{V_a \sin\theta}{V_a \cos\theta + \omega R} \quad (2.22)$$

Non-dimensionalizing the equation,

$$\tan\alpha = \frac{\frac{V_a}{V_\infty} \sin\theta}{\frac{V_a}{V_\infty} \cos\theta + \frac{\omega R}{V_\infty}} \quad (2.23)$$

$$\alpha = \tan^{-1} \left[ \frac{(1-a)\sin\theta}{(1-a)\cos\theta + \lambda} \right]$$

The directions of the lift and drag forces and their normal and tangential components are shown in Figure 2.6. The tangential force coefficient,  $C_t$  is basically the difference between the tangential components of lift and drag forces. Similarly, the normal force coefficient,  $C_n$  is the difference between the normal components of lift and drag forces.

The expressions of  $C_t$  and  $C_n$  can be written as:

$$C_n = C_L \cos\alpha + C_D \sin\alpha \quad (2.24)$$

$$C_t = C_L \sin\alpha - C_D \cos\alpha \quad (2.25)$$

where  $C_L$  and  $C_D$  is the lift coefficient and drag coefficient respectively.

The instantaneous thrust force,  $T_i$  on one single airfoil with respect of azimuth angle,  $\theta$  is:

$$T_i = \frac{1}{2} \rho V_R^2 (hc) (C_l \cos \theta - C_n \sin \theta) \quad (2.26)$$

where  $h$  is the blade height and  $c$  is the blade chord length.

The instantaneous torque,  $Q_i$  on one single airfoil with respect to azimuth angle,  $\theta$  is:

$$Q_i = \frac{1}{2} \rho V_R^2 (hc) C_T R \quad (2.27)$$

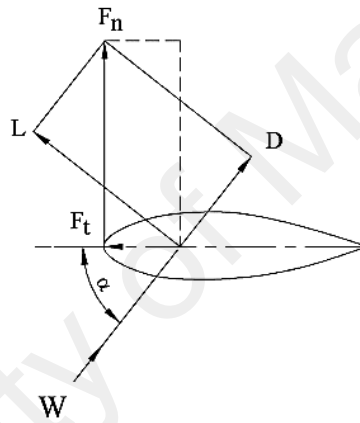


**Figure 2.6 Force diagram of an airfoil blade (Islam et al., 2008).**

### 2.1.1.2 Aerodynamic prediction models for vertical axis wind turbine

Several aerodynamic prediction models currently exist for studying the Darrieus vertical axis wind turbines. Generally, the main objective of all aerodynamic models is to evaluate the induced velocity field of the turbine since knowledge of this velocity field allows all the forces on the blade and the power generated by the turbine to be determined (Brahimi, Allet, & Paraschivoiu, 1995).

Different momentum models (also specified as Blade Element Momentum or BEM model) are basically based on calculation of flow velocity through the turbine by equating the stream wise aerodynamic force on the blades with the rate of change of momentum of air, which is equal to the overall change in velocity times the mass flow rate (Islam et



al., 2008). The force is also equal to the average pressure difference across the rotor. Bernoulli's equation is applied in each stream tube. The main drawback of these models is that they become invalid for large tip speed ratios and also for high rotor solidities because the momentum equations in these particular cases are inadequate (Paraschivoiu, 2002). Over the years, several approaches were attempted to utilize this concept, which are discussed briefly in the following headings.

(a) *Single stream tube model*

The first approach to analyze the flow field around a vertical-axis wind turbine was developed by Templin (1974) who considered the rotor as an actuator disk enclosed in a simple stream tube. For the analysis, the induced velocity through the swept volume of the turbine is assumed to be constant throughout the disk within a single stream tube as shown in Figure 2.7. In the assumption, the actuator disc is considered as the surface of the imaginary body of revolution. It is assumed that the flow velocity is constant throughout the upstream and downstream side of the swept volume. This theory takes into account the effect of airfoil stalling on the performance characteristics. The effects of geometric variables such as blade solidity and rotor height–diameter ratio have been included in the analysis. The effect of zero-lift-drag coefficient on the performance characteristics has also been included. Wind shear effect cannot be incorporated into the model.

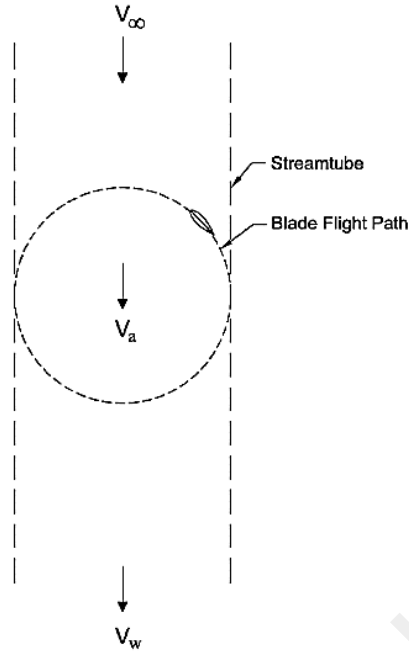


**Figure 2.7 Schematic of single stream tube model (Islam et al., 2008).**

Now, according to Glauert Actuator Disk theory, the expression of the uniform velocity through the rotor is:

$$V_a = \frac{V_\infty + V_w}{2} \quad (2.28)$$

where  $V_w$  is the wake velocity. All the calculations in this model are performed for a single blade whose chord equals the sum of the chords of the actual rotor's blade. The streamwise drag force,  $F_D$  due to the rate of change of momentum is expressed as:

$$F_D = \dot{m}(V_\infty - V_w) \quad (2.29)$$

The rotor drag coefficient,  $C_{DR}$  is defined as:

$$C_{DR} = \frac{F_D}{\frac{1}{2} \rho A V_a^2} \quad (2.30)$$

Merging Equations 2.29 and 2.30, the equation becomes:

$$C_{DR} = 4 \left( \frac{V_\infty - V_a}{V_a} \right) \quad (2.31)$$

and

$$\frac{V_a}{V_\infty} = \left( \frac{1}{1 + C_{DR}/4} \right) \quad (2.32)$$

Utilizing the expression 2.32, the overall torque and power coefficient of the VAWT can be calculated.

This model can predict the overall performance of a lightly loaded wind turbine (Jin, Zhao, Gao, & Ju, 2015). However, it always predicts higher power compared to the experimental results. It is because the model does not predict the wind velocity variations across the rotor where these variations gradually increase with the increase of the blade solidity and tip speed ratio (Islam et al., 2008).

(b) ***Multiple stream tube model***

Wilson and Lissaman (1974) assumed a sinusoidal variation in inflow velocity across the width of the turbine to account for non-uniform flow. An extension of this method to the multiple stream tube model was then developed by Strickland (1975) who considered the swept volume of the turbine as a series of adjacent stream tubes. The momentum balance is carried out separately for each stream tube, allowing an arbitrary variation in inflow. The schematic for the multiple stream tube model is illustrated in Figure 2.8.

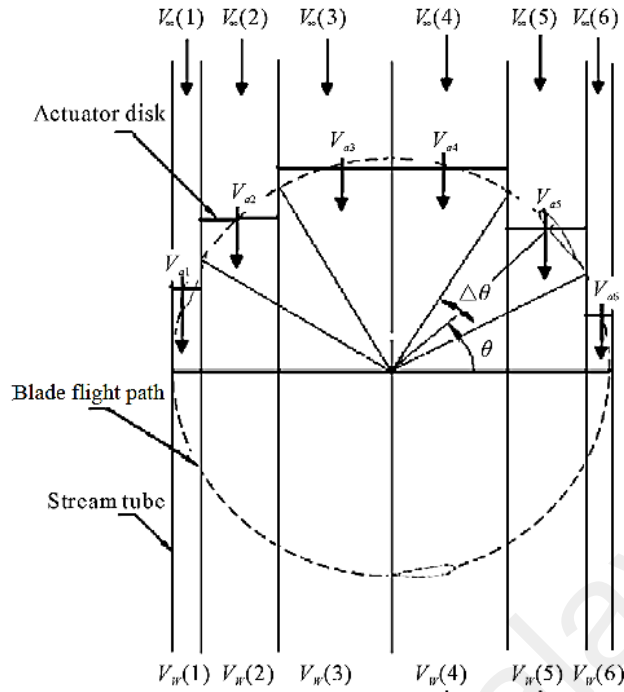


**Figure 2.8 Principle of multiple stream tube model with 6 stream tubes divided by uniform  $\Delta\theta$  (Beri & Yao, 2011).**

A single blade passes each stream tube twice per revolution in the upstream and downstream. The instantaneous thrust force on one single blade is given in Equation 2.23. The average thrust force,  $T_{avg}$  acting in a stream tube by the  $N$  number of blades and twice per revolution can be expressed as:

$$T_{avg} = 2NT_i \left( \frac{\Delta\theta}{\pi} \right) \quad (2.33)$$

The average aerodynamic thrust can be characterized by a non-dimensional thrust coefficient:

$$C_T = \frac{T_a}{\frac{1}{2} \rho V^2 (hR \Delta\theta \sin \theta)}$$

$$= \left( \frac{Nc}{2R} \right) \left( \frac{V_R}{V_\infty} \right)^2 \frac{2}{\pi} \left( C_t \frac{\cos \theta}{\sin \theta} - C_n \right) \quad (2.34)$$

The instantaneous torque on a single blade is given in Equation 2.27. The average torque,  $Q_{avg}$  on rotor by  $N$  number of blades in one complete revolution and calculated in  $m$  number of stream tubes is then given as:

$$Q_{avg} = N \times \sum_{i=1}^{2m} \left[ \frac{\frac{1}{2} \rho V_R^2 (hc) C_t R}{2m} \right] \quad (2.35)$$

The torque coefficients,  $C_Q$  and power coefficients,  $C_P$  are given as

$$\begin{aligned} C_Q &= \frac{Q_a}{\frac{1}{2} \rho V^2 (Dh) R} \\ &= \left( \frac{Nc}{D} \right) \sum_{i=1}^{2m} \left[ \frac{\left( \frac{V_R}{V_\infty} \right)^2 C_t}{2m} \right] \end{aligned} \quad (2.36)$$

$$C_P = C_Q \lambda \quad (2.37)$$

where  $D$  represents the diameter of the turbine.

### (c) *Double multiple stream tube*

The widely used aerodynamic prediction model recently is the double-multiple stream tube (DMST) which was developed by Paraschivoiu (1981). In this model the calculation is done separately for the upstream and downstream half cycles of the turbine. At each level of the rotor, the induced velocities at upstream and downstream are obtained using the principle of two actuator discs in tandem. The concept of the two actuator discs in tandem for a Darrieus wind turbine was originally given by Lapin (1975). DMST applies the concept like the multiple stream tube model with variation of induced velocity in vertical direction but extracted into upstream and downstream half cycles. The downwind

half of the rotor is assumed to be in the fully expanded wake of the upwind half and the model neglects the effect of the downwind half of the rotor on the upwind half (Simao Ferreira et al., 2014). In the horizontal direction, the induced velocity is assumed to be constant like that of a single stream tube model. Figure 2.9 depicts the schematic of the double multiple stream tube. The induced velocities for the upstream and downstream are differentiated by the subscripts *au* and *ad* respectively.  $V_e$  represents the equilibrium velocity between upstream and downstream.

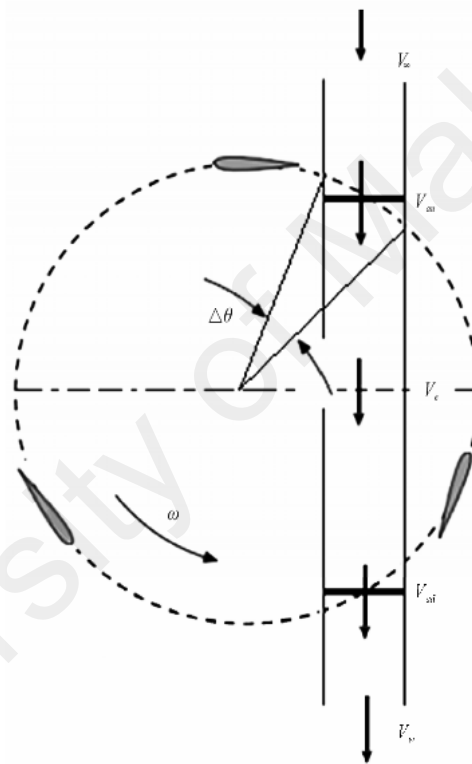


**Figure 2.9 DMST with actuator discs and velocity vectors  $V_{au}$  is induced velocity at upstream actuator disc,  $V_e$  is equilibrium value, and  $V_{ad}$  induced velocity at downstream actuator disc (Beri & Yao, 2011).**

The turbine interacts with the wind in the upwind and downwind passes of the blades separately. The assumption is made that the wake from the upwind pass is fully expanded and the ultimate wake velocity has been reached before the interaction with the blades in the downwind pass. The downwind blades therefore see a reduced ‘free-stream’ velocity. This approach more accurately represents the variation in flow through the turbine. Each stream tube in the DMST model intersects the airfoil path twice; once on the upwind pass,

and again on the downwind pass. At these intersections we imagine the turbine replaced by a tandem pair of actuator discs, upon which the flow may exert force. The DMST model simultaneously solves two equations for the stream-wise force at the actuator disk; one obtained by conservation of momentum and other based on the aerodynamic coefficients of the airfoil (lift and drag) and the local wind velocity. These equations are solved twice; for the upwind and for the downwind part of the rotor.

According to the actuator disk theory shown in Equation 2.11, the induced velocity,  $V_{au}$  on the upstream wind will be the average of the air velocity at far upstream,  $V_{\infty}$  and the air velocity at equilibrium,  $V_e$ . Thus

$$V_{au} = \frac{1}{2}(V_{\infty} + V_e)$$

and

$$V_e = 2V_{au} - V_{\infty} \quad (2.38)$$

### 2.1.2 Research development on wind energy

Wind energy has been developing very quickly in the past years. Installation of wind turbines grew at an annual average rate of 30% between 2000 and 2009 and global installed capacity up to 2013 represents 318 GW (Fried, 2013). It is projected to grow by 350% when wind power projects currently in development come online in the next few years (Hallgren, Gunturu, & Schlosser, 2014) and is predicted to be the second largest right after hydro-power in 2030 (Fazelpour, Soltani, Soltani, & Rosen, 2015). The trend of wind energy research is also becoming more widespread. However, penetration of wind power is challenged by intermittent and fluctuating wind speeds restricting the dispatchability of wind power to meet daily and seasonal patterns of energy demand (Huffaker & Bittelli, 2015). Thus, the research mainly covers the area of improving the wind turbine power coefficient, wind concentrator, extracting energy at low wind speed

conditions, and building integrated wind turbines. There are also research works in introducing wind energy systems that can possibly be installed in urban settings for local energy generation. These systems feature additional augmentation systems, either utilizing the building geometry or retrofitted onto the building or a combination of these.

Both the horizontal axis wind turbine (HAWT) and vertical axis wind turbine (VAWT) designs are efficient, however both are being rigorously tested and improved (Bellarmine & Urquhart, 1996; Joselin Herbert, Iniyar, Sreevalsan, & Rajapandian, 2007). In terms of wind turbine design, HAWT is considered a matured design. Most wind farms globally are dominated by HAWTs. Recent researches are more focused on improving and introducing new designs of VAWTs. A variety of steps have been tried to improve self-starting performance: increasing blade chord length, adding more blades, using drag-driven wind turbines as a starter, and designing blade airfoils for high aerodynamic performance (Tanino, Fujikawa, Nakao, & Takahashi, 2010). A comparative study by Eriksson et al. has shown that VAWTs are advantageous compared to HAWTs in several aspects (Eriksson, Bernhoff, & Leijon, 2008). Generally, the VAWTs have the advantages such as ease of installation and maintenance (due to the generator being located beneath the turbine), omni-direction wind power extraction and no yawing mechanism is required. In comparison between H-rotor and Darrieus turbines, H-rotor seems more beneficial than the Darrieus. The possibility of simple structure and lower level of maintenance are the strengths of the H-rotor turbine. Clear advantage of the VAWTs is that they can handle the wind from any direction regardless of orientation (Riegler, 2003). VAWTs can work even when the wind is very unstable making them suitable for urban and small-scale applications (Armstrong, Fiedler, & Tullis, 2012). Their particular axial symmetry means they can obtain energy where there is high turbulence (Brusca, Lanzafame, & Messina, 2014). With its robust design, this research utilizes the VAWT in generating energy.



### 2.1.2.1 Recent design of vertical axis wind turbine

Even though the Savonius VAWT has a low power coefficient (as depicted in Figure 2.3), the fact that the drag-type turbines have better self-starting behavior attracts researchers to find ways to improve its performance. Saha, Thotla, and Maity (2008) studied the optimum design configuration of Savonius rotor through wind tunnel experiments. There are three parameters that determine the configurations which are the stages (single, 2-stage and 3-stage), number of blades (2 and 3 blades) and the blade shapes (semi-circle and twisted). The 2-stage 3-bladed with twisted blade Savonius rotor system is superior among all the configurations with a power coefficient of up to 0.32. Taking the advantage of the self-starting behavior, Savonius wind turbine is also coupled with lift-type VAWT. A group of researchers in Japan introduced the hybrid configuration of Darrieus and Savonius rotors for stand-alone wind turbine-generator systems. Two Savonius rotors as the Darrieus starter are rigidly installed with an angular difference of 90 degrees on the same axis (Wakui, Tanzawa, Hashizume, & Nagao, 2005). Gupta, Biswas, and Sharma (2008) also studied the same configurations but with the Savonius' blades at 150 degrees arc.

Other recent designs of VAWTs is the helical wind turbine as patented by Gray, Lewis, MacLean, Naskali, and Newall (2008). The key feature of the VAWT is that of the orientation of the helical blade design. According to the published patent document, the blades orientation is designed to provide a lifting force on the turbine section that will raise the rotor section off of the base section. As the wind will impact the blade on the radially inward and downward facing surface and thus creating both a rotation force and a lifting force. As a result, some of the wind energy is used to reduce the effective rotation weight of the rotor. Researchers from Korea and Japan introduced the butterfly wind turbine (BWT) which is the transformation of their own idea of a double-blade wind turbine (Hara et al., 2014). The double-blade idea is to improve self-starting behavior of

an H-rotor VAWT by adding another set of blade with smaller radius to the existing blade. By combining the blades, a BWT is established. The BWT may offer reduced costs, good self-starting performance, high energy efficiency, and good vibration handling because of the direct installation of the armless looped blades on the central axis. The double-blade VAWT and BWT are illustrated in Figure 2.10.

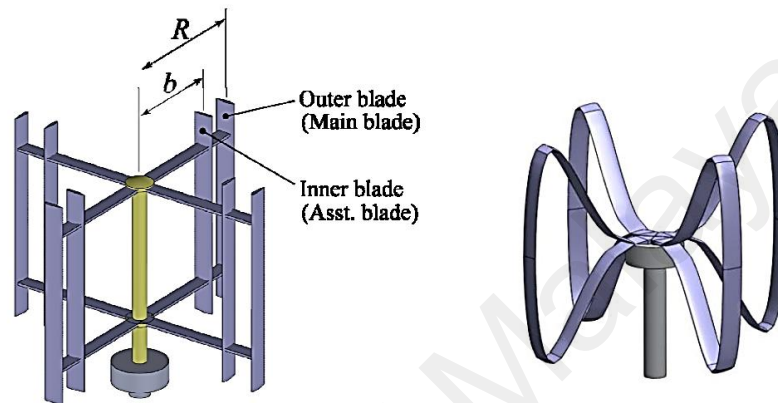


**Figure 2.10 Double-blade vertical axis wind turbine (left) and butterfly wind turbine (right) (Hara et al., 2014).**

#### 2.1.2.2 Wind turbine power-augmentation system

Besides focusing on improving the performance of wind turbines by the aerodynamic study of the turbine blades, increasing the on-coming wind speed before it interacts with the wind turbine also provides a significant result in power generation increment (W. T. Chong, Fazlizan, Omar, et al., 2012). Over decades, researchers have studied and reported different designs of ducted or funneled wind turbine systems. A lot of research had been done to improve the performance of horizontal axis wind turbine (HAWT). Frankovic and Vrsalovic (2001) proposed a nozzle augmented wind turbine that is able to produce 3.28 times more energy than a conventional HAWT. From the computational fluid dynamics (CFD) analysis by Hu and Cheng (2008) on their innovatory design of ducted wind turbine, the optimal shape for the interior of the duct appears to be an unconventional nozzle which widens the range of operating wind speeds by 60%. Grant, Johnstone, and Kelly (2008) proposed a roof mounted ducted wind turbine where the duct

linked a high pressure zone (stagnation) on the building with the zone of very low pressure for better power output compared to the bare roof-mounted wind turbine.

As for the VAWT, by adopting the guide vane row to a straight-bladed VAWT, the power coefficient was increased by 1.5 times compared to a wind turbine without guide vane (Takao et al., 2008). Altan and Atllgan (2010) proposed three configurations of curtain design to be integrated with the Savonius rotor in which the power coefficient of the rotor with one of the curtain designs was approximately 2 times higher than the rotor without curtain. However, the amount of performance improvement on each mentioned system depends on the size of the augmentation device to wind rotor ratio. Chong et al. proposed a novel omni-direction-guide-vane (ODGV) that surrounds a VAWT to further improve the VAWT performance (W. T. Chong, Fazlizan, et al., 2013; W. T. Chong, Pan, et al., 2013). This performance augmentation device can help to address the problem of low wind speed where the wind turbine can start producing energy at a lower wind speed in urban areas. The VAWT's self-starting behavior is improved where the cut-in speed was reduced with the integration of the ODGV. At 6 m/s, the power output at maximum torque was 3.48 times higher for the ODGV integrated VAWT compared to the bare VAWT.

### **2.1.2.3 Urban wind energy generation system**

Increase in urbanization and industrialization around the world in recent years has led to a consequent rise in energy demand (Ishugah, Li, Wang, & Kiplagat, 2014). The United Nations Centre for Human Settlements has stated that approximately 75% of generated power is consumed in cities (Dodman, 2009). Generation of power within the city could be of great importance to help reduce both the generation load and transmission infrastructure (Ishugah et al., 2014), and minimize transmission losses due to reduced distance from users (El-Khattam & Salama, 2004). Wind energy is one of the brightest

prospects for the urban energy generation system. However, the idea of bringing the wind energy system into urban areas is more challenging because of limited available space and the adaptation of the wind turbine to the existing infrastructure (Bohrer, Zhu, Jones, & Curtis, 2013). The scope for integrating wind energy in urban areas with good wind resources is extensive.

Many researchers have proposed the idea of wind energy systems that can possibly be installed in urban settings for local energy generation. These systems feature additional augmentation systems, either utilizing the building geometry or retrofitted onto the building or a combination of these. Three main categories of project can be identified: small wind and retrofitting, large-scale stand-alone turbines and building-integrated turbines (where the buildings are shaped with wind energy in mind) (Stankovic, Campbell, & Harries, 2009). However, siting wind turbines in urban areas require careful evaluation on wind availability and patterns due to factors such as the urban terrain roughness and the adjacent buildings that can cause wind shadows (Walker, 2011). At the moment, building integrated wind turbines are gaining more attention for urban on-site clean energy generation. The concept of on-site renewable energy generation is to extract energy from renewable sources close to the populated area where the energy is required (W. T. Chong, Naghavi, Poh, Mahlia, & Pan, 2011).

(a) *Stand-alone wind turbines*

Stand-alone wind energy systems are generally known to be utilized for remote or isolated applications (Alnasir & Kazerani, 2013; Malla & Bhende, 2014; Mesbahi et al., 2014). High energy demand and increase of awareness on the need of renewable energy makes the stand-alone small wind turbines an attractive alternative on generating energy in populated areas. Although wind speeds are generally lower in built-up areas, large-scale urban wind energy systems have been successfully implemented in some areas as

shown in Figure 2.11. However, it may encounter constraints such as limitation of land in urban areas and low wind speeds due to other existing high rise buildings. It may also give rise to public concern over safety, issues of noise and visual impact (W. T. Chong, Fazlizan, Poh, Pan, & Ping, 2012).



**Figure 2.11 Stand-alone wind turbine at McGlynn Elementary School, Boston (left) and Great Lakes Science Center, Cleveland.**

The stand-alone wind turbine can be a completely off-grid system where the energy generated is stored in a battery or a grid-connected system. For the grid-connected system, the generated energy can be supplied to the grid depending on local regulation. In some countries, the Feed-in Tariffs (FiT) is introduced to encourage the stand-alone renewable energy generation (Couture & Gagnon, 2010). It is a large foreseen potential market for wind turbines to be installed as stand-alone units in urban environment. Thus, to make it more reliable, technical solutions are being proposed every day to include the aspects of difficult operating conditions within the urban environment, challenges of low capacity factor, high battery costs, and finite capacity to store electricity that leads to wastage of the extra energy generated (Khan & Iqbal, 2005).

**(b) *Retrofitting wind turbines onto existing buildings***

Retrofitting wind turbines onto existing buildings is also addressed as building integrated/mounted wind turbine. For this case, the wind turbines are physically linked to

the building where the building is being used to tower the wind turbines in a desirable wind flow, e.g. on the roof top and building edge (Dutton, Halliday, & Blanch, 2005). Small-scale turbines have proven to be viable as building retrofit solution especially with micro-wind turbines of various types which are commercially available (Bahaj, Myers, & James, 2007). The government of UK provided attractive schemes which accounted for approximately 17% of state grant aid to encourage the application of micro-wind turbines in urban areas (Peacock, Jenkins, Ahadzi, Berry, & Turan, 2008). However, such small-scale wind turbines for building integration may not always be aesthetically pleasing and may also be hazardous due to turbine blade failures occurring. For retrofitting wind turbine into an existing building, there is an obvious difference in visual impact between the conventional wind turbine and the one that is specially designed for urban area as illustrated by Sharpe and Proven (2010).

One iconic application of this concept is the Boston Logan airport building ("Logan Airport Wind Turbines,") as shown in Figure 2.12. Twenty wind turbines are specifically installed to take advantage of the acceleration effect of wind as it passes over the building parapet. Each one kilowatt six-foot-tall turbine is affixed at a unique angle to capture the wind that gusts through Boston Harbor and climb the building's walls. The installation was estimated to generate about 60,000 kW h annually, which is equivalent to 3% of the building's energy needs ("Architectural Wind™ Installation at Boston's Logan International Airport," 2008). Another installation is at The Hilton Fort Lauderdale Beach Resort where six 4 kW wind turbines were installed on its rooftop ("UGE Turbines Powering a Hilton Resort," 2013). The turbines are expected to produce 10 % of the hotel's electricity and will power lighting in 372 guestrooms and public areas (Grozdanic, 2014).



**Figure 2.12 A fleet of micro wind turbines at Boston Logan International Airport (Yu, 2008).**

**(c) *Full integration of wind turbines together with architectural form***

The strategy of a fully integrated solution involves a well-defined construction plan and huge capital. A matrix of generic options for integrating wind turbines into the building was developed during the initial phase of the project (Campbell et al., 2001). It might seem fascinating from both the architectural and aerodynamics point of view. However, the issues of safety, noise, vibration and visual impact should not be underestimated. Examples of full integration of wind turbines together with architectural form is shown in Figure 2.13. The large-scale building integrated wind turbines have been demonstrated in some countries where these buildings have been established as iconic buildings (W. T. Chong, Fazlizan, Poh, et al., 2012). The first large-scale integration of wind turbines with a building is the Bahrain World Trade Centre. This 240 m high building harmoniously integrates building augmented design with three horizontal axis wind turbines of 29 m diameter (Smith & Killa, 2007). The Strata Tower in London was built to incorporate wind turbines within its structure. The three wind turbines at the top of the building are rated at 19 kW each and are anticipated to produce 8% of electricity

needed by the building . In Guangzhou, China, the Pearl River Tower was designed to harness the energy from solar and wind to sustain the building. The wind is funneled down from the vertical face of the tower toward a series of wind turbines for energy generation ("Pearl River Tower,").



**Figure 2.13 Top: Bahrain World Trade Centre ("Bahrain world trade centre (BWTC)," 2015); Bottom left: Strata Tower ; Bottom right: Pearl River Tower ("Pearl River Tower,").**



With further consideration of building and architectural integration, Müller et al. (2009) has proposed and architecturally demonstrated a wind energy converter with a cylindrical form to facilitate current building design. Grant et al. (2008) also reported and concluded that ducted wind turbines which are attached to the building roof have a significant potential for retrofitting into a building with small concern of visual impact. A concept and early development of the wind turbine called Crossflex utilized an existing Darrieus turbine concept, but it was applied in a novel form for building integration (Sharpe & Proven, 2010). The demonstrative study for the wind and solar power hybrid system from Ashikaga Institute of Technology in Japan shows that the generated power by photovoltaic cells is abundant in the summer season and that by wind powered generator increases from autumn to winter. An innovative design of power-augmentation-guide-vane (PAGV) to integrate several green elements (urban wind turbine, solar array for electricity and hot water, and rain water collector) is introduced by Tong et al. (2010). It is compact and can be built on the top (or between upper levels) of high rise buildings or structures in order to provide on-site green power to the building.

### **2.1.3 Wind energy generation system implementation in Malaysia**

Government initiative is essential in order to boost the utilization of renewable energy in a country. Thus, the government of Malaysia has also played the role in order to promote the implementation of renewable energy generation via policies, incentives, etc. Renewable energy was first introduced officially in the country's energy mix through the Fifth-Fuel Policy which was formulated under the Eighth Malaysia Plan (2001–2005) to reduce dependency on fossil fuel and to address the rising global concern on climate change (Hashim & Ho, 2011). However, despite rigorous initiatives, the renewable target set out under the Ninth Malaysia Plan (2006–2010) period was not achieved (Rahim & Hasanuzzaman, 2012). Under the Tenth Plan (2011–2015), several new initiatives anchored upon the Renewable Energy Policy and Action Plan is undertaken to achieve a

renewable energy target of 5.5% to Malaysia's total electricity generation mix in 2015 (2010).

However, the implementation of wind energy generation system has a slow start in Malaysia. Malaysia has a hot, humid tropical climate with two monsoon seasons, namely a southwest monsoon season and a northeast monsoon season; the latter (from November to February) is characterized by heavy rainfall and thunderstorms (Suhaila, Deni, Zin, & Jemain, 2010). Meanwhile wind speed is relatively low all through the year. A study on wind energy potential in nine coastal sites in Malaysia showed that the average wind speed for these sites is in the range of (1.8-2.9) m/s while the annual energy of the wind hitting a wind turbine with a 1 m<sup>2</sup> swept area is in the range of (15.4-25.2) kWh/m<sup>2</sup> (Sopian & Khatib, 2013). Akorede, Mohd Rashid, Sulaiman, Mohamed, and Ab Ghani (2013) presented that the maximum of monthly average wind speed in the country is only 5.4 m/s at 10 m altitude in Mersing with a capacity factor of 4.39%. It is far lower than the values obtained in Europe (Boccard, 2009). However, from the economic analysis, it is found that unlike what is widely touted, there is an actual potential of wind energy in Malaysia, manifested through the several economically viable wind turbine generating sites (Nor, Shaaban, & Rahman, 2014). In 2013, eleven sites had been identified by the government authority for wind resource mapping which will provide the essential information on wind energy generation potential. The data collection is expected to come into completion in mid-2015 ("SEDA Annual Report 2013," 2014). It is hopeful that the outcome of the wind resource mapping will boost the implementation of wind energy generation in Malaysia.

## **2.2 Exhaust air system**

### **2.2.1 Basics of cooling tower**

Most air-conditioning systems and industrial processes generate heat that must be removed and dissipated. Water is commonly used as a heat transfer medium to remove heat from refrigerant condensers or industrial process heat exchangers (ASHRAE, 2008). Cooling towers are commonly used to dissipate heat from water-cooled refrigeration, air-conditioning systems, and industrial process systems (Jeong, Chung, Bae, Kim, & Shin, 2005). Cooling towers are heat removal devices used to transfer waste heat to the atmosphere; large office buildings, hospitals and schools typically install one or more cooling towers for building ventilation systems.

A cooling tower cools water by a combination of heat and mass transfer. Water to be cooled is distributed in the tower by spray nozzles, splash bars, or film-type fill, which exposes a very large water surface area to atmospheric air. Atmospheric air is circulated by fans, convective currents, natural wind currents, or induction effect from sprays. A portion of the water absorbs heat to change from a liquid to a vapor at a constant pressure. This heat of vaporization at the atmospheric pressure is transferred from the water remaining in the liquid state into the airstream.

There are two basic types of cooling towers. The first type is the direct-contact or open cooling tower where the source of heat is transferred directly to the air by exposing water to the cooling atmosphere (Xu, Wang, & Ma, 2008). For the second of type, the closed circuit cooling tower that combines a heat exchanger and cooling tower into one relative compact device, the heat is dissipated by indirect contact between heated fluid and atmosphere (ASHRAE, 2008). Induced-draft towers, chimney towers and non-mechanical-draft towers are the types of direct-contact cooling towers while the types of indirect-contact cooling towers are closed-circuit cooling towers and coil shed towers

(both are mechanical-draft). The temperature of the water leaving the tower and the packing depth needed to achieve the desired leaving water temperature are of primary interest for design (ASHRAE, 2001).

## 2.2.2 Cooling tower behavior and factors affecting its performance

There are a lot of factors which affect a cooling tower's performance. However, those factors whose effects predominate and related to the air flow are identified and discussed in this section. This is because the study of exhaust air energy recovery turbine generator at the outlet of a cooling tower is only related to the cooling tower air flow.

### 2.2.2.1 Interference

Figure 2.14 depicts a phenomenon called "interference" that happens when a portion of the wind from the outlet of a cooling tower contaminates with the air intake of another cooling tower. A cooling tower is designed so that the fresh air is induced into the cooling tower and travels to the discharge outlet carrying the heat. The interference of wind that forces the discharge air to be induced back into the cooling tower will affect the cooling tower performance. Therefore, a proper design especially on the discharge height and the distance between the cooling towers is necessary to minimize the interference effect. The study on the local wind condition will be a baseline for the design.

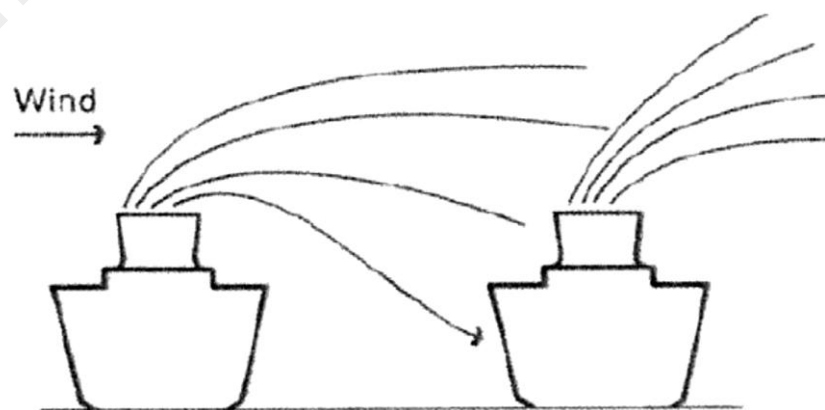
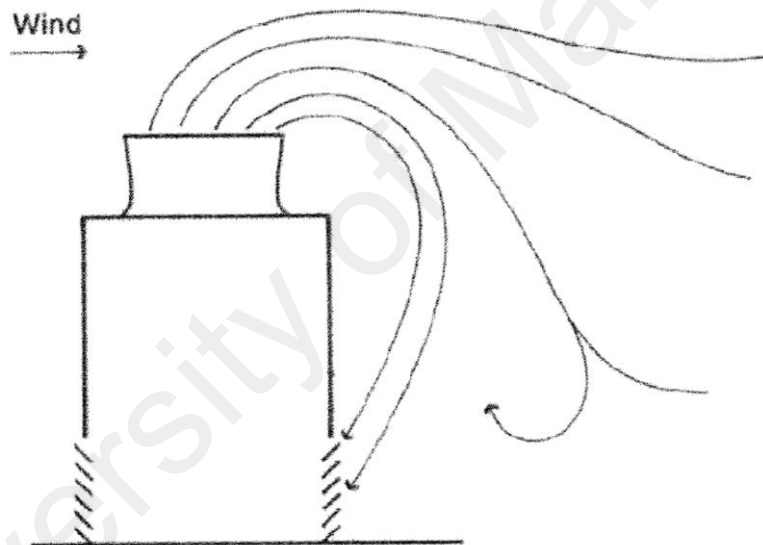


Figure 2.14 Interference phenomenon on cooling towers (Hensley, 2009).

### 2.2.2.2 Re-entrainment

Re-entrainment as shown in Figure 2.15 is another undesirable situation that affects the cooling tower performance. The basic principle of the cooling tower is to take the fresh ambient air into the compartment for the air to absorb and carry the heat out of the cooling tower through the outlet. If the discharged air is recirculated by contamination with the intake air, the performance of the cooling tower will be affected. The potential for recirculation is primarily related to wind force and direction. It tends to increase as the wind velocity increases. From a test, the limit of wind velocity is up to 4.5 m/s in order to acquire an accepted thermal performance of cooling towers (Hensley, 2009).



**Figure 2.15 Recirculation phenomenon on cooling towers (Hensley, 2009).**

## 2.3 Existing energy recovery system

Most of the available energy recovery systems are related to recover energy from waste heat from a process. Malmrup (2006) filed a patent for a system to recover waste heat from heat exchangers of a process. The system generates electricity from heat that is transferred from heat exchanger with a subsystem called turbocharger. The subsystem contains turbine, generator, compressor and main shaft (that connects turbine, generator and compressor together). Surplus electric energy or heat can be supplied to the process, according to above, in order to increase the overall efficiency. One of the most popular

energy recovery systems is the turbocharger in a car engine. In a normal engine the exhaust gas from the engine is wasted and dissipated to the environment. In an engine with turbocharger, the turbocharger uses the exhaust flow from the engine to spin a turbine, which in turn spins an air pump (Saidur et al., 2012). The power generated from the turbocharger system is used to boost the engine performance.

As for energy recovery system from wind resources, Berenda and Ferenci (1996) filed a patent on a system to capture and convert to electrical energy by using the horizontal axis wind turbine that is positioned in front of an exhaust fan. Referring to the patent document, the exhaust air from a system is blown horizontally while the HAWTs are arranged in line perpendicular to the exhaust wind flow. Another patent is by (Cohen, 2002) on an invention to generate electricity from an air conditioning exhaust. A shroud is mounted as an extension to the exhaust air outlet to enclose the discharged air. Wind from the outlet will turn the turbine that is placed in the shroud. The system is likely to cause an obvious blockage effect to the outlet and the exhaust heat might accumulate at the shroud. This will negatively affect the air conditioning exhaust performance.

## CHAPTER 3: DESIGN DESCRIPTION AND METHODOLOGY

### 3.1 Design description of the exhaust air energy recovery turbine generator

#### 3.1.1 General arrangement and working principles of the system

The exhaust air energy recovery wind turbine generator is a novel idea on generating green energy by harnessing unnatural wind resources using a micro-wind generation system. The unnatural wind resources can be from cooling towers, air ventilation systems, humidification plants or any system that produce strong and consistent winds. However, the integration of the exhaust air energy recovery wind turbine generator is not identical for all the unnatural wind resources. This is due to different systems having different characteristics and geometry. A specific configuration has to be designed in order to recover the maximum amount of energy from the exhaust air system without any significant negative effect to the original system. In this study, the exhaust air energy recovery wind turbine generator is specifically designed for integration with a cooling tower. The design was patented in 2011 with a patent number PCT/MY2012/000274 (Wen Tong Chong, Kong, & Fazlizan, 2011). The general arrangement of this innovative system is illustrated in Figure 3.1.

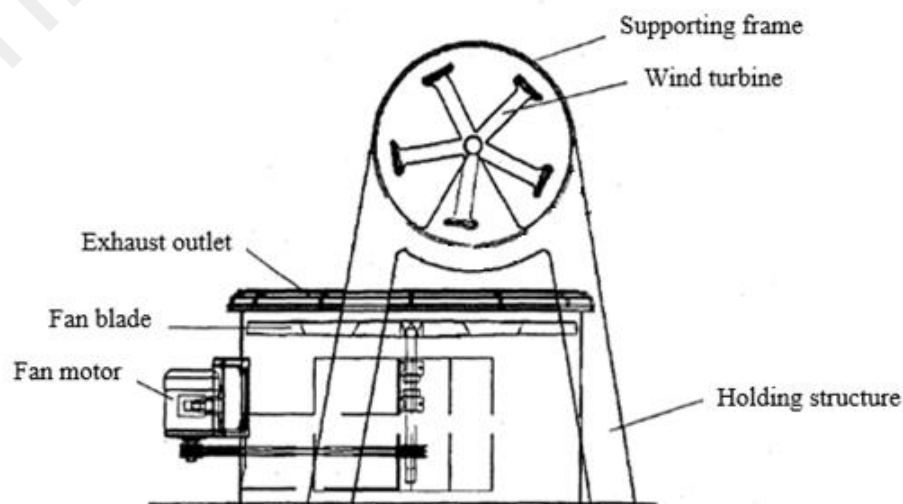


**Figure 3.1 General arrangement of the exhaust air energy recovery wind turbine generator.**

A VAWT in cross-wind orientation is mounted above a cooling tower outlet by a supporting structure to extract the wind energy. The supporting structure is the main structure to hold the VAWT and enclosure. It can be installed above any ventilation outlet either in a horizontal or vertical position depending on the direction of the approaching wind. A predefined location for positioning the VAWT facing the cooling tower's outlet is essential to ensure zero or minimum negative effect on the performance of the original system. The radial position (on elevated plane above the exhaust air outlet) of the VAWT is set to match with the exhaust air speed profile. A portion of the VAWT blades rotating path is located slightly out of the discharged air stream (slightly out of the cooling tower exhaust outlet) so that the highest wind speed can interact with the wind turbine blades at the positive torque areas and hence maximizes the VAWT performance. The selection of wind turbine type and size is also critical to ensure its operation would not cause the blockage effect to the original exhaust air system. It can be installed horizontally where it is supported at both ends of the power transmission shaft with the generator on one side in order to harness the outlet air that is blowing from the bottom. It is also able to be mounted in a vertical direction with the generator placed on the floor.

In order to maximize the energy recovery from the exhaust air, the diffuser-plates are designed to be integrated with the system as a power augmentation device. It is an expanding duct inclined outwardly at an optimum angle relative to their vertical axis at both sides of the VAWT. Air flow characteristic improvement can be obtained and more output power can be acquired as compared to a bare wind turbine. In addition, the concern on the safety issue is minimized by integrating the wind turbine with an enclosure. The possibility of danger caused by blade failure can be reduced by using a layer of mesh to cover the enclosure. It blocks flying creatures like birds from striking the turbine. Since the VAWT is installed within the diffuser-plates, the noise generated is lower and no negative visual impact is produced.



### **3.1.2 Benefits of the energy recovery wind turbine generator**

This innovative system is aimed at generating on-site clean energy by converting wasted wind energy from a cooling tower to a useful form of energy. The energy generated is predictable and continuous because the exhaust wind is readily available whenever the cooling tower is switched on. In other words, exhaust air consists of wind characteristic that is predictable and consistent. Thus, statistical analysis of wind characteristic over a period of time is not required. In addition, the turbine is expected to spin at a constant rotational speed and therefore, over speed control is not necessary because only minimum rotational speed fluctuation is experienced. For that reason, the energy generation over the lifespan of the turbine is expected to be higher.

The efficiency of the wind turbine is greatly improved when it is integrated with a diffuser-plates. The diffuser-plate is an expanding duct that cause a pressure drop that effectively improves the air flow. In addition, more air will be discharged and will interact with the wind turbine due to the suction effect resulting from the low pressure zone around the VAWT. This advantage promotes better self-starting behavior and the turbine is able to rotate close to its rated speed. Besides, hazards during maintenance and installation can be reduced to a great extent by integrating the VAWT with diffuser-plates. The diffuser-plates (with meshes) can work as a safety cover because the turbine is enclosed within it.

This energy recovery system has a high market potential due to abundant usage of exhaust air systems. It is a green energy invention which investigates visionary and technology-driven solution that is able to supply a portion of the energy demand of a metropolis. Figure 3.2 shows an artist's impression of the energy recovery wind turbine generator mounted above an exhaust air system.

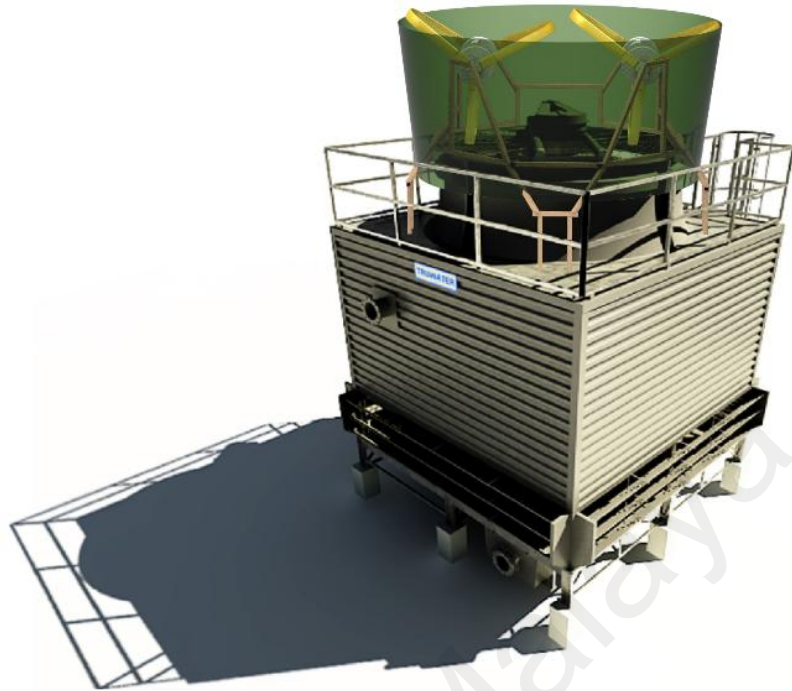


**Figure 3.2 Artist's impression of the energy recovery wind turbine generator mounted above an exhaust air system.**

### **3.1.3 Variations of exhaust air energy recovery wind turbine**

The exhaust air energy recovery turbine generator can be installed in a number of variations. For a big size of exhaust air outlet, more than one turbine can be installed to utilize the discharged air. However, it depends on the space availability, structural strength and most importantly, it should not negatively affect the performance of the original exhaust air system. As an example, Figure 3.3 (a) shows a single rotor of 1.2 m diameter VAWT at the outlet of a cooling tower with 2 m outlet diameter. Figure 3.3 (b) illustrates a cooling tower with a discharge outlet diameter of 2.6 m that can accommodate an exhaust air energy recovery turbine generator that consists of two VAWTs of 1.2 m diameter. For a bigger size of cooling tower, there can be more VAWTs installed.

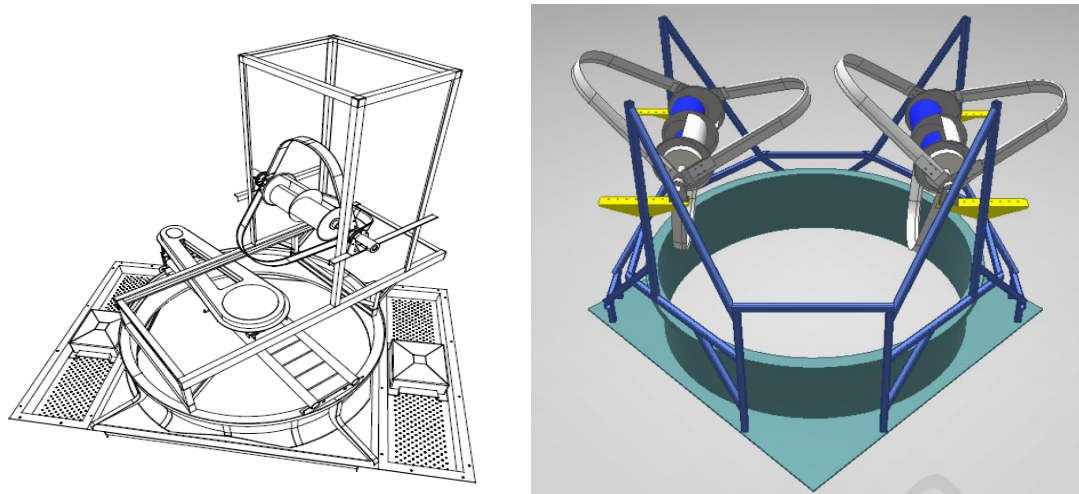


**Figure 3.3 (a) Single rotor exhaust air energy recovery turbine generator; (b) Twin-rotor exhaust air energy recovery turbine generator**

### **3.2 Cooling tower model and exhaust air energy recovery turbine generator test rig fabrication**

#### **3.2.1 Cooling tower model fabrication**

A scaled-down model of a cooling tower is constructed for the laboratory test. The model consists of an axial flow fan, the body and an outlet duct which is similar to the common counter-flow cooling tower. The cooling tower model is mainly built from fiber reinforced material (FRP) which is similar to an actual cooling tower. The FRP square channels with dimensions of 50 mm x 50 mm and thickness of 5 mm are used as the main internal structure of the cooling tower model. Figure 3.4 shows the FRP square channel while Figure 3.5 shows several views of the internal structure of the model.

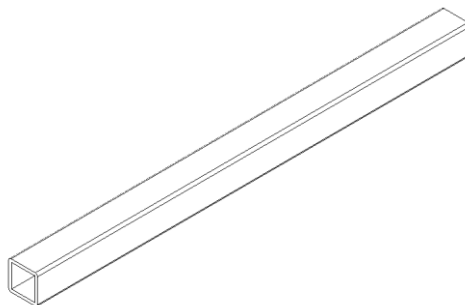


**Figure 3.4 FRP square channel.**

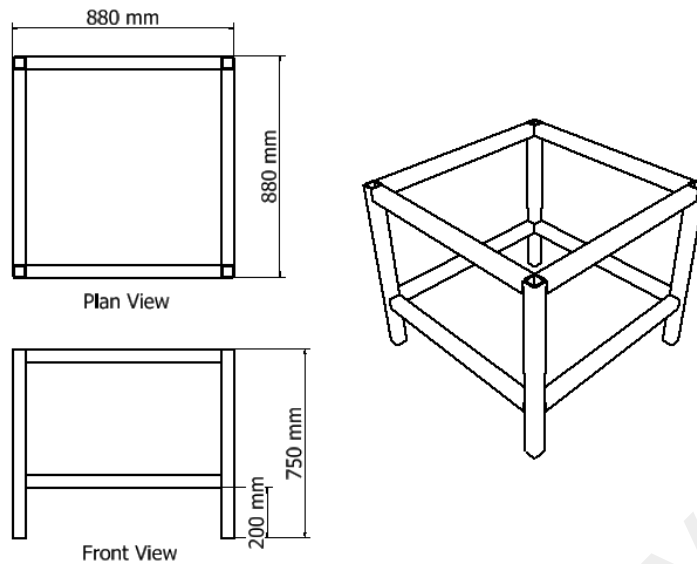


**Figure 3.5 Internal structure of the cooling tower model.**

The side of the cooling tower model is attached with an array of corrugated FRP plates, the top part is attached with FRP plane and the FRP L channel is attached at every corner of the cooling tower. These materials are depicted in Figure 3.6. The outlet duct is also fabricated using the FRP material using mold as illustrated in Figure 3.7. The assembly and exploded view of the cooling tower box is shown in Figure 3.8. For the model, there are openings with 200 mm distance to the floor at all sides for the air inlet. The air is discharged through the cylindrical outlet duct with a diameter of 730 mm.

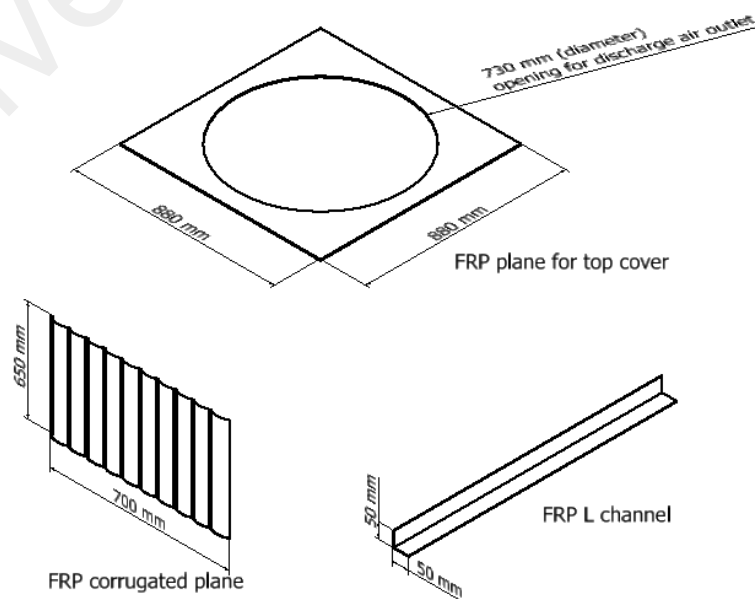


**Figure 3.6 FRP plane for top cover, FRP corrugated plane for side cover and L channel for corner.**

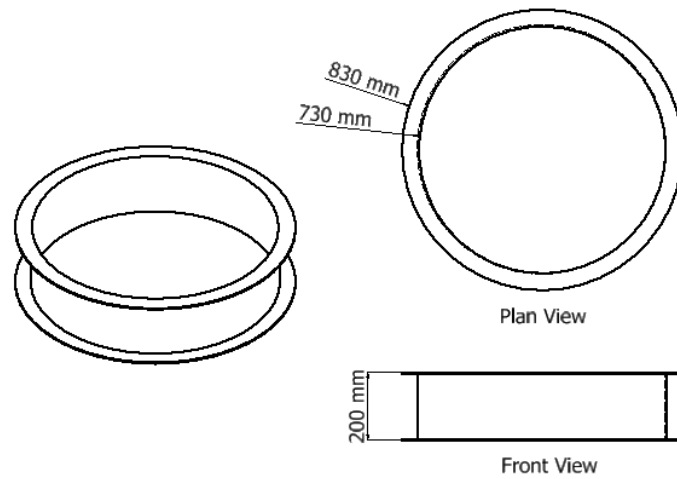


**Figure 3.7 Discharged air outlet duct.**

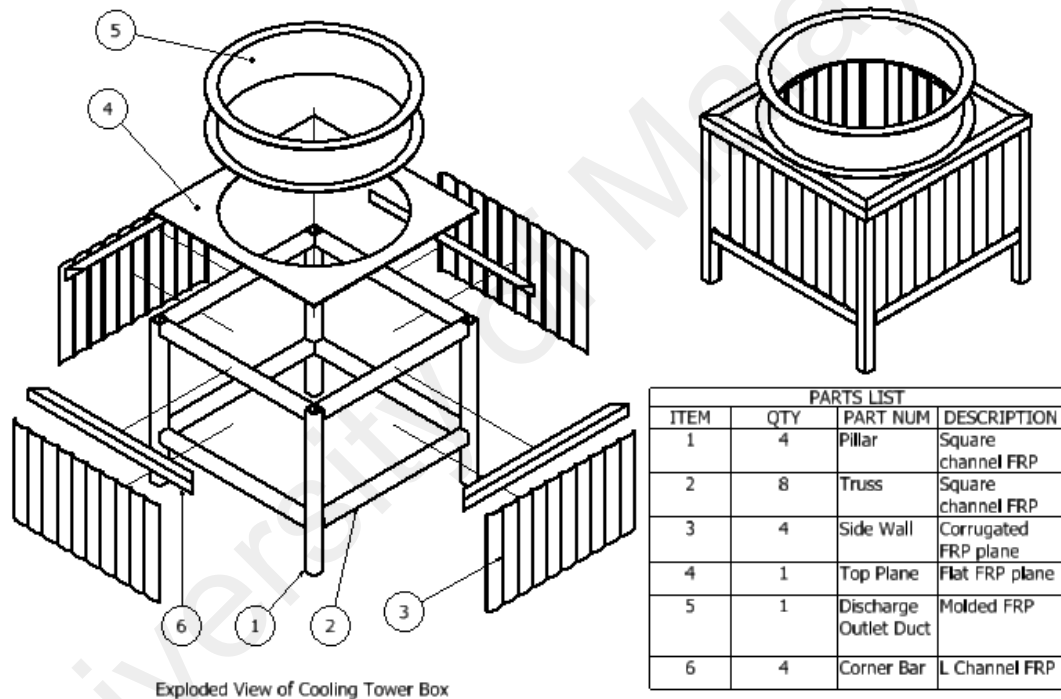


**Figure 3.8 Assembly and exploded view of the cooling tower box**

The fan mechanism is mounted inside the box of the cooling tower model. It is a 5-bladed fan powered by a 0.75 kW three-phase asynchronous motor. The fan rotational speed can be controlled with a fan driver with the highest fan speed at 910 rpm. The fan system needs a strong supporting structure in order to withstand the force generated from the fan. Thus, it is fabricated with steel material with a thickness of 5 mm. Figure 3.9 shows the assembly of the fan mechanism while Figure 3.10 illustrates the assembly of the fan mechanism inside the cooling tower box.

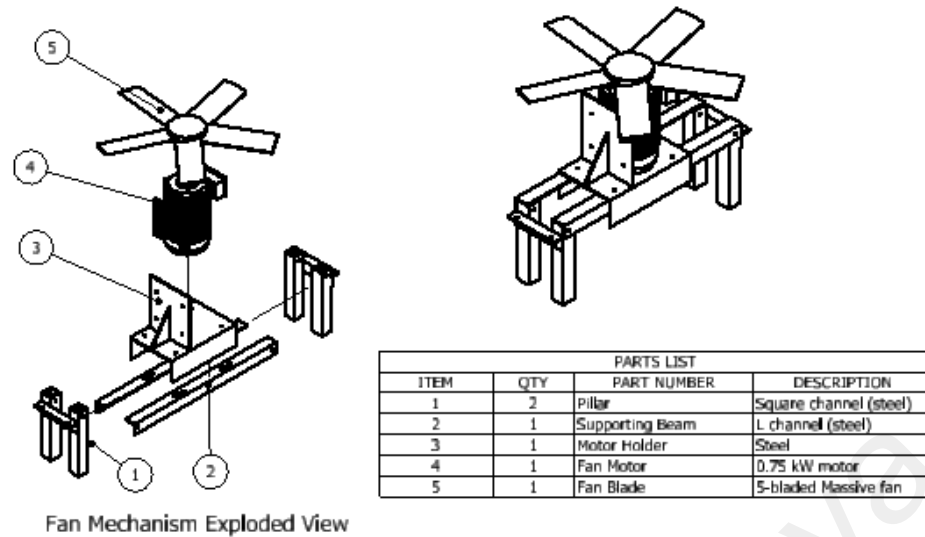


**Figure 3.9 Fan mechanism assembly**

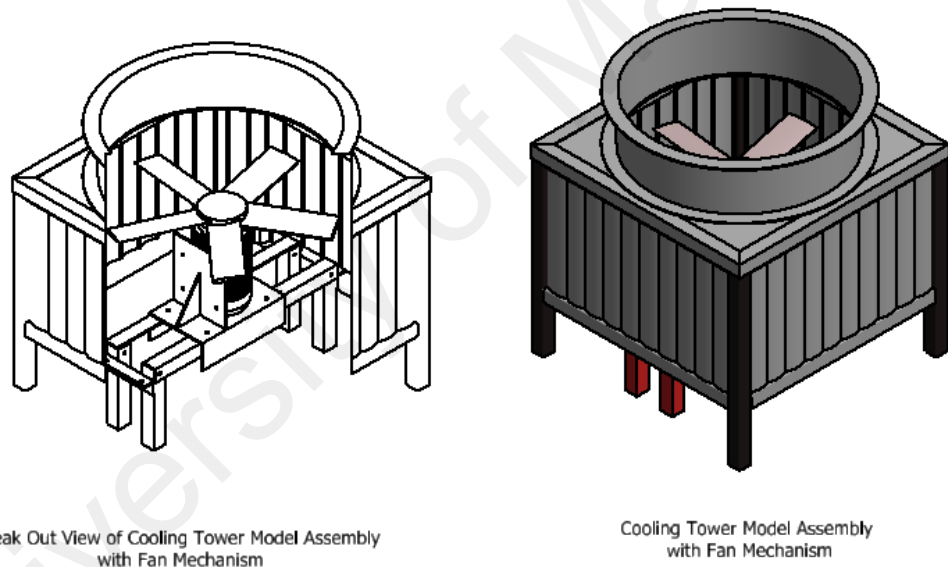


**Figure 3.10 Break out view and isometric view of the cooling tower model assembly with fan mechanism.**

### 3.2.2 Exhaust air energy recovery turbine generator test rig fabrication

The wind turbine that is used for this fabrication is a commercially available 10 W H-rotor VAWT which was purchased from Shanghai Aeolus Wind Power Technology Co. Ltd. ("P10: 10W Vertical Axis Wind Turbine,"). The turbine is composed of five airfoils with a rotor diameter of 30 cm, chord length of 4.5 cm and height of 30 cm. For the case of a cooling tower with turbine, a supporting frame for the wind turbine and dynamometer is constructed. The whole supporting frame is fabricated using the extruded aluminium

modular profile and accessories. This material is chosen because of its modularity and assembly flexibility which is suitable for changing wind turbine and dynamometer positions. The extruded aluminium for this fabrication is depicted in Figure 3.11. Figure 3.12 illustrates the assembled aluminium profile as the supporting structure for the wind turbine and dynamometer. The wind turbine and dynamometer position can be easily adjusted on this supporting frame.

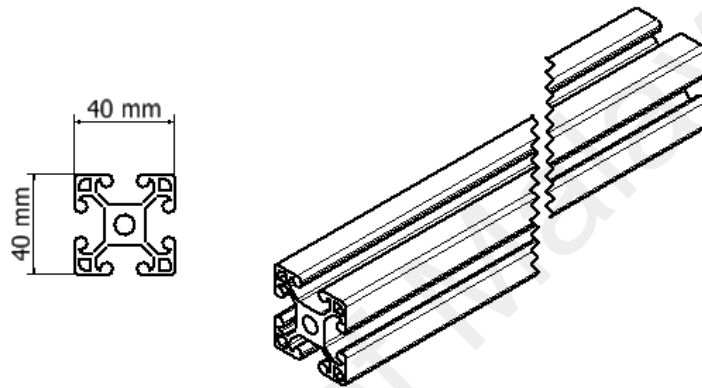


**Figure 3.11 Extruded aluminum modular profile.**

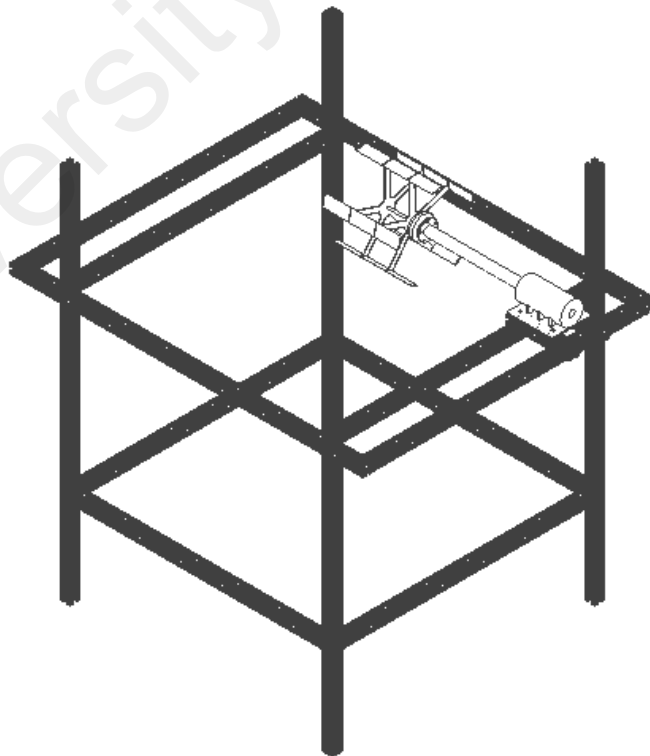


**Figure 3.12 Assembled aluminium profile as the supporting structure for wind turbine and dynamometer.**

### 3.3 Experimental methodology

#### 3.3.1 Cooling tower model performance evaluation

The bare cooling tower model performance is evaluated by the air flow rate and the power consumption by the fan motor. Air flow rate is obtained from the multiplication of average air velocity and area at the inlet of the model. The average inlet air velocity is calculated by averaging measured air velocities from all sides of the model. These measurements are conducted using a vane-type anemometer. Power consumption by the fan motor is measured using a power analyzer (Fluke 435 Series II). A suitable method for measuring air velocity of a circular duct is by dividing the area into several concentric parts of equal area and velocities are taken at every quarter of the circle (Herrman, 1962). In order to determine the points for the measurement, the area of discharge outlet is divided into five equal concentric areas and the radius to the center of each area is obtained. Each of these concentric areas is named as a band where the bands are numbered as shown in Figure 3.13 and the measuring points for each band is tabulated in Table 3.1. These discharge velocities are plotted onto a graph to determine the discharge air distribution profile. The overall outlet area for this model is  $0.42 \text{ m}^2$  and the area of each band is  $0.084 \text{ m}^2$ . The performance of the bare cooling tower model will be the benchmark for the entire experiment. For this experiment, two sets of fan speed are used, i.e. 910 rpm and 708 rpm.

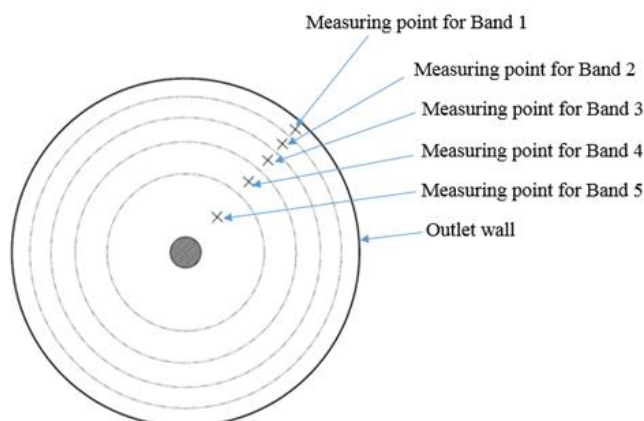


**Figure 3.13 Measuring points for each band at the discharge outlet.**



**Table 3.1 Wind outlet velocity measuring points.**

Band	Inner radius (mm)	Outer radius (mm)	Measuring point (mm) (distance to the center of outlet)
1	0	163	82
2	163	231	197
3	231	283	257
4	283	326	305
5	326	365	346

### 3.3.2 Cooling tower model with exhaust air energy recovery turbine generator

Figure 3.14 shows the cooling tower model with the test rig of the exhaust air energy recovery turbine generator. To determine the optimum wind turbine position at the outlet of the cooling tower, several positions are set and the wind turbine performance as well as the cooling tower model airflow performance are collected at all positions. Taking the center of the turbine as a reference, the turbine position is vertically varied from 200 mm to 400 mm range to the cooling tower discharge outlet. For horizontal position variation, the center of the discharge outlet (also the center of the fan) is taken as the reference. The turbine is moved in the range from -250 mm to 250 mm with the distance of every position as 50 mm. Figure 3.15 illustrates the wind turbine position setting.



**Figure 3.14 Test rig, consisting of cooling tower model, wind turbine, dynamometer and supporting frame.**

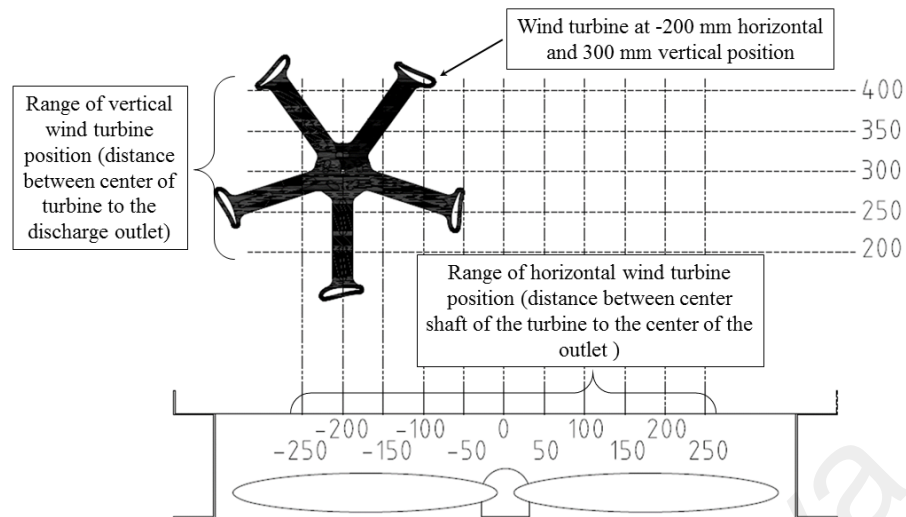


**Figure 3.15 Horizontal and vertical range for turbine positioning experiment.**

The wind turbine performance is logged using the dynamometer system. The parameters that are recorded are the rotational speed, torque and power. All the parameters taken from the bare cooling tower model are also recorded for the cooling tower with wind turbine at the outlet. This is to compare the cooling tower performance between all configurations. The outlet air velocity measurement is to determine the outlet air flow rate and wind velocity profile.

### **3.4 Double multiple stream tube analysis for the exhaust air energy recovery turbine generator**

The experiments as explained in Section 3.3 use a commercial 10 W straight-bladed VAWT. Based on the comparison in the airfoil databases, the airfoil type is assumed as the Martin Hepperle MH114 (MH114) airfoil with maximum thickness of 13% (Hepperle, 2008; "UIUC Airfoil Coordinate Database,"). The airfoil cross section is illustrated in Figure 3.16. Semi-empirical approach is applied in this theoretical study where the parameter of wind velocities and rotor rotational speeds is taken from the experiment. In order to proceed for the computation of the performance of the turbine, the lift and drag coefficients of the airfoil section are needed. The data is obtained from

the online airfoil database (Airfoil Investigation Database) at Reynolds number of 25000 ("AID Airfoil Investigation Database, "). The data is presented in Appendix B1.

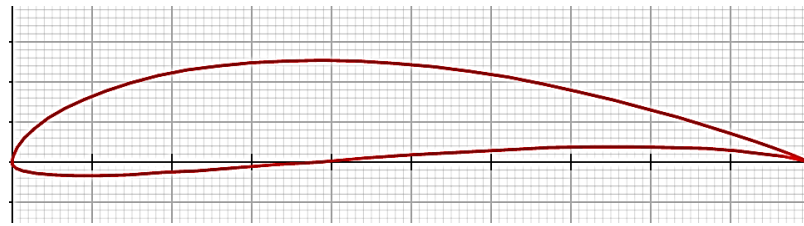


**Figure 3.16 Cross section of MH114 air foil.**

An airfoil of a vertical axis wind turbine is subjected to a continually changing angle of attack cycling from positive to negative back to positive as it revolves about the vertical axis. At low tip speed ratios, it is possible to be at an angle of attack approaching  $\pm 180^\circ$  throughout the revolution (Sheldahl & Klimas, 1981). However, the available data is only limited to a small range of angle of attack since most of the airfoil study is focused on aircraft wing application. To get a complete range of angle of attack ( $\pm 180^\circ$ ), an extrapolation model developed by Montgomerie (2004) is applied. It is essential due to the fact that the aerodynamic angle of attack of the blades varies continually during the rotation. Moreover, one blade moves on the downwind side of the other blade in the range of  $180^\circ$  to  $360^\circ$  of rotational angle so that the wind speed in this area is already reduced due to the energy extracted by the upwind blades (D'Ambrosio & Medaglia, 2010). The extrapolated airfoil aerodynamic data is tabulated in Appendix B2.

### **3.4.1 Stream tube**

For the analysis in the DMST theory, the swept volume of the turbine is divided into 18 stream tubes for each of upstream and downstream. Illustration of the stream tube for the calculation is shown in Figure 3.17. Each stream tube in the DMST model intersects the airfoil path twice; once on the upwind pass, and again on the downwind pass. At these intersections, the turbine is replaced by a tandem pair of actuator discs, upon which the flow may exert force. The DMST model simultaneously solves two equations for the

stream-wise force at the actuator disk; one obtained by conservation of momentum and other based on the aerodynamic coefficients of the airfoil (lift and drag) and the local wind velocity. These equations are solved twice; for the upwind and for the downwind part of the rotor. The equations are explained in Chapter 2. With the size of the stream tubes at  $10^\circ$ , there will be 36 values of the instantaneous parameters. Figure 3.17 also illustrates the rotation direction of the turbine and  $0^\circ$  azimuth angle reference to be used in the DMST calculation. Azimuth angle is represented by  $\theta$  while  $\Delta\theta$  represents the angular size of the stream tube.

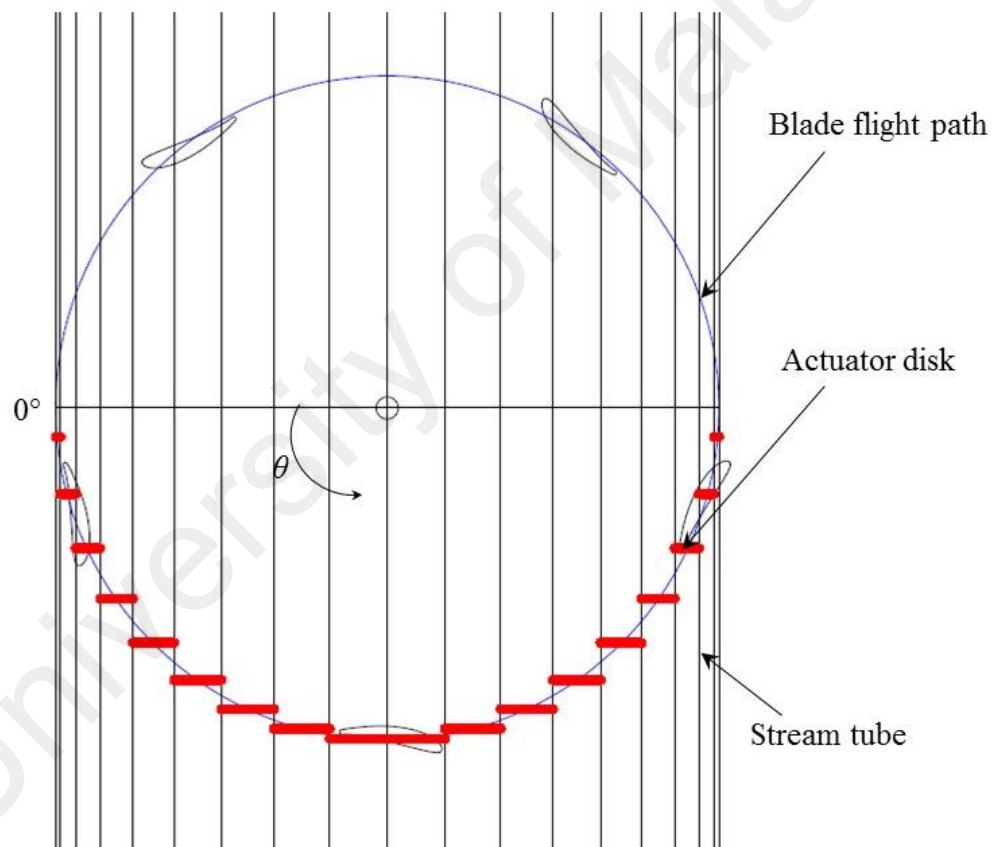


**Figure 3.17 Double multiple stream tube model with 18 stream tubes divided by uniform  $\Delta\theta$  ( $10^\circ$ )**

### 3.4.2 Assumptions

Wind velocity profiles that are recorded as mentioned in Section 3.3 are taken as the wind velocity for each stream tube. The determination is done by matching the stream

tube positions at the outlet of the cooling tower to the wind profile. The wind velocity values are taken based on the trend line generated from wind velocity profile experiment (as mentioned in section 3.3.1) where the midline of the stream tube crosses the velocity trend line. There will be one wind velocity value for each of the stream tube. The stream and induced velocity is assumed as perpendicular to the turbine swept plane and the effect of gravity is neglected.

For the computations, the axial induction factor,  $a$  is assumed as  $1/3$  at all conditions. It is the optimum value of axial induction factor where in this situation, the flow is decelerated to  $2/3$  and  $1/3$  of its original free-stream velocity at the rotor-disc and in the far wake respectively (Geurts, Simao Ferreira, & Van Bussel, 2010). The turbine is divided into 18 stream tubes (each of upwind and downwind) with the size of each tube at  $10^\circ$ .

### **3.4.3 Calculation procedure**

The parameters needed for the calculation in the DMST theory are the wind velocity, turbine rotational speed, turbine and airfoil dimensions, azimuth angle, and the angular size of the stream tube. With respect to the airfoil type and Reynolds number, the airfoil aerodynamic constants are acquired from the reliable database. The aerodynamic constants are lift and drag coefficient at particular angle of attack. The calculations are performed in the Excel spreadsheet. For the 18 stream tubes, 36 sets of calculations to get the instantaneous values for the stream tubes (18 for each of upstream and downstream). The calculation flow for each stream tube is illustrated in Figure 3.18.

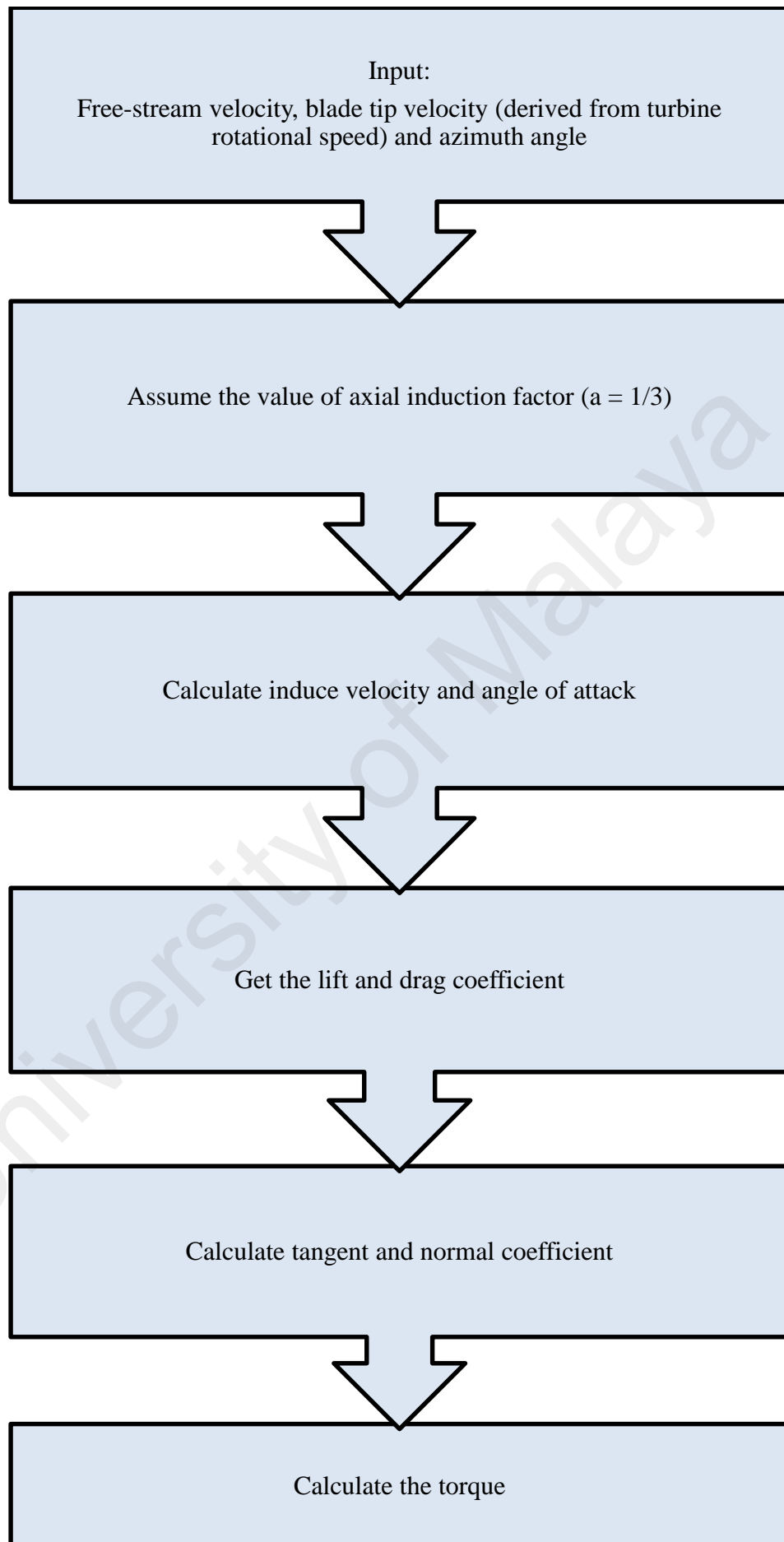


**Figure 3.18** Calculation flow chart of the DMST theory.

Since there is a non-uniform wind profile, the blade of the wind turbine also experiences different wind velocities along its length. This is because the wind profile is changing radially about the center of the exhaust air outlet as illustrated in Figure 3.19. Thus, the blade is divided into 5 sections of equal length for the analysis as shown in Figure 3.20. Each section experience different wind velocities based on exhaust air outlet air flow distribution.

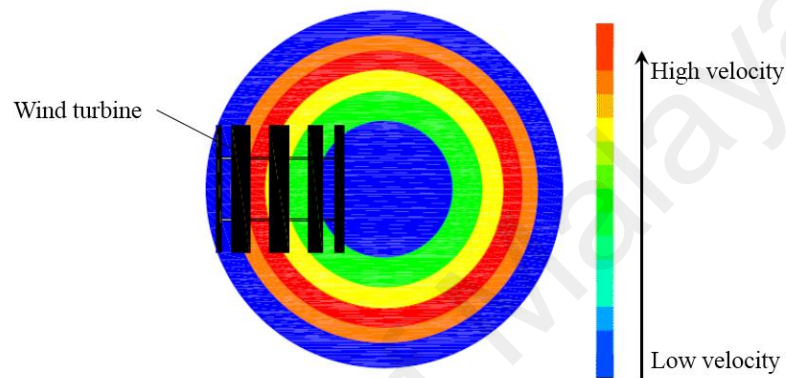


**Figure 3.19 Velocity contour of non-uniform wind (not to scale) from exhaust air outlet and wind turbine position.**

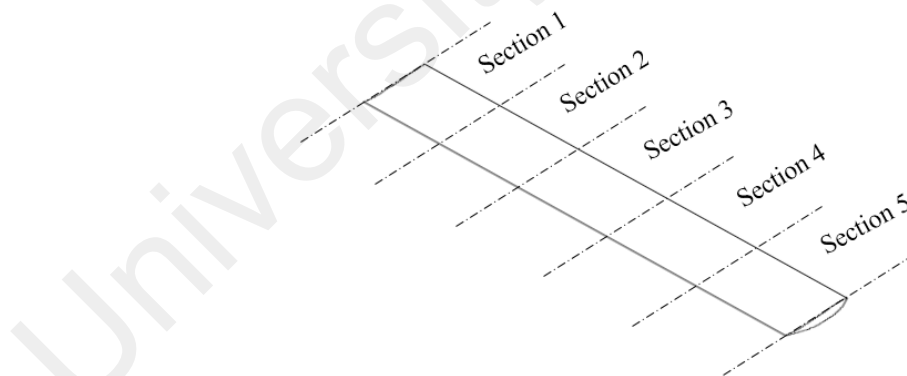


**Figure 3.20 The wind turbine blade is equally divided to 5 sections for analysis.**

The average torque of each section for one complete revolution and  $N$  number of blades is calculated independently by using equation 2.35. Then, the total average torque generated by the turbine is calculated by the summation of average torque from all sections.

### 3.5 Dual rotor exhaust air energy recovery turbine generator with and without the integration of diffuser-plates

#### 3.5.1 Dual rotor exhaust air energy recovery setup

As mentioned in the design description section, the exhaust energy recovery turbine generator can be more than one turbine depending on the discharge outlet and the turbine size. For the fabricated cooling tower model, the outlet area is possible to accommodate 2 units of wind turbine to become a dual rotor exhaust air energy recovery turbine generator. The best wind turbine horizontal positions, i.e. 250 mm and -250 mm from the experiments as mentioned in section 3.2 is taken as the configuration of each turbine. The position is symmetrical which makes the VAWTs rotate in opposite directions (counter rotating) as shown in Figure 3.21. Figure 3.22 shows the assembly of the cooling tower model with dual rotor exhaust air energy recovery turbine generator. The experiment was conducted by varying the vertical VAWT position in the range of from 200 mm to 400 mm. Similar to the previous experiments the VAWT performance is done by the rotational speed while the cooling tower performance assessment is by referring to the fan motor power consumption and intake air flow rate.

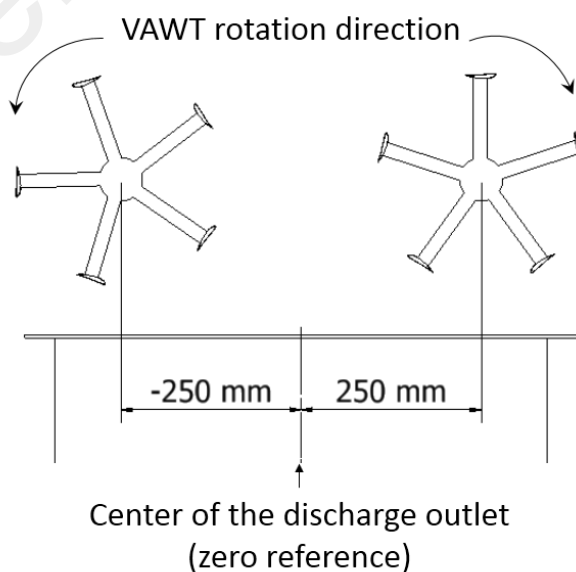


**Figure 3.21 VAWT position at the cooling tower outlet.**



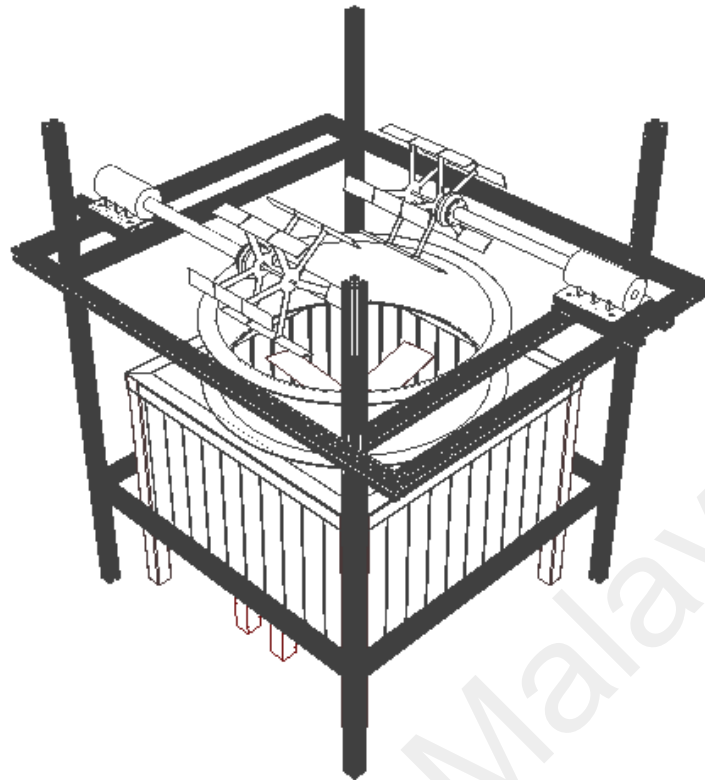


**Figure 3.22 Assembly of cooling tower model with dual rotor exhaust air energy recovery turbine generator.**

### **3.5.2 Integration of diffuser-plates onto the exhaust air energy recovery turbine generator**

A simple diffuser is introduced to be integrated with the exhaust air energy recovery turbine generator. It is a combination of two flat plates to enclose the wind turbine at both ends of the turbine blades. The diffuser-plates are mounted on the outlet of the circular duct with a slant angle of  $7^\circ$  relative to its vertical axis. This slant angle is set to be the preferable angle for diffuser-plates according to the experimental investigation carried out by Abe et al. (2005). This slant angle has also been used in the formulation by Monroe (2000) and Kwon (1994). Figure 3.23 illustrates the assembly of the diffuser, energy recovery turbine generator and the cooling tower.

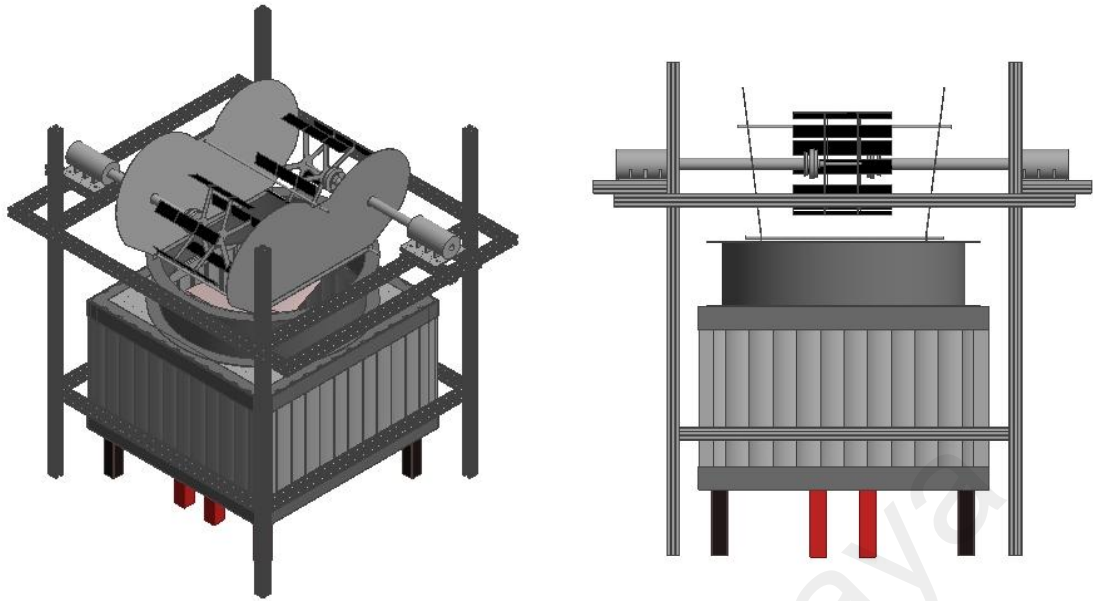


**Figure 3.23 Isometric view and side view of the assembly of the diffuser, energy recovery turbine generator and the cooling tower model.**

Based on the obtained results in the VAWT positioning experiment, the best horizontal position for the wind turbine placement is when the center of the wind turbine is at a distance of 250 mm to the center of the fan. Thus, the experiment for exhaust air energy recovery integrated with diffuser is conducted at this horizontal position and by varying the vertical position. The vertical VAWT positions are varied in the range between 200 mm to 400 mm (based on the distance between the center of the VAWT to the outlet plane). It is illustrated in Figure 3.24.

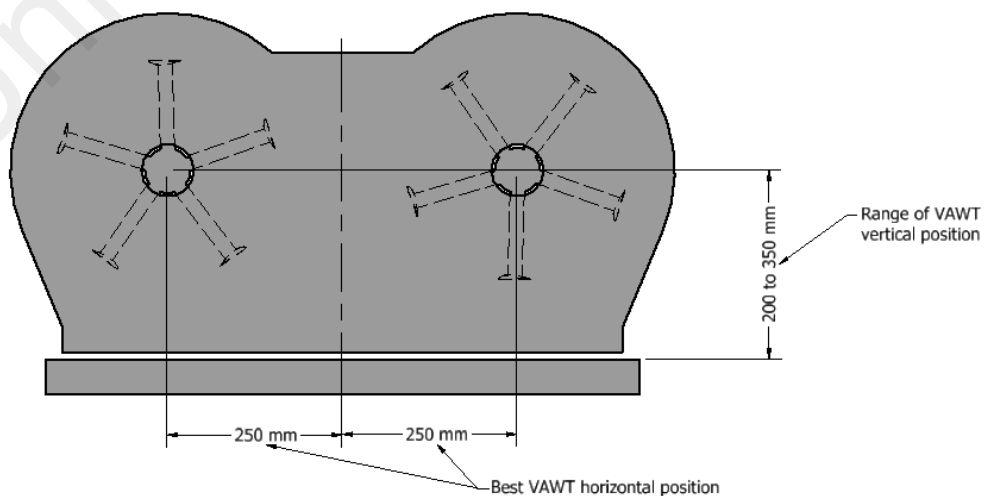


**Figure 3.24 Position of dual rotor VAWT for the diffuser-augmented exhaust air energy recovery turbine generator.**

The procedure of the previous experiment is repeated but this time with the presence of the diffuser. In term of cooling tower performance, the comparison is made according to the fan power consumption and intake air flow rate. The VAWT performance is compared in its rotational speed and power generation.

University of Malaya

## CHAPTER 4: RESULTS AND DISCUSSION

### 4.1 Performance of bare cooling tower

The speed of the fan that is used for this experiment can be regulated adjustable speed drive controller. The speed drive controller allows the fan to be adjusted at 10 variations and the maximum rotational speed is 910 rpm. From the preliminary study, at 910 rpm, the highest wind velocity discharged from the cooling tower model is at about 9 m/s. This wind velocity is acceptable where for an induced draft cooling tower, the normal discharged air velocity is about 9 m/s in order to sufficiently reject the heat to the environment (Hensley, 2009). To observe the variation in different speed of fan, the third highest fan rotational speed, i.e. 708 rpm is selected. The second highest rotational speed is not selected because based on the preliminary study, the difference wind velocity is not so much. Thus, the fan rotational speeds of 910 rpm and 708 rpm are selected for the entire experiment.

The performance of the bare cooling tower is evaluated to compare its performance with and without the integration of the exhaust air energy recovery turbine generator. The parameters are the flow rate and the fan motor power consumption as tabulated in Table 4.1. These parameters will be the bench mark for the experiments.

**Table 4.1 Performance of bare cooling tower.**

Fan speed (rpm)	Average intake air flow rate (m <sup>3</sup> /s)	Average fan motor power consumption (Watt)
910	3.05	672.78
708	2.60	334.88

#### 4.1.1 Blockage effect assessment

To assess the blockage effect to the cooling tower's flow rate and fan motor power consumption, a simple experiment is conducted where a variety of flat planes is placed at the outlet of the cooling tower as the blockage. The sizes of the blockage are set to cover 25%, 50% and 100% of the outlet area. The blockage effect on the cooling tower model is indicated by the decrease of the intake of air flow rate or the increase of the fan motor power consumption or both. The results are depicted in Figure 4.1 and Figure 4.2.

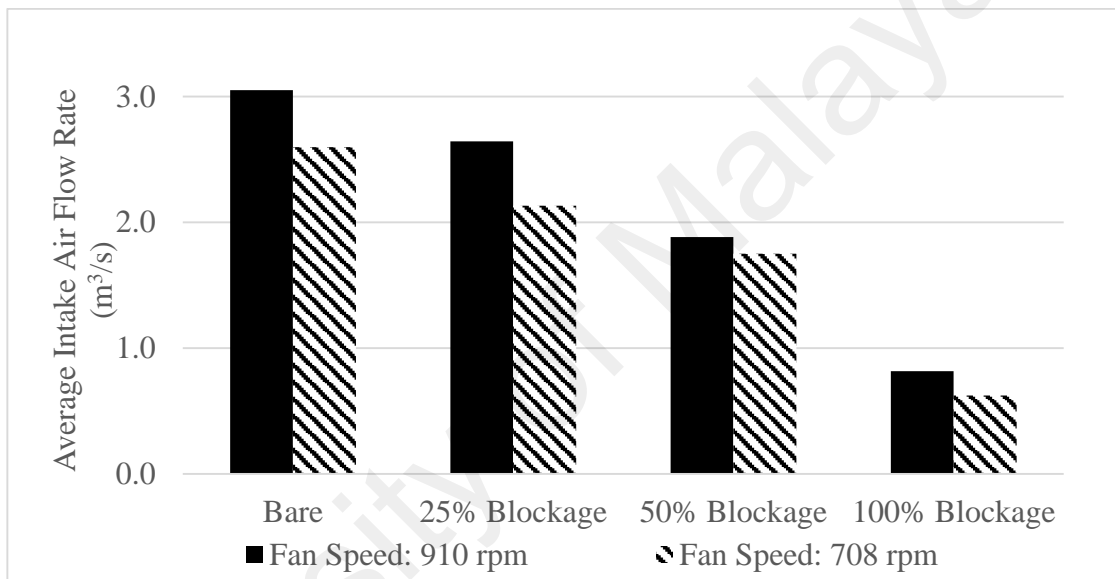


**Figure 4.1** The effect of blockage to the cooling tower air flow rate.

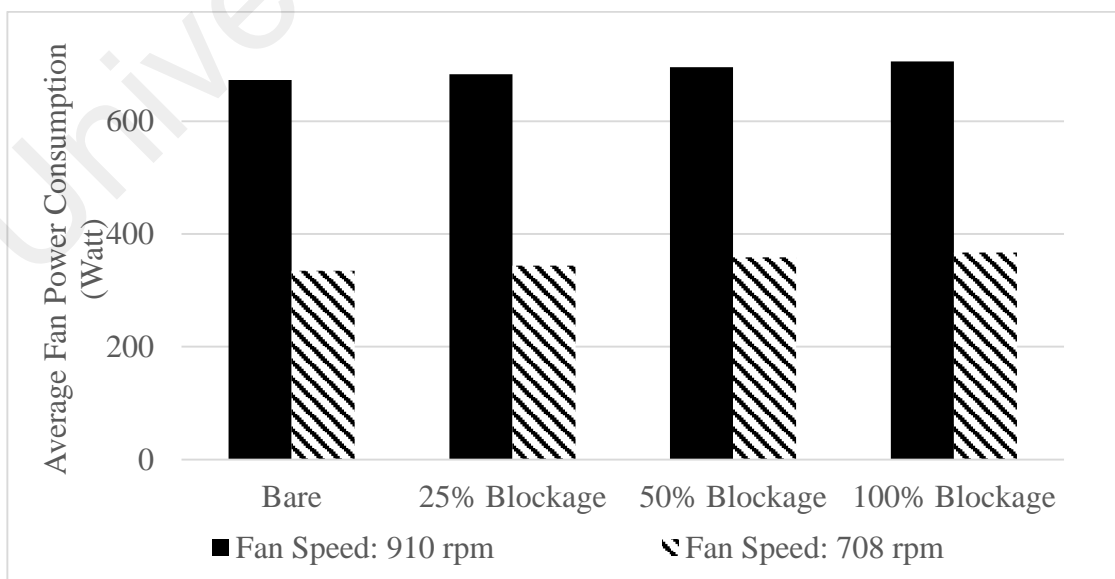


**Figure 4.2** The effect of blockage to the cooling tower fan power consumption.

Referring to Figure 4.1, it is observed that the intake air flow rate significantly decreases with the increase of blockage area at the outlet of the cooling tower. The blockage applied at the outlet blocks the air path causing less air to travel within the cooling tower model. In Figure 4.2, slight increment in power consumption is observed with the increase of blockage. The increment is because the fan requires more power in order to push the air when there is a blockage at the outlet of the cooling tower model. Considering the results from both figures, it can be concluded that the presence of blockage significantly reduces the flow rate of the cooling tower for both fan speeds while the fan power consumption increases slightly. These results prove that the additional obstruction at the path of the cooling tower airflow may cause negative effect on the cooling tower performance.

#### **4.1.2 Wind velocity profile**

Different configurations of exhaust air systems produce different profiles of outlet wind. Thus, wind turbine matching has to be made according to wind velocity profile. The mean velocity profile for all configurations (with and without turbine) are plotted in Figure 4.3. The radius of the fan duct is 365 mm which is represented by the dashed line and the wind velocity distribution is assumed as symmetrical with center of the outlet is  $X = 0$ . Since there is a fan blade hub at the center of the outlet and the measured velocity is zero, the graph is assumed to cross the y-axis at 0 m/s. For both fan speeds, the wind velocities gradually increase along the outlet radius until maximum at about 300 mm distance to the center of the outlet before slightly decreasing close to the outlet wall. The standard error for these measurements are less than 5%.

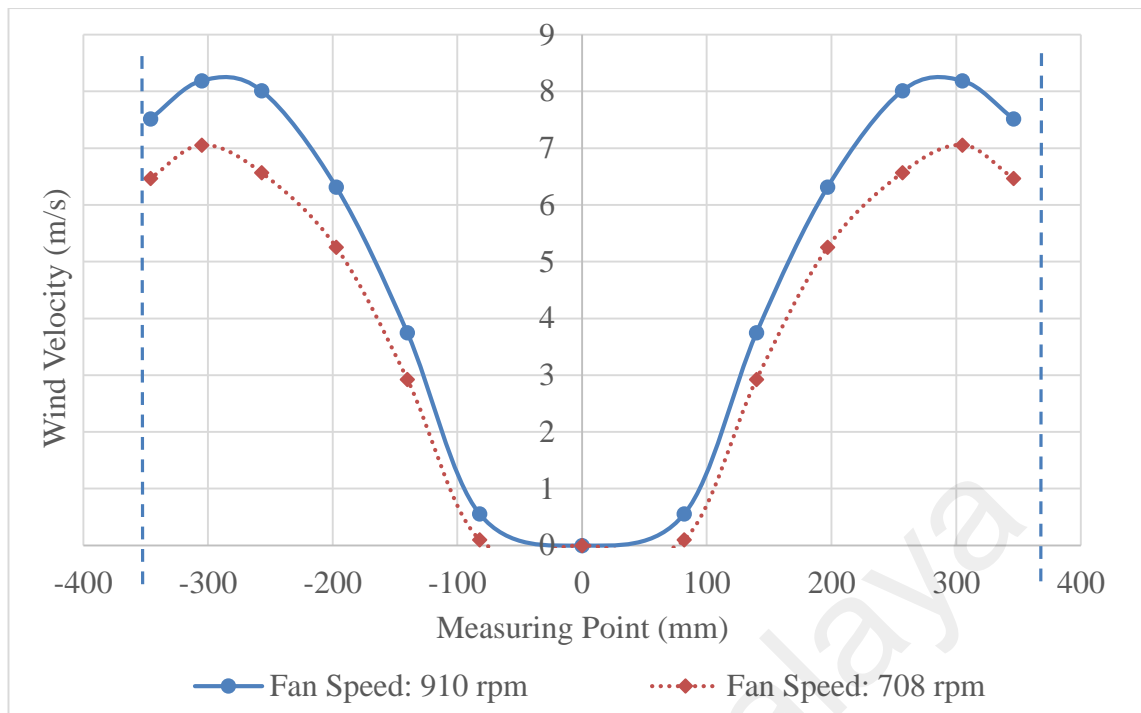


**Figure 4.3 Mean wind velocity at the outlet of the cooling tower model.**

## 4.2 Cooling tower with exhaust air energy recovery wind turbine generator

### 4.2.1 Wind turbine performance

#### 4.2.1.1 Wind turbine rotational speed

Figure 4.4 and 4.5 depict the rotational speed of the free running wind turbine in various configurations at the fan speed of 708 rpm and 910 rpm respectively. Both figures show similar trend where the rotational speeds are higher when the turbine is placed close to the outer radius of the discharge outlet. The rotational speeds of the wind turbine are significantly low when the turbine is placed close to the center of the outlet ( $X = -100$  mm to  $100$  mm) for all vertical turbine positions. This is because the wind speed at this region is very low (refer to Figure 4.3). Generally, the closer the distance between the turbine to the outlet plane, the higher the rotational speed.

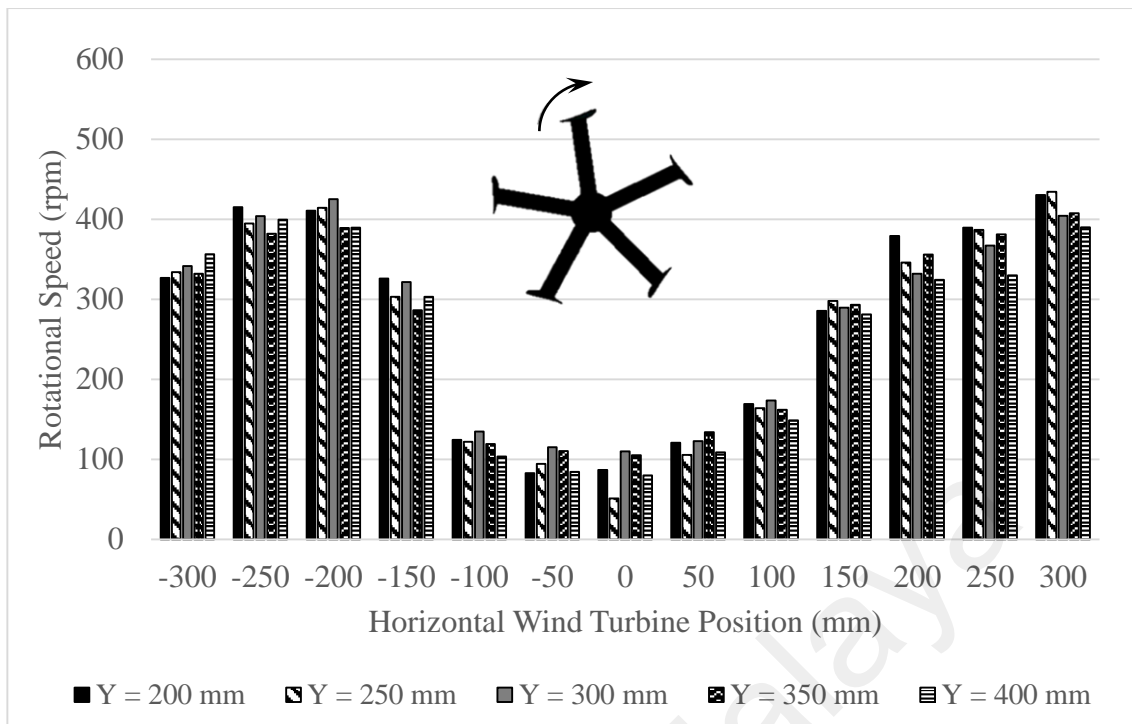


**Figure 4.4 Rotational speed of wind turbine at various positions for fan speed of 708 rpm (VAWT rotates in clockwise direction).**

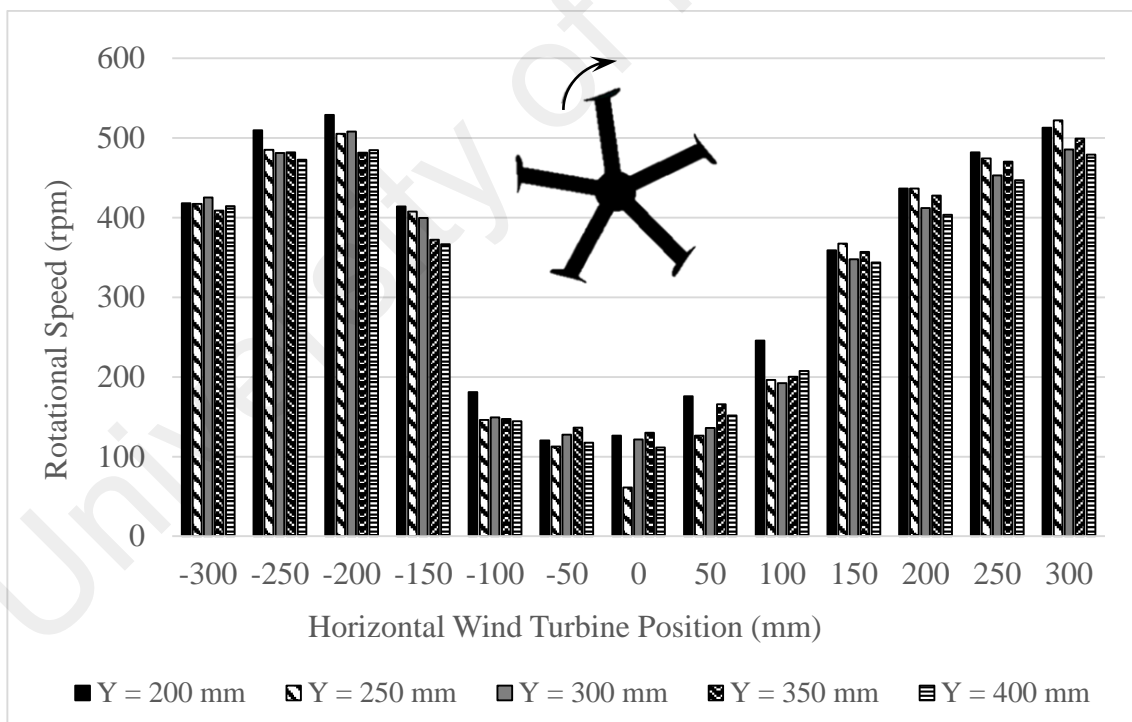


**Figure 4.5 Rotational speed of wind turbine at various positions for fan speed of 910 rpm (VAWT rotates in clockwise direction).**

On the positive side of the horizontal position, the rotational speeds show an increasing trend toward the wall of the outlet duct. On the other hand, at the negative side of the horizontal position, the rotational speeds increase until the maximum either at  $X = -200$



mm or  $X = -250$  mm before decreasing at  $X = -300$  mm. For the fan speed of 708 rpm, the highest rotational speed of the wind turbine occurs at  $X = -200$  mm and  $Y = 300$  mm with a speed of 425 rpm. While for fan speed of 910 rpm, the highest wind turbine rotational speed is 529 rpm at  $X = -200$  mm and  $Y = 200$  mm. These results show a good agreement with the wind speed profile as in Figure 4.3. Comparing the wind turbine rotational speeds between both fan settings, the fan speed of 910 rpm produces on average 23% higher rotational speeds compared to fan speed of 708 rpm. The standard deviations of rotational speeds of the VAWT for both fan speeds is about 3 rpm and standard error of less than 1%.

#### **4.2.1.2 Wind turbine power generation**

Wind turbine performance at various positions at the outlet of the cooling tower is illustrated in Figure 4.6 and 4.7. For both fan speeds, higher power is generated when the wind turbine is placed closer to the outlet duct. This is because the wind velocities are higher at this position (as illustrated in Figure 4.3). Power generation at the positions close to the fan center are significantly low, thus, the discussion will focus on the wind turbine positions other than these areas ( $X = -100$  mm to 100 mm). Inconsistent trends are demonstrated in power generation at the fan speed of 708 rpm. The highest power is generated at the wind turbine position of  $X = 200$  mm and  $Y = 200$  mm. Wind turbine at horizontal position of  $Y = 200$  mm is the highest for the horizontal positions of -300 mm, -250 mm, 200 mm and 250 mm. Comparing the negative and positive side of the horizontal positions, the wind turbine at the positive side of the cooling tower outlet produce higher power compared to the negative side. This is because the outlet flow pattern has a better matching to the wind turbine position. This will be explained theoretically in the double multiple stream tube discussions. Fan speed of 910 rpm produces a similar trend to the fan speed of 708 rpm. The highest power generation is demonstrated at wind turbine position of  $X = 250$  mm and  $Y = 200$  mm with 1.24 W.

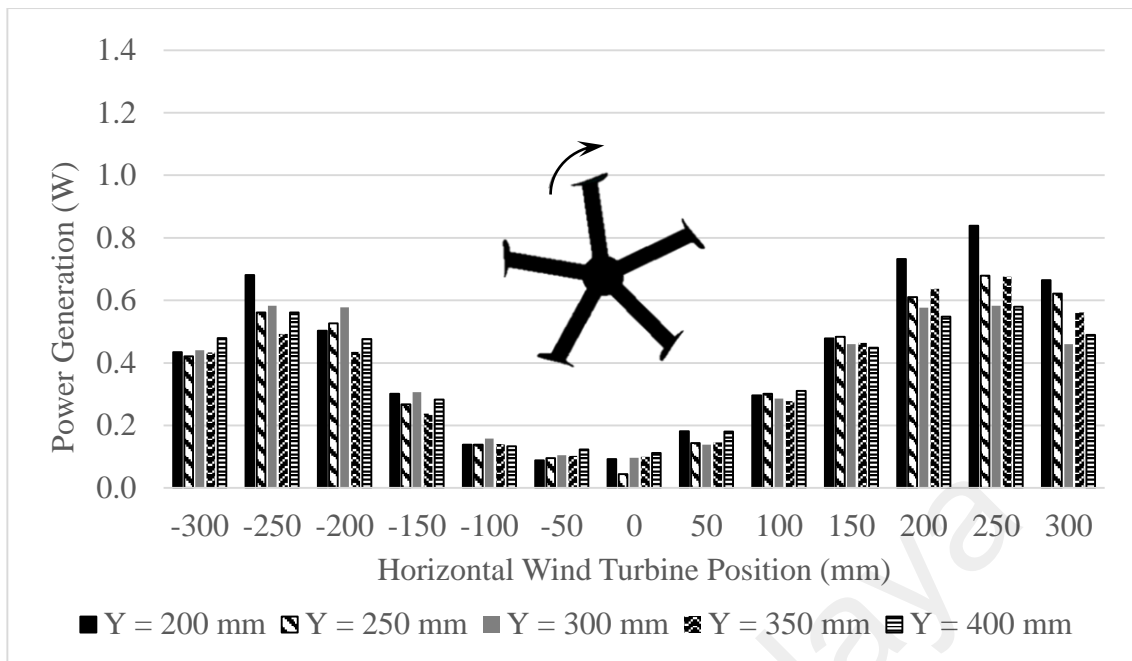


**Figure 4.6 Energy generated by the wind turbine at various positions for the fan speed of 708 rpm.**

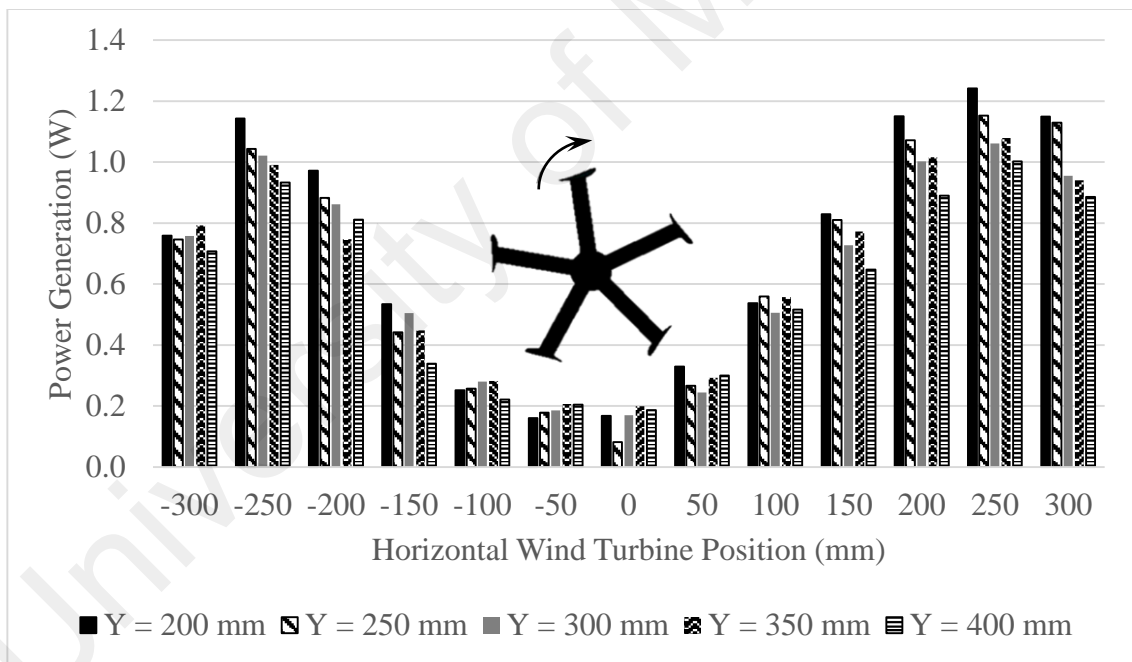


**Figure 4.7 Energy generated by the wind turbine at various positions for the fan speed of 910 rpm.**

Comparing the turbine performance between the different heights (vertical wind turbine position), the turbine closer to the outlet produced higher power. Since the air is blown upwards, the gravity effect will cause an additional loss to the wind velocity, hence lowering the wind turbine power output. However, other than power generation, the consideration of cooling tower air flow rate and power consumption are also needed for

wind turbine position determination. The standard deviations for both fan speeds are acceptable which less than 0.08 W and standard error of less than 1%.

#### 4.2.1.3 Coefficient of power of wind turbine

Since the fan produces a non-uniform wind profile, the turbine at each position experiences different wind velocity and hence different amounts of available wind energy to be extracted. The wind velocity is considered by averaging the wind velocity from Figure 4.3 at every 10° of azimuth angle at the upstream of the turbine. For this case, the air is assumed flowing at constant velocity in a vertical direction perpendicular to the turbine swept plane and the effect of gravity is negligible. The average wind velocity is tabulated in Table 4.2.

**Table 4.2 Average free-stream wind velocity on each wind turbine configuration.**

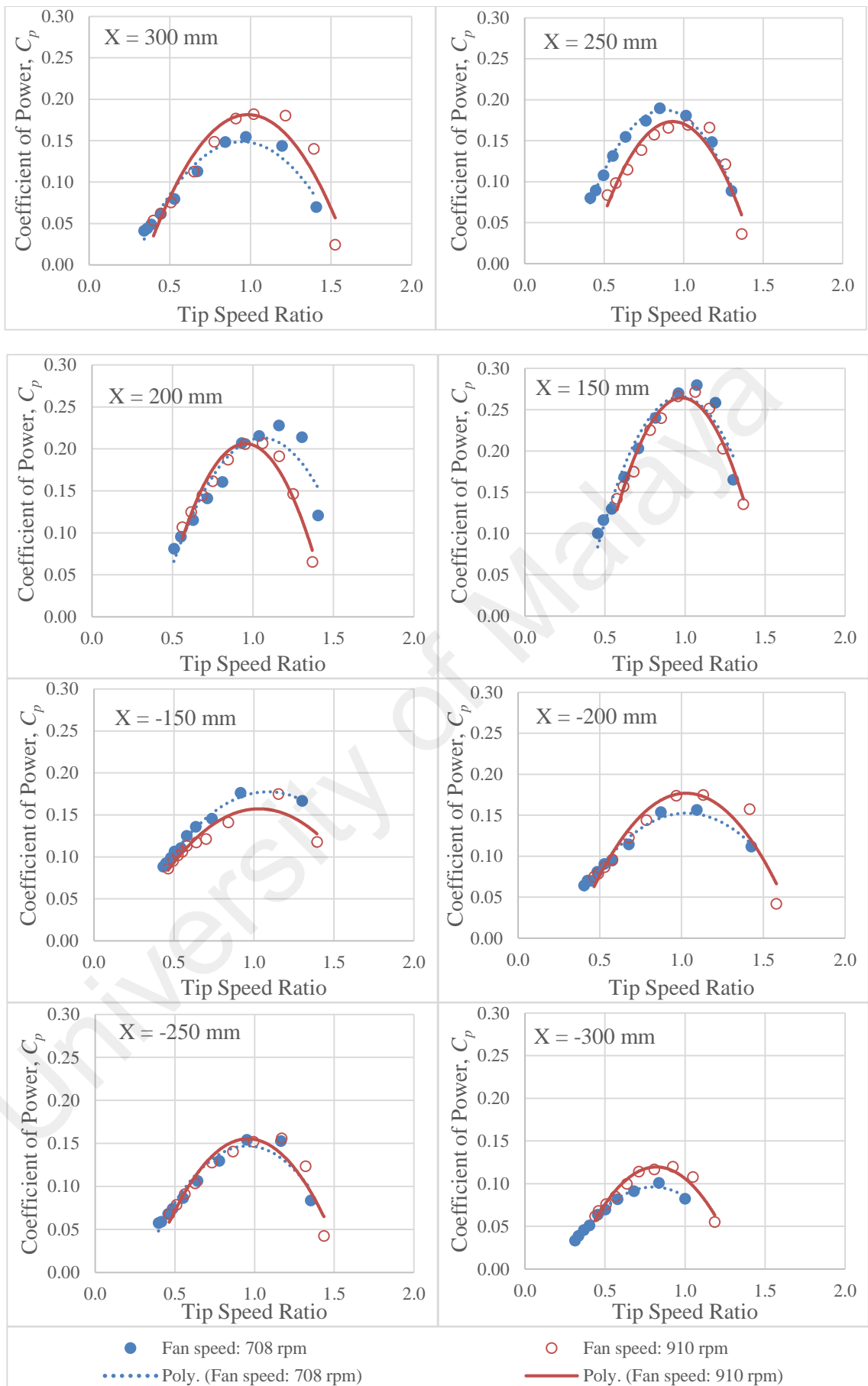
Wind turbine horizontal position, X (mm)	Average wind velocity (m/s)	
	Fan speed: 708 rpm	Fan speed: 910 rpm
300	4.273	4.856
250	4.312	5.102
200	3.876	4.654
150	3.141	3.811
-150	3.141	3.811
-200	3.876	4.654
-250	4.312	5.102
-300	4.273	4.856

The coefficient of power,  $C_p$  versus tip speed ratio (TSR) graphs for the considered wind turbine configurations are tabulated for comparison. The coefficient of power,  $C_p$  is defined as  $2P/(\rho AV^3)$ , where  $\rho$  is the air density and  $A$  is the frontal swept area of the turbine. The power generated by the turbine,  $P$  is measured by a controller which consists of rectifier and resistive dump load. AC voltage from the generator will be rectified to DC for current and voltage measurements and dumped to resistive load inside the

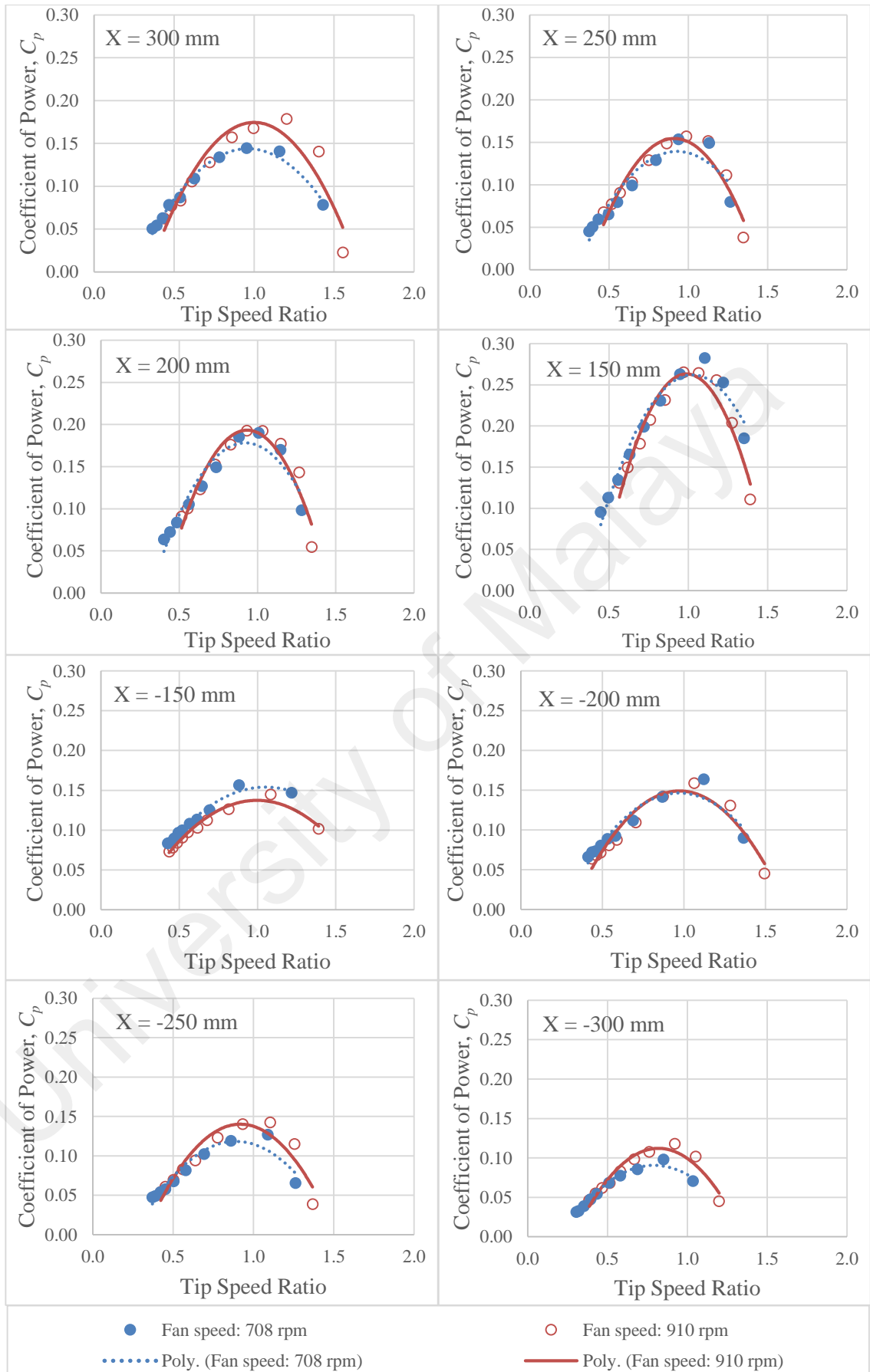
controller. Low power generation is expected, according to the previous study that utilized the same wind turbine model, the turbine producing much less than 1 W at wind velocity lower than 8.5 m/s (Kim & Gharib, 2013). It was also reported that the maximum  $C_p$  was 0.03 at a TSR of 0.98 and wind velocity of 8.5 m/s.

Figure 4.8-4.12 illustrate the graphs of coefficient of power against tip speed ratio of the wind turbine at the respective vertical positions. All the graphs show similar trends where the coefficient of power,  $C_p$  of the wind turbine reach its peak at the tip speed ratio, TSR of between 0.8 to 1.2 for both fan speeds. This is a normal range for micro wind turbines. Unlike the large scale wind turbine, the micro wind turbines normally operate at a tip speed ratio between 0 to 2 (Johnson, 2006; Leung, Deng, & Leung, 2010; Park, Lee, Sabourin, & Park, 2007). At the positive side of the horizontal position, the highest  $C_p$  occur at the horizontal position of 150 mm for all vertical positions. However, this position has the lowest wind speed which according to Table 4.2, the wind speed at this wind turbine position is 3.141 m/s and 3.811 m/s respectively. The higher  $C_p$  at this position is due to highest wind speed area (of non-uniform wind profile) matches with the wind turbine at the azimuth angle of between 45° to 100°. This range of azimuth angle is the range where the turbine produces the most torque. This factor is discussed further in result and discussion of double multiple stream tube analysis.

On the other hand, the  $C_p$  at the negative side of the wind turbine horizontal position is relatively low compared to the positive side. This is because the wind speed profiles are not favorable to the wind turbine rotation and azimuth angle. The highest wind speed (of the non-uniform wind profile) matches to the turbine at the second quarter of azimuth angle. At this azimuth angle, the wind turbine either generates low torque value or negative torque which results in a low value of  $C_p$ . The analysis of this is discussed in the double multiple stream tube analysis.



**Figure 4.8 Coefficient of power against tip speed ratio wind turbine at the considered horizontal position and vertical position of  $Y = 200$  mm.**



**Figure 4.9 Coefficient of power against tip speed ratio wind turbine at the considered horizontal position and vertical position of  $Y = 250$  mm.**

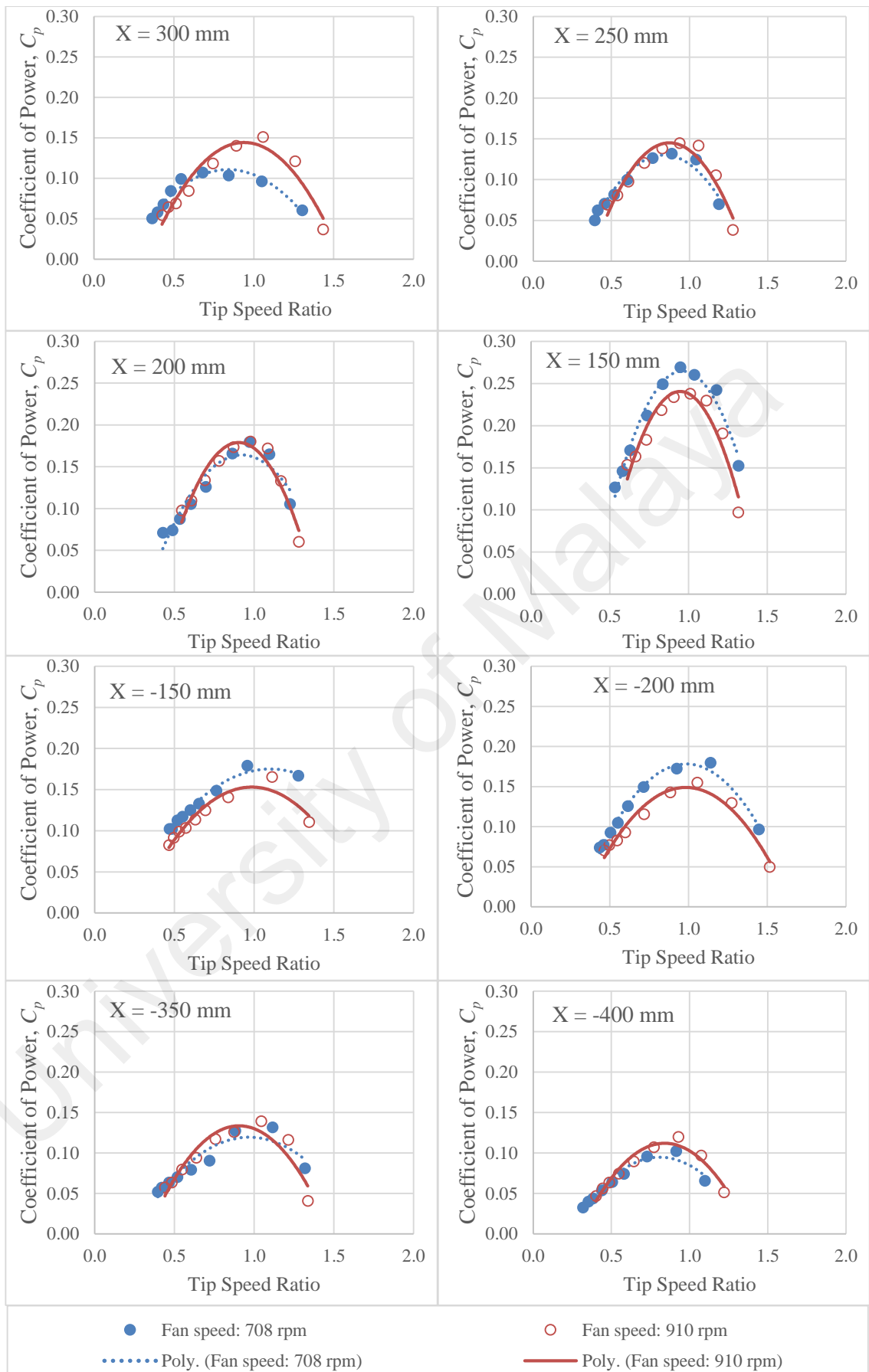


**Figure 4.10** Coefficient of power against tip speed ratio wind turbine at the considered horizontal position and vertical position of  $Y = 300$  mm.

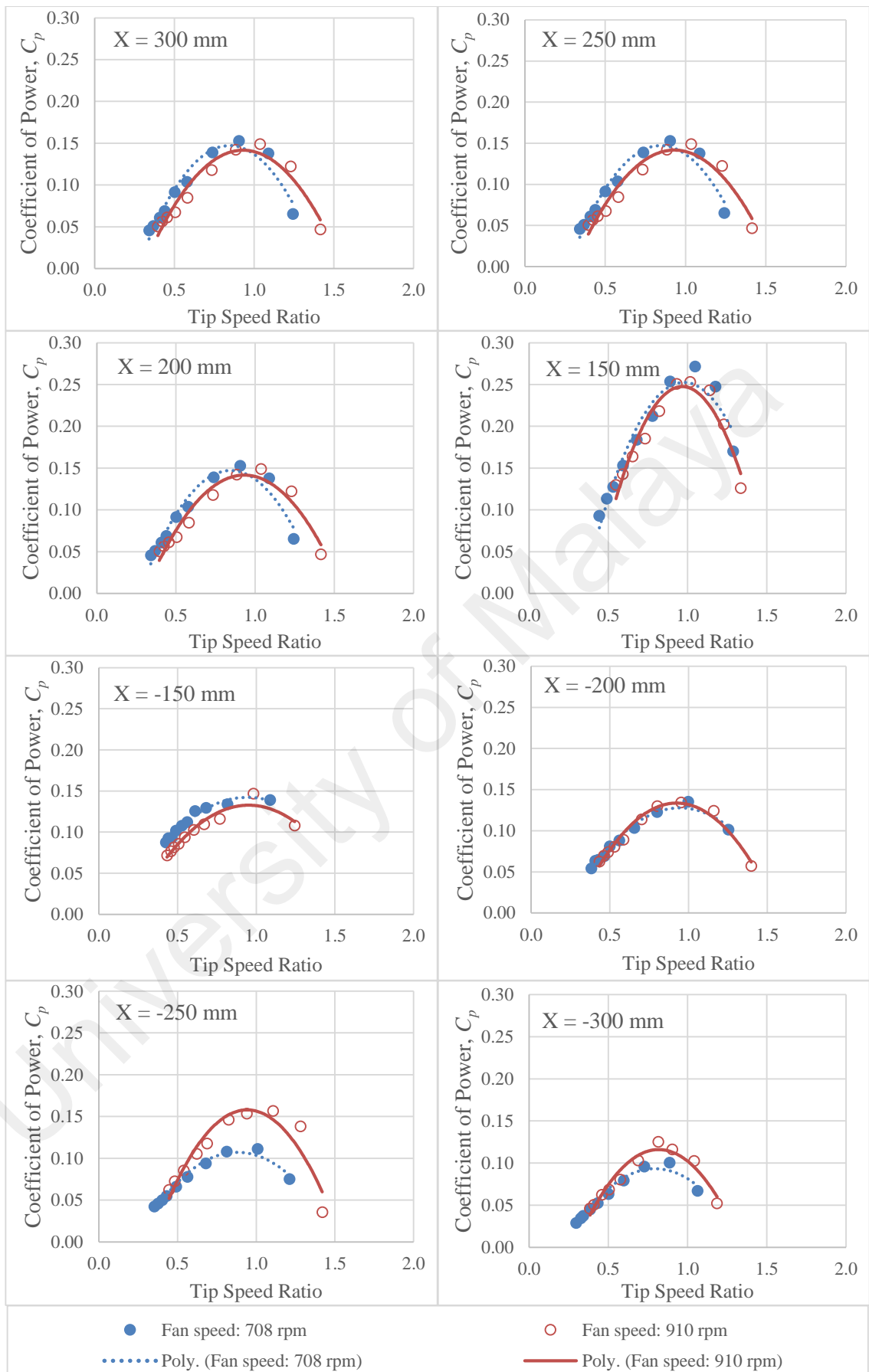


**Figure 4.11** Coefficient of power against tip speed ratio wind turbine at the considered horizontal position and vertical position of  $Y = 350$  mm.



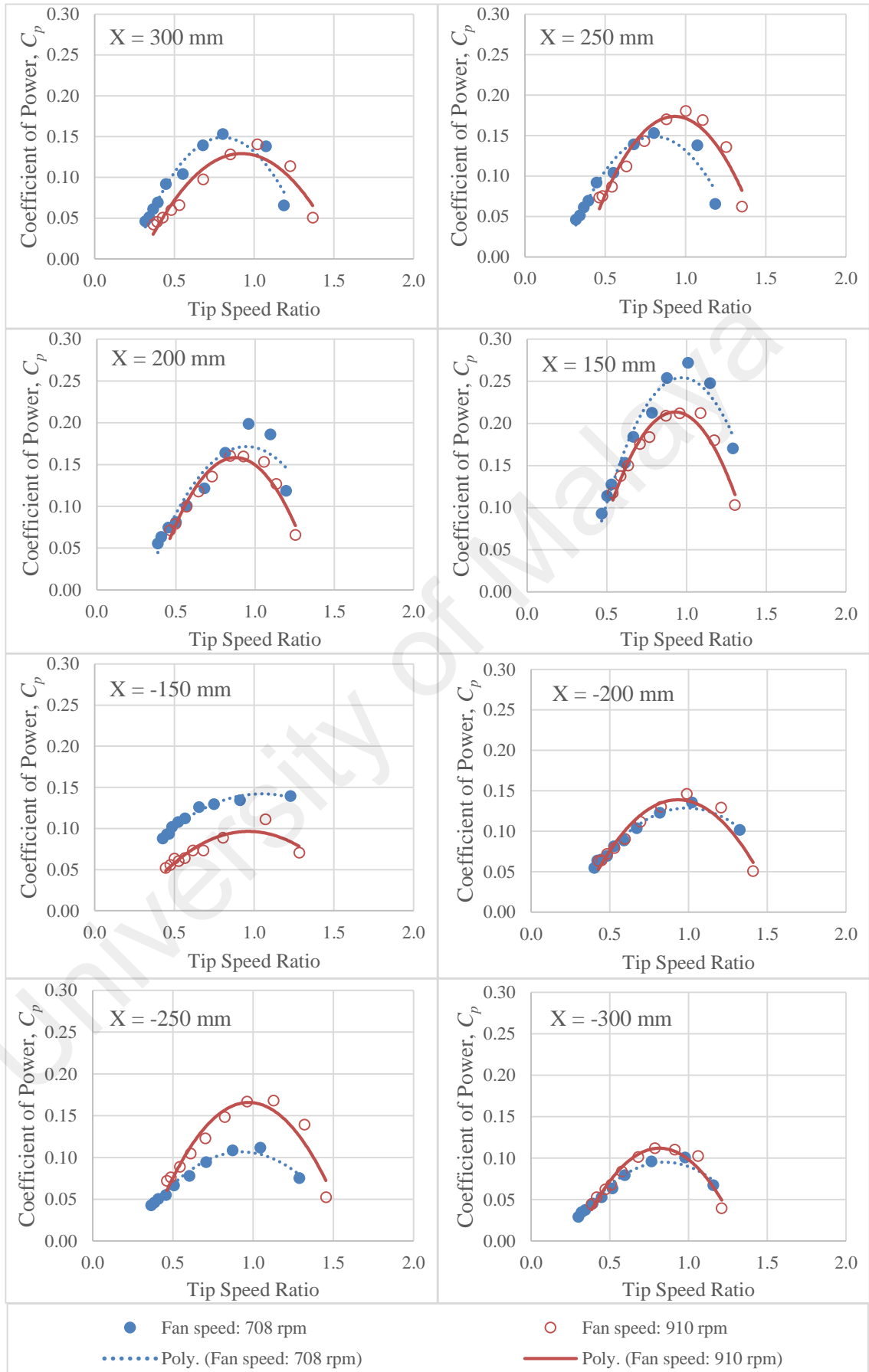


**Figure 4.12 Coefficient of power against tip speed ratio wind turbine at the considered horizontal position and vertical position of  $Y = 400$  mm.**

## **4.2.2 Cooling tower performance**

### **4.2.2.1 Air flow rate of the cooling tower model**

The intake flow rates are obtained by multiplying the average intake velocity with the intake area which is equal to 0.584 m<sup>2</sup>. The flow rate of the original operation of the cooling tower model at 2.60 m<sup>3</sup>/s for fan speed of 708 rpm and 3.05 m<sup>3</sup>/s for 910 rpm are the benchmark for the assessment. Flow rate lower than the benchmark value represents the negative effect to the cooling tower model while a higher flow rate represents an improvement of its air flow.

Figure 4.13 and 4.14 depict the average flow rate of the cooling tower model with various configurations for the fan speed of 708 rpm and 910 rpm respectively. For both fan speeds, at all wind turbine positions at the outlet of the cooling tower, the air flow rates of the cooling tower show greater values than the cooling tower without the wind turbine. The results show that the presence of the wind turbine at the outlet of the cooling tower improves the flow rate of the cooling tower. This is because when the wind turbine is spinning at a high rotational speed, a low pressure region is created and hence possibly creates a suction effect which improves the air flow (W. T. Chong et al., 2014; W.T. Chong, Fazlizan, Yip, Poh, & Hew, 2014).

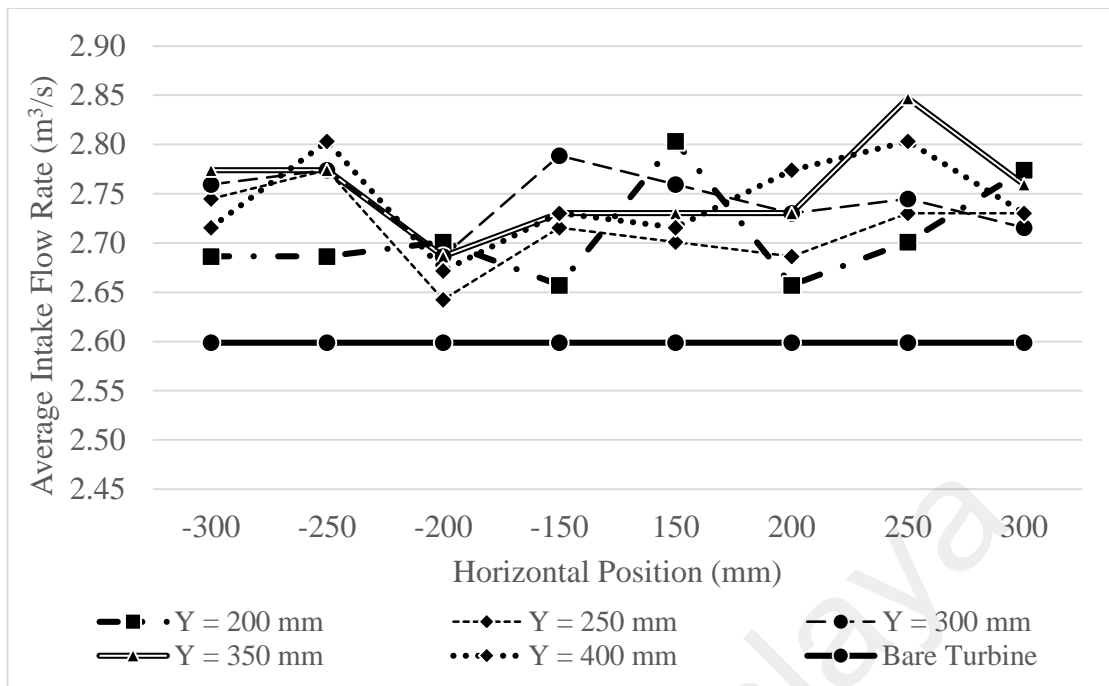


**Figure 4.13 Average flow rate of the cooling tower model with various configurations for the fan speed of 708 rpm.**

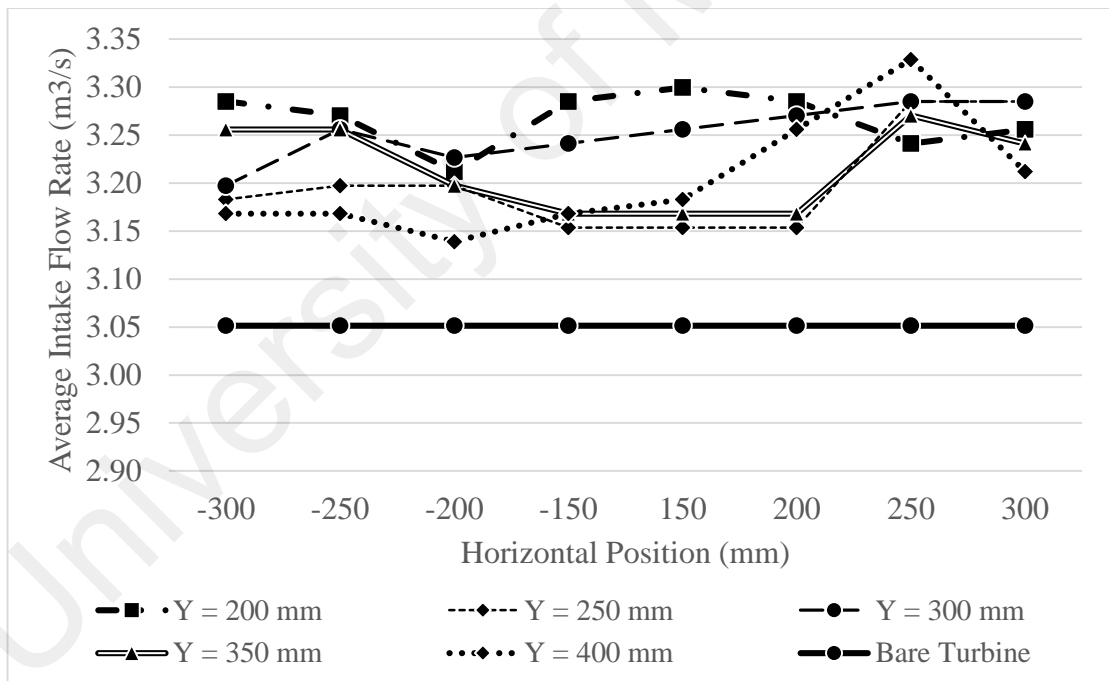


**Figure 4.14 Average flow rate of the cooling tower model with various configurations for the fan speed of 910 rpm.**

#### 4.2.2.2 Cooling tower fan motor power consumption

The cooling tower power consumption for the fan speed of 708 rpm is plotted in Figure 4.15. It can be seen that the fan motor for most of the horizontal position of the wind turbine at vertical position for 200 mm and 250 mm consumes higher power than the bare

cooling tower. While for  $Y = 300$  mm, 350 mm and 400 mm, the fan motor consumes less power than the benchmark value except at  $X = -150$  mm. Comparing the negative and positive side of wind turbine horizontal position, it shows that the positive side makes the motor consume less power. The lowest fan motor power consumption occurs at  $X = 250$  mm and  $Y = 400$  mm. Figure 4.16 depicts the fan motor power consumption for the fan speed of 910 rpm. It is clearly shown that the presence of the wind turbine decreases the power consumption of the fan motor except at the position of  $X = -150$  mm and  $Y = 200$  mm. The highest power consumption for all vertical positions is at  $X = -150$  mm. Overall, the further the wind turbine distance from the cooling tower, the lower the fan power consumption and the lowest power consumption occurs at  $X = 250$  mm and  $Y = 400$  mm for both fan speeds.

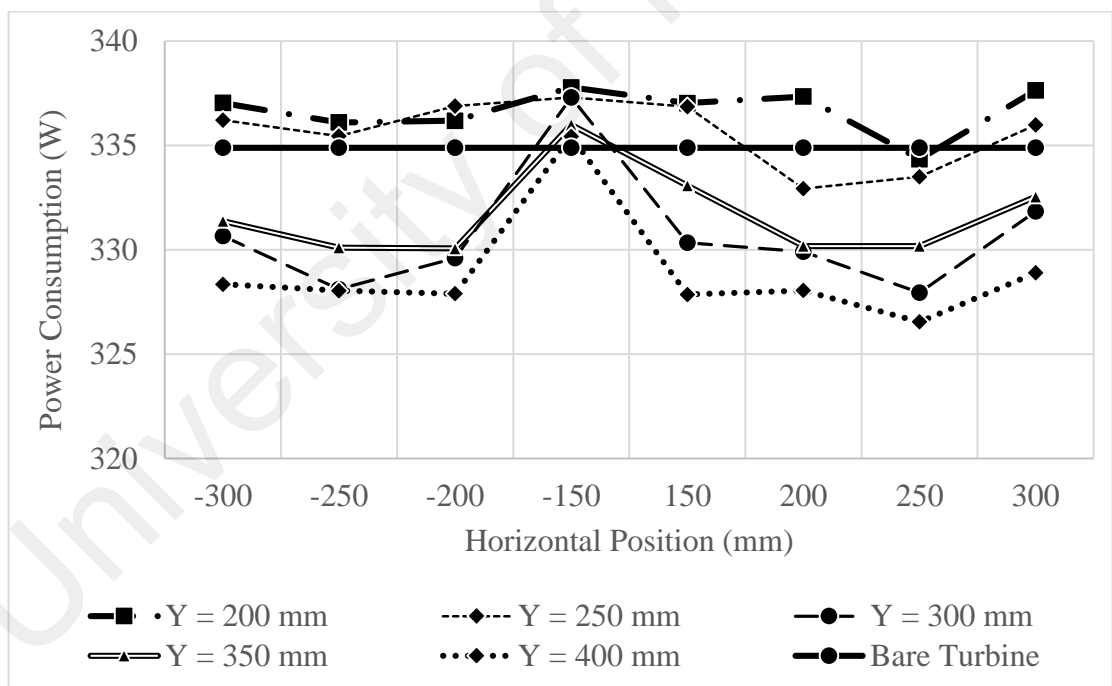


**Figure 4.15 Average fan motor power consumption of the cooling tower model with various configurations for the fan speed of 708 rpm.**

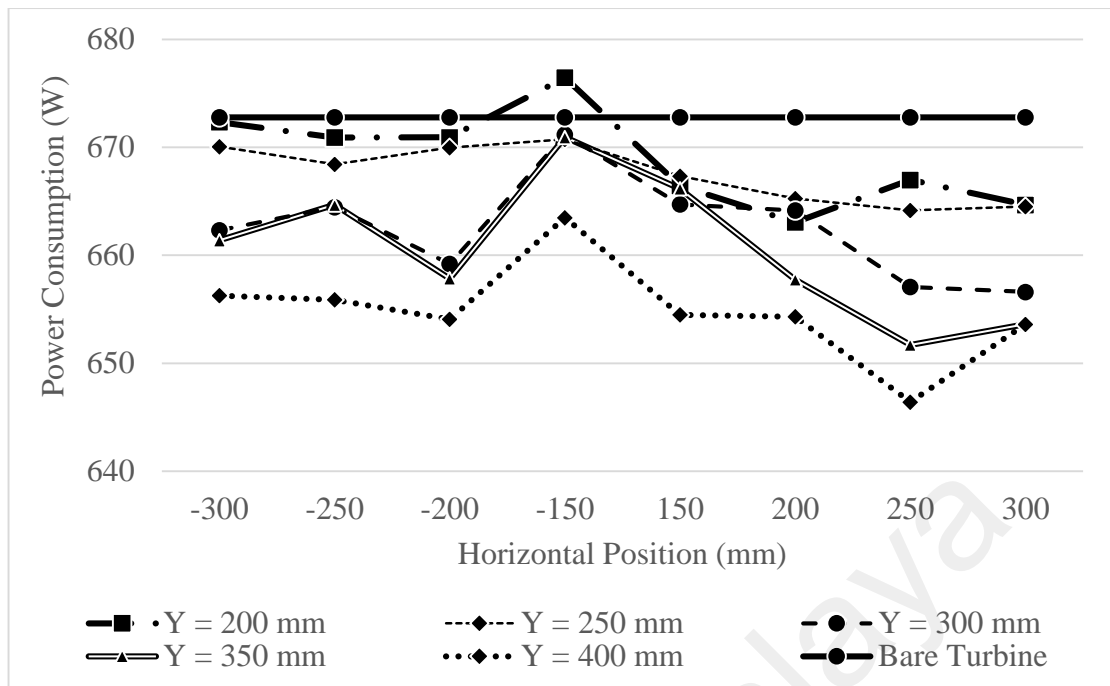


**Figure 4.16 Average fan motor power consumption of the cooling tower model with various configurations for the fan speed of 910 rpm.**

Among all configurations, the wind turbine horizontal position of -150 mm consumes the highest power at each of the vertical positions for both fan speeds. This is because the matching of the wind turbine and the outlet with profile is causing the blockage effect to the airflow which makes the motor consume more power.

### 4.2.3 Overall performance comparison

The presented results suggest that the preferable position for the turbine is when the turbine is spinning clockwise at the right side, i.e.  $X = 150$  mm,  $200$  mm,  $250$  mm and  $300$  mm for all vertical distances. This is due to the higher energy generation by the turbine while lower power consumption and higher flow rate by the cooling tower at this side. Thus, these configurations are selected for further evaluation. Table 4.3 presents the comparative performance of cooling tower and wind turbine compared to bare cooling tower at positive side of horizontal position and fan speed of 708 rpm. At this fan speed, the cooling tower has the highest flow rate at  $X = 250$  mm and  $Y = 350$  mm with the increment of 9.55% compared to the bare cooling tower. The lowest power consumption occurs at 3 configurations, i.e.  $X = 250$  mm and  $Y = 300$  mm,  $X = 250$  mm and  $Y = 350$

mm, and  $X = 250$  mm and  $Y = 400$  mm with 2.1% decrease compared to the bare cooling tower. However, the highest power generation and energy recovery percentage is observed at  $X = 250$  mm and  $Y = 200$  mm. The results clearly show that the best horizontal position is at  $X = 250$  mm for all vertical positions. In selecting the best configuration, the priority is to either improve or maintain cooling tower performance, then only consider the energy recovery percentage. If the presence of the wind turbine negatively affects the cooling tower performance, the configuration should not be accepted. Thus, wind turbine at  $X = 250$  mm and  $Y = 350$  mm is selected as best configuration for the fan speed of 708 rpm.

The comparative performance of cooling tower and wind turbine compared to bare cooling tower at positive side of horizontal position and fan speed of 910 rpm is tabulated in Table 4.4. Similar to the fan speed of 708 rpm, the horizontal position of 250 mm is also the best for all vertical positions at fan speed of 910 rpm. The highest air flow rate and lowest power consumption of the cooling tower is at  $X = 250$  mm and  $Y = 400$  mm with 9.09% increase and 3.92% decrease respectively compared to the bare cooling tower. The highest energy recovery with 0.19% is at  $X = 250$  mm and  $Y = 200$  mm. Since at highest energy recovery, the cooling tower performance is also improved, this configuration is selected as best configuration for the fan speed of 910 rpm.

**Table 4.3 Comparative performance of cooling tower and wind turbine compared to bare cooling tower at positive side of horizontal position and fan speed of 708 rpm.**

Configuration		Cooling Tower				Wind Turbine				Percentage of Energy Recovery
		Intake Flow Rate		Fan Motor Consumption		Maximum Power Generation	Free Running Rotational Speed (RPM)	Maximum $C_p$	TSR at Maximum $C_p$	
		Flow Rate (m <sup>3</sup> /s)	% Difference	Input Power (W)	% Difference					
Y (mm)	X (mm)									
200	150	2.80	7.87%	337	0.64%	0.48	286	0.280	1.07	0.14%
	200	2.66	2.25%	337	0.73%	0.73	379	0.228	1.04	0.22%
	250	2.70	3.93%	335	0.14%	0.84	390	0.190	1.01	0.25%
	300	2.77	6.74%	338	0.82%	0.66	430	0.155	0.97	0.20%
250	150	2.70	3.93%	337	0.59%	0.48	298	0.283	1.10	0.14%
	200	2.69	3.37%	333	-0.59%	0.61	346	0.190	1.01	0.18%
	250	2.73	5.06%	333	-0.41%	0.68	387	0.154	0.94	0.20%
	300	2.73	5.06%	336	0.32%	0.62	434	0.145	0.95	0.19%
300	150	2.76	6.18%	330	-1.36%	0.46	289	0.283	0.95	0.14%
	200	2.73	5.06%	330	-1.49%	0.58	332	0.190	0.97	0.17%
	250	2.74	5.62%	328	-2.07%	0.58	367	0.154	0.89	0.18%
	300	2.72	4.49%	332	-0.91%	0.46	404	0.145	0.68	0.14%
350	150	2.73	5.06%	330	-1.36%	0.46	293	0.269	1.05	0.14%
	200	2.73	5.06%	330	-1.49%	0.64	356	0.180	1.04	0.19%
	250	2.85	9.55%	328	-2.07%	0.68	381	0.132	0.90	0.21%
	300	2.76	6.18%	332	-0.91%	0.56	407	0.107	0.87	0.17%
400	150	2.72	4.49%	330	-1.36%	0.45	281	0.272	1.01	0.14%
	200	2.77	6.74%	330	-1.49%	0.55	324	0.198	0.96	0.17%
	250	2.80	7.87%	328	-2.07%	0.58	330	0.153	1.07	0.18%
	300	2.73	5.06%	332	-0.91%	0.49	390	0.131	0.95	0.15%
Bare cooling tower		2.60	2.60	-	335	-	-	-	-	-

**Table 4.4 Comparative performance of cooling tower and wind turbine compared to bare cooling tower at positive side of horizontal position and fan speed of 910 rpm.**

Configuration		Cooling Tower				Wind Turbine				Percentage of Energy Recovery
		Intake Flow Rate		Fan Motor Consumption		Maximum Power Generation	Free Running Rotational Speed (RPM)	Maximum $C_p$	TSR at Maximum $C_p$	
		Flow Rate (m <sup>3</sup> /s)	% Difference	Input Power (W)	% Difference					
Y (mm)	X (mm)									
200	150	3.30	8.13%	666	-0.94%	0.83	359	0.272	1.06	0.12%
	200	3.29	7.66%	663	-1.45%	1.15	436	0.207	1.06	0.17%
	250	3.24	6.22%	667	-0.86%	1.24	482	0.170	1.03	0.19%
	300	3.26	6.70%	665	-1.21%	1.15	513	0.182	1.02	0.17%
250	150	3.15	3.35%	667	-0.81%	0.81	368	0.265	0.97	0.12%
	200	3.15	3.35%	665	-1.12%	1.07	437	0.193	0.93	0.16%
	250	3.29	7.66%	664	-1.28%	1.15	475	0.157	0.99	0.17%
	300	3.29	7.66%	665	-1.23%	1.13	522	0.179	1.20	0.17%
300	150	3.26	6.70%	665	-1.20%	0.73	348	0.238	1.01	0.11%
	200	3.27	7.18%	664	-1.28%	1.00	412	0.180	0.98	0.15%
	250	3.29	7.66%	657	-2.33%	1.06	453	0.145	0.94	0.16%
	300	3.29	7.66%	657	-2.40%	0.96	486	0.151	1.06	0.14%
350	150	3.17	3.83%	666	-0.98%	0.77	357	0.238	1.02	0.12%
	200	3.17	3.83%	658	-2.23%	1.02	428	0.180	1.00	0.15%
	250	3.27	7.18%	652	-3.13%	1.08	470	0.145	1.08	0.17%
	300	3.24	6.22%	654	-2.85%	0.94	499	0.151	1.04	0.14%
400	150	3.18	4.31%	654	-2.72%	0.65	344	0.253	1.09	0.10%
	200	3.26	6.70%	654	-2.75%	0.89	404	0.183	0.84	0.14%
	250	3.33	9.09%	646	-3.92%	1.00	447	0.147	0.91	0.16%
	300	3.21	5.26%	654	-2.85%	0.89	479	0.149	1.02	0.14%
Bare cooling tower		3.05	-	673	-	-	-	-	-	-



### **4.3 Double multiple stream tube analysis for the exhaust air energy recovery turbine generator**

#### **4.3.1 Comparison between the experimental result and the calculated result**

Comparisons between the experiment and the calculated result using DMST are depicted in Figure 4.17 and 4.18. The graphs show similar trends for all configurations except at  $X = -300$  mm. The calculated wind turbine power falls lower than the power generation obtained from the experiment. This can be justified by considering that, for high values of the angle of attack, the blades fall into stall for a large angular sector of rotor rotation about the turbine axis. In fact, since the local Reynolds number is low, the lift and drag coefficients are much influenced by the profile geometrical characteristics for angles of attack higher than the stall limit (Camporeale & Magi, 2000). The wind that discharge from the outlet tends to expand because of the pressure difference with the surroundings. The expansion makes the wind direction to change and may not be in vertical direction from the outlet. Due to the complexity of the flow, in the calculation, the wind direction is assumed as perpendicular to the turbine swept plane. This is another justification for the deviation between experimental result and DMST calculation.

It is noticeable that at  $X = -300$  mm fan speed of 708 rpm and all vertical wind turbine positions, the power value from experiment and DMST calculation is very close to each other. This is because of the initial assumption that considers the flow direction is perpendicular to the swept plane and the instantaneous velocities. At this turbine position, some of the wind turbine swept area is outside the outlet area (365 mm radius) of the cooling tower and the instantaneous wind velocity at these areas are determined by the polynomial trend line of the mean velocity. Since there is no wind source outside the outlet area, the wind from the duct will expand to this area, hence the wind direction is no longer perpendicular to the swept plane. Thus, lesser wind is experienced by the wind turbine and consequently, the wind generation is lower.

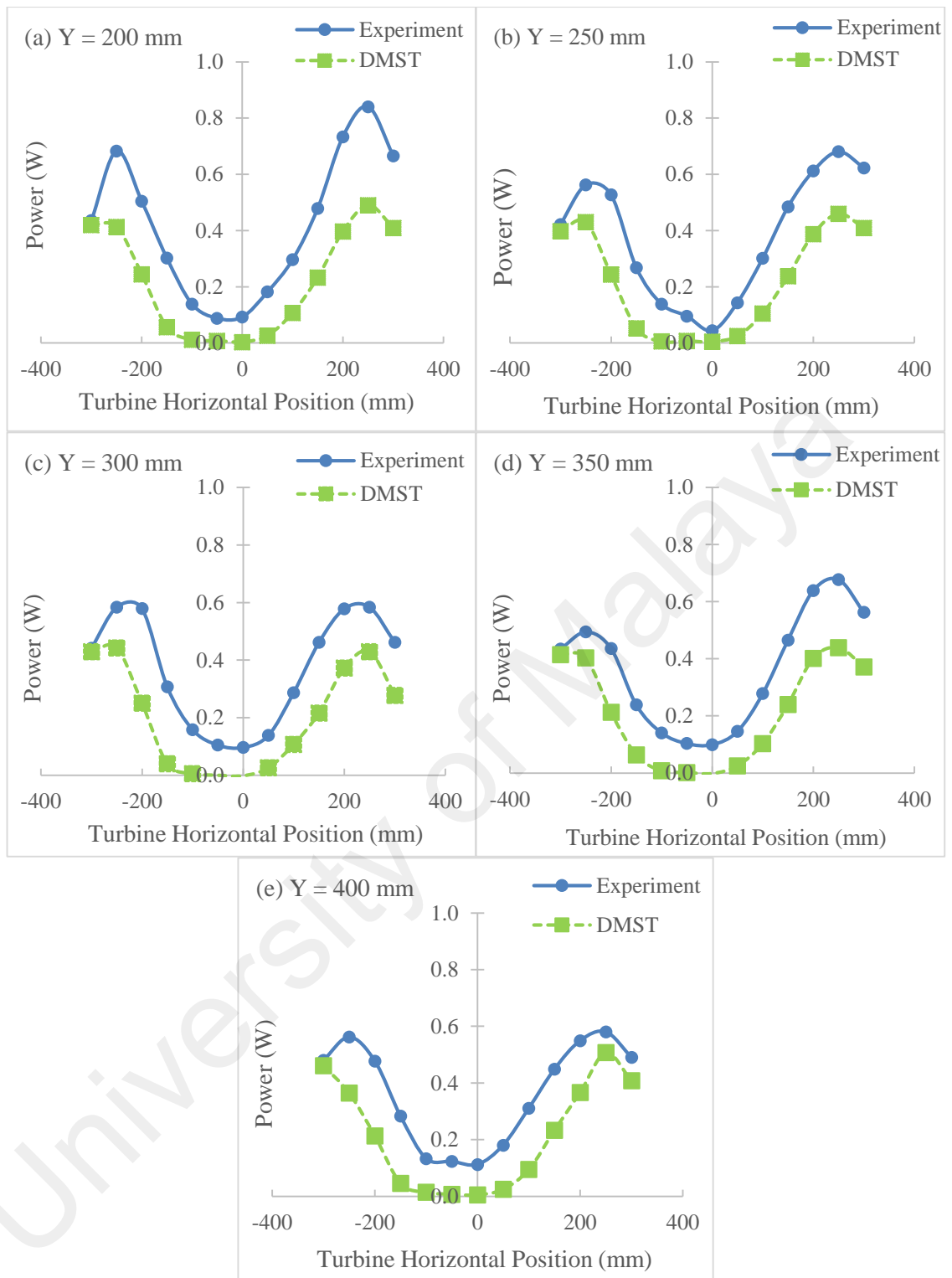


**Figure 4.17 Comparison between the power obtained from the experiments and obtained from the DMST calculations for the fan speed of 708 rpm. (a) For the wind turbine at 200 mm distance, (b) for the wind turbine at 250 mm distance, (c) for the wind turbine at 300 mm distance, and (d) for the wind turbine at 400 mm distance.**

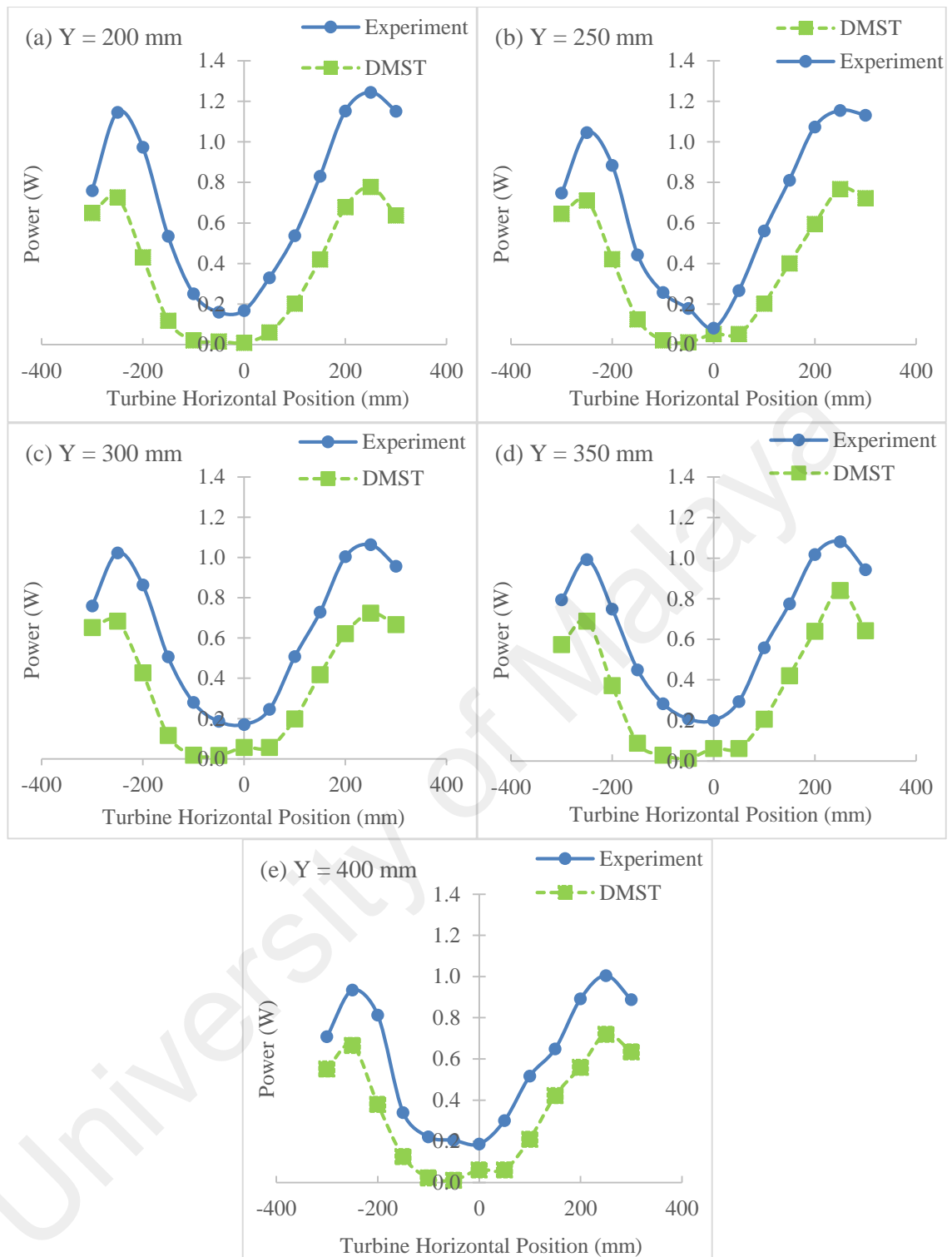


**Figure 4.18 Comparison between the power obtained from the experiments and obtained from the DMST calculations for the fan speed of 910 rpm. (a) For the wind turbine at 200 mm distance, (b) for the wind turbine at 250 mm distance, (c) for the wind turbine at 300 mm distance, and (d) for the wind turbine at 400 mm distance.**

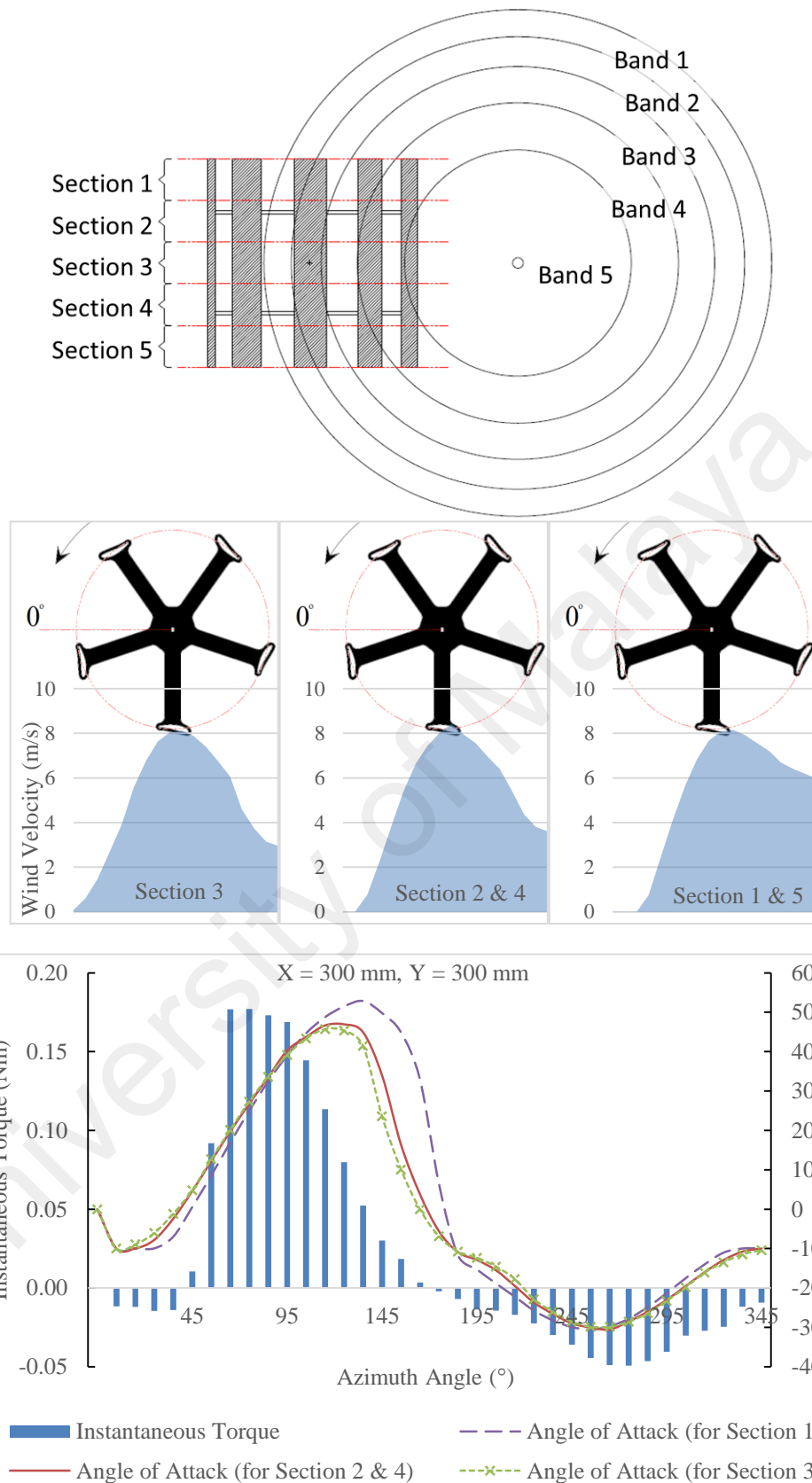
According to the wind velocity profiles (Figure 4.3), the highest velocity occurs at about 300 mm radius of the discharge outlet. Thus, the wind turbine performs best when it is positioned at this area. This condition happens at all wind turbine vertical distance

and fan wind speed. Comparing the trends for power obtained from experiment and from DMST calculation, a good agreement is observed for the configuration that produce the highest power, i.e. at  $X = 250$  mm for both fan speed and all vertical wind turbine position.

#### **4.3.2 Wind turbine power generation against non-uniform wind velocity profile**

The angle of attack and power generation at every  $10^\circ$  (starting from  $5^\circ$ ) azimuth angle for all wind turbine configurations are presented in Appendix B. Since the graphs' trends are similar, some configurations are selected for the discussion which are at the vertical position of  $Y = 300$  mm and fan speed of 910 rpm. Figure 4.19 depicts the plan view of the turbine position against circular bands of exhaust air outlet, side view of wind turbine against the wind stream, instantaneous torque against azimuth angle and angle of attack versus azimuth angle at horizontal position of  $X = 300$  mm and vertical position of  $Y = 300$  mm for the fan speed of 910 rpm. At this configuration, the highest wind speed region matches to the wind turbine at about  $90^\circ$  azimuth angle for all blade sections. The angle of attack of the turbine blade at this azimuth angle is more than  $30^\circ$  for all blade sections which is high and not preferable to produce high torque. Similar trends are demonstrated for the angle of attack against azimuth angle for all sections except Section 1 and 5 where the angle of attack at between  $105^\circ$  to  $185^\circ$  are higher compared to others.

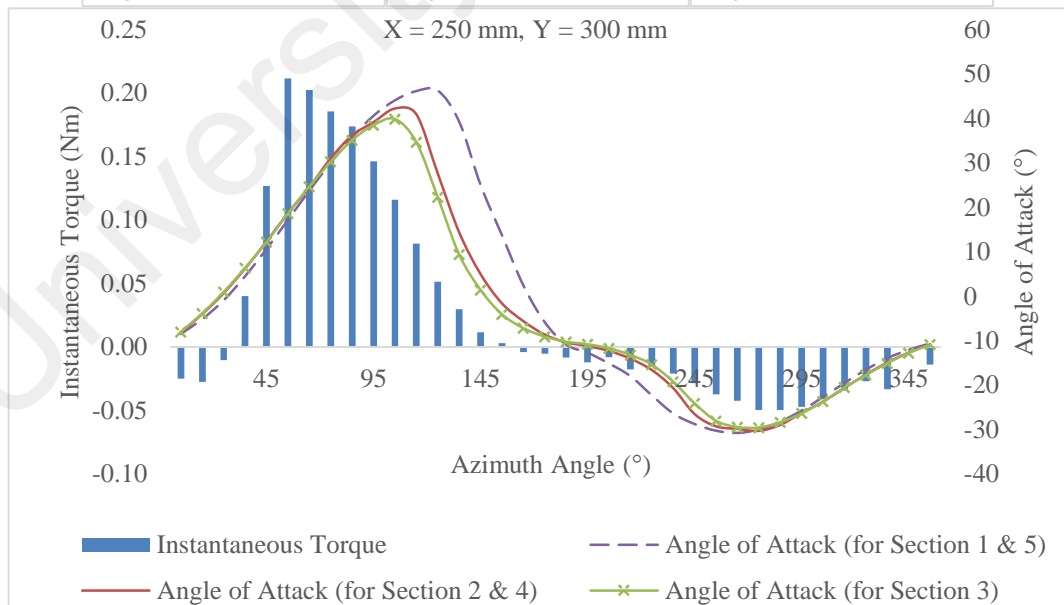
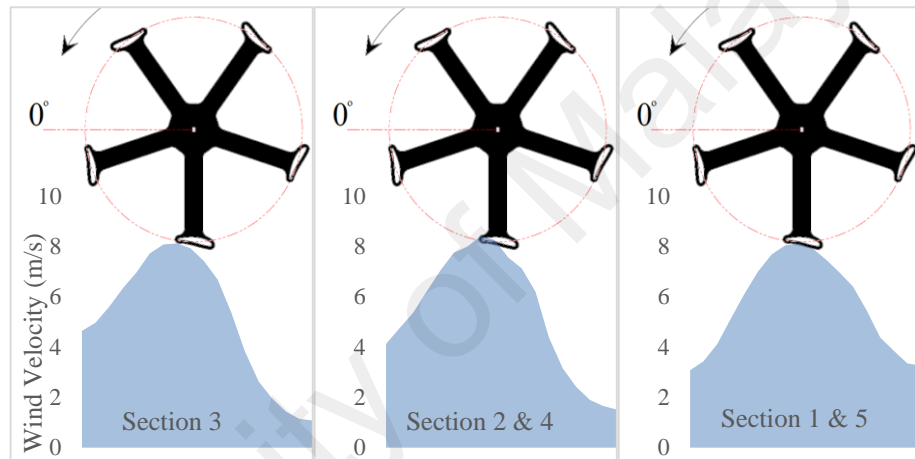
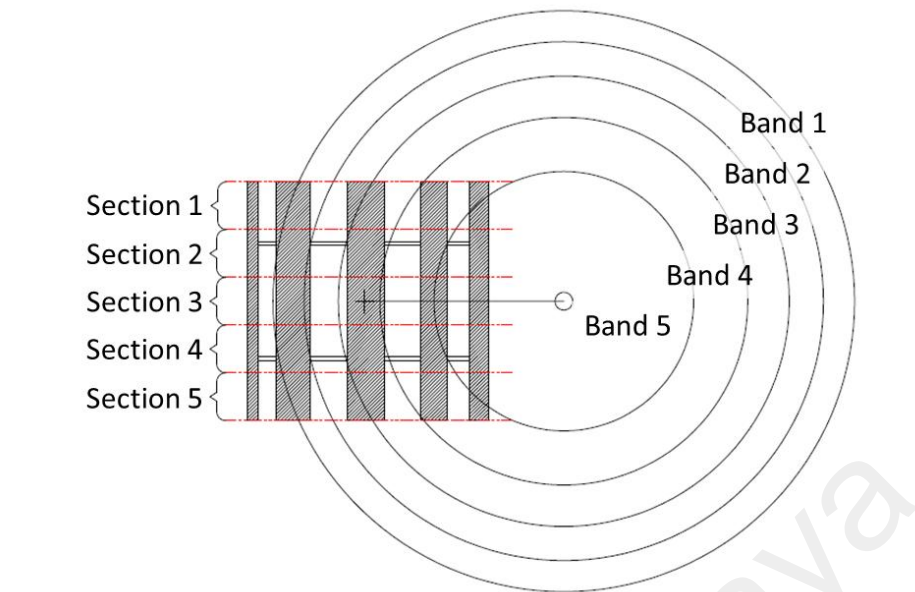
The turbine produces the highest power at the azimuth angle of  $65^\circ$  where at this azimuth angle, the angle of attacks are  $16.9^\circ$  for blade section 1 and 5,  $19.7^\circ$  for blade section 2 and 4, and  $20.1^\circ$  for blade section 3. Only the azimuth angles ranging from  $45^\circ$  to  $155^\circ$  are producing positive torque, hence positive power. The advantage of this configuration is the low wind velocity at the azimuth angle of  $0^\circ$  to  $35^\circ$  where at this range, the whole blade experiences negative angle of attacks and the wind power is converted into negative torque. The mean torque for this configuration is 0.019 Nm and the turbine power generation is 0.666 W.



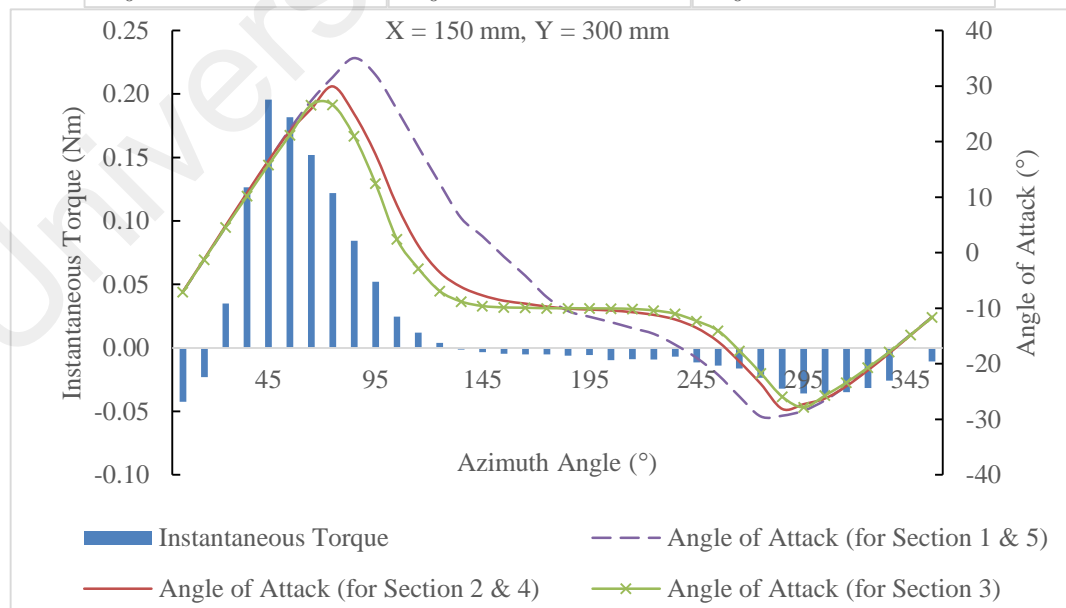
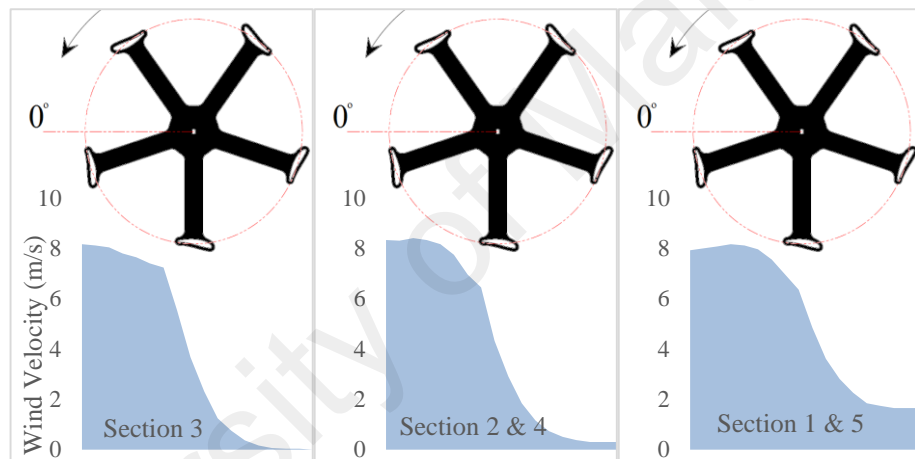
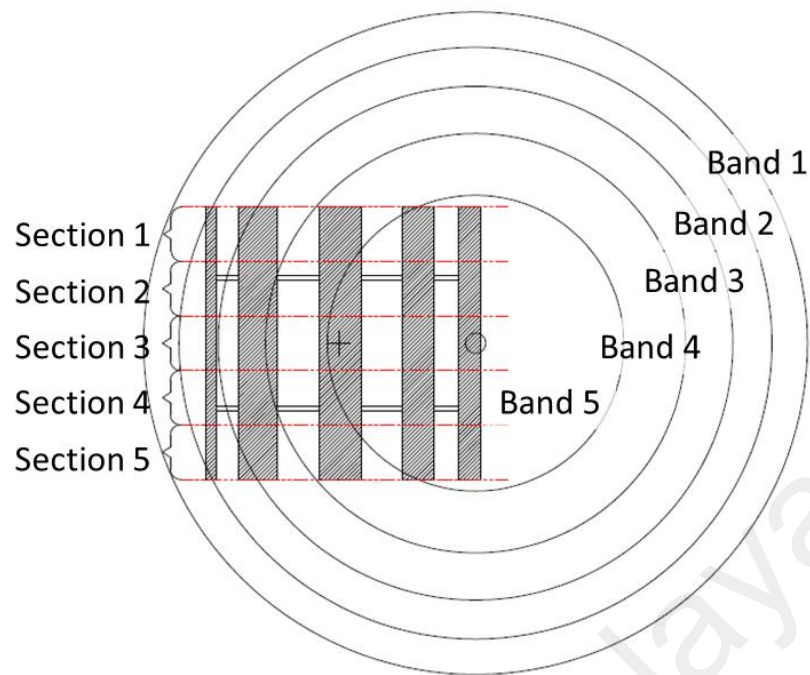
**Figure 4.19 (a) Plan view of wind turbine position against circular bands of exhaust air outlet; (b) Side view of wind turbine against the wind stream; (c) Instantaneous torque against azimuth angle and angle of attack versus azimuth angle at horizontal position of  $X = 300$  mm and vertical position of  $Y = 300$  mm for the fan speed of 910 rpm.**

Figure 4.20 depicts the plan view of the turbine position against circular bands of exhaust air outlet, side view of wind turbine against the wind stream, instantaneous torque against azimuth angle and angle of attack versus azimuth angle at horizontal position of  $X = 250$  mm and vertical position of  $Y = 300$  mm for the fan speed of 910 rpm. At this configuration, the highest wind speed matches to the wind turbine at  $45^\circ$  to  $95^\circ$  azimuth angle. At this region, the turbine produces higher torque and the highest torque, i.e. 0.211 Nm is generated at the azimuth angle of  $55^\circ$  with angle of attacks of  $17.1^\circ$  for blade section 1 and 5,  $18.7^\circ$  for blade section of 2 and 4, and  $18.6^\circ$  for blade section 3. The blade experiences negative angle of attack for all sections starting from azimuth angle of  $145^\circ$  and throughout the downstream side of the wind turbine. At these negative angle of attacks the instantaneous torques of the turbine rotation are negative. The mean torque for this configuration is 0.023 Nm and the turbine power generation is 0.724 W.

Figure 4.21 depicts the plan view of the turbine position against circular bands of exhaust air outlet, side view of wind turbine against the wind stream, instantaneous torque against azimuth angle and angle of attack versus azimuth angle at horizontal position of  $X = 150$  mm and vertical position of  $Y = 300$  mm for the fan speed of 910 rpm. At this configuration, the highest wind velocity region is matched with the wind turbine at the azimuth angle of  $0^\circ$  to  $45^\circ$ . However, since the turbine blades have a pitch angle of  $10^\circ$ , it is not able to generate torque at small azimuth angle (less than  $15^\circ$ ) and the sum of average torque is only generated starting from  $25^\circ$  to  $125^\circ$ . The highest torque generated is at azimuth angle of  $45^\circ$  with a value of 0.196 Nm and angle of attacks of  $16.5^\circ$  for blade section 1 and 5,  $16.6^\circ$  for blade section of 2 and 4, and  $21.1^\circ$  for the blade section 3. At the second quarter of azimuth angle, the wind velocity significantly drops until almost zero at  $180^\circ$  azimuth angle. Due to the component of velocity from the turbine rotation, this region produces negative torque.



**Figure 4.20 (a) Plan view of wind turbine position against circular bands of exhaust air outlet; (b) Side view of wind turbine against the wind stream; (c) Instantaneous torque against azimuth angle and angle of attack versus azimuth angle at horizontal position of  $X = 250$  mm and vertical position of  $Y = 300$  mm for the fan speed of 910 rpm.**

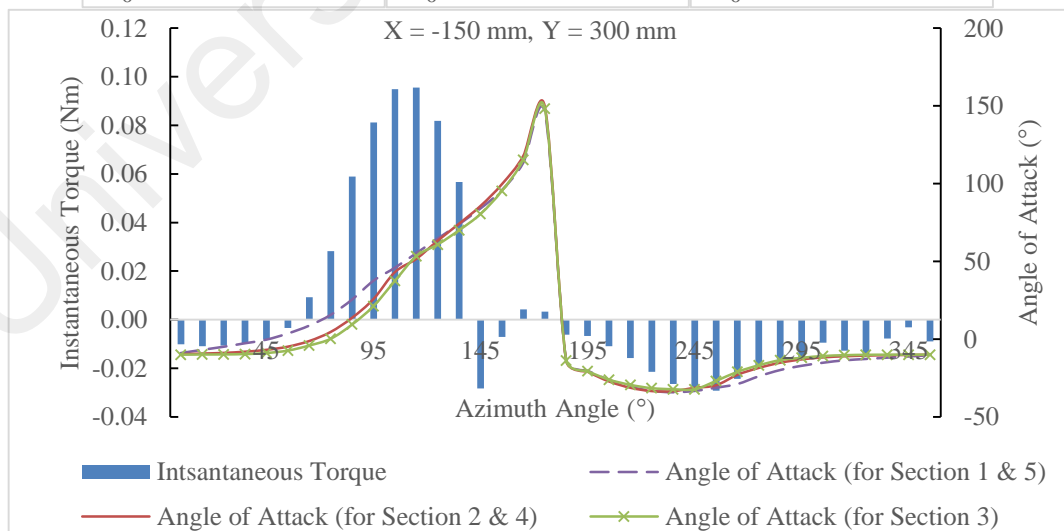
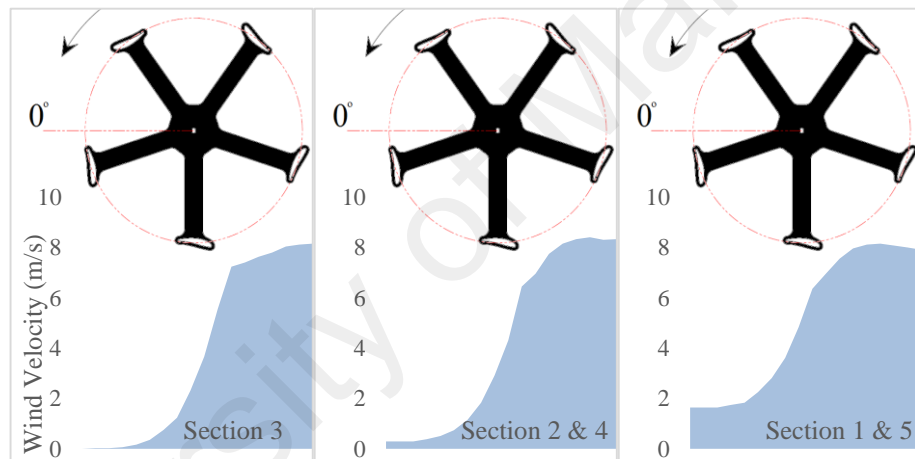
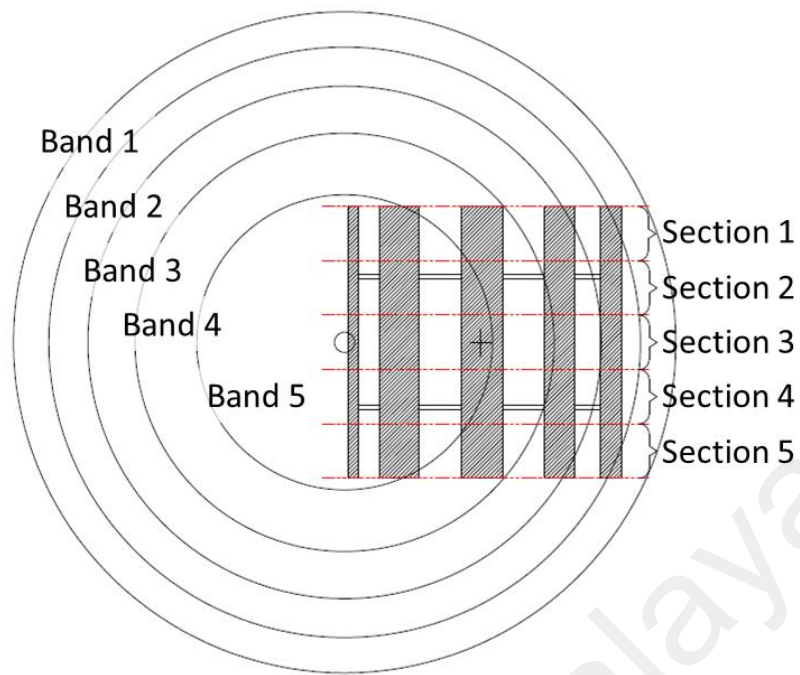


**Figure 4.21 (a) Plan view of wind turbine position against circular bands of exhaust air outlet; (b) Side view of wind turbine against the wind stream; (c) Instantaneous torque against azimuth angle and angle of attack versus azimuth angle at horizontal position of  $X = 150 \text{ mm}$  and vertical position of  $Y = 300 \text{ mm}$  for the fan speed of 910 rpm.**

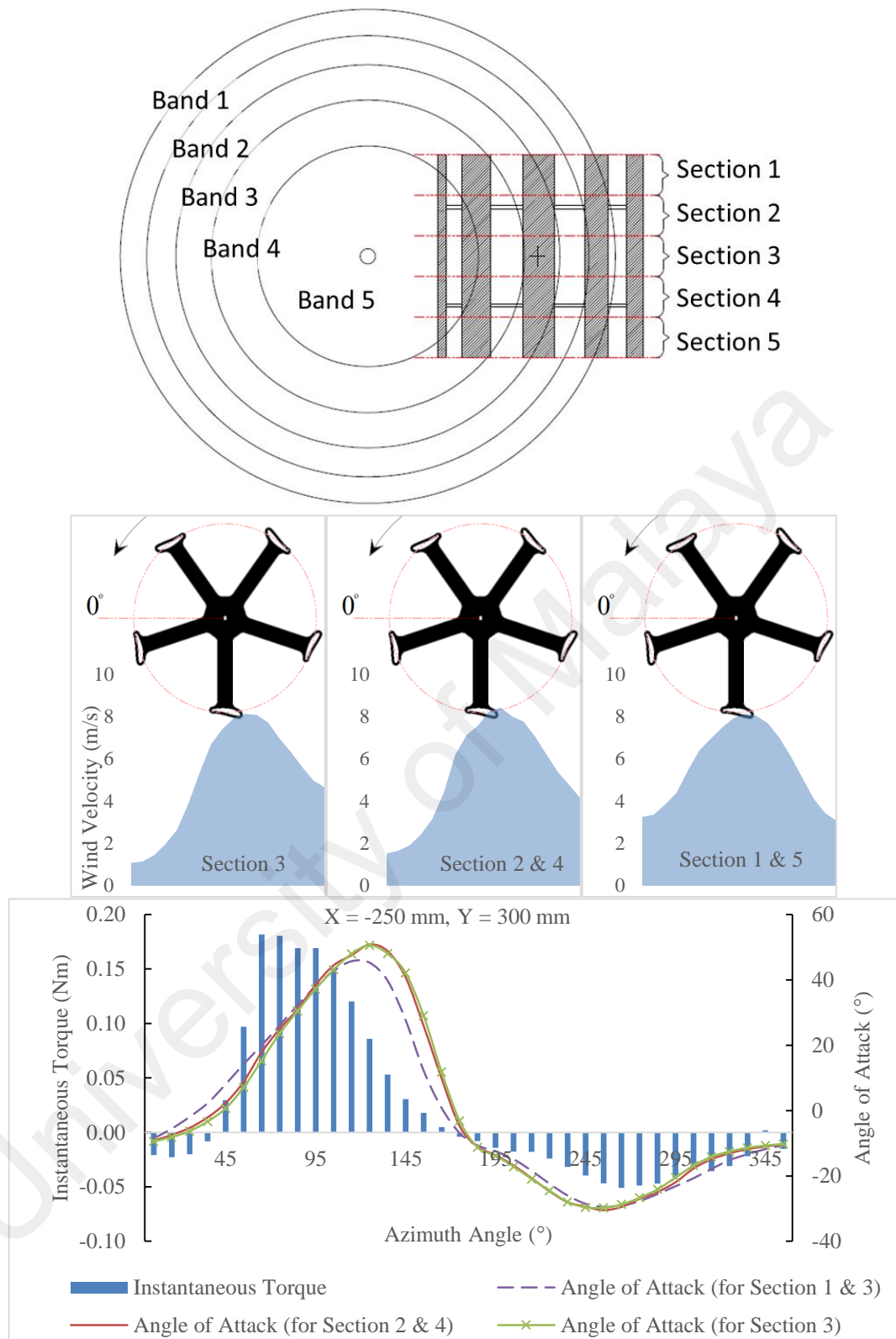


Figure 4.22 depicts the plan view of the turbine position against circular bands of exhaust air outlet, side view of wind turbine against the wind stream, instantaneous torque against azimuth angle and angle of attack versus azimuth angle at horizontal position of  $X = -150$  mm and vertical position of  $Y = 300$  mm for the fan speed of 910 rpm. This is the least preferable position in this comparison. At the first quarter of azimuth angle, the wind velocity is very low, thus the angle of attacks become negative and the blades generate negative torque. The positive torque is only generated starting from azimuth angle of  $65^\circ$  to  $135^\circ$ . However, the angle of attacks for all blade sections at this region are already high, thus the amount of positive torque generated is low. The angle of attack continues to increase until the end for the upstream azimuth angle ( $180^\circ$ ) before becoming negative at the downstream.

Figure 4.23 depicts the plan view of the turbine position against circular bands of exhaust air outlet, side view of wind turbine against the wind stream, instantaneous torque against azimuth angle and angle of attack versus azimuth angle at horizontal position of  $X = -250$  mm and vertical position of  $Y = 300$  mm for the fan speed of 910 rpm. At this configuration, the highest wind velocity region is in the range of  $75^\circ$  to  $145^\circ$  for all blade sections. The angle of attacks start with a negative value at azimuth angle of  $0^\circ$  to  $35^\circ$  for all blade sections and gradually increase until maximum at azimuth angle of  $125^\circ$ . The angle of attacks decrease after that and become negative at the downstream. The positive torque is generated between  $45^\circ$  to  $165^\circ$  with the highest torque of 0.182 Nm at azimuth angle  $75^\circ$  and angle of attacks of  $0.8^\circ$  for blade section 1 and 5,  $9.8^\circ$  for blade section of 2 and 4, and  $11.9^\circ$  for the blade section 3. The trend at this configuration ( $X = -250$  mm) is similar to the configuration at the other side ( $X = 250$  mm) because of the highest wind velocity region matches the wind turbine at almost the same azimuth angle.



**Figure 4.22 (a) Plan view of wind turbine position against circular bands of exhaust air outlet; (b) Side view of wind turbine against the wind stream; (c) Instantaneous torque against azimuth angle and angle of attack versus azimuth angle at horizontal position of  $X = -150$  mm and vertical position of  $Y = 300$  mm for the fan speed of 910 rpm.**



**Figure 4.23** Plan view of wind turbine position against circular bands of exhaust air outlet; (b) Side view of wind turbine against the wind stream; (c) Instantaneous torque against azimuth angle and angle of attack versus azimuth angle at horizontal position of  $X = -250$  mm and vertical position of  $Y = 300$  mm for the fan speed of 910 rpm.

Figure 4.24 depicts the plan view of the turbine position against circular bands of exhaust air outlet, side view of wind turbine against the wind stream, instantaneous torque against azimuth angle and angle of attack versus azimuth angle at horizontal position of  $X = -300$  mm and vertical position of  $Y = 300$  mm for the fan speed of 910 rpm. At this configuration, the highest wind velocity region matches with the wind turbine at  $45^\circ$  to  $115^\circ$  azimuth angle. The positive torque is generated between azimuth angles of  $45^\circ$  to  $135^\circ$ . The highest torque of 0.193 Nm is generated at the azimuth angle of  $55^\circ$  with the angle of attack of  $19.2^\circ$  for blade section 1 and 5,  $17.9^\circ$  for blade section of 2 and 4, and  $17.5^\circ$  for the blade section 3. According to Figure 4.18 (c), the power obtained from experiment and DMST calculation shows the closest value at configuration of  $X = -300$  mm for all vertical positions. Since some portion of the wind turbine is outside the outlet area of the cooling tower, the wind speed is determined by extrapolation of the wind velocity curve. The change of wind direction is assumed as negligible. Thus, an over prediction of power generation at  $X = -300$  mm is expected.

The behaviour of wind turbine in the non-uniform wind stream is investigated using the double multiple stream tube theory. Similar patterns of energy generation against wind turbine position are produced by the experimental result and DMST calculation. Both methods agree that the best horizontal position for the wind turbine at the outlet of the cooling tower is at  $X = 250$  mm. However, the DMST calculations result showed a lower value in power generation compared to the experimental result.

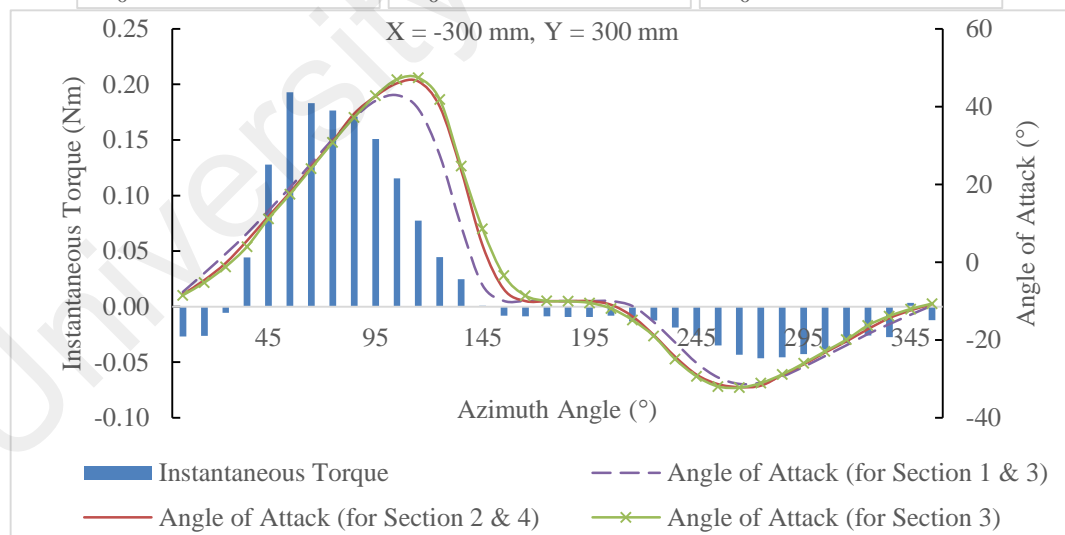
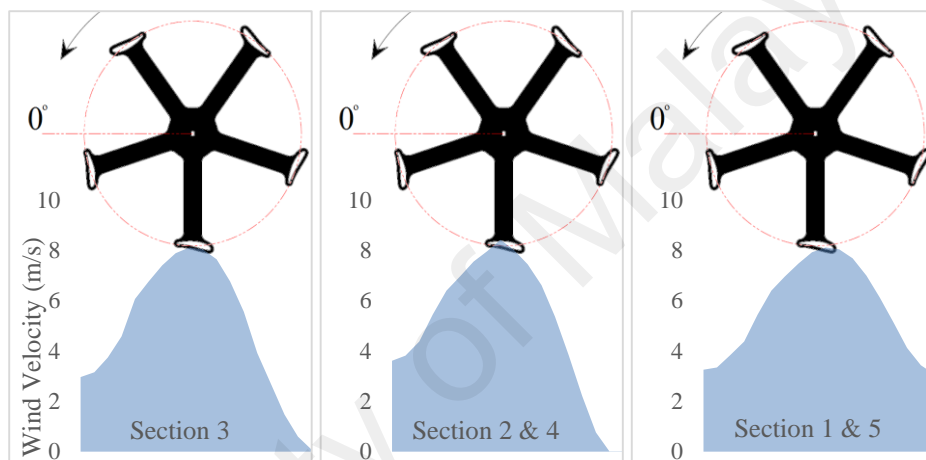
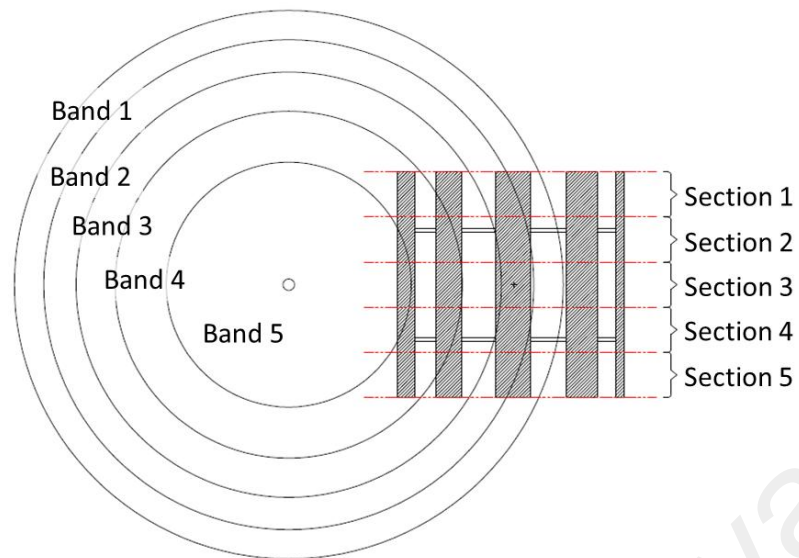


**Figure 4.24** Plan view of wind turbine position against circular bands of exhaust air outlet; (b) Side view of wind turbine against the wind stream; (c) Instantaneous torque against azimuth angle and angle of attack versus azimuth angle at horizontal position of  $X = -300$  mm and vertical position of  $Y = 300$  mm for the fan speed of 910 rpm.

The instantaneous torque against azimuth angle and angle of attack against azimuth angle is plotted for the analysis. It is clearly shown that the positioning of wind turbine in the non-uniform wind stream has a great impact on power generation. For the selected wind turbine, it is the best to matching between the highest wind velocity region to the wind turbine at the range of  $45^\circ$  to  $115^\circ$  azimuth angle. This is as shown by the wind turbine at the positions of  $X = 250$  mm and  $-250$  mm. At this range of azimuth angle, the turbine produces higher instantaneous torque and better angle of attack compared to the other azimuth angle.

#### **4.4 Dual rotor exhaust air energy recovery turbine generator with and without the diffuser-plates**

As mentioned in the methodology section, the VAWTs are placed at the horizontal position of 250 mm and -250 mm. The VAWTs are in counter-rotation where in clockwise direction for 250 mm and counterclockwise for the -250 mm (with respect to the viewing point). Figure 4.25 shows the comparison of the average rotational speed of the VAWT with and without diffuser-plates for the fan speed of 708 rpm and 910 rpm. For the fan speed of 708 rpm, there is no significant improvement at the VAWT vertical positions of 200 mm and 350 mm while at the vertical positions of 250 mm and 300 mm, the improvement of VAWT rotational speeds are 3.3% and 5.9% respectively. The low improvement of rotational speed at the wind turbine position close to the outlet is because at this position the area surrounded by the diffuser is almost the same as the outlet duct. Thus, the pressure at this area is also about the same as at the outlet plane. Then, at the vertical position of 250 mm and 300 mm, due to the slanted angle of the diffuser, the flow area has been further expanded which causes the pressure drop. According to Bernoulli's principle, a decrease in pressure or potential energy of inviscid fluid occurs simultaneously with an increase of speed (Spurk & Aksel, 2008). The effect of gravity is assumed negligible. The same trend is observed for the fan speed of 910 rpm where there

are significant improvements in rotational speeds at the vertical positions of 250 mm and 300 mm. The improvements are 8.1% and 10.3% respectively.

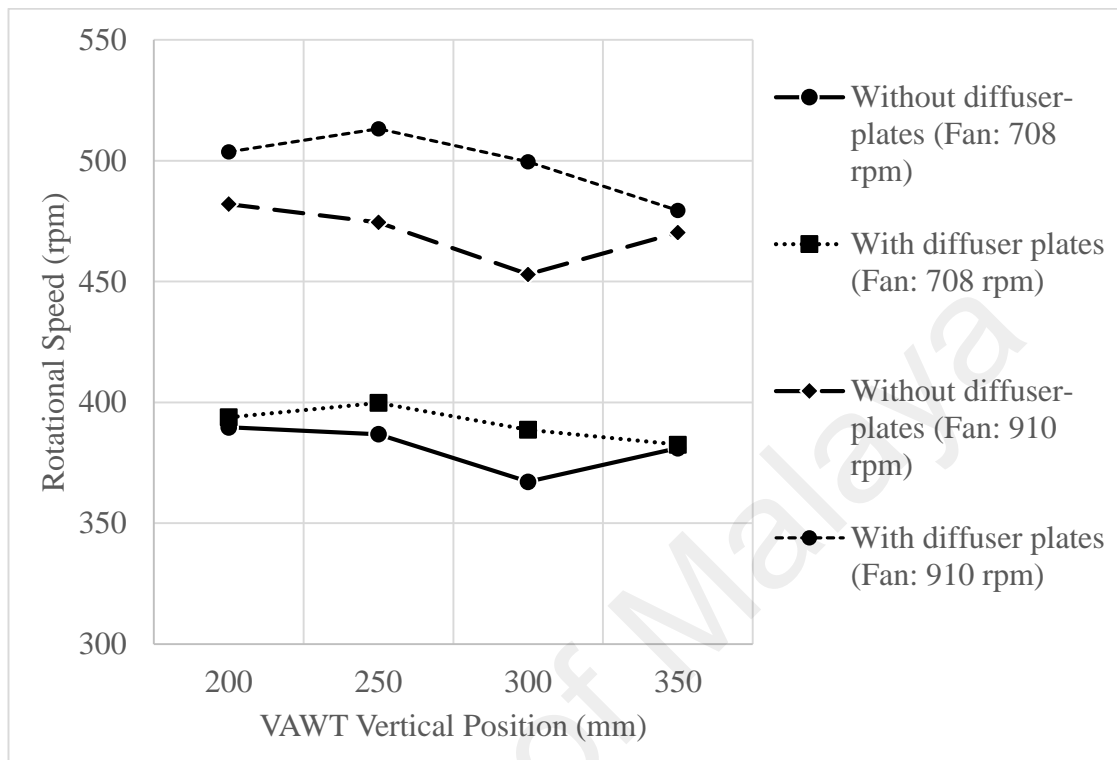


**Figure 4.25 Comparison of free running rotational speed of VAWT for the condition with and without the integration of diffuser-plates. The rotational speed values are the average from 2 VAWTs.**

Figure 4.26 depicts the comparison for the average power generation by the VAWT for the condition with and without the integration of diffuser-plates. The VAWT average power generations demonstrate similar trends to the rotor rotational speeds. At both fan speeds, the highest improvement in power generation with the integration of diffuser-plates is at the vertical distance of 300 mm with the increments of 20% and 27% for fan speed of 708 rpm and 910 rpm respectively. These results of wind turbine performance show that the best horizontal position for the exhaust air energy recovery turbine generator with the integration of diffuser-plates is at 300 mm distance to the exhaust air outlet plane. This distance is equivalent to the radius of the wind turbine.

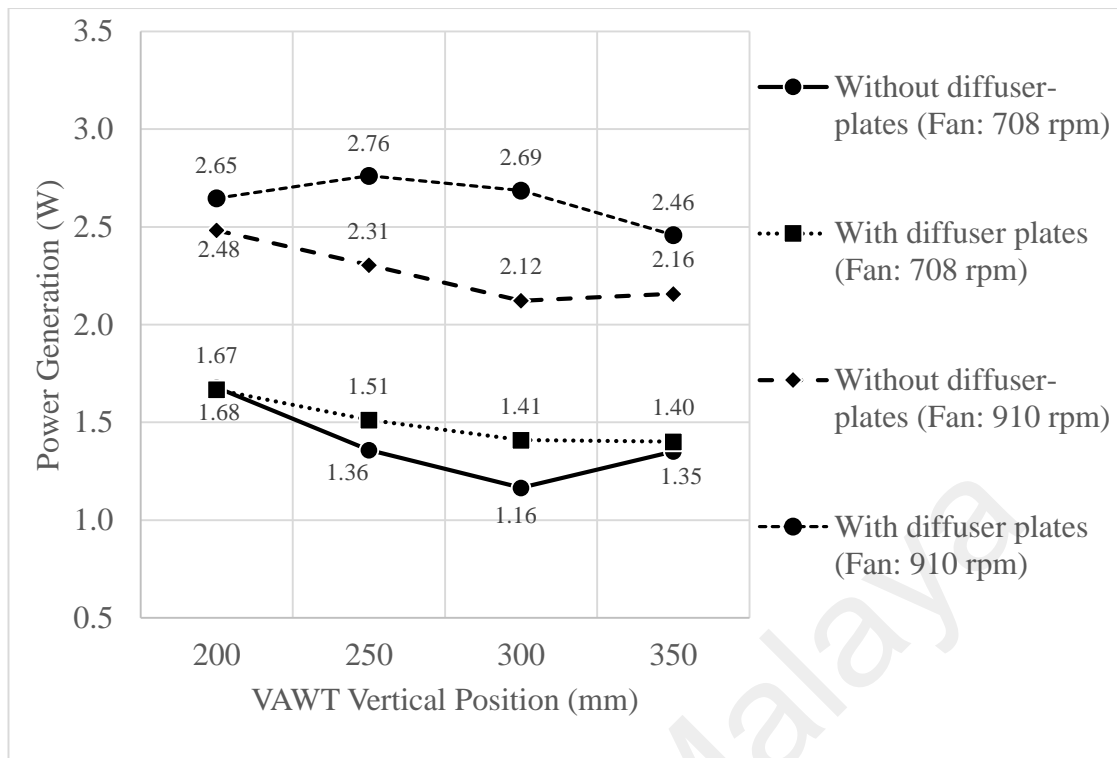


**Figure 4.26 Comparison the average power generation by the VAWT for the condition with and without the integration of diffuser-plates**

#### 4.4.1 Cooling tower performance

Figure 4.27 illustrates the comparison of the fan motor power consumption for the bare cooling tower, cooling tower with the VAWT and the cooling tower with the VAWT integrated with diffuser-plates at various vertical VAWT positions. Significant increases in fan motor power consumption are shown for the cooling tower with the VAWT integrated with diffuser-plates at the vertical position of 200 mm for both fan speeds. This is due to the blockage effect created by the presence of the diffuser and the VAWT at the position very close to the exhaust air outlet plane. At this distance, the expansion of the diffuser is still very small, thus the pressure drop is yet to be significant. The power consumption of the configuration of VAWT with diffuser-plates is lower than the bare cooling tower at the vertical position of 350 mm for both fan speeds.



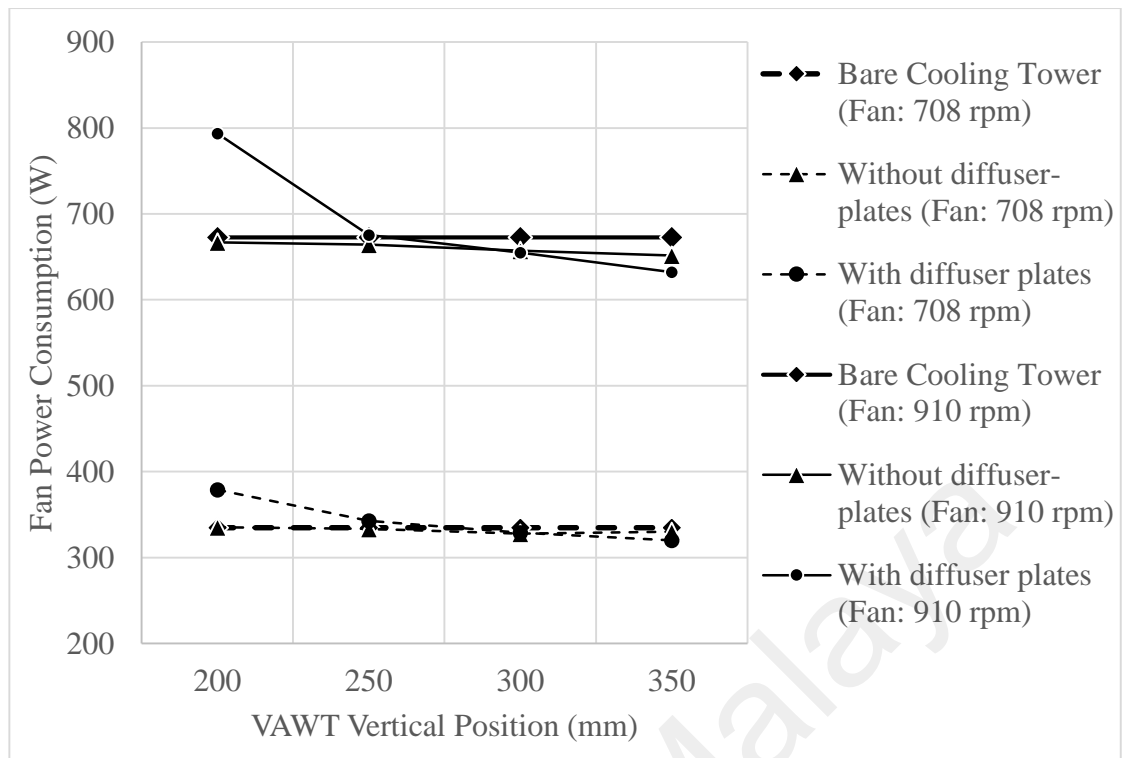


**Figure 4.27 Comparison of the fan motor power consumption for the bare cooling tower, cooling tower with the VAWT and the cooling tower with the VAWT integrated with diffuser-plates at various vertical VAWT positions.**

Figure 4.28 shows the comparison of the cooling tower intake flow rate for the bare cooling tower, cooling tower with the VAWTs and the cooling tower with the VAWTs integrated with diffuser-plates at various vertical VAWT positions. As discussed in the previous section, the presence of wind turbine at the outlet of the cooling tower improves its intake flow rate. With the integration of diffuser to the VAWT, there are no significant improvements in the air flow rate of the cooling tower compared to the cooling tower with VAWT only. Since both conditions produce higher flow rate compared to the bare cooling tower, these conditions are considered as positively affecting the cooling tower air flow rate performance.

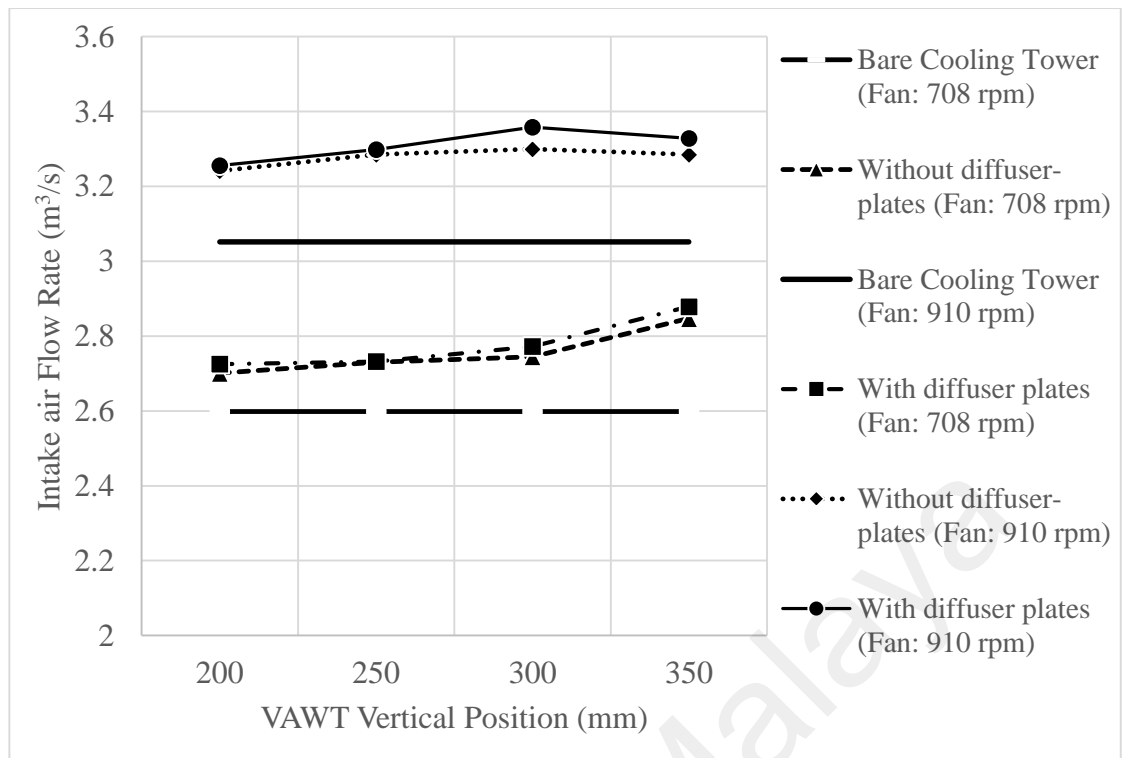


**Figure 4.28 Comparison of the cooling tower intake flow rate for the bare cooling tower, cooling tower with the VAWT and the cooling tower with the VAWT integrated with diffuser-plates at various vertical VAWT positions.**

#### 4.4.2 Overall performance comparison

Conclusion remark is made based on the summary in Table 4.5 and 4.6. For the fan speed of 708 rpm, the amount of energy recovery is about the same to each other for all vertical VAWT positions with 0.44%. However, considering the cooling tower performance, when the VAWT distance is at 250 mm or closer to the outlet plane, the power consumption of the fan motor is increased. This negatively affected the cooling tower performance and hence the coefficient of performance of the cooling system. Integration of the VAWT with diffuser at the outlet of the cooling tower at distances of 300 mm and 350 mm do not negatively affect the cooling tower performance. Thus, this configuration can be accepted for the energy recovery application. On the other hand, for the fan speed of 910 rpm, the highest energy recovery for the VAWT with diffuser at the outlet of the cooling tower occurs at the vertical position of 300 mm with 0.41%. At this condition, the cooling tower's airflow rate is improved while the fan consumption is

reduced. Comparing the configuration with and without diffuser-plates, energy recovery at 300 mm vertical distance also shows the highest increment, i.e. by 27%.

University of Malaya

**Table 4.5 Summary of cooling tower performance and wind turbine performance for the bare cooling tower, cooling tower with diffuser-plates integrated VAWT and cooling tower with VAWT only for the fan speed of 708 rpm.**

Fan speed: 708 rpm																	
Wind Turbine Position		Airflow rate			Fan consumption				Average VAWT Rotational Speed			Average Maximum Power Generation			Energy Recovery		
VAWT Horizontal Position, X (mm)	VAWT Vertical Position, Y (mm)	Bare Cooling Tower (m <sup>3</sup> /s)	Without diffuser-plates	With diffuser-plates	Bare Cooling Tower (W)	Without diffuser-plates	With diffuser-plates	% of difference with diffuser-plates compared to without diffuser -plates	Without diffuser-plates	With diffuser-plates	% of difference with diffuser-plates compared to without diffuser-plates	Without diffuser-plates (W)	With diffuser-plates (W)	% of difference with diffuser-plates compared to without diffuser-plates	Without diffuser-plates (%)	With diffuser-plates (%)	% of difference with diffuser-plates compared to without diffuser-plates
			% of difference compared to bare cooling tower			% of difference compared to bare cooling tower											
250	200	2.60	3.93%	4.86%	335	0.14%	13.17%	13.02%	390	394	1.07%	1.68	1.67	-0.60%	0.50	0.44	-12.05%
250	250	2.60	5.06%	5.14%	335	-0.41%	2.34%	2.77%	387	400	3.35%	1.36	1.51	11.29%	0.41	0.44	8.29%
250	300	2.60	5.62%	6.68%	335	-2.07%	-1.76%	0.32%	367	389	5.86%	1.16	1.41	20.25%	0.36	0.43	19.86%
250	350	2.60	9.55%	10.78%	335	-1.41%	-4.38%	-3.01%	381	383	0.38%	1.35	1.40	4.27%	0.41	0.44	7.51%

**Table 4.6 Summary of cooling tower performance and wind turbine performance for the bare cooling tower, cooling tower with diffuser-plates integrated VAWT and cooling tower with VAWT only for the fan speed of 910 rpm.**

Fan speed: 910 rpm																	
Wind Turbine Position		Airflow rate			Fan consumption				Average VAWT Rotational Speed			Average Maximum Power Generation			Energy Recovery		
VAWT Horizontal Position, X (mm)	VAWT Vertical Position, Y (mm)	Bare Cooling Tower (m <sup>3</sup> /s)	Without diffuser-plates	With diffuser-plates	Bare Cooling Tower (W)	Without diffuser-plates	With diffuser-plates	% of difference with diffuser-plates compared to without diffuser -plates	Without diffuser-plates	With diffuser-plates	% of difference with diffuser-plates compared to without diffuser-plates	Without diffuser-plates (W)	With diffuser-plates (W)	% of difference with diffuser-plates compared to without diffuser-plates	Without diffuser-plates (%)	With diffuser-plates (%)	% of difference with diffuser-plates compared to without diffuser-plates
			% of difference compared to bare cooling tower			% of difference compared to bare cooling tower											
250	200	3.05	6.22%	6.70%	673	-0.86%	17.95%	18.98%	482	504	4.49%	2.48	2.65	6.63%	0.37%	0.33%	-10.38%
250	250	3.05	7.66%	8.09%	673	-1.28%	0.37%	1.68%	475	513	8.15%	2.31	2.76	19.82%	0.35%	0.41%	17.85%
250	300	3.05	8.13%	10.05%	673	-2.33%	-2.68%	-0.35%	453	500	10.30%	2.12	2.69	26.58%	0.32%	0.41%	27.03%
250	350	3.05	7.66%	9.09%	673	-3.13%	-6.05%	-3.02%	470	480	1.95%	2.16	2.46	13.96%	0.33%	0.39%	17.50%

Further discussion is made based on the best configuration of dual rotor exhaust air energy recovery turbine generator for the cooling tower fan speed of 910 rpm, i.e. at vertical position of 300 mm and horizontal position of 250 mm (for clockwise turbine) and -250 mm (for counter clockwise turbine). The results from all the three configurations, i.e. 1) bare cooling tower, 2) cooling tower with dual-rotor exhaust air energy recovery turbine generator, and 3) cooling tower with diffuser integrated dual-rotor exhaust air energy recovery turbine generator, are evaluated. The first configuration (bare cooling tower) is considered as the baseline for the experiment where it represents the performance of an original cooling tower without any additional feature. The results are tabulated in Table 4.7.

**Table 4.7 Test results of different configurations of cooling tower model.**

Configuration	Intake Flow Rate (m <sup>3</sup> /s)	Fan Motor Power Consumption (W)	Rotational Speed (rpm)		
			VAWT 1	VAWT 2	Average
Bare Cooling	3.05	672.8	-	-	
Cooling Tower with Dual-rotor Exhaust Air Energy Recovery Turbine Generator	3.45	660.8	453.0	459.9	456.4
Cooling Tower with Diffuser Integrated Dual-rotor Exhaust Air Energy Recovery Turbine Generator	3.36	656.34	502.2	497.0	499.6

The original cooling tower model performance is considered when there is no additional feature on the model. In this condition, the intake flow rate is 3.05 m<sup>3</sup>/s and the power consumption by the fan motor is 672.8 W (for the fan rotational speed of 910 rpm). When the 2 units of VAWT are installed at the outlet of the cooling tower model, the average maximum rotational wind speed for both VAWTs is 456.4. The intake air flow rate increases to 3.45 m/s while the power consumption drops to 660.76 W. Theoretically,

this may be due to the speed of the turbines being faster than the discharged wind speed. When the speed of the turbine is higher than the incoming wind, a low pressure region is created surrounding the wind turbine swept area, which may help the cooling tower to draw more air due to the suction effect. This condition contributed to the increase in intake wind speed and reduction of fan motor power consumption.

When the diffuser is in place with the VAWTs, the performance of the cooling tower model and VAWTs is further improved. The fan power consumption is further reduced to 656.3 W which is 1.76% and 0.67% compared to the bare cooling tower and the cooling tower with the VAWTs respectively. The intake air flow rate is increased by 10% compared to the bare cooling tower, but reduced by comparison to the cooling tower with the VAWT. The average rotational speed for the VAWTs with diffuser is 499.6 rpm, a 9.75% increase from the VAWTs without diffuser. These results proved that the diffuser has served its purpose in improving the VAWTs performance without negatively affecting the performance of the cooling tower.

## **CHAPTER 5: ENERGY RECOVERY ESTIMATION AND TECHNO- ECONOMIC ANALYSIS OF THE EXHAUST AIR ENERGY RECOVERY TURBINE GENERATOR ON AN ACTUAL COOLING TOWER**

### **5.1 Introduction**

In this chapter, an energy recovery estimation is conducted based on an actual size of a cooling tower that is commonly installed in Malaysia. The projection is based on the life-span of the designed system according to THE life cycle analysis (LCA). This analysis takes into account the time value of money and allows detail consideration of the complete range of costs. It also includes inflation rates when estimating future expenses (Kalogirou, 2013). It is an analytical procedure for the systematic evaluation of the environmental aspects of a product, process, or service system throughout its life cycle (Bhakar, Uppala, Digalwar, & Sangwan, 2013). However, challenges in using LCA include poor data availability, erratic economic changes, uncertainties regarding discount rate, inflation rate, asset life, and estimating future operating and maintenance costs (Naghavi, 2010).

Many researchers have applied this approach in the renewable energy sector with the main purpose of identifying the environmental impacts on goods and services during the whole life cycle of the product or service. Guezuraga, Zauner, and Pölz (2012) made a conclusion that wind energy is among the cleanest sources of energy available nowadays based on the LCA on 2 MW class wind turbines. The evaluation of electricity supply between standalone renewable energy system and national grid network to the remote area has also been investigated by this approach. From a case study in Turkey, an optimized size of PV/wind hybrid energy system with battery storage is more economical than the extension of electricity to a remote area (Ekren, Ekren, & Ozerdem, 2009).



According to the net present value, the feasible power supply system has been sorted to assess the possibility of supplying electricity from a solar–wind hybrid renewable system to a remotely located model community detached from the main electricity grid in Ethiopia (Bekele & Palm, 2010).

For the exhaust energy recovery turbine generator, the economic analysis is conducted to evaluate the payback period and the earnings from the energy recovery generated by the system. Capital cost, component replacement cost, operation and maintenance cost, and energy cost will be included in this study.

## **5.2 Methodology**

### **5.2.1 Cooling tower and wind turbine matching**

The assessment common size of cooling tower in Malaysia's market is referred to market share by the cooling tower manufacturer, Truwater Cooling Towers Sdn. Bhd. (Truwater). Truwater is the largest cooling tower manufacturer in Malaysia which specializes in the wet and hybrid type of cooling towers since the last 20 years. The company has constructed very highly efficient and environmentally friendly cooling towers for the various industries such as air-conditioning, power generation, biomass co-generation, petrochemical, chemical, oil & gas, steel mills, food and other processing industries ("Truwater Cooling Towers Sdn. Bhd.,"). According to Truwater, its market share is approximately 45% of the total industry in Malaysia with their installed quantity about 11,000 units up to September 2012. One of the most common sizes of cooling towers that is being installed in Malaysia is the induced-draft counter-flow cooling tower with the outlet diameter of 2.4 m and powered by a 7.5 kW fan motor. Thus, this cooling tower specification is chosen for the energy recovery estimation and techno-economic analysis of the exhaust air energy recovery turbine generator. Figure 5.1 shows the drawing of a modular counter-flow cooling tower manufactured by Truwater. It is

designed for air conditioning and industrial process cooling applications (Truwater, 2011).

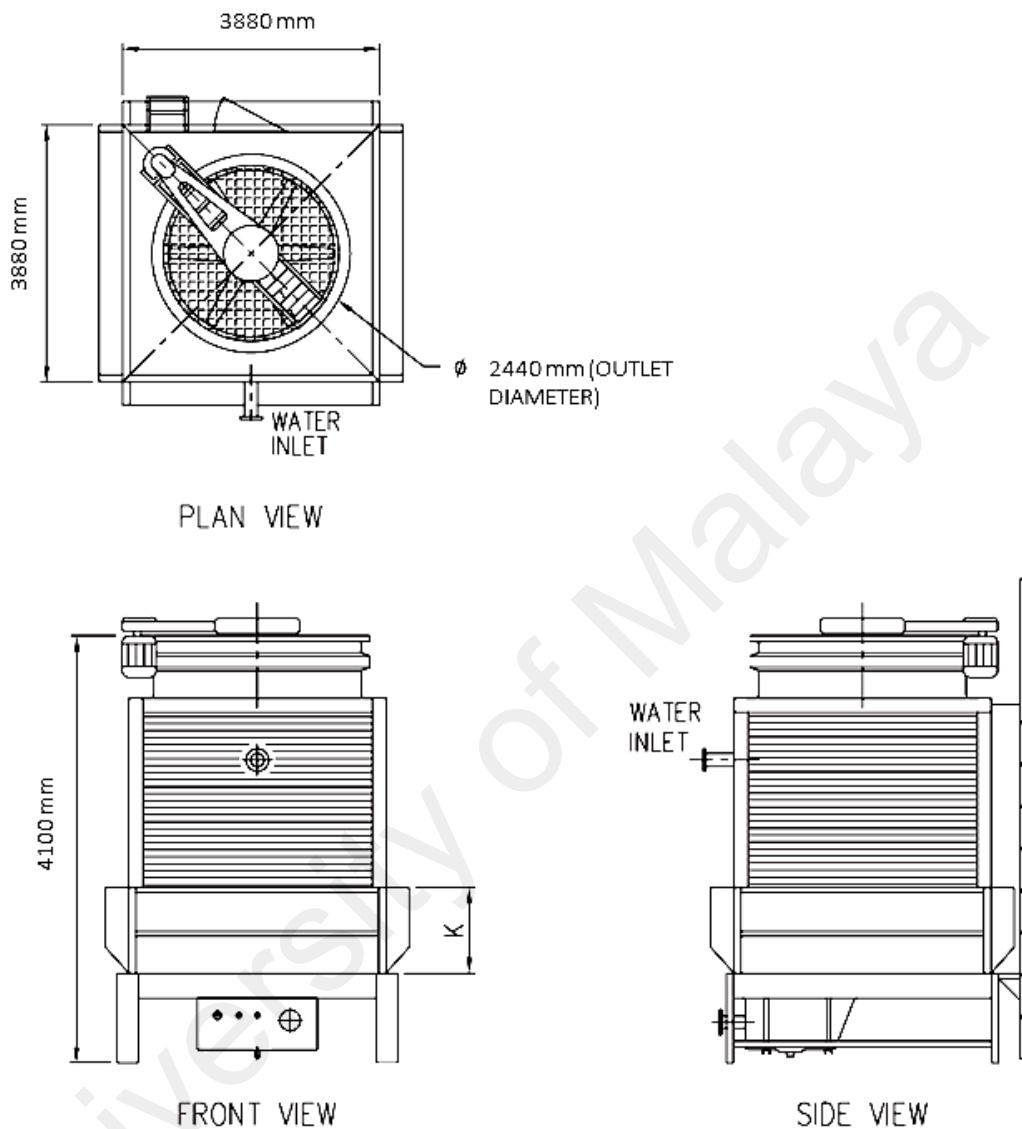


**Figure 5.1 Modified screenshot of the cooling tower model TCS 300-1B from Truwater (Truwater, 2011).**

A preliminary test is carried out at the Truwater factory which has a ready demonstration unit of this model. This unit of cooling tower was certified by Cooling Tower Institute from the US. The purpose of this preliminary test is to assess the outlet wind velocity and its profile. Using the same procedure as explained in Chapter 4, the obtained data is plotted in Figure 5.2. The overall average outlet wind velocity is calculated as 8.5 m/s. Based on this wind velocity and the cooling tower outlet area, the calculated available wind power is about 2000 W.

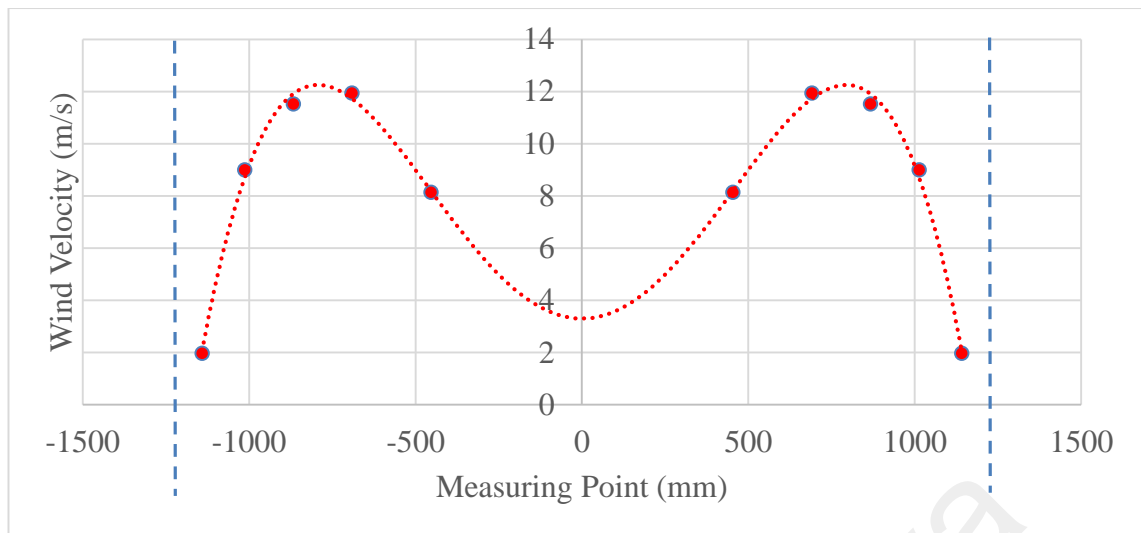


**Figure 5.2 Mean wind velocity at the outlet of the cooling tower.**

Based on the outlet area and the discharge velocity of the cooling tower, a commercially available wind turbine is selected for the installation. A curved-blade Darrieus VAWT is suitable for this purpose due to its shape matches well with the cooling tower outlet. A company in Taiwan, i.e. Hi-VAWT Technology Corporation manufactures wind turbines of this type. Based on available area at the outlet of the cooling tower, 500 W curved-blade Darrieus is used in this estimation. A supporting structure is used to support the entire system at both ends of the transmission shaft. It was installed above a demonstration unit of the cooling tower, and positioned in cross-wind orientation with the generator at a side and the bearings at the other side. Figure 5.3 depicts installation set-up of 500 W VAWT with diffuser at the outlet of cooling tower. Surrounding the wind turbine, a supporting structure is expected to be built in the shape of a diffuser. According to the discharged wind velocity, power augmentation by the diffuser and VAWT specifications, the VAWT is expected to generated power at its rated value.

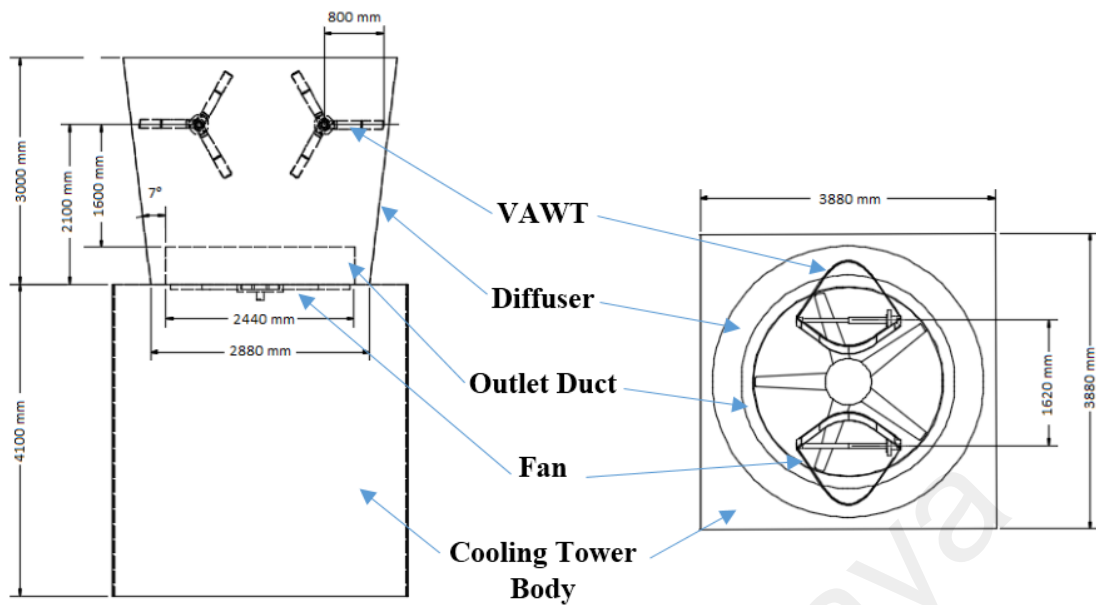


**Figure 5.3 Simplified front view and top view of the installation setup.**

### 5.2.2 Economic assessment

Initial capital, operating cost and payback time for any system is very important for investors. Renewable energy systems are generally characterized by high capital cost but low operation costs make it cost-effective in the long run (Hafez & Bhattacharya, 2012). For the assessment, the economic analysis is done by using the life-cycle costing (LCC) method to calculate the entire life-cycle cost such as the net present value and payback period of both capital and operating expenses over the life of the system. The analysis only considers the cost of additional installation and maintenance of the exhaust air energy recovery wind turbine generator and does not include the cooling tower economic aspect. The initial capital of the investment includes the purchase of the wind turbine system, supporting structure and the first year of operation and maintenance. The wind turbine system is the combination of 2 units of VAWT, an inverter, a controller and a set of batteries. The battery set needs to be replaced in 5 years and the inverter and controller need to be replaced in 10 years. The supporting structure design is inclusive of the diffuser. The estimated costs for the economic analysis is tabulated in Table 5.1. These

costs are estimated based on the information acquired from and presented in the Appendix E.

**Table 5.1 Estimated system components price and operating cost.**

Description	Cost (RM)
Initial Costs	
Turbine generator (2 units including inverter and controller)	11,000.00
Batteries	2,000.00
Diffuser and supporting structure	2,500.00
<b>Total capital cost</b>	<b>15,500.00</b>
Operating costs	
Batteries (every 5 years)	1,000.00
Inverter (every 10 years)	2,000.00
Controller (every 10 years)	1,500.00
Estimated annual operation and maintenance cost	1,000.00

The cooling towers for commercial buildings commonly operate for long-hours per day. For the economic assessment, the cooling towers are assumed to be installed at commercial areas (i.e. shopping malls, hospitals, etc.) in Peninsular Malaysia using low voltage commercial tariff operating for 20 h daily and 30 days in a month. The commercial tariff of electricity provided by the utility provider is RM 0.43/kWh ("Low Voltage Commercial Tariff.," 2015). According to the electricity price trend, tariff rate is predicted to rise by 10% annually (W. T. Chong et al., 2011). Apart from that, inflation rate for components replacement cost and operation and maintenance cost is taken into account which will increase by of 4% yearly as reported by the Department of Statistics Malaysia ("Malaysia Inflation Rate," 2014). To determine the present value (*PV*) of income for  $N^{th}$  period (usually year) in the future, the following equation is used

$$PV = \frac{1}{(1+i)^N} \quad (5.1)$$

where  $i$  represents the estimated annual inflation rate.  $PV$  is used to return the value of the future payments or incomes on a given period to present value (Newnan, Eschenbach, & Lavelle, 2012). Then, the net present value ( $NPV$ ) is calculated to obtain the sum of the present values of the individual cash flow. The economic parameter for the exhaust air energy recovery turbine generator system assessment are tabulated in Table 5.2.

**Table 5.2 Economic parameters**

<b>Economic Parameter</b>	<b>Value</b>	<b>Reference</b>
Electricity price (per kWh)	RM 0.43	("Low Voltage Commercial Tariff.," 2015)
Annual electricity price increment	10%	(W. T. Chong et al., 2011)
Inflation rate of inverter price	4%	("Malaysia Inflation Rate," 2014)
Inflation rate of battery price	4%	
Inflation rate of inverter price	4%	
Inflation rate of operation and maintenance cost	4%	

### **5.3 Results and discussion**

#### **5.3.1 Energy recovery estimation**

For the considered size of cooling tower with 2.4 m outlet diameter, 2 units of VAWT is expected to be installed at the exhaust air energy recovery turbine generator. As its design includes the diffuser for power augmentation and the high wind velocity available, both turbines are expected to generate power at the rated value. Thus, 1 kW of power is expected to be generated by the twin rotors as energy recovery from a 7.5 kW rated cooling tower power consumption. The estimation of energy recovery is tabulated in Table 5.3. Based on this estimation, the exhaust air energy recovery turbine generator is expected to recover 13.3% of the energy consumed by the fan motor of the cooling tower.

**Table 5.3 Projection of power recovered by an exhaust air energy recovery turbine generator with twin-rotor installed on a single unit of cooling tower.**

Mode	Operating Hour	Fan Motor Power Consumption	Total Power recovered	Percentage of Energy Recovery
Day	20 h / day	150 kWh / day	20 kWh / day	13.3%
Year	7300 h / year	54,750 kWh / year	7,300 kWh / year	

### 5.3.2 Economic assessment

The economic analysis is done with the consideration of operation cost and energy generated by the system based on a 20-year life cycle analysis. This is because according to ASHRAE, the life expectancy of a cooling tower to work in acceptable efficiency is 20 years (2013). An optimized exhaust air energy recovery turbine generator is considered to generate 13.3% of discharged energy tabulated from the power consumption of the cooling tower fan as estimated in the previous section. The initial capital required for the entire system is RM 15,500 which consists of 2 units of wind turbines, inverter, diffuser-plates and supporting structure. The life cycle analysis is illustrated in Figure 5.4. It is observed that the designed system has a payback period of 7 years with net present value of RM 1,536. Even though some components need to be replaced every 5 years the earnings from the energy savings will be able to compensate the replacement cost of the breakeven year. The net present value of the system at the end of the life cycle of the analysis is RM 25,347. The cumulative recovered energy value at the end of the life cycle of the system is RM 179,189 (Figure 5.5).

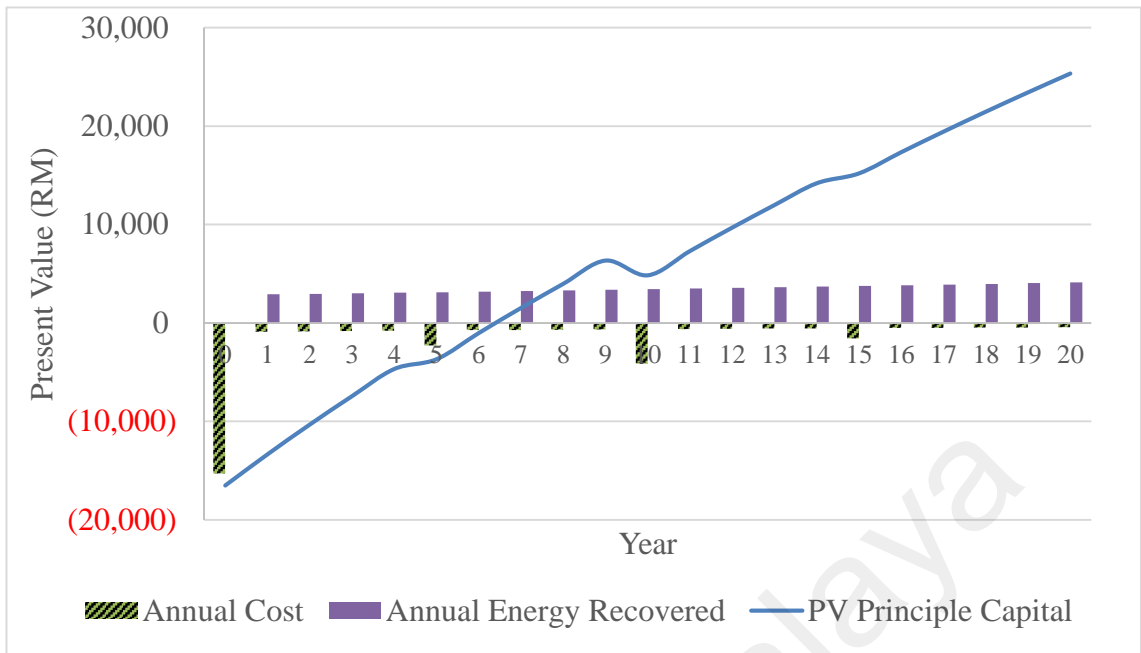


**Figure 5.4 Cost analysis of the exhaust air energy recovery generator (20 years life cycle).**

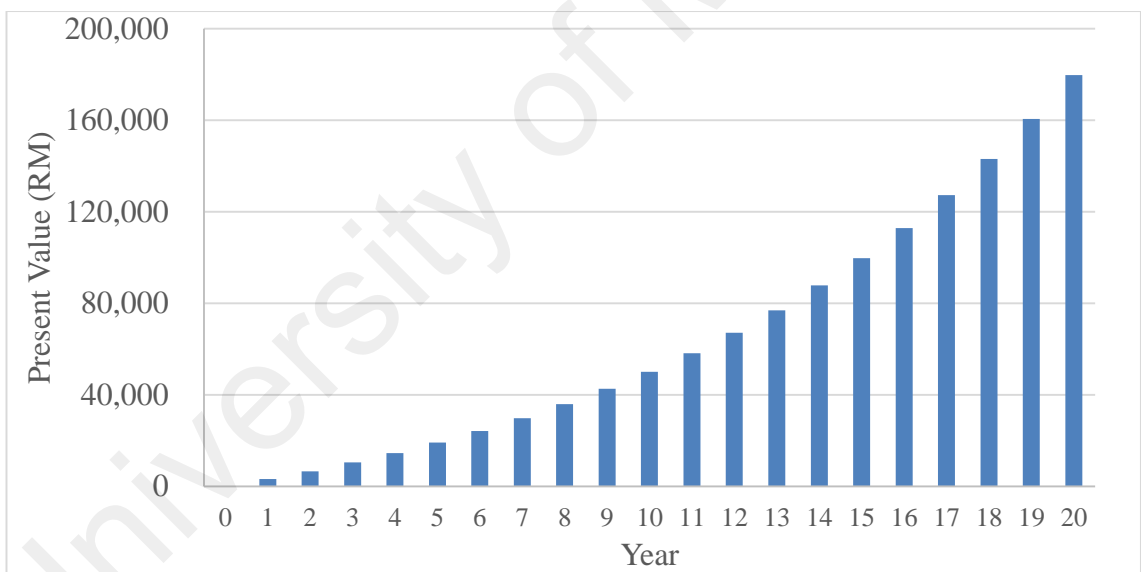


**Figure 5.5 Cumulative value of recovered energy**

#### 5.4 Summary

In this chapter, a techno-economic analysis has been carried out on the novel exhaust air energy recovery wind turbine generator installed on a cooling tower commonly used in Malaysia. For the cooling tower with a 7.5 kW rated fan motor, 13.3% of the discharged energy is expected to be recovered. For a year of operation of the cooling tower with this system, approximately 7.3 MWh is estimated to be recovered. Economic analysis shows



that capital, components replacement, and operation and maintenance costs of the system are covered in the lifetime of the system. For this project, the NPV is RM 25,347 for the 20-years lifetime.

University of Malaya

## CHAPTER 6: CONCLUSIONS AND RECOMMENDATIONS

### 6.1 Conclusions

In this thesis, a novel exhaust air energy recovery turbine generator is designed to recover part of the energy discharged from an exhaust air system. A vertical axis wind turbine (VAWT) in cross-wind orientation is mounted above a cooling tower's exhaust fan to harness the wind energy for producing electricity. The performance of the VAWT and its effects on the cooling tower were investigated by experiment. A small scale cooling tower is fabricated to mimic the actual counter-flow induced draft cooling tower. To hold the VAWT and dynamometer in place, a supporting structure is constructed independently of the cooling tower model. The supporting structure is a modular design where the wind turbine position can be moved vertically and horizontally to study the performance in various configurations.

The wind from the discharge outlet is generated by fan which is not uniform in profile. Thus, the VAWT behavior is different depending on its position in the non-uniform wind stream. From the experiments, it is determined that the best horizontal position of the VAWT with a diameter of 300 mm at the outlet of the cooling tower with an outlet diameter of 730 mm is when the center of the turbine is at a distance of 250 mm from the center of the outlet. The distance is about  $\frac{2}{3}$  of the outlet radius. However, the vertical distance of the VAWT to the outlet is different depending on the fan speed. Based on the evaluation on the VAWT performance as well as the cooling tower performance, the best configuration of the system at fan speed of 708 rpm is when the VAWT is at horizontal position of 250 mm and vertical position of 350 mm. At this configuration, the cooling tower's flow rate was improved by 9.55%, the fan motor power consumption was reduced by 2.07% while the turbine was generating energy. For the fan speed of 910 rpm, the best

VAWT position at the outlet of the cooling tower is at horizontal position of 250 mm and vertical position of 400 mm where the air flow rate of the cooling tower and fan motor consumption showed a 9.09% increase and 3.92% decrease respectively.

The theoretical analysis is conducted based on the double multiple stream tube (DMST) theory. It is done via a semi-empirical approach where the wind velocities and the wind turbine rotational speeds are taken from the experiment. The DMST analysis produced similar patterns of graphs to the experimental result which indicates an agreement between these two analyses. Theoretical analysis explains the wind turbine behavior in the not uniform wind stream as acquired from the experiment. It is concluded that the positioning of the wind turbine in the non-uniform wind stream has a great impact on power generation. For the selected wind turbine, it is best to match the highest wind velocity region to the wind turbine at the range of  $45^\circ$  to  $115^\circ$  azimuth angle. This is as shown by the wind turbine at the positions of  $X = 250$  mm and  $-250$  mm. At this range of azimuth angle, the turbine produces higher instantaneous torque and better angle of attack compared to the other azimuth angles.

For the fabricated cooling tower model, it is possible to accommodate 2 units of VAWT to become a dual rotor energy recovery turbine generator. Thus, the experiment on this configuration was conducted with the best VAWT horizontal position and varying the vertical position. With the same setup, a pair of diffuser-plates was added as a power-augmentation device. It is found that the dual rotor exhaust air energy recovery turbine generator produced the best performance at the VAWT vertical distance of 300 mm to the outlet plane. The integration of diffuser-plates further improved the VAWT performance with 20% and 27% for the fan speed of 708 rpm and 910 rpm respectively. At 910 rpm, with the diffuser-plates, the cooling tower air flow rate improved by 10.05% and the fan consumption decreased by 2.68% compared to the bare cooling tower. It also

improved the energy recovery by 27.03% compared to the VAWT without diffuser-plates.

For long term projection, energy recovery estimation and techno-economic analysis of exhaust air energy recovery turbine generator on an actual cooling tower is conducted. It is estimated that 13% of the energy from the common cooling tower with the outlet size of 2.4 m and rated motor consumption of 7.5 kW is recovered. For the cooling tower that operates for 20 hours per day, every day throughout the year, a sum of 7,300 kWh/year is expected to be recovered. Life cycle assessment for 20-year life span which takes into account full range of costs showed that the payback period for the system of this size is 7 years. The net present value of the system at the end of the life cycle of the analysis is RM 25,347. The cumulative recovered energy value at the end of the life cycle of the system is RM 179,786.

## **6.2 Contributions**

The thesis provides an innovative contribution to the development of energy recovery methods. It is aimed at generating on-site clean energy by converting wasted wind energy from an exhaust air system to a useful form of energy. The energy generated is predictable and continuous because the exhaust wind is readily available whenever the cooling tower is switched on. In other words, exhaust air consists of wind characteristic that is predictable and consistent. Thus, statistical analysis of wind characteristic over a period of time is not required. This energy recovery system has a high market potential due to abundant usage of exhaust air systems. It promotes the sustainability, energy conservations and green technologies.

Another contribution is on the analysis of non-uniform wind turbine using the DMST theory. The existing theory is applied in a novel way to get the aerodynamic parameters at various azimuth angle along the rotation of the vertical axis wind turbine. The

developed model can be used for both uniform and non-uniform wind conditions. It is a useful model for prediction the torque and power for vertical axis wind turbine.

### **6.3 Limitations**

The presented result is only valid for the specific geometry of the design only. This is because there are many varieties of wind turbines and exhaust air systems available. Different types exhaust air system may be in different configuration and use different type of fan that produce different wind characteristic. Similarly, the wind turbines may also have different airfoil types and shapes that respond differently to the wind. However, the methodology presented the method of analyzing the system with different geometry.

### **6.4 Recommendations**

It needs to be understood that there are so many variations of exhaust air systems available for different types of applications. This study focuses on the cooling towers as one of the exhaust air systems. However, different types of cooling towers that have different shapes and components produce different kinds of airflow patterns. Thus, the methodology and results presented in this thesis could be used to study the feasibility of installing the exhaust air energy recovery turbine generator for different variations. The power augmentation device for the system can also be improved with the introduction of guide-vanes. Based on the literature review, it is another value that potentially can be added in the system. The system has a great potential for commercialization since there are abundant quantities of exhaust air systems globally and the increase of awareness for sustainability development. The cooling tower manufacturer could make the system as another variant of cooling tower which comes together with the energy recovery feature as one unit. It is very hopeful that the exhaust air energy recovery turbine generator can be another solution for reducing the carbon emissions for a cleaner and healthier environment.

## REFERENCES

- Abe, K., Nishida, M., Sakurai, A., Ohya, Y., Kihara, H., Wada, E., & Sato, K. (2005). Experimental and numerical investigations of flow fields behind a small wind turbine with a flanged diffuser. *Journal of Wind Engineering and Industrial Aerodynamics*, 93(12), 951-970.
- Ackermann, Thomas. (2005). Historical development and current status of wind power. In T. Ackermann (Ed.), *Wind power in power systems*. Sussex, England: John Wiley & Sons.
- Ahmad, Salsabila, Kadir, Mohd Zainal Abidin Ab, & Shafie, Suhaidi. (2011). Current perspective of the renewable energy development in Malaysia. *Renewable and Sustainable Energy Reviews*, 15(2), 897-904.
- AID (Airfoil Investigation Database.). *MH114* 13.02%. 2013, from <http://www.airfoildb.com/foils/481>
- Akorede, Mudathir Funsho, Mohd Rashid, Muhd Ikram, Sulaiman, Mohd Herwan, Mohamed, Norainon Binti, & Ab Ghani, Suliana Binti. (2013). Appraising the viability of wind energy conversion system in the Peninsular Malaysia. *Energy Conversion and Management*, 76(0), 801-810.
- Ali, Rosnazri, Daut, Ismail, & Taib, Soib. (2012). A review on existing and future energy sources for electrical power generation in Malaysia. *Renewable and Sustainable Energy Reviews*, 16(6), 4047-4055.
- Alnasir, Zuher, & Kazerani, Mehrdad. (2013). An analytical literature review of stand-alone wind energy conversion systems from generator viewpoint. *Renewable and Sustainable Energy Reviews*, 28(0), 597-615.
- Altan, Burçin Deda, & Atılgan, Mehmet. (2010). The use of a curtain design to increase the performance level of a Savonius wind rotors. *Renewable Energy*, 35(4), 821-829.
- . Architectural Wind™ Installation at Boston's Logan International Airport. (2008): Architectural Wind™.
- Armstrong, Shawn, Fiedler, Andrzej, & Tullis, Stephen. (2012). Flow separation on a high Reynolds number, high solidity vertical axis wind turbine with straight and canted blades and canted blades with fences. *Renewable Energy*, 41, 13-22.
- ASHRAE. (2001). ASHRAE Handbook: Fundamental. *American Society of Heating, Refrigerating and Air Conditioning Engineers, Atlanta*.
- ASHRAE. (2008). ASHRAE Handbook: HVAC Systems and Equipment (SI). *American Society of Heating, Refrigerating and Air Conditioning Engineers, Atlanta*.

- ASHRAE. (2013). ASHRAE Equipment Life Expectancy chart: American Society of Heating, Refrigerating and Air Conditioning Engineers, Atlanta.
- Bahaj, A. S., Myers, L., & James, P. A. B. (2007). Urban energy generation: Influence of micro-wind turbine output on electricity consumption in buildings. *Energy and Buildings*, 39(2), 154-165.
- Bahrain world trade centre (BWTC). (2015). Retrieved August 2015, 2015, from <http://www.bahrainwtc.com/>
- Bekele, Getachew, & Palm, Björn. (2010). Feasibility study for a standalone solar–wind-based hybrid energy system for application in Ethiopia. *Applied Energy*, 87(2), 487-495.
- Bellarmino, G. Thomas, & Urquhart, Joe. (1996). Wind energy for the 1990s and beyond. *Energy Conversion and Management*, 37(12), 1741-1752.
- Berenda, Robert M, & Ferenci, Jack. (1996). United State Patent No. US5512788 A. U. S. P. a. T. Office.
- Beri, Habtamu, & Yao, Yingxue. (2011). Double Multiple Streamtube Model and Numerical Analysis of Vertical Axis Wind Turbine. *Energy and Power Engineering*, 3(03), 262.
- Bhakar, Vikrant, Uppala, Venkata Vamsi K., Digalwar, A. K., & Sangwan, K. S. (2013). Life Cycle Assessment of Smithy Training Processes. *Procedia Engineering*, 64, 1267-1275.
- Bhatia, S C. (2014). *Advanced Renewable Energy Systems* (Vol. Part 1). New Delhi, India: Woodhead Publishing India.
- Biadgo, Asress Mulugeta, Simonovic, Aleksandar, Komarov, Dragan, & Stupar, Slobodan. (2013). Numerical and Analytical Investigation of Vertical Axis Wind Turbine. *FME Transactions*, 41(1), 49-58.
- Boccard, Nicolas. (2009). Capacity factor of wind power realized values vs. estimates. *Energy Policy*, 37(7), 2679-2688.
- Bohrer, Gil, Zhu, Kunpeng, Jones, Robert L., & Curtis, Peter S. (2013). Optimizing wind power generation while minimizing wildlife impacts in an urban area. *PLoS ONE*, 8(2), e56036.
- Brahimi, MT, Allet, A, & Paraschivoiu, I. (1995). Aerodynamic analysis models for vertical-axis wind turbines. *International Journal of Rotating Machinery*, 2(1), 15-21.
- Brusca, S, Lanzafame, R, & Messina, M. (2014). Design of a vertical-axis wind turbine: how the aspect ratio affects the turbine's performance. *International Journal of Energy and Environmental Engineering*, 5(4), 333-340.
- Campbell, N., Stankovic, S., Graham, M., Parkin, P., Duijvendijk, M. V., Gruiter, T. D., . . . Blanch, M. (2001). *Wind energy for built environment (Project WEB)*. Paper

presented at the Proceedings of the European Wind Energy Conference & Exhibition, Copenhagen, Denmark.

- Camporeale, Sergio M, & Magi, Vinicio. (2000). Streamtube model for analysis of vertical axis variable pitch turbine for marine currents energy conversion. *Energy conversion and management*, 41(16), 1811-1827.
- Chauhan, Sonika, & Singh, Ravinder. (2014). Design of domestic helix vertical axis wind turbine to extract energy from exhaust fans. *Innovative Systems Design and Engineering*, 5(12), 23-28.
- Chen, Damir Cosic, Gong, Xinghao, Raju Huidrom, Ekaterine, Vashakmadze, Jiayi Zhang, & Zhao, Tianli. (2015). Understanding the plunge in oil prices: Sources and implications *Global Energy Prospect* (Vol. Chapter 4): The World Bank.
- Chong, W. T., Fazlizan, A., Omar, W. Z. W., Mansor, S., Zain, Z. M., Pan, K. C., & Oon, C. S. (2012). Wind Tunnel Testing of 5-bladed H-rotor Wind Turbine with the Integration of the Omni-Direction-Guide-Vane. In M. A. Wahid, S. Samion, J. M. Sheriff & N. A. C. Sidik (Eds.), *4th International Meeting of Advances in Thermofluids* (Vol. 1440, pp. 507-512). Melville: Amer Inst Physics.
- Chong, W. T., Fazlizan, A., Poh, S. C., Pan, K. C., Hew, W. P., & Hsiao, F. B. (2013). The design, simulation and testing of an urban vertical axis wind turbine with the omni-direction-guide-vane. *Applied Energy*, 112(0), 601-609.
- Chong, W. T., Fazlizan, A., Poh, S. C., Pan, K. C., & Ping, H. W. (2012). Early development of an innovative building integrated wind, solar and rain water harvester for urban high rise application. *Energy and Buildings*, 47(0), 201-207.
- Chong, W. T., Hew, W. P., Yip, S. Y., Fazlizan, A., Poh, S. C., Tan, C. J., & Ong, H. C. (2014). The experimental study on the wind turbine's guide-vanes and diffuser of an exhaust air energy recovery system integrated with the cooling tower. *Energy Conversion and Management*, 87(0), 145-155.
- Chong, W. T., Naghavi, M. S., Poh, S. C., Mahlia, T. M. I., & Pan, K. C. (2011). Techno-economic analysis of a wind-solar hybrid renewable energy system with rainwater collection feature for urban high-rise application. *Applied Energy*, 88(11), 4067-4077.
- Chong, W. T., Pan, K. C., Poh, S. C., Fazlizan, A., Oon, C. S., Badarudin, A., & Nik-Ghazali, N. (2013). Performance investigation of a power augmented vertical axis wind turbine for urban high-rise application. *Renewable Energy*, 51(0), 388-397.
- Chong, W.T., Fazlizan, A., Yip, S.Y., Poh, S.C., & Hew, W.P. (2014). *Performance and Environmental Evaluation of an On-site Waste-to-energy Conversion System by Using Exhaust Air Energy Recovery Turbine Generator*. Paper presented at the International Green Energy Conference (IGEC-IX), Tianjin, China. 25-28th May 2014.
- Chong, Wen Tong, Kong, Y. Y., & Fazlizan, A. (2011). WO2013073930-A1. Patentscope (WIPO): I. P. C. o. Malaysia.



- Cohen, Lawrence J. (2002). United State Patent No. US6365985 B1. U. S. P. a. T. Office.
- Couture, Toby, & Gagnon, Yves. (2010). An analysis of feed-in tariff remuneration models: Implications for renewable energy investment. *Energy Policy*, 38(2), 955-965.
- D'Ambrosio, Marco, & Medaglia, Marco. (2010). *Vertical axis wind turbines: History, technology and applications*. (Master), Halmstad University, Halmstad, Sweden.
- Dodman, David. (2009). Blaming cities for climate change? An analysis of urban greenhouse gas emissions inventories. *Environment and Urbanization*, 21(1), 185-201.
- Duran, Seraht. (2005). Computer aided design of horizontal axis wind turbine blades. *Master's thesis, Middle East Technical University, Ankara, Turkey*.
- Dutton, A. G., Halliday, J. A., & Blanch, M. J. (2005). The feasibility of building-mounted/integrated wind turbines (BUWTs): Achieving their potential for carbon emission reductions: Council for the Central Laboratory of the Research Councils (CCLRC).
- Ekren, Orhan, Ekren, Banu Y., & Ozerdem, Baris. (2009). Break-even analysis and size optimization of a PV/wind hybrid energy conversion system with battery storage – A case study. *Applied Energy*, 86(7–8), 1043-1054.
- El-Khattam, W., & Salama, M. M. A. (2004). Distributed generation technologies, definitions and benefits. *Electric Power Systems Research*, 71(2), 119-128.
- Eriksson, Sandra, Bernhoff, Hans, & Leijon, Mats. (2008). Evaluation of different turbine concepts for wind power. *Renewable and Sustainable Energy Reviews*, 12(5), 1419-1434.
- Fazelpour, Farivar, Soltani, Nima, Soltani, Sina, & Rosen, Marc A. (2015). Assessment of wind energy potential and economics in the north-western Iranian cities of Tabriz and Ardabil. *Renewable and Sustainable Energy Reviews*, 45(0), 87-99.
- Frankovic, Bernard, & Vrsalovic, Ivan. (2001). New high profitable wind turbines. *Renewable Energy*, 24(3-4), 491-499.
- Fried, Lauha. (2013). *Global Wind Statistics 2013*. Brussels, Belgium: Global Wind Energy Council.
- Gasch, R. (1982). *Wind turbine generators*. USA: MIT Press.
- Geurts, BM, Simao Ferreira, C, & Van Bussel, GJW. (2010). *Aerodynamic Analysis of a Vertical Axis Wind Turbine in a Diffuser*. Paper presented at the 3rd EWEA Conference-Torque 2010: The Science of making Torque from Wind, Heraklion, Crete, Greece, 28-30 June 2010.
- . Global Wind Energy Report: Annual Market Update 2014. (2015). In L. Fried, L. Qiao, S. Sawyer & S. Shukla (Eds.). Brussels, Belgium: Global Wind Energy Council.

- Grant, Andrew, Johnstone, Cameron, & Kelly, Nick. (2008). Urban wind energy conversion: The potential of ducted turbines. *Renewable Energy*, 33(6), 1157-1163.
- Gray, Neil CC, Lewis, J Harry, MacLean, Angus, Naskali, Pertti H, & Newall, A Patrick. (2008). Helical wind turbine: Google Patents.
- Grozdanic, Lidija. (2014). Hilton Fort Lauderdale Beach Resort Installs Six Wind Turbines on its Hotel Rooftop. *Energy*. Retrieved May, 2015, from <http://inhabitat.com/hilton-fort-lauderdale-beach-resort-installs-six-wind-turbines-on-its-hotel-rooftop/>
- Guezuraga, Begoña, Zauner, Rudolf, & Pölz, Werner. (2012). Life cycle assessment of two different 2 MW class wind turbines. *Renewable Energy*, 37(1), 37-44.
- Gupta, R., Biswas, A., & Sharma, K. K. (2008). Comparative study of a three-bucket Savonius rotor with a combined three-bucket Savonius–three-bladed Darrieus rotor. *Renewable Energy*, 33(9), 1974-1981.
- Hafez, Omar, & Bhattacharya, Kankar. (2012). Optimal planning and design of a renewable energy based supply system for microgrids. *Renewable Energy*, 45, 7-15.
- Hallgren, Willow, Gunturu, Udaya Bhaskar, & Schlosser, Adam. (2014). The Potential Wind Power Resource in Australia: A New Perspective. *PLoS ONE*, 9(7), e99608.
- Hara, Yutaka, Kawamura, Takafumi, Akimoto, Hiromichi, Tanaka, Kenji, Nakamura, Takuju, & Mizumukai, Kentaro. (2014). Predicting Double-Blade Vertical Axis Wind Turbine Performance by a Quadruple-Multiple Streamtube Model. *International Journal of Fluid Machinery and Systems*, 7(1), 16-27.
- Hashim, Haslenda, & Ho, Wai Shin. (2011). Renewable energy policies and initiatives for a sustainable energy future in Malaysia. *Renewable and Sustainable Energy Reviews*, 15(9), 4780-4787.
- Hau, Erich. (2006). *Wind Turbines: Fundamentals, Technologies, Application, Economics* (2nd ed.). New York: Springer.
- Hensley, John C. (Ed.). (2009). *Cooling Tower Fundamental* (2nd ed.). Kansas, USA: SPX Cooling Technologies Inc.
- Hepperle, Martin. (2008). Aerodynamics of Model Aircraft: MH Airfoils. Retrieved July 2015, from Martin Hepperle <http://www.mh-aerotools.de/airfoils/mh114koo.htm>
- Herrman, D. D. (1962). Field tests of fan performance on induced draft cooling towers. *Cooling Tower Institute*.
- Hu, S. Y., & Cheng, J. H. (2008). Innovatory designs for ducted wind turbines. *Renewable Energy*, 33(7), 1491-1498.

- Huffaker, Ray, & Bittelli, Marco. (2015). A nonlinear dynamics approach for incorporating wind-speed patterns into wind-power project evaluation. *PLoS ONE*, 10(1), e0115123.
- Ishugah, T. F., Li, Y., Wang, R. Z., & Kiplagat, J. K. (2014). Advances in wind energy resource exploitation in urban environment: A review. *Renewable and Sustainable Energy Reviews*, 37(0), 613-626.
- Islam, Mazharul, Ting, David S. K., & Fartaj, Amir. (2008). Aerodynamic models for Darrieus-type straight-bladed vertical axis wind turbines. *Renewable and Sustainable Energy Reviews*, 12(4), 1087-1109.
- Jeong, Hyo Min, Chung, Han Shik, Bae, Kang Youl, Kim, Se Hyun, & Shin, You Sik. (2005). Water cooling characteristics in an enclosed vacuum tank by water driven ejector. *Journal of mechanical science and technology*, 19(1), 164-172.
- Jin, Xin, Zhao, Gaoyuan, Gao, KeJun, & Ju, Wenbin. (2015). Darrieus vertical axis wind turbine: Basic research methods. *Renewable and Sustainable Energy Reviews*, 42(0), 212-225.
- Johnson, Gary L. (2006). *Wind energy systems*: Gary L. Johnson.
- Joselin Herbert, G. M., Iniyan, S., Sreevalsan, E., & Rajapandian, S. (2007). A review of wind energy technologies. *Renewable and Sustainable Energy Reviews*, 11(6), 1117-1145.
- Kalantar, M., & Mousavi G, S. M. (2010). Dynamic behavior of a stand-alone hybrid power generation system of wind turbine, microturbine, solar array and battery storage. *Applied Energy*, 87(10), 3051-3064.
- Kalogirou, Soteris A. (2013). *Solar energy engineering: processes and systems*: Academic Press.
- Khan, M. J., & Iqbal, M. T. (2005). Pre-feasibility study of stand-alone hybrid energy systems for applications in Newfoundland. *Renewable Energy*, 30(6), 835-854.
- Kim, Daegyoum, & Gharib, Morteza. (2013). Efficiency improvement of straight-bladed vertical-axis wind turbines with an upstream deflector. *Journal of Wind Engineering and Industrial Aerodynamics*, 115, 48-52.
- Kwon, Oick. (1994). *Velocity Recovery at Fan Stack Cooling Tower Thermal Design*. Gyungnam, Korea: Daeil Aqua Co. Ltd.
- Lapin, EE. (1975). Theoretical performance of vertical axis wind turbines. *American Society of Mechanical Engineers*, 1.
- Leung, DYC, Deng, Y, & Leung, MKH. (2010). *Design optimization of a cost-effective micro wind turbine*. Paper presented at the WCE 2010-World Congress on Engineering 2010.
- Logan Airport Wind Turbines. ((Accessed: May 2015)). from <http://www.cityofboston.gov/eeos/conservation/wind.asp>

- Low Voltage Commercial Tariff. (2015). Retrieved August, 2015
- Mahlia, T. M. I., & Saidur, R. (2010). A review on test procedure, energy efficiency standards and energy labels for room air conditioners and refrigerator–freezers. *Renewable and Sustainable Energy Reviews, 14*(7), 1888-1900.
- Mahlia, T. M. I., Saidur, R., Memon, L. A., Zulkifli, N. W. M., & Masjuki, H. H. (2010). A review on fuel economy standard for motor vehicles with the implementation possibilities in Malaysia. *Renewable and Sustainable Energy Reviews, 14*(9), 3092-3099.
- . Malaysia Energy Statistics 2015. (2015). Putrajaya, Malaysia: Energy Commission of Malaysia.
- Malaysia Inflation Rate. (2014). *Trading Economics*,. Retrieved Accessed: May 2014
- Malla, S. G., & Bhende, C. N. (2014). Voltage control of stand-alone wind and solar energy system. *International Journal of Electrical Power & Energy Systems, 56*(0), 361-373.
- Malmrup, Lars. (2006). US20080315589 A1. U. S. P. a. T. Office.
- Manan, Zainuddin Abdul, Shiun, Lim Jeng, Alwi, Sharifah Rafidah Wan, Hashim, Haslenda, Kannan, K. S., Mokhtar, Norhasliza, & Ismail, Ahmad Zairin. (2010). Energy Efficiency Award system in Malaysia for energy sustainability. *Renewable and Sustainable Energy Reviews, 14*(8), 2279-2289.
- Manwell, J. F., McGowan, J. G., & Rogers, A. L. (2002). *Wind Energy Explained: Theory, Design and Application*: John Wiley & Sons, Ltd.
- Mathew, Sathyajith. (2006). *Wind Energy: Fundamentals, Resource Analysis and Economics*. New York: Springer.
- Meinhold, Bridgette. (2010). Strata Tower. *Architecture*. Retrieved August 2015, 2015, from <http://inhabitat.com/first-skyscraper-with-built-in-wind-turbines-opens-in-london/>
- Mesbahi, Tedjani, Ouari, Ahmed, Ghennam, Tarak, Berkouk, El Madjid, Rizoug, Nassim, Mesbahi, Nadhir, & Meradji, Moudrik. (2014). A stand-alone wind power supply with a Li-ion battery energy storage system. *Renewable and Sustainable Energy Reviews, 40*(0), 204-213.
- Mirchi, Ali, Hadian, Saeed, Madani, Kaveh, Rouhani, Omid M., & Rouhani, Azadeh M. (2012). World energy balance outlook and opec production capacity: Implications for global oil security. *Energies, 5*(8), 2626-2651.
- Mohamed, M. H., Janiga, G., Pap, E., & Thévenin, D. (2010). Optimization of Savonius turbines using an obstacle shielding the returning blade. *Renewable Energy, 35*(11), 2618-2626.
- Monroe, Robert C. (2000). *The Basics of Axial Flow Fans*. Houston, Texas: Hudson Products Corporation.

- Montgomerie, Björn. (2004). Methods for root effects, tip effects and extending the angle of attack range to  $\pm 180$ , with application to aerodynamics for blades on wind turbines and propellers: Tech. Rep FOI.
- Müller, Gerald, Jentsch, Mark F., & Stoddart, Euan. (2009). Vertical axis resistance type wind turbines for use in buildings. *Renewable Energy*, 34(5), 1407-1412.
- Naghavi, Mohammad Sajad. (2010). *Technical feasibility and economic viability of a wind-solar hybrid renewable energy generation system*. (Master of Engineering), University of Malaya, Kuala Lumpur.
- Newnan, Donald G, Eschenbach, Ted, & Lavelle, Jerome P. (2012). *Engineering Economic Analysis* (11th ed.). New York: Oxford University Press.
- Nor, Khalid Mohamed, Shaaban, Mohamed, & Rahman, Hasimah Abdul. (2014). Feasibility assessment of wind energy resources in Malaysia based on NWP models. *Renewable Energy*, 62, 147-154.
- Ohya, Yuji, & Karasudani, Takashi. (2010). A shrouded wind turbine generating high output power with wind-lens technology. *Energies*, 3(4), 634-649.
- OPEC. (2014). OPEC monthly oil market report (Vol. December 2014). Vienna, Austria: Organization of the Petroleum Exporting Countries.
- . The Outlook for Energy: A view to 2040. (2012): ExxonMobil.
- P10: 10W Vertical Axis Wind Turbine.). Retrieved November, 2014, from <http://www.sawtenergy.com/product/p10.php>
- Paraschivoiu, Ion. (1981). *Double-multiple streamtube model for Darrieus in turbines*. Paper presented at the Wind Turbine Dynamics.
- Paraschivoiu, Ion. (2002). *Wind Turbine Design: With Emphasis on Darrieus Concept*. Montreal: Polytechnic International Press.
- Park, JY, Lee, S, Sabourin, T, & Park, K. (2007). A Novel Vertical-Axis Wind Turbine for Distributed & Utility Deployment. *Dept. of Mechanical Engineering, Inha University, Korea KR Wind Energy Research Institute, Korea. KR WindPower, Inc., USA*.
- Patel, M. (2006). *Wind and solar power systems: design, analysis, and operation*. Florida: Taylor & Francis.
- Peacock, A. D., Jenkins, D., Ahadzi, M., Berry, A., & Turan, S. (2008). Micro wind turbines in the UK domestic sector. *Energy and Buildings*, 40(7), 1324-1333.
- Pearl River Tower.). Retrieved August 2011, 2011, from [http://smithgill.com/#/work/pearl\\_river\\_tower](http://smithgill.com/#/work/pearl_river_tower)
- Ponta, F. L., Seminara, J. J., & Otero, A. D. (2007). On the aerodynamics of variable-geometry oval-trajectory Darrieus wind turbines. *Renewable Energy*, 32, 35-56.

- Prambudia, Yudha, & Nakano, Masaru. (2012). Integrated simulation model for energy security evaluation. *Energies*, 5(12), 5086-5110.
- Ragheb, Magdi, & Ragheb, Adam M. (Eds.). (2011). *Wind Turbines Theory - The Betz Equation and Optimal Rotor Tip Speed Ratio*. Rijeka, Croatia: InTech.
- Rahim, Nasrudin Abd, & Hasanuzzaman, Md. (2012). Energy situation in Malaysia: Present and its future *Country Report*. Brunei Darussalam: SUSTAINABLE FUTURE ENERGY 2012 and 10th SEE FORUM.
- Resch, Gustav, Held, Anne, Faber, Thomas, Panzer, Christian, Toro, Felipe, & Haas, Reinhard. (2008). Potentials and prospects for renewable energies at global scale. *Energy Policy*, 36(11), 4048-4056.
- REUK.co.uk. (2007). Darrieus Wind Turbines. from <http://www.reuk.co.uk/Darrieus-Wind-Turbines.htm>
- Riegler, H. (2003). HAWT versus VAWT: Small VAWTs find a clear niche. *Refocus*, 4(4), 44-46.
- Saha, U. K., Thotla, S., & Maity, D. (2008). Optimum design configuration of Savonius rotor through wind tunnel experiments. *Journal of Wind Engineering and Industrial Aerodynamics*, 96(8-9), 1359-1375.
- Saidur, R., Rezaei, M., Muzammil, W. K., Hassan, M. H., Paria, S., & Hasanuzzaman, M. (2012). Technologies to recover exhaust heat from internal combustion engines. *Renewable and Sustainable Energy Reviews*, 16(8), 5649-5659.
- Savonius, S. J. (1931). The S-Rotor and its applications. *Mech Eng*, 53(5), 333-338.
- Schaeffer, Roberto, Szklo, Alexandre Salem, Pereira de Lucena, André Frossard, Moreira Cesar Borba, Bruno Soares, Pupo Nogueira, Larissa Pinheiro, Fleming, Fernanda Pereira, . . . Boulahya, Mohammed Sadeck. (2012). Energy sector vulnerability to climate change: A review. *Energy*, 38(1), 1-12.
- . SEDA Annual Report 2013. (2014). Putrajaya: Sustainable Energy Development Authority Malaysia.
- Shan, Zhongde, Qin, Shaoyan, Liu, Qian, & Liu, Feng. (2012). Key manufacturing technology & equipment for energy saving and emissions reduction in mechanical equipment industry. *International Journal of Precision Engineering and Manufacturing*, 13(7), 1095-1100.
- Sharpe, Tim, & Proven, Gordon. (2010). Crossflex: Concept and early development of a true building integrated wind turbine. *Energy and Buildings*, 42(12), 2365-2375.
- Shekarchian, M., Moghavvemi, M., Mahlia, T. M. I., & Mazandarani, A. (2011). A review on the pattern of electricity generation and emission in Malaysia from 1976 to 2008. *Renewable and Sustainable Energy Reviews*, 15(6), 2629-2642.
- Sheldahl, R E, & Klimas, P C. (1981). Aerodynamic characteristics of seven symmetrical airfoil sections through 180-degree angle of attack for use in aerodynamic analysis

of vertical axis wind turbines (pp. Medium: ED; Size: Pages: 120). Albuquerque, United States: Sandia National Laboratories.

- Simao Ferreira, Carlos, Barone, Matthew F, Madsen, Helge A, Roscher, Bjorn, Deglaire, Paul, & Arduin, Igor. (2014). Comparison of aerodynamic models for vertical axis wind turbines: Sandia National Laboratories (SNL-NM), Albuquerque, NM (United States).
- Smith, R. F., & Killa, S. (2007). Bahrain World Trade Center (BWTC): the first large-scale integration of wind turbines in a building. *The Structural Design of Tall and Special Buildings*, 16(4), 10.
- Solomon, S., Qin, D., Manning, M., Chen, Z., Marquis, M., Averyt, K.B., . . . Miller, H.L. (2007). *Climate Change 2007: The Physical Science Basis IPCC Fourth Assessment Report (AR4)*. New York: International Governmental Panel on Climate Change.
- Sopian, Kamaruzzaman, & Khatib, Tamer. (2013). Wind energy potential in nine Coastal Sites in Malaysia. *Palestine Tech Univ Res J*, 1, 10-15.
- Spurk, Joseph H., & Aksel, Nuri. (2008). *Fluid Mechanics*. Berlin, Germany: Springer Berlin Heidelberg.
- Stankovic, Sinisa, Campbell, Neil, & Harries, Alan. (2009). *Urban wind energy*. London, UK: Earthscan.
- Strickland, James H. (1975). Darrieus turbine: a performance prediction model using multiple streamtubes: Sandia Labs., Albuquerque, N. Mex.(USA).
- Suhaila, Jamaludin, Deni, Sayang Mohd, Zin, Wan Zawiah Wan, & Jemain, Abdul Aziz. (2010). Trends in Peninsular Malaysia rainfall data during the southwest monsoon and northeast monsoon seasons: 1975–2004. *Sains Malaysiana*, 39(4), 533-542.
- Takao, Manabu, Maeda, Takao, Kamada, Yasunari, Oki, Michiaki, & Kuma, Hideki. (2008). A straight-bladed vertical axis wind turbine with a directed guide vane row. *Journal of Fluid Science and Technology*, 3(3), 8.
- Tanino, Tadakazu, Fujikawa, Takuji, Nakao, Shinichiro, & Takahashi, Kazunobu. (2010). Influence of Reynolds Number and Scale on Performance Evaluation of Lift-type Vertical Axis Wind Turbine by Scale-model Wind Tunnel Tests. *Turbomachinery*, 38(6), 345-351.
- Templin, RJ. (1974). Aerodynamic performance theory for the NRC vertical-axis wind turbine. *NASA STI/Recon Technical Report N*, 76, 16618.
- Tong, Chong Wen, Zainon, M. Z., Chew, Poh Sin, Kui, Soo Chun, Keong, Wee Seng, & Chen, Pan Kok. (2010). Innovative power-augmentation-guide-vane design of wind-solar hybrid renewable energy harvester for urban high rise application. *AIP Conference Proceedings*, 1225(1), 507-521.
- Truwater. (2011). TC-M Series Cooling Tower - Modular Design Counterflow Type. In T. C. T. S. Bhd (Ed.).

- Truwater Cooling Towers Sdn. Bhd.). *About us*. Retrieved August, 2015, from <http://www.truwater.com.my/about-us/>
- UGE Turbines Powering a Hilton Resort. (2013). 2015, from [http://www.ugei.com/case\\_study/enterprise/hilton](http://www.ugei.com/case_study/enterprise/hilton)
- UIUC Airfoil Coordinate Database. Retrieved Accessed: August 2014, from UIUC Applied Aerodynamics Group, University of Illinois [http://aerospace.illinois.edu/m-selig/ads/coord\\_database.html](http://aerospace.illinois.edu/m-selig/ads/coord_database.html)
- Unit, Economic Planning. (2010). *10 th Malaysia Plan, Chapter 6: Building an Environment that Enhances Quality of Life*. Putrajaya.
- Wakui, Tetsuya, Tanzawa, Yoshiaki, Hashizume, Takumi, & Nagao, Toshio. (2005). Hybrid configuration of Darrieus and Savonius rotors for stand-alone wind turbine-generator systems. *Electrical Engineering in Japan*, 150(4), 13-22.
- Walker, Sara Louise. (2011). Building mounted wind turbines and their suitability for the urban scale--A review of methods of estimating urban wind resource. *Energy and Buildings*, 43(8), 1852-1862.
- Wang, Wen-Xue, Matsubara, Terutake, Hu, Junfeng, Odahara, Satoru, Nagai, Tomoyuki, Karasutani, Takashi, & Ohya, Yuji. (2015). Experimental investigation into the influence of the flanged diffuser on the dynamic behavior of CFRP blade of a shrouded wind turbine. *Renewable Energy*, 78(0), 386-397.
- Wilson, Robert Elliot, & Lissaman, Peter BS. (1974). Applied aerodynamics of wind power machines. *NASA STI/Recon Technical Report N*, 75, 22669.
- . World Economic Situation and Prospects 2015 (2015) (Vol. Chapter 1). New York.
- Xu, Xinhua, Wang, Shengwei, & Ma, Zhenjun. (2008). Evaluation of plume potential and plume abatement of evaporative cooling towers in a subtropical region. *Applied Thermal Engineering*, 28(11-12), 1471-1484.
- Yu, Roger. (2008). Airports go for green with eco-friendly efforts. *USA Today*.



## APPENDIX A

**Appendix A1: Sample of data collected by the dynamometer  
Data at 40% load (peak power) from X = 250 mm, Y = 350 mm.**

Time	RPM	Torque (Nm)	% Load	Current	Voltage	Electrical Power (W)	Mechanical Power (W)
849.13	347.19	0.161911	40	0.034681	12.41935	0.430714	0.981126
850.124	346.60	0.195676	40	0.038816	13.3871	0.51964	1.18369
851.121	345.80	0.190949	40	0.040561	12.47312	0.505921	1.152439
852.119	342.90	0.206916	40	0.041956	12.95699	0.543629	1.238335
853.116	339.95	0.202707	40	0.043073	12.25806	0.52799	1.202711
854.113	337.97	0.193632	40	0.042011	11.93548	0.501422	1.14219
855.109	336.49	0.218027	40	0.044681	12.58065	0.56211	1.280433
856.109	334.24	0.218499	40	0.045252	12.36559	0.55957	1.274646
857.106	332.62	0.207656	40	0.043363	12.2043	0.52922	1.205513
858.105	331.31	0.194146	40	0.042243	11.66667	0.49284	1.122642
859.107	330.66	0.213192	40	0.043302	12.47312	0.540117	1.230334
860.097	327.83	0.208736	40	0.042586	12.31183	0.524307	1.194322
861.096	324.91	0.211743	40	0.043576	12.09677	0.527132	1.200756
862.091	322.96	0.192243	40	0.043587	10.91398	0.475704	1.083609
863.086	321.48	0.224719	40	0.044377	12.47312	0.553521	1.260867
864.09	319.24	0.211556	40	0.0454	11.39785	0.517467	1.17874
865.083	317.62	0.216142	40	0.043873	11.98925	0.526004	1.198188
866.082	316.31	0.196871	40	0.04226	11.29032	0.47713	1.086857
867.076	315.65	0.177272	40	0.041752	10.26882	0.428741	0.976632
868.115	315.33	0.203382	40	0.042909	11.45161	0.491379	1.119314
869.075	315.16	0.195829	40	0.041489	11.39785	0.472885	1.077187
870.069	313.58	0.201581	40	0.041135	11.77419	0.48433	1.103258
871.068	312.29	0.182031	40	0.042416	10.26882	0.435558	0.99216
872.062	310.15	0.179269	40	0.041485	10.26882	0.426004	0.970396
873.059	308.07	0.214687	40	0.041523	12.2043	0.506757	1.154345
874.074	308.04	0.214075	40	0.043508	11.6129	0.505254	1.150921
875.056	308.52	0.199494	40	0.041968	11.23656	0.471577	1.074207
876.058	307.76	0.207355	40	0.0423	11.55914	0.488954	1.11379
877.059	306.88	0.2136	40	0.044912	11.1828	0.502241	1.144056
878.044	305.94	0.206643	40	0.0427	11.34409	0.484395	1.103405
879.057	305.47	0.203038	40	0.042495	11.1828	0.475211	1.082486
880.039	303.73	0.175369	40	0.04194	9.731183	0.408122	0.929662
881.035	302.37	0.208016	40	0.041886	11.50538	0.481918	1.097764
882.031	301.18	0.180032	40	0.040671	10.21505	0.415454	0.946365
883.033	300.59	0.175762	40	0.04048	10	0.404803	0.922103
884.027	300.30	0.173834	40	0.039155	10.21505	0.39997	0.911093
885.024	300.15	0.205232	40	0.040832	11.55914	0.471979	1.075123
886.042	300.07	0.179483	40	0.042173	9.784946	0.412661	0.940002

## Appendix A2: Sample of uncertainty analysis

At each of the load applied, the data is collected for 20 minutes in order to let all the parameters to be stabilized. Only the data for the last 2 minutes (after the parameters are stabilized) is considered for the experimental analysis. As a sample, data from the dynamometer system as shown in Appendix 2 is used for the uncertainty analysis.

The parameters that are taken for the analysis are the rotational speed, torque and mechanical power. The calculation of mean values is as below:

$$mean = \frac{1}{N} \sum_{i=1}^N x_i = \frac{1}{N} (x_1 + x_2 + x_3 + \dots + x_{N-1} + x_N)$$

With the above formula, the mean values for the turbine rotational speed, torque and mechanical power are 308.0 rpm, 0.2024 Nm and 1.0889 W. Then, the standard deviation,  $\sigma$  is calculated as below:

$$\sigma_x = \sqrt{\frac{1}{N-1} \sum_{i=1}^N (x_i - mean)^2}$$

The standard deviation values for the turbine rotational speed, torque and mechanical power are 9.47 rpm, 0.0135 Nm and 0.0793 W respectively. These values are acceptable for the experimental result. The normal distribution curves are illustrated in Appendix A2(a-c).

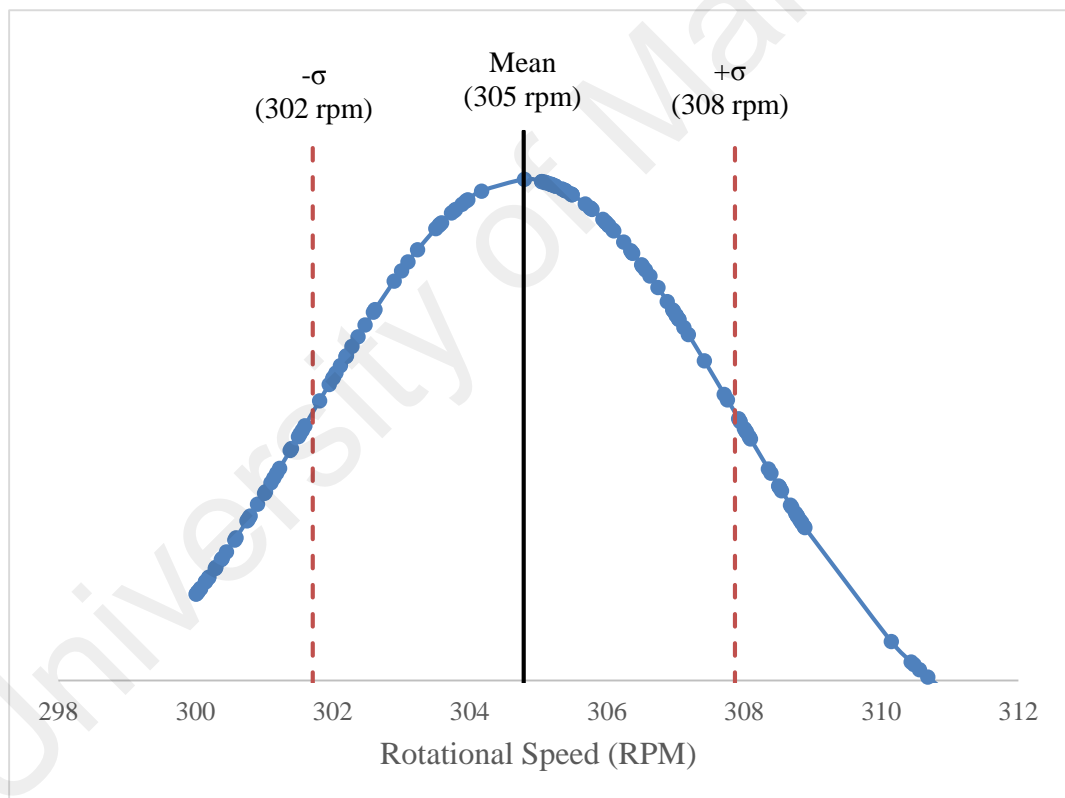
The general rule of acceptable margin of error in research 5% (Bartlett, Kotrlík & Higgins, 2001). The standard error,  $SE$  is calculated using the following formula:

$$SE = \frac{\sigma}{\sqrt{N}}$$

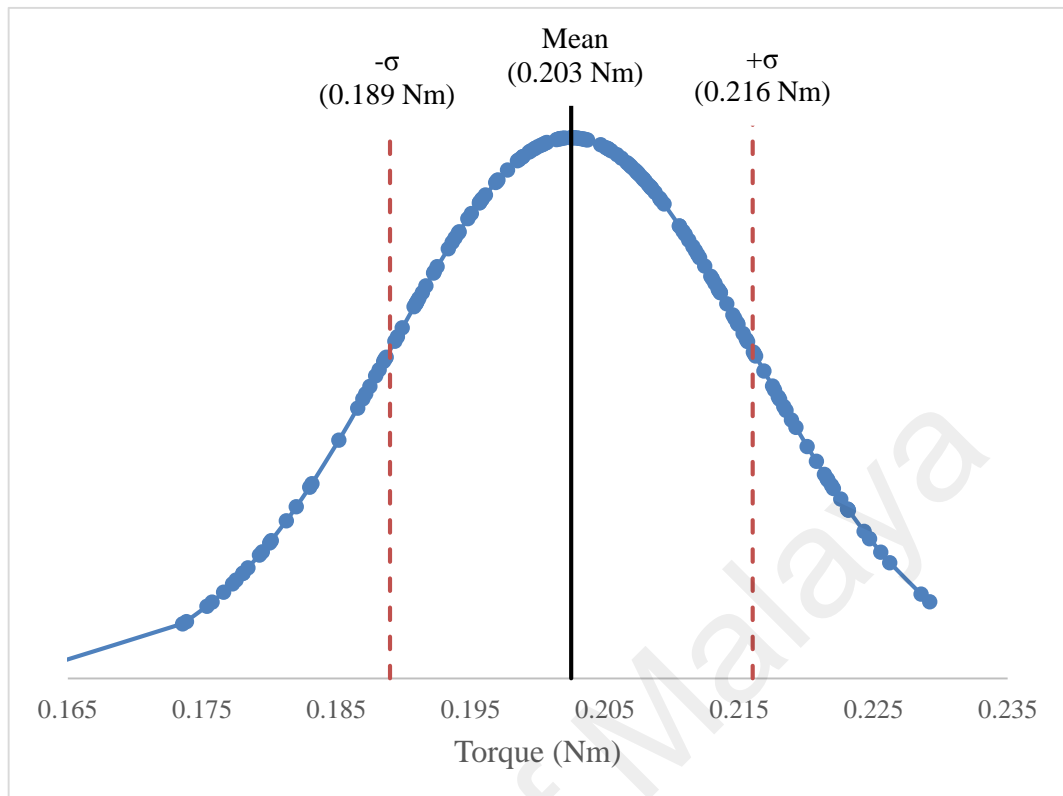
The standard deviation values for the turbine rotational speed, torque and mechanical power are less than 1% which is within the acceptable value.

**Reference:** Bartlett, J. E., Kotrlik, J. W. & Higgins, C. C. (2001). *Organizational research: Determining appropriate sample size in survey research appropriate sample size in survey research. Information technology, learning, and performance journal, 19(1), 43.*

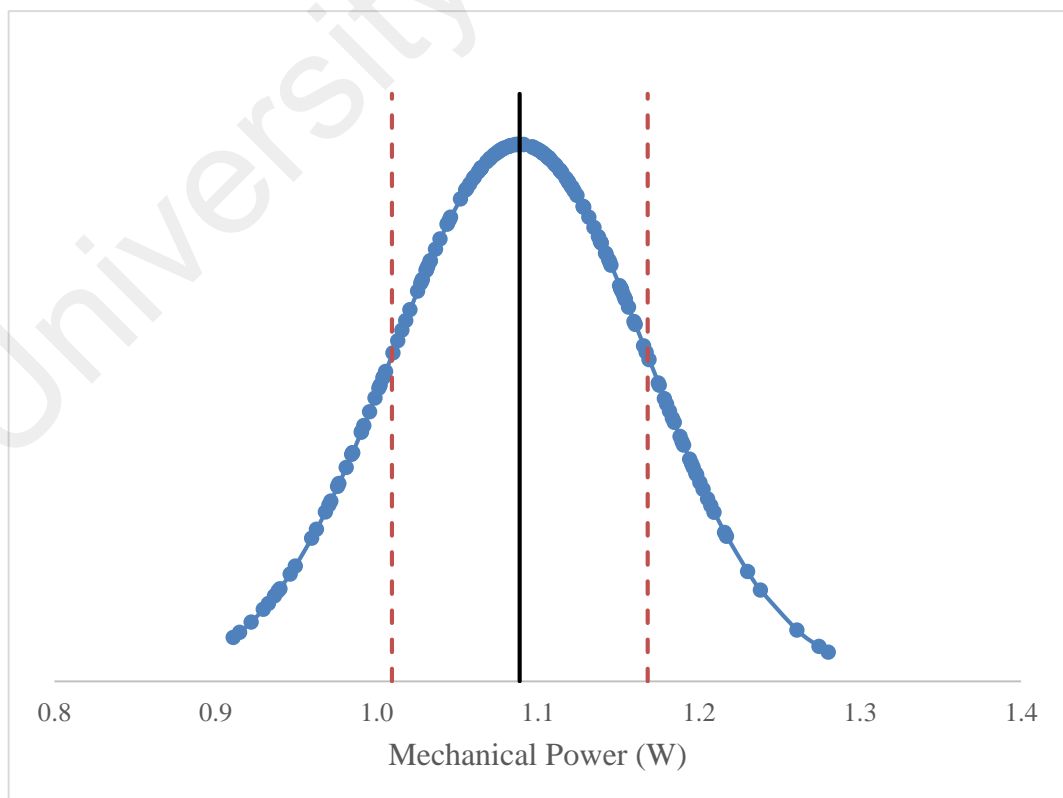
**Appendix A2(a): Normal distribution of turbine rotational speed**



### Appendix A2(b): Normal distribution of torque generation

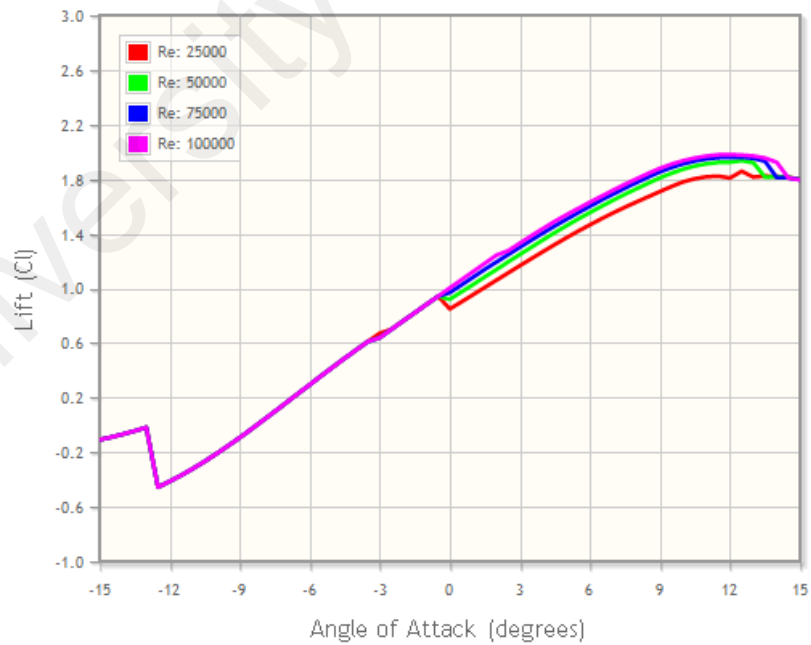
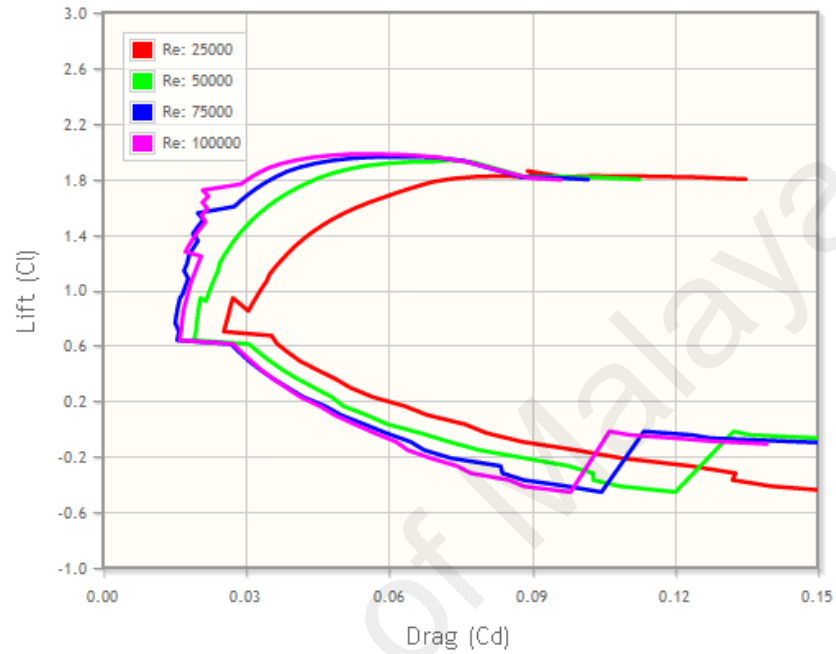


### Appendix A2(b): Normal distribution of mechanical power



## APPENDIX B

**Appendix B1: Lift coefficient against drag coefficient and lift coefficient against angle of attack of the MH 114 airfoil (Airfoil Investigation Database).**

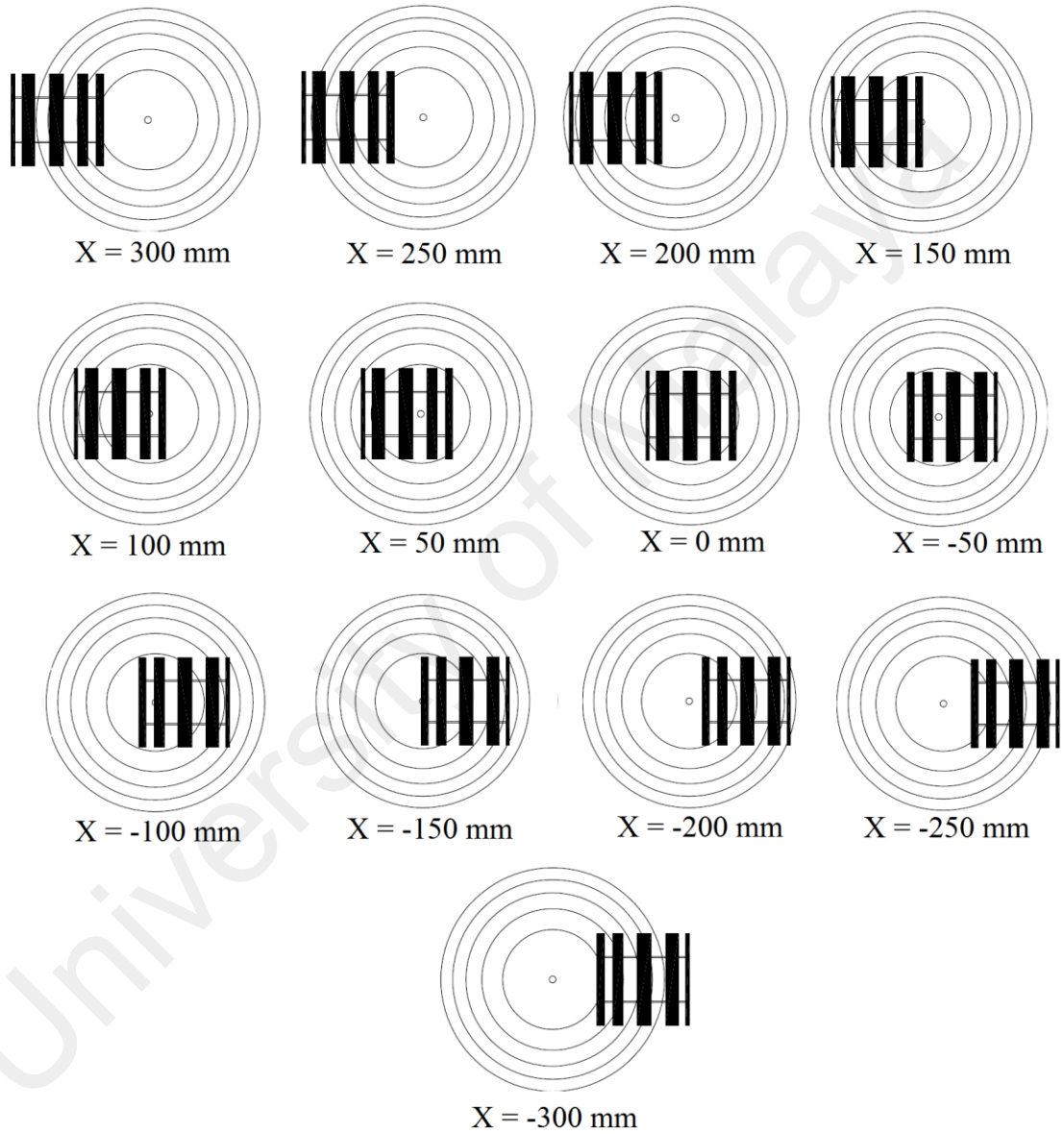


## Appendix B2: Extrapolated aerodynamic data of MH114 airfoil (angle of attack, $\alpha$ against lift coefficient, $C_L$ and drag coefficient, $C_D$ )

$\alpha$	$C_L$	$C_D$	$\alpha$	$C_L$	$C_D$	$\alpha$	$C_L$	$C_D$	$\alpha$	$C_L$	$C_D$	$\alpha$	$C_L$	$C_D$	$\alpha$	$C_L$	$C_D$
-180.0	-0.37	0.01	-113.0	-0.06	1.38	-45.0	-0.11	0.82	4.0	1.27	0.04	61.0	1.51	1.37	129.0	-1.41	1.08
-179.0	-0.29	0.01	-112.0	-0.06	1.39	-44.0	-0.12	0.80	4.5	1.32	0.04	62.0	1.48	1.39	130.0	-1.42	1.05
-178.0	-0.23	0.01	-111.0	-0.07	1.41	-43.0	-0.13	0.77	5.0	1.37	0.04	63.0	1.46	1.42	131.0	-1.44	1.02
-177.0	-0.18	0.01	-110.0	-0.07	1.43	-42.0	-0.14	0.74	5.5	1.42	0.04	64.0	1.43	1.45	132.0	-1.46	0.99
-176.0	-0.14	0.01	-109.0	-0.07	1.45	-41.0	-0.15	0.71	6.0	1.47	0.05	65.0	1.41	1.47	133.0	-1.47	0.96
-175.0	-0.11	0.02	-108.0	-0.07	1.47	-40.0	-0.15	0.68	6.5	1.51	0.05	66.0	1.38	1.50	134.0	-1.48	0.92
-174.0	-0.09	0.02	-107.0	-0.06	1.48	-39.0	-0.16	0.66	7.0	1.55	0.05	67.0	1.35	1.52	135.0	-1.49	0.89
-173.0	-0.07	0.03	-106.0	-0.06	1.50	-38.0	-0.16	0.63	7.5	1.59	0.05	68.0	1.31	1.54	136.0	-1.50	0.86
-172.0	-0.05	0.04	-105.0	-0.06	1.51	-37.0	-0.17	0.60	8.0	1.63	0.06	69.0	1.28	1.56	137.0	-1.51	0.83
-171.0	-0.02	0.05	-104.0	-0.06	1.52	-36.0	-0.17	0.58	8.5	1.67	0.06	70.0	1.25	1.59	138.0	-1.51	0.80
-170.0	0.00	0.06	-103.0	-0.05	1.54	-35.0	-0.18	0.55	9.0	1.71	0.06	71.0	1.21	1.61	139.0	-1.51	0.77
-169.0	0.02	0.07	-102.0	-0.05	1.55	-34.0	-0.18	0.52	9.5	1.75	0.07	72.0	1.17	1.63	140.0	-1.51	0.74
-168.0	0.04	0.08	-101.0	-0.04	1.56	-33.0	-0.18	0.50	10.0	1.78	0.07	73.0	1.14	1.64	141.0	-1.51	0.70
-167.0	0.06	0.09	-100.0	-0.04	1.57	-32.0	-0.18	0.47	10.5	1.80	0.07	74.0	1.10	1.66	142.0	-1.50	0.67
-166.0	0.08	0.10	-99.0	-0.03	1.58	-31.0	-0.18	0.45	11.0	1.82	0.08	75.0	1.05	1.68	143.0	-1.50	0.64
-165.0	0.10	0.12	-98.0	-0.03	1.58	-30.0	-0.18	0.42	11.5	1.82	0.08	76.0	1.01	1.69	144.0	-1.49	0.61
-164.0	0.11	0.13	-97.0	-0.02	1.59	-29.0	-0.18	0.40	12.0	1.81	0.09	77.0	0.97	1.71	145.0	-1.48	0.58
-163.0	0.13	0.15	-96.0	-0.02	1.60	-28.0	-0.18	0.37	12.5	1.86	0.09	78.0	0.92	1.72	146.0	-1.47	0.56
-162.0	0.14	0.17	-95.0	-0.01	1.60	-27.0	-0.17	0.35	13.0	1.82	0.10	79.0	0.88	1.74	147.0	-1.46	0.53
-161.0	0.16	0.18	-94.0	0.00	1.61	-26.0	-0.17	0.33	13.5	1.82	0.10	80.0	0.83	1.75	148.0	-1.44	0.50
-160.0	0.17	0.20	-93.0	0.01	1.61	-25.0	-0.16	0.30	14.0	1.82	0.11	81.0	0.79	1.76	149.0	-1.43	0.47
-159.0	0.18	0.22	-92.0	0.01	1.61	-24.0	-0.15	0.28	14.5	1.81	0.12	82.0	0.74	1.77	150.0	-1.41	0.44
-158.0	0.19	0.24	-91.0	0.02	1.61	-23.0	-0.14	0.26	15.0	1.80	0.13	83.0	0.69	1.78	151.0	-1.39	0.42
-157.0	0.20	0.26	-90.0	0.03	1.61	-22.0	-0.13	0.24	16.0	1.82	0.07	84.0	0.64	1.78	152.0	-1.37	0.39
-156.0	0.21	0.28	-89.0	0.03	1.61	-21.0	-0.12	0.22	17.0	1.79	0.09	85.0	0.59	1.79	153.0	-1.35	0.37
-155.0	0.22	0.30	-88.0	0.04	1.61	-20.0	-0.11	0.20	18.0	1.76	0.10	86.0	0.54	1.80	154.0	-1.33	0.34
-154.0	0.22	0.33	-87.0	0.05	1.61	-19.0	-0.10	0.18	19.0	1.72	0.12	87.0	0.49	1.80	155.0	-1.30	0.32
-153.0	0.22	0.35	-86.0	0.05	1.61	-18.0	-0.09	0.16	20.0	1.70	0.14	88.0	0.43	1.80	156.0	-1.28	0.29
-152.0	0.23	0.37	-85.0	0.06	1.60	-17.0	-0.08	0.15	21.0	1.67	0.17	89.0	0.38	1.80	157.0	-1.25	0.27
-151.0	0.23	0.40	-84.0	0.06	1.60	-16.0	-0.08	0.13	22.0	1.65	0.19	90.0	0.33	1.80	158.0	-1.23	0.25
-150.0	0.23	0.42	-83.0	0.07	1.59	-15.0	-0.11	0.22	23.0	1.63	0.22	91.0	0.28	1.80	159.0	-1.20	0.23
-149.0	0.23	0.45	-82.0	0.07	1.58	-14.5	-0.09	0.21	24.0	1.62	0.24	92.0	0.22	1.80	160.0	-1.18	0.21
-148.0	0.22	0.47	-81.0	0.08	1.58	-14.0	-0.07	0.19	25.0	1.61	0.27	93.0	0.17	1.80	161.0	-1.16	0.19
-147.0	0.22	0.50	-80.0	0.08	1.57	-13.5	-0.05	0.18	26.0	1.60	0.29	94.0	0.11	1.80	162.0	-1.14	0.17
-146.0	0.22	0.52	-79.0	0.08	1.56	-13.0	-0.02	0.19	27.0	1.60	0.32	95.0	0.06	1.79	163.0	-1.13	0.15
-145.0	0.21	0.55	-78.0	0.09	1.55	-12.5	-0.46	0.16	28.0	1.59	0.35	96.0	0.00	1.78	164.0	-1.12	0.14
-144.0	0.21	0.58	-77.0	0.09	1.54	-12.0	-0.41	0.14	29.0	1.60	0.38	97.0	-0.05	1.78	165.0	-1.12	0.12
-143.0	0.20	0.60	-76.0	0.09	1.52	-11.5	-0.37	0.13	30.0	1.60	0.41	98.0	-0.10	1.77	166.0	-1.14	0.11
-142.0	0.19	0.63	-75.0	0.09	1.51	-11.0	-0.32	0.13	31.0	1.60	0.44	99.0	-0.16	1.76	167.0	-1.16	0.09
-141.0	0.18	0.66	-74.0	0.09	1.50	-10.5	-0.27	0.12	32.0	1.61	0.47	100.0	-0.21	1.75	168.0	-1.19	0.08
-140.0	0.17	0.68	-73.0	0.09	1.48	-10.0	-0.21	0.11	33.0	1.62	0.50	101.0	-0.27	1.74	169.0	-1.19	0.07
-139.0	0.16	0.71	-72.0	0.09	1.47	-9.5	-0.15	0.10	34.0	1.62	0.53	102.0	-0.32	1.73	170.0	-1.17	0.06
-138.0	0.15	0.74	-71.0	0.09	1.45	-9.0	-0.09	0.09	35.0	1.63	0.56	103.0	-0.37	1.71	171.0	-1.12	0.05
-137.0	0.14	0.77	-70.0	0.09	1.43	-8.5	-0.03	0.08	36.0	1.64	0.59	104.0	-0.43	1.70	172.0	-1.04	0.04
-136.0	0.13	0.80	-69.0	0.08	1.41	-8.0	0.03	0.08	37.0	1.64	0.62	105.0	-0.49	1.68	173.0	-0.96	0.03
-135.0	0.12	0.82	-68.0	0.08	1.39	-7.5	0.10	0.07	38.0	1.65	0.65	106.0	-0.54	1.67	174.0	-0.87	0.02
-134.0	0.11	0.85	-67.0	0.08	1.38	-7.0	0.16	0.06	39.0	1.66	0.68	107.0	-0.59	1.65	175.0	-0.79	0.02
-133.0	0.10	0.88	-66.0	0.07	1.36	-6.5	0.23	0.06	40.0	1.66	0.72	108.0	-0.64	1.63	176.0	-0.71	0.01
-132.0	0.09	0.91	-65.0	0.07	1.33	-6.0	0.29	0.05	41.0	1.67	0.75	109.0	-0.69	1.61	177.0	-0.62	0.01
-131.0	0.08	0.94	-64.0	0.06	1.31	-5.5	0.36	0.05	42.0	1.67	0.78	110.0	-0.73	1.59	178.0	-0.54	0.01
-130.0	0.07	0.96	-63.0	0.05	1.29	-5.0	0.42	0.04	43.0	1.67	0.81	111.0	-0.78	1.57	179.0	-0.45	0.01
-129.0	0.06	0.99	-62.0	0.05	1.27	-4.5	0.49	0.04	44.0	1.68	0.84	112.0	-0.83	1.55	180.0	-0.37	0.01
-128.0	0.04	1.02	-61.0	0.04	1.25	-4.0	0.55	0.04	45.0	1.68	0.88	113.0	-0.87	1.52	131.0	-1.44	1.02
-127.0	0.03	1.04	-60.0	0.03	1.22	-3.5	0.61	0.04	46.0	1.68	0.91	114.0	-0.92	1.50	132.0	-1.46	0.99
-126.0	0.02	1.07	-59.0	0.02	1.20	-3.0	0.67	0.04	47.0	1.68	0.94	115.0	-0.96	1.48	133.0	-1.47	0.96
-125.0	0.01	1.10	-58.0	0.01	1.17	-2.5	0.70	0.03	48.0	1.67	0.97	116.0	-1.00	1.45	134.0	-1.48	0.92
-124.0	0.00	1.12	-57.0	0.01	1.15	-2.0	0.76	0.03	49.0	1.67	1.01	117.0	-1.04	1.43	135.0	-1.49	0.89
-123.0	0.00	1.15	-56.0	0.00	1.12	-1.5	0.82	0.03	50.0	1.66	1.04	118.0	-1.08	1.40	136.0	-1.50	0.86
-122.0	-0.01	1.17	-55.0	-0.01	1.10	-1.0	0.88	0.03	51.0	1.66	1.07	119.0	-1.12	1.37	137.0	-1.51	0.83
-121.0	-0.02	1.20	-54.0	-0.02	1.07	-0.5	0.94	0.03	52.0	1.65	1.10	120.0	-1.15	1.35	138.0	-1.51	0.80
-120.0	-0.03	1.22	-53.0	-0.03	1.04	0.0	0.85	0.03	53.0	1.64	1.13	121.0	-1.19	1.32	139.0	-1.51	0.77
-119.0	-0.04	1.25	-52.0	-0.04	1.02	0.5	0.90	0.03	54.0	1.63	1.16	122.0	-1.22	1.29	140.0	-1.51	0.74
-118.0	-0.04	1.27	-51.0	-0.05	0.99	1.0	0.95	0.03	55.0	1.62	1.19	123.0	-1.25	1.26	141.0	-1.51	0.70
-117.0	-0.05	1.29	-50.0	-0.06	0.96	1.5	1.01	0.03	56.0	1.60	1.22	124.0	-1.28	1.23	142.0	-1.50	0.67
-116.0	-0.05	1.31	-49.0	-0.07	0.94	2.0	1.06	0.03	57.0	1.59	1.25	125.0	-1.31	1.20	143.0	-1.50	0.64
-115.0	-0.06	1.33	-48.0	-0.08	0.91	2.5	1.11	0.03	58.0	1.57	1.28	126.0	-1.34	1.17	144.0	-1.49	0.61
-115.0	-0.06	1.33	-47.0	-0.09	0.88	3.0	1.17	0.04	59.0	1.55	1.31	127.0	-1.36	1.14	145.0	-1.48	0.58
-114.0	-0.06	1.36	-46.0	-0.10	0.85	3.5	1.22	0.04	60.0	1.53	1.34	128.0	-1.38	1.11			

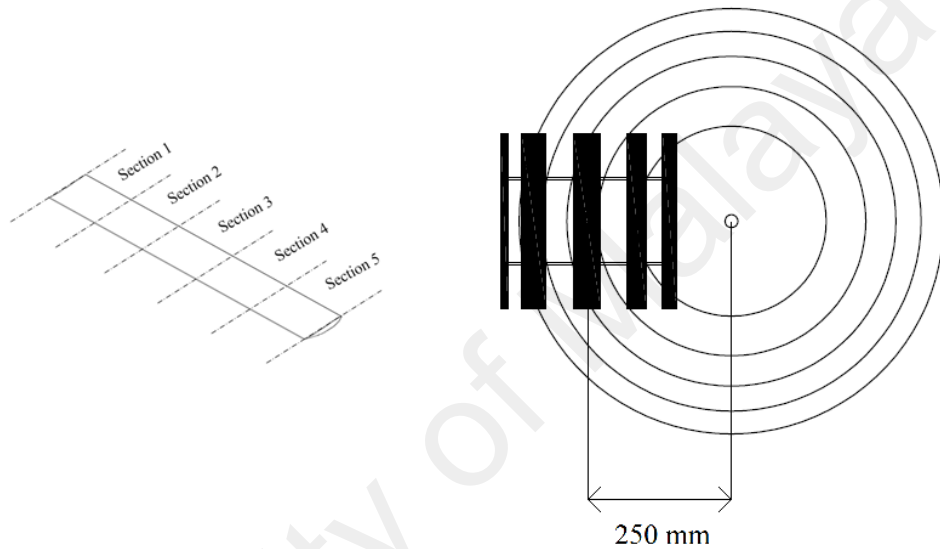
## APPENDIX C

**Appendix C1: Plan view of the wind turbine position against the circular band of the cooling tower model outlet. X indicates the distance of the wind turbine center from the center of the outlet.**



## Appendix C2: Sample of double multiple stream tube calculation

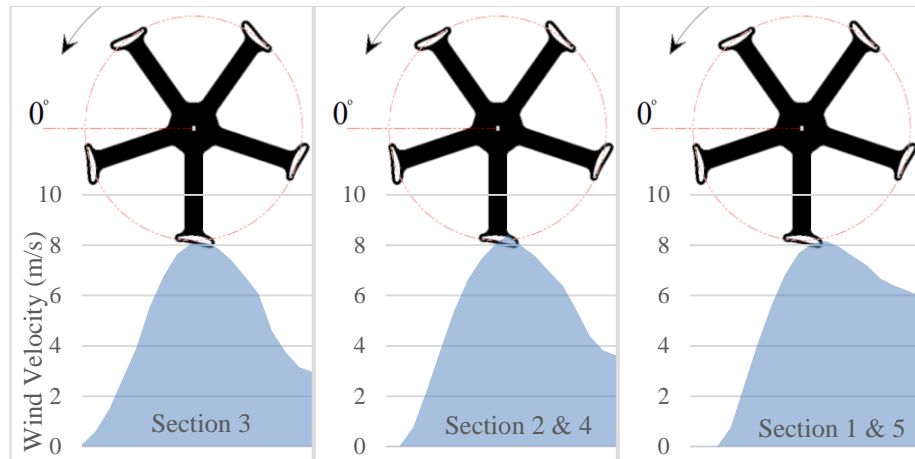
As a sample of calculation, configuration of  $X = 250$  mm and  $Y = 300$  mm is presented. The configuration of is as displayed below. The airfoil blade is divided into 5 sections of equal length as blow:



Parameters from experiments:

- Rotational speed
- Free-stream velocities for the not uniform wind is made according the plotted graph from the measured wind velocity. Wind velocity interacting to the wind turbine section is as below:





- The axial induction factor,  $a$  is assumed as  $1/3$  for all conditions

The blade is divided into 5 sections of equal length and the calculations are made separately on every sections. For this DMST analysis, since the wind velocity is in non-uniform pattern, the wind velocity for each stream tube is assume as different according to the measured wind velocity profile. The measured and extrapolated wind velocities at the upwind of the wind turbine for each blade section are as below.

Stream Tube	Azimuth Angle (°)	Blade Section 3 (m/s)	Blade Section 2 & 4 (m/s)	Blade Section 1 & 5 (m/s)
1	5	4.64	4.12	3.08
2	15	4.96	4.75	3.44
3	25	5.60	5.37	4.12
4	35	6.32	6.21	5.12
5	45	6.96	7.04	6.12
6	55	7.72	7.75	7.00
7	65	8.08	8.00	7.68
8	75	8.12	8.42	8.04
9	85	7.92	8.25	8.12
10	95	7.40	7.56	7.92
11	105	6.68	7.12	7.48
12	115	5.35	6.19	6.96
13	125	3.83	4.38	6.40
14	135	2.64	3.16	5.45
15	145	1.96	2.42	4.38
16	155	1.44	1.9	3.84
17	165	1.15	1.65	3.35
18	175	1.08	1.52	3.26

For this sample of calculation, stream tube 4 (azimuth angle of  $35^\circ$ ) and blade section 3 is selected to be presented. The parameters and calculation procedure is as below:

$$\text{Rotor rotational speed} = 304.3 \text{ rpm}$$

$$\text{Rotational speed, } \omega = 31.87 \text{ rad/s}$$

$$\text{Azimuth angle, } \theta = 35^\circ$$

$$= 0.6109 \text{ rad}$$

$$\text{Stream tube size, } \Delta\theta = 10^\circ$$

$$= .1745 \text{ rad}$$

$$\text{Free-stream wind, } V_\infty = 5.32 \text{ m/s}$$

$$\text{Local tip speed ratio, } \lambda = \frac{\omega R}{V_\infty}$$

$$= 0.76$$

$$\text{Induce Velocity, } V_a = V_\infty (1 - a)$$

$$= 4.213 \text{ m/s}$$

$$\text{Relative velocity, } V_R = \sqrt{(V_a \sin \theta)^2 + (\omega R + V_a \cos \theta)^2}$$

$$= 8.5788 \text{ m/s}$$

$$\text{Flow angle, } \phi = \tan^{-1} \left[ \frac{(1 - a) \sin \theta}{(1 - a) V_a + \lambda} \right]$$

$$= 16.362^\circ$$

The turbine blades have a pitch angle,  $\beta$  of  $10^\circ$ . Therefore,

$$\text{Angle of attack, } \alpha = \phi - \beta$$

$$= 6.362^\circ$$

With the obtained angle of attack, the lift coefficient,  $C_L$  and drag coefficient,  $C_D$  can be acquired from the particular Airfoil data (Appendix).

$$\text{Lift coefficient, } C_L = 1.465$$

$$\text{Drag coefficient, } C_D = 0.046$$

$$\text{Normal coefficient, } C_n = C_L \cos \alpha + C_D \sin \alpha$$

$$= 1.4611$$

$$\text{Tangential coefficient, } C_t = C_L \sin \alpha - C_D \cos \alpha$$

$$= 0.1166$$

$$\text{Instantaneous torque, } Q_i = \frac{1}{2} \rho V_R^2 (hc) C_t R$$

$$= 0.0021 \text{ Nm}$$

Instantaneous torque for upwind side of the stream tube 4 for single blade turbine is 0.0021 Nm. Since the turbine has five blades, the instantaneous torque for five blades are obtained by multiplying the value with the number of blade which is 0.106 Nm.

The same procedure is repeated for the downwind side of the same stream tube with the equilibrium velocity,  $V_e$  is assumed as the free-stream velocity for the downwind.  $V_e$  is calculated as below:

$$V_e = (1 - 2a)$$

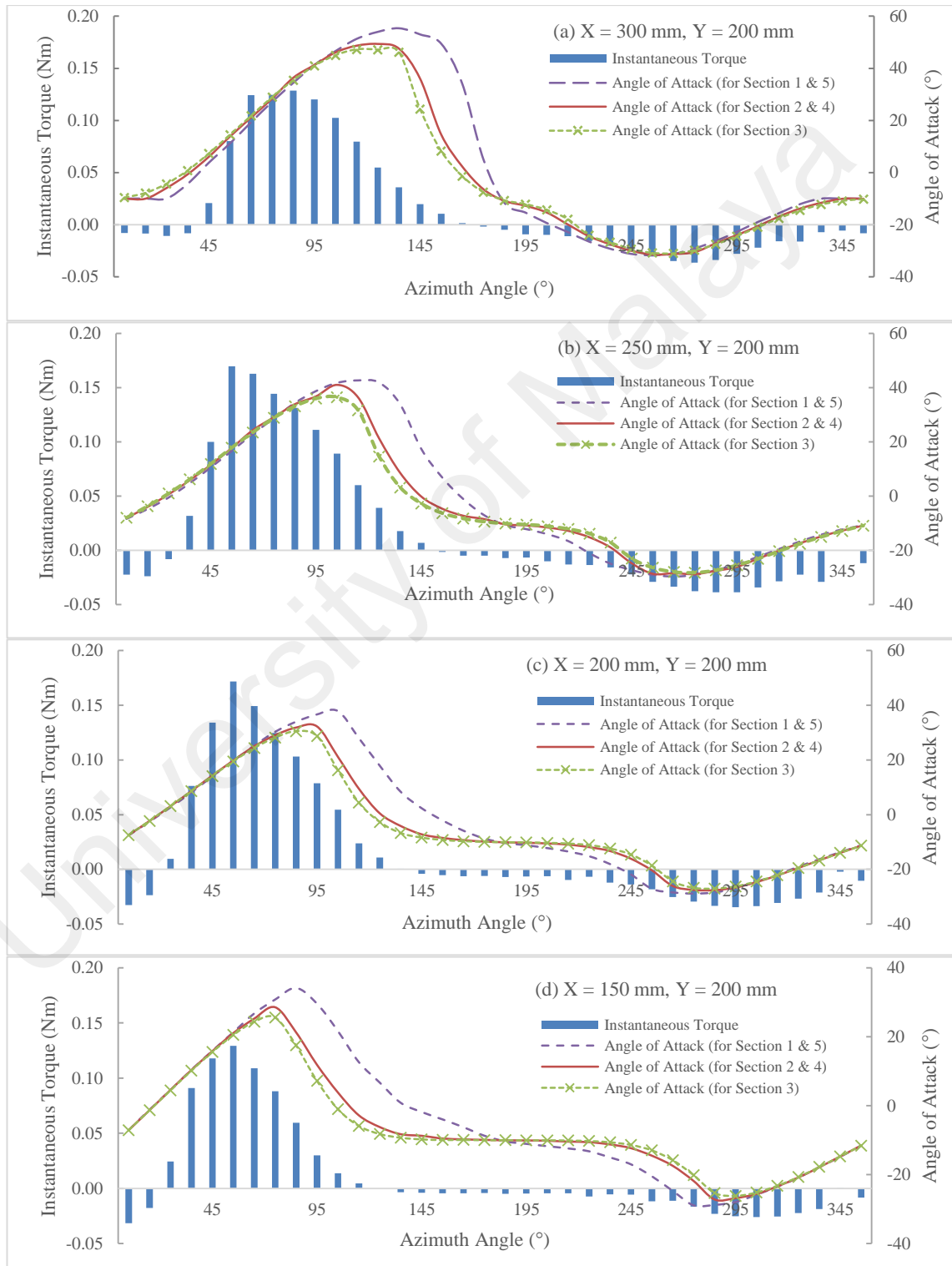
The same calculation procedure (for upwind and downwind) is repeated for all stream tube of the blade sections. Then, the data as tabulated in table below is obtained.

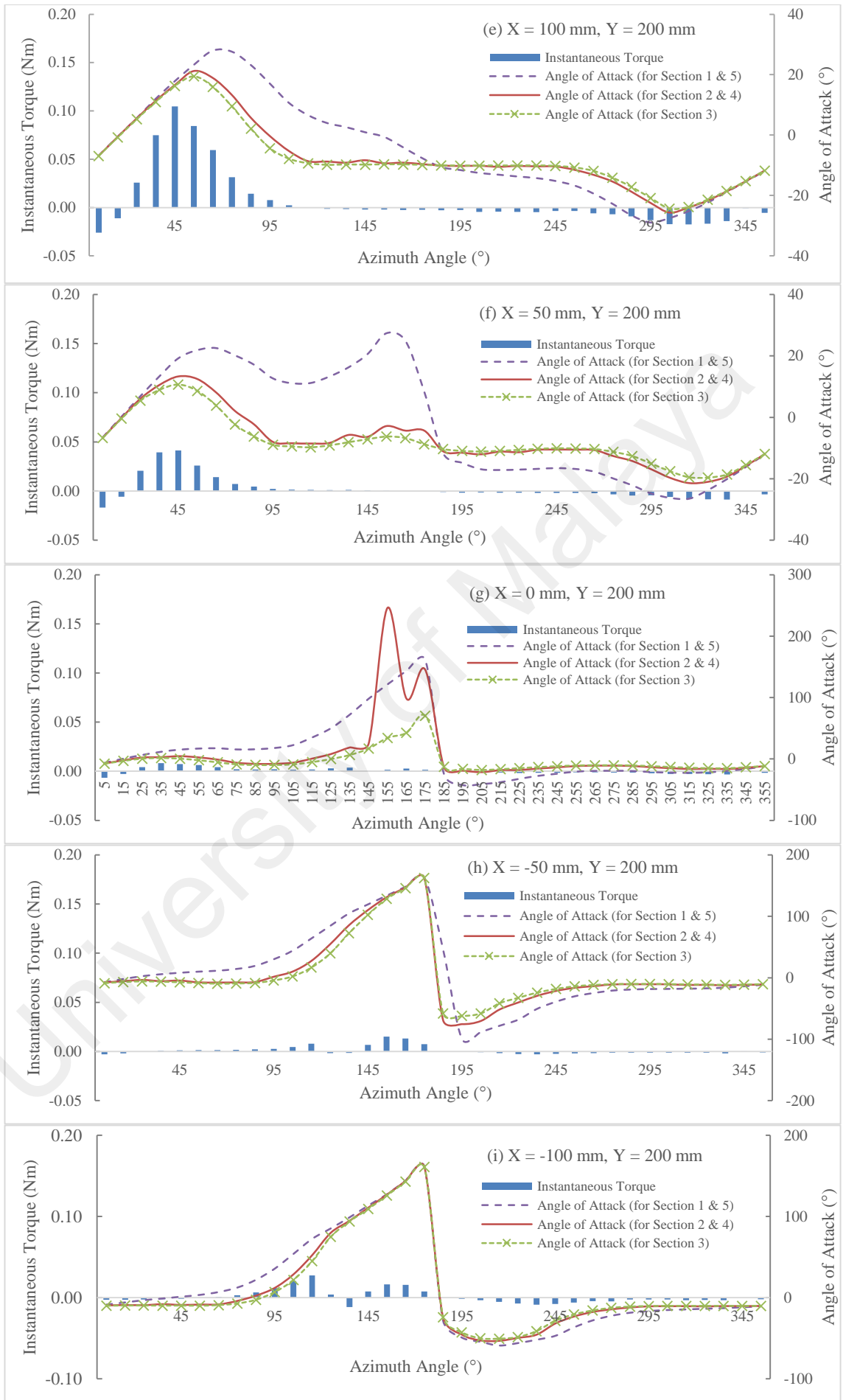
Stream tube	Azimuth angle (°)	Instantaneous torque, $Q_i$ (Nm)					
		Section 1	Section 2	Section 3	Section 4	Section 5	
Upwind	1	5	-0.0023	-0.0053	-0.0058	-0.0053	-0.0023
	2	15	-0.0023	-0.0058	-0.0061	-0.0058	-0.0023
	3	25	-0.0023	-0.0017	-0.0014	-0.0017	-0.0023
	4	35	-0.0031	0.0101	0.0106	0.0101	-0.0031
	5	45	-0.0012	0.0280	0.0273	0.0280	-0.0012
	6	55	0.0118	0.0448	0.0444	0.0448	0.0118
	7	65	0.0325	0.0407	0.0416	0.0407	0.0325
	8	75	0.0339	0.0383	0.0369	0.0383	0.0339
	9	85	0.0333	0.0352	0.0329	0.0352	0.0333
	10	95	0.0334	0.0282	0.0277	0.0282	0.0334
	11	105	0.0297	0.0228	0.0211	0.0228	0.0297
	12	115	0.0239	0.0158	0.0129	0.0158	0.0239
	13	125	0.0173	0.0087	0.0085	0.0087	0.0173
	14	135	0.0117	0.0056	0.0038	0.0056	0.0117
	15	145	0.0068	0.0012	-0.0002	0.0012	0.0068
	16	155	0.0035	-0.0008	-0.0015	-0.0008	0.0035
	17	165	0.0015	-0.0014	-0.0016	-0.0014	0.0015
	18	175	0.0002	-0.0013	-0.0015	-0.0013	0.0002
Downwind	19	185	-0.0010	-0.0018	-0.0019	-0.0018	-0.0010
	20	195	-0.0019	-0.0014	-0.0018	-0.0014	-0.0019
	21	205	-0.0026	-0.0013	-0.0013	-0.0013	-0.0026
	22	215	-0.0037	-0.0042	-0.0040	-0.0042	-0.0037
	23	225	-0.0047	-0.0027	-0.0025	-0.0027	-0.0047
	24	235	-0.0063	-0.0037	-0.0036	-0.0037	-0.0063
	25	245	-0.0074	-0.0056	-0.0051	-0.0056	-0.0074
	26	255	-0.0089	-0.0074	-0.0070	-0.0074	-0.0089
	27	265	-0.0095	-0.0082	-0.0083	-0.0082	-0.0095
	28	275	-0.0094	-0.0101	-0.0094	-0.0101	-0.0094
	29	285	-0.0084	-0.0100	-0.0100	-0.0100	-0.0084
	30	295	-0.0072	-0.0097	-0.0097	-0.0097	-0.0072
	31	305	-0.0053	-0.0086	-0.0086	-0.0086	-0.0053
	32	315	-0.0069	-0.0072	-0.0072	-0.0072	-0.0069
	33	325	-0.0020	-0.0057	-0.0058	-0.0057	-0.0020
	34	335	-0.0024	-0.0079	-0.0046	-0.0079	-0.0024
	35	345	-0.0020	-0.0015	-0.0014	-0.0015	-0.0020
	36	355	-0.0025	-0.0028	-0.0029	-0.0028	-0.0025
<b>Average</b>			<b>0.0038</b>	<b>0.0045</b>	<b>0.0043</b>	<b>0.0045</b>	<b>0.0038</b>

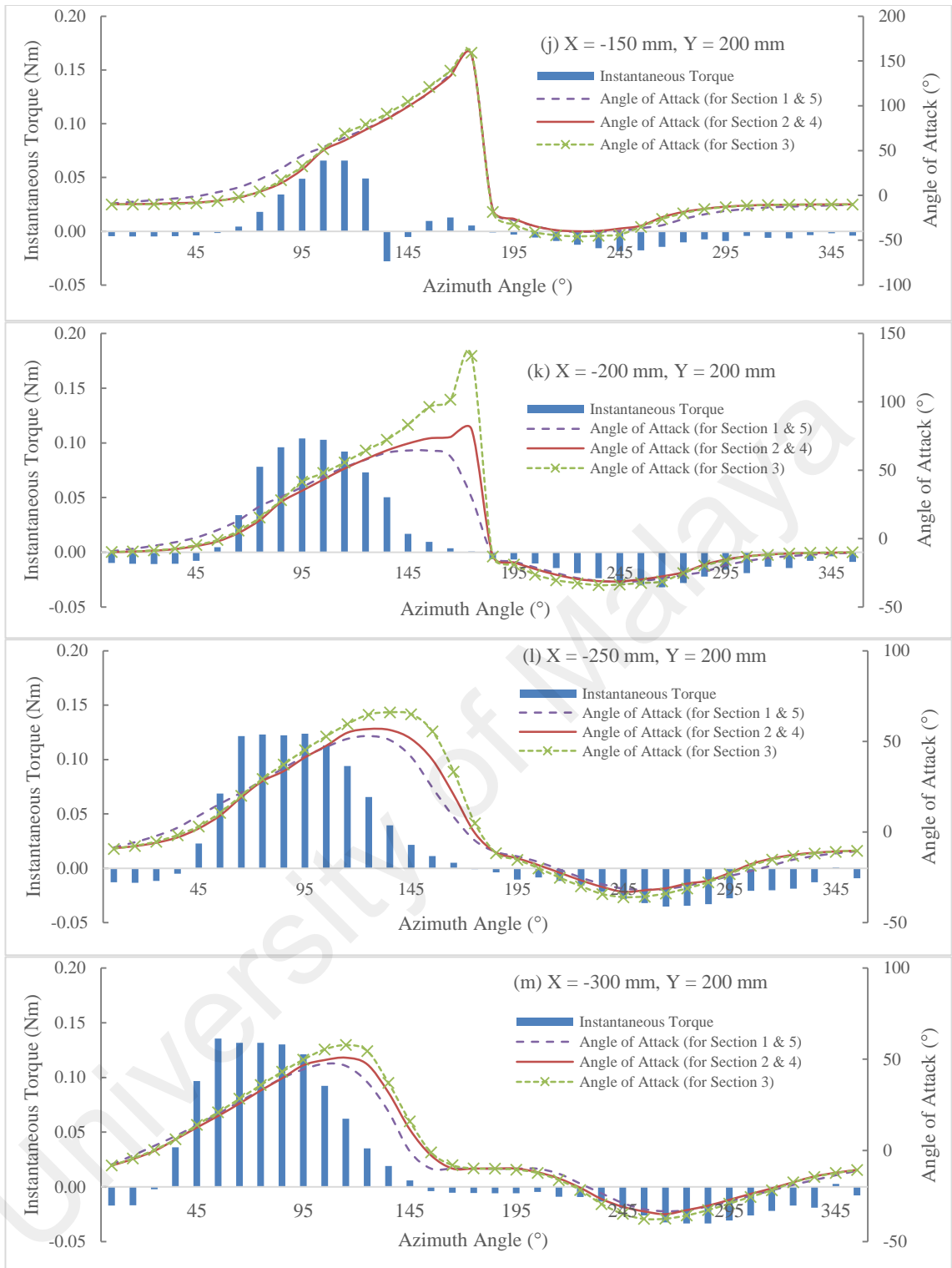
The total average torque generated by the turbine at this configuration by the summation of the average torque from all sections.

## APPENDIX D

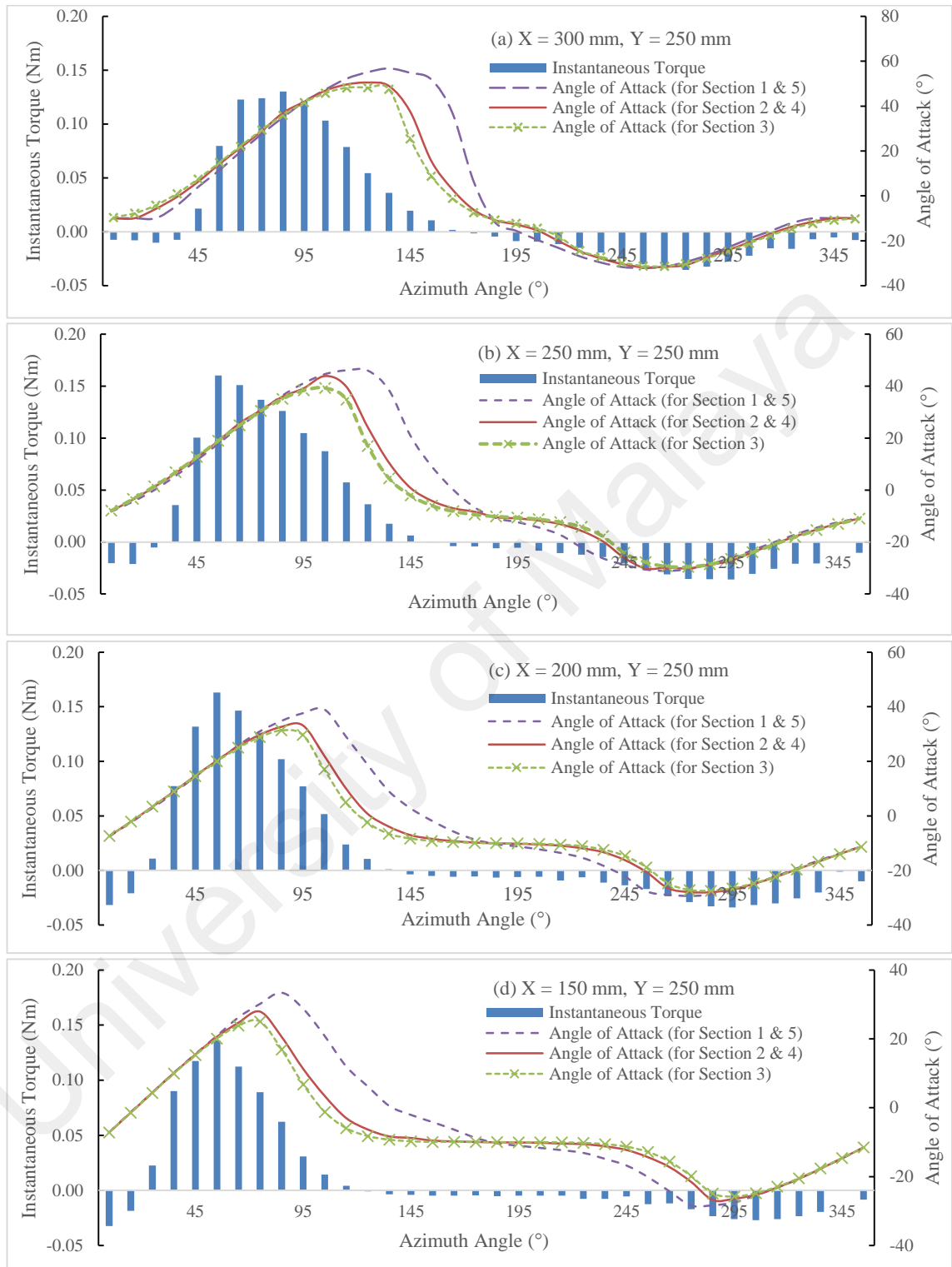
**Appendix D1: Instantaneous torque against azimuth angle and angle of attack versus azimuth angle at vertical position of  $Y = 200$  mm for the fan speed of 708 rpm.**



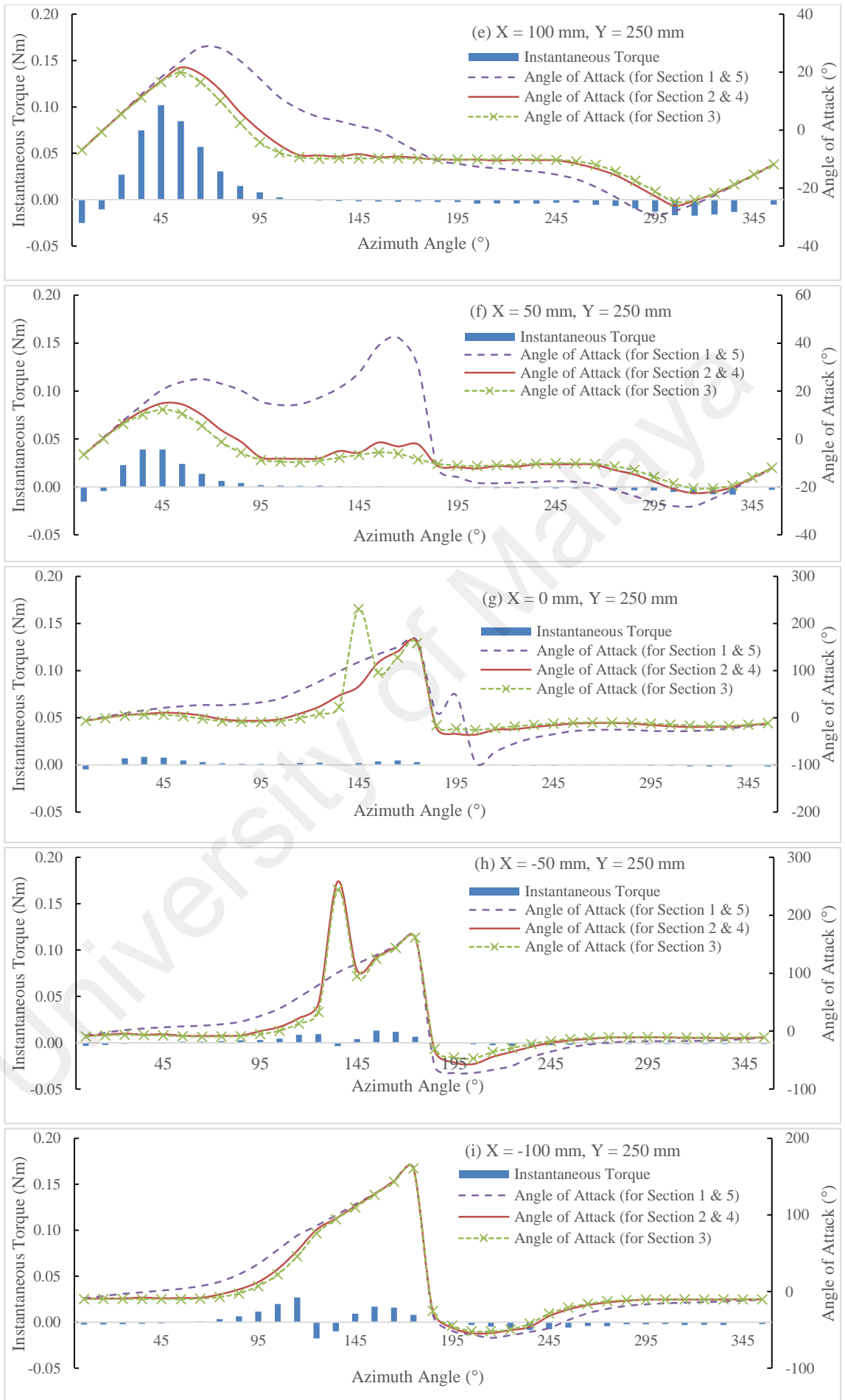


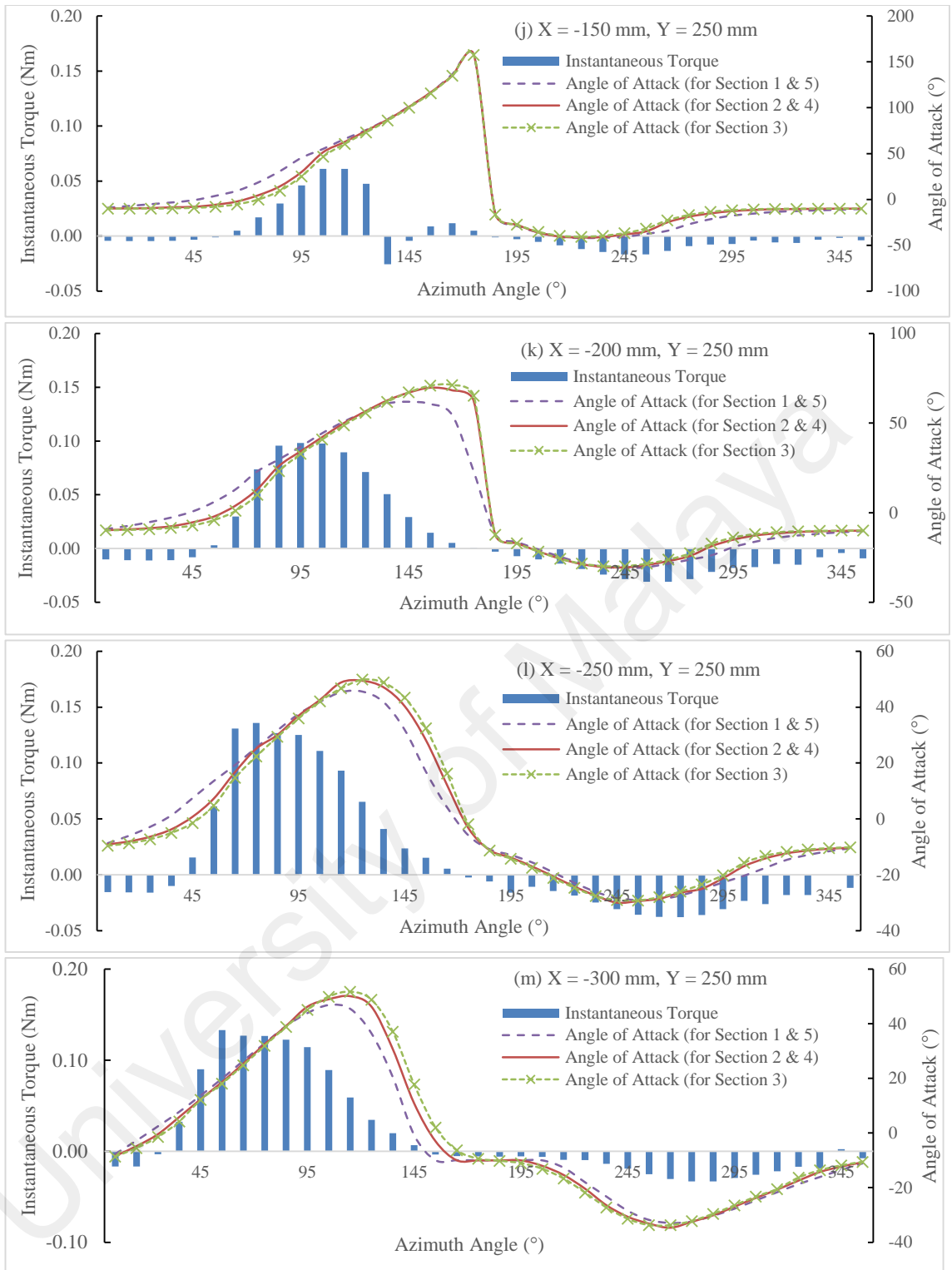


**Appendix D2: Instantaneous torque against azimuth angle and angle of attack versus azimuth angle at vertical position of  $Y = 250$  mm for the fan speed of 708 rpm.**

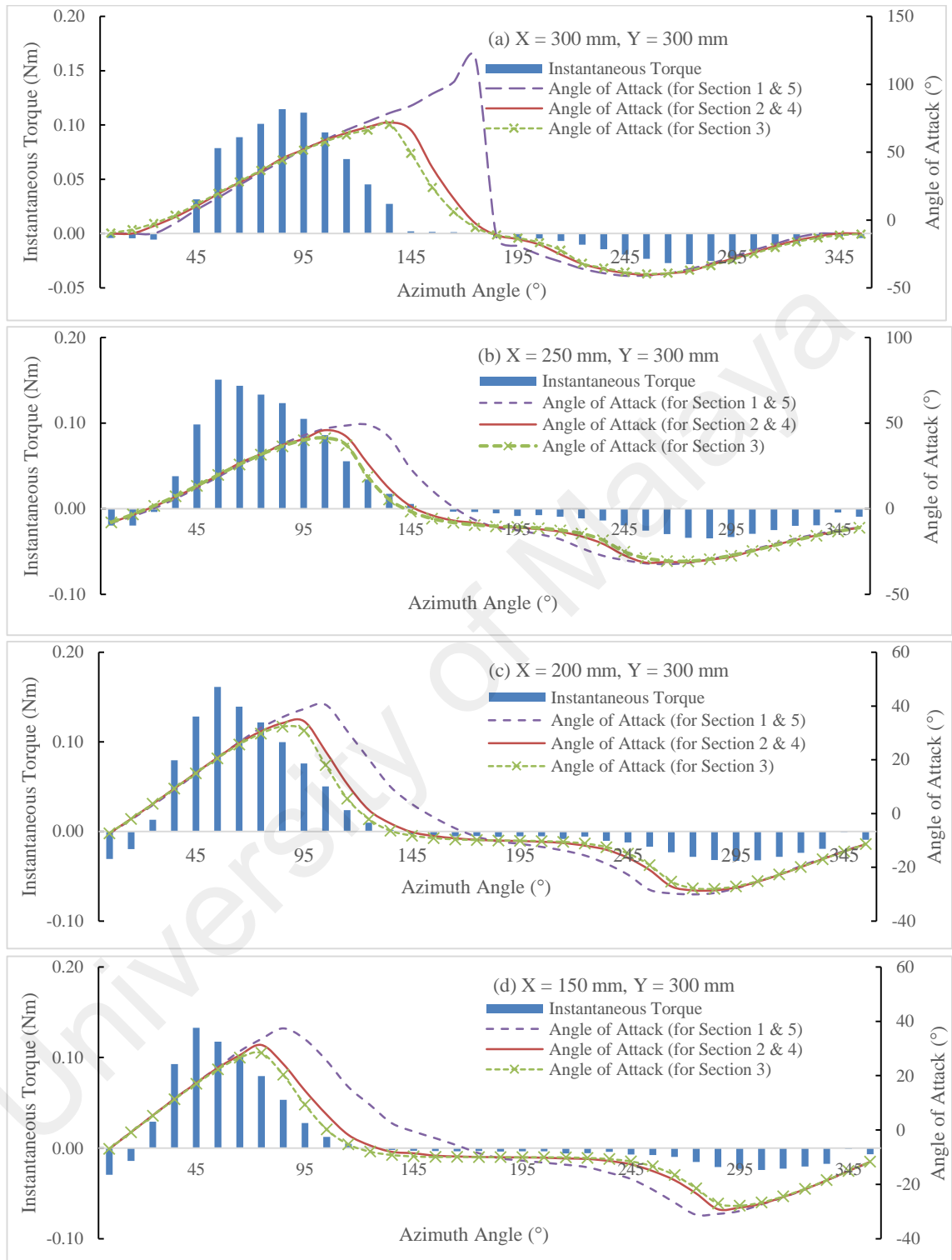


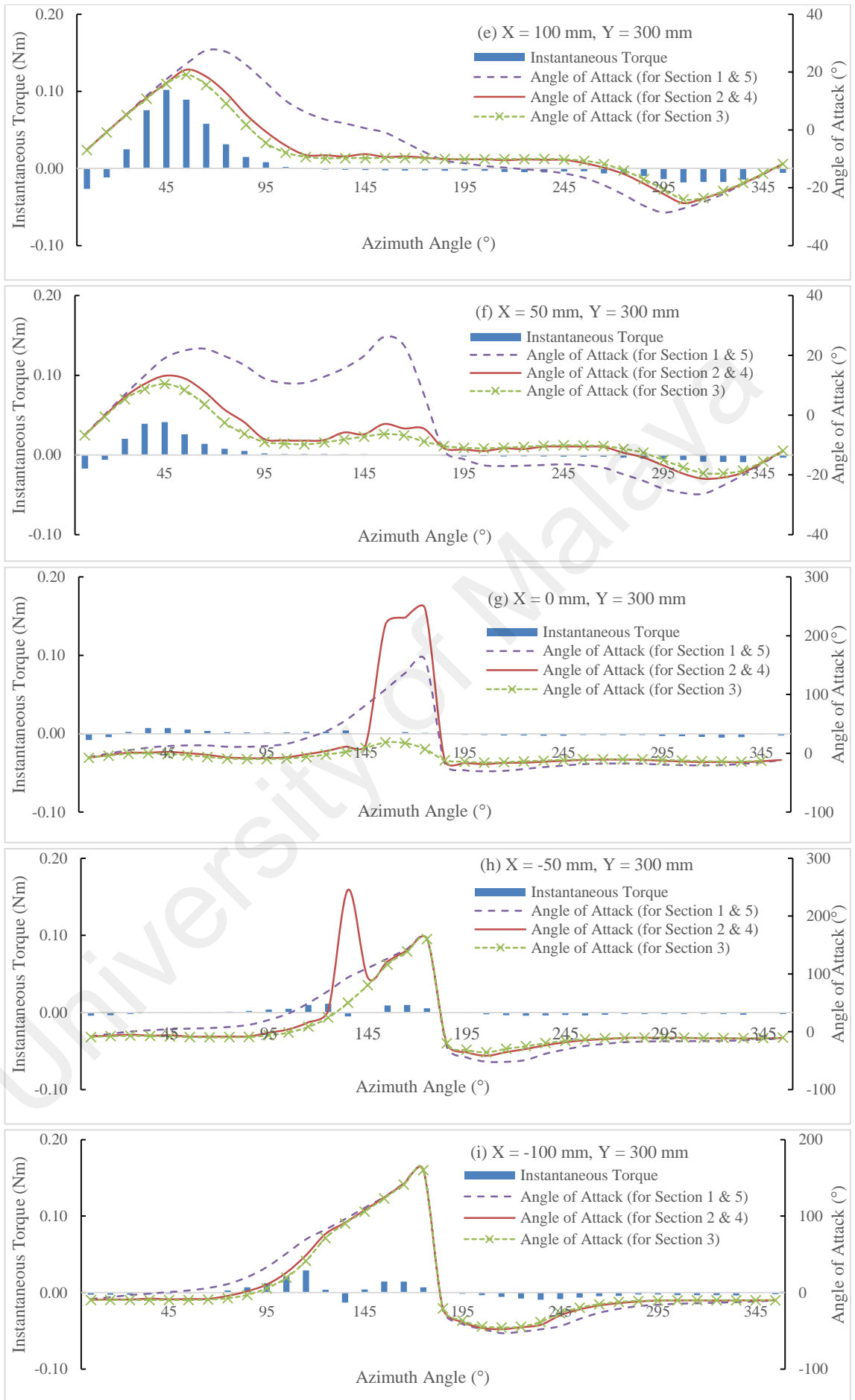


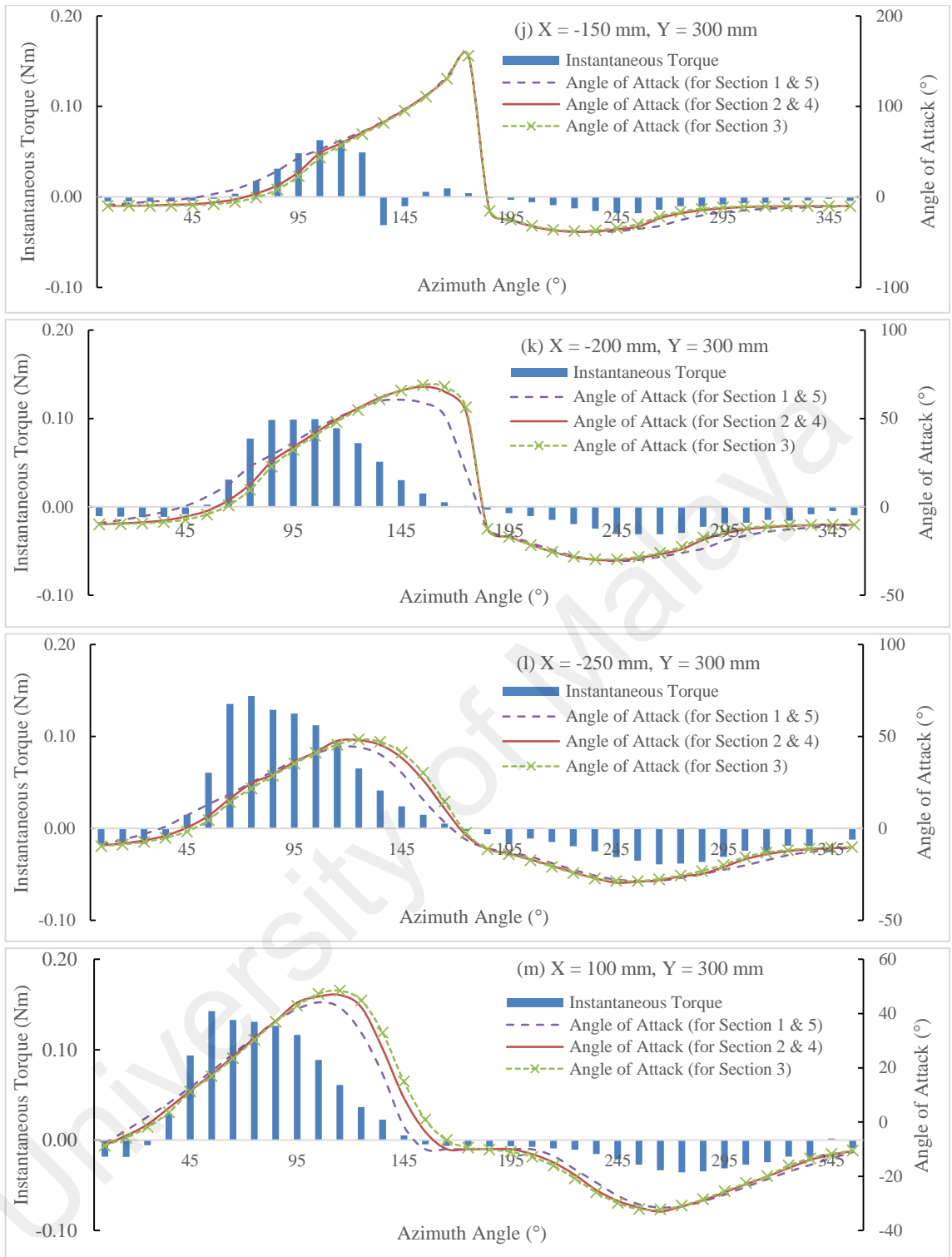




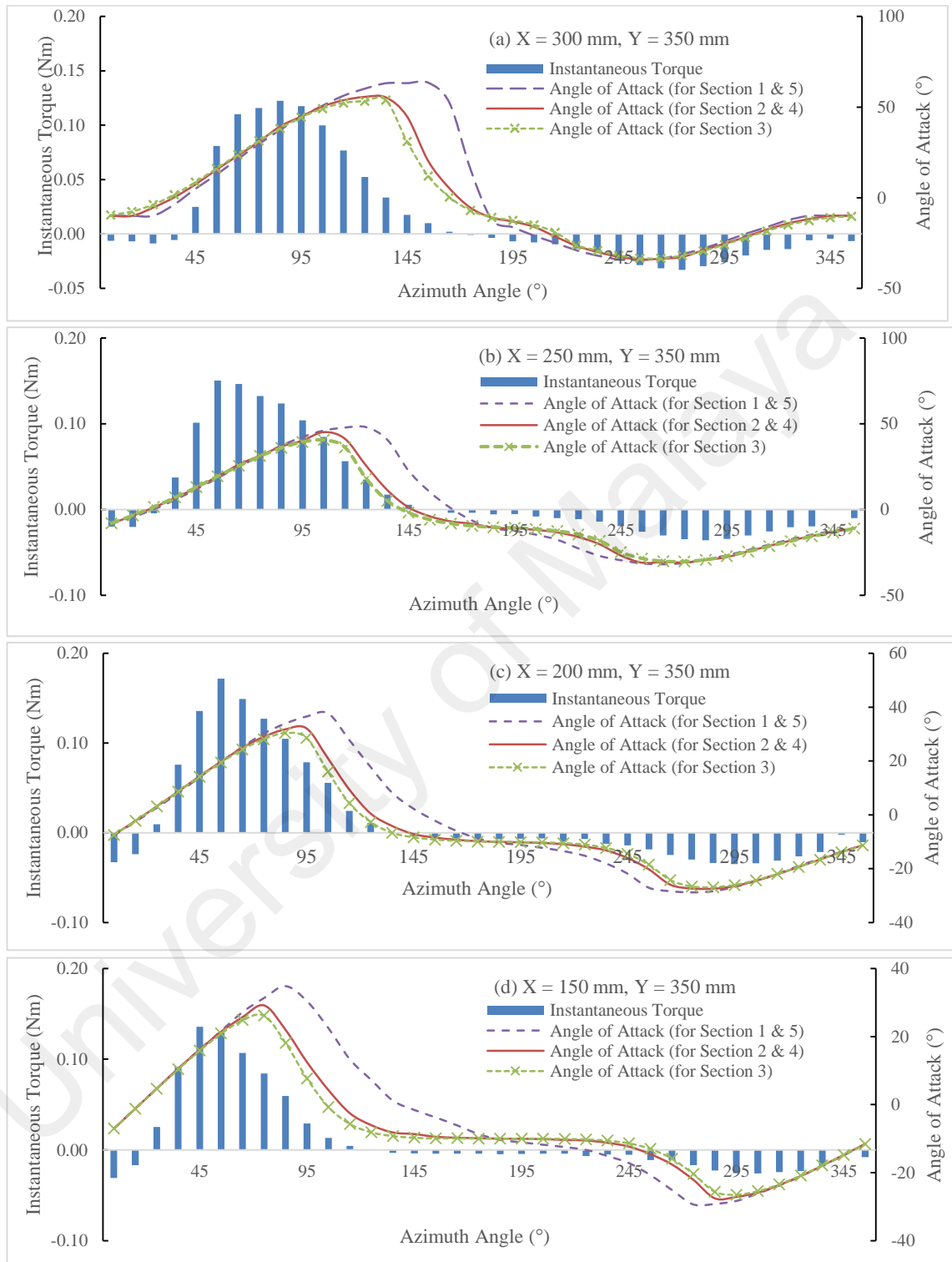
**Appendix D3: Instantaneous torque against azimuth angle and angle of attack versus azimuth angle at vertical position of  $Y = 300$  mm for the fan speed of 708 rpm.**

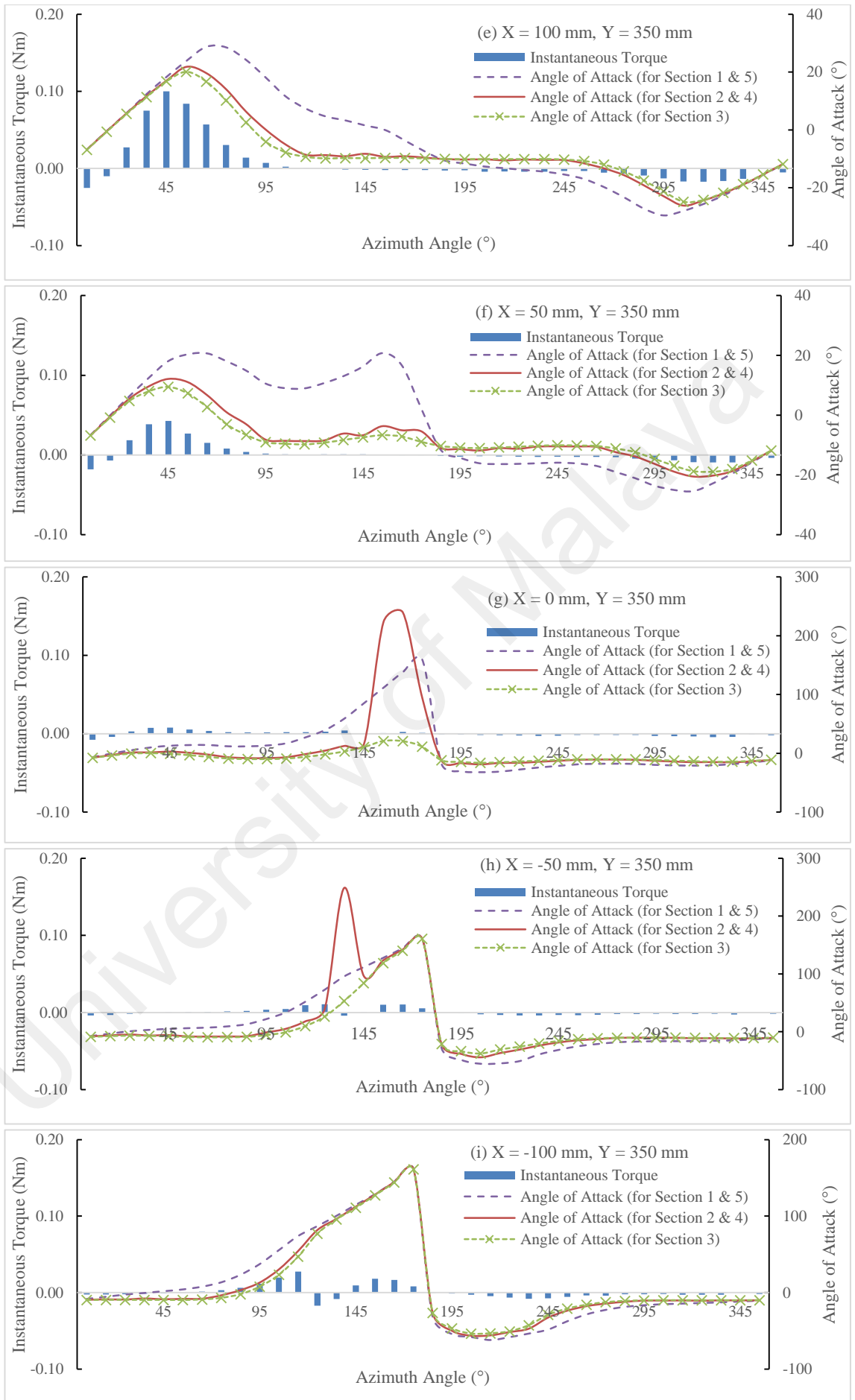


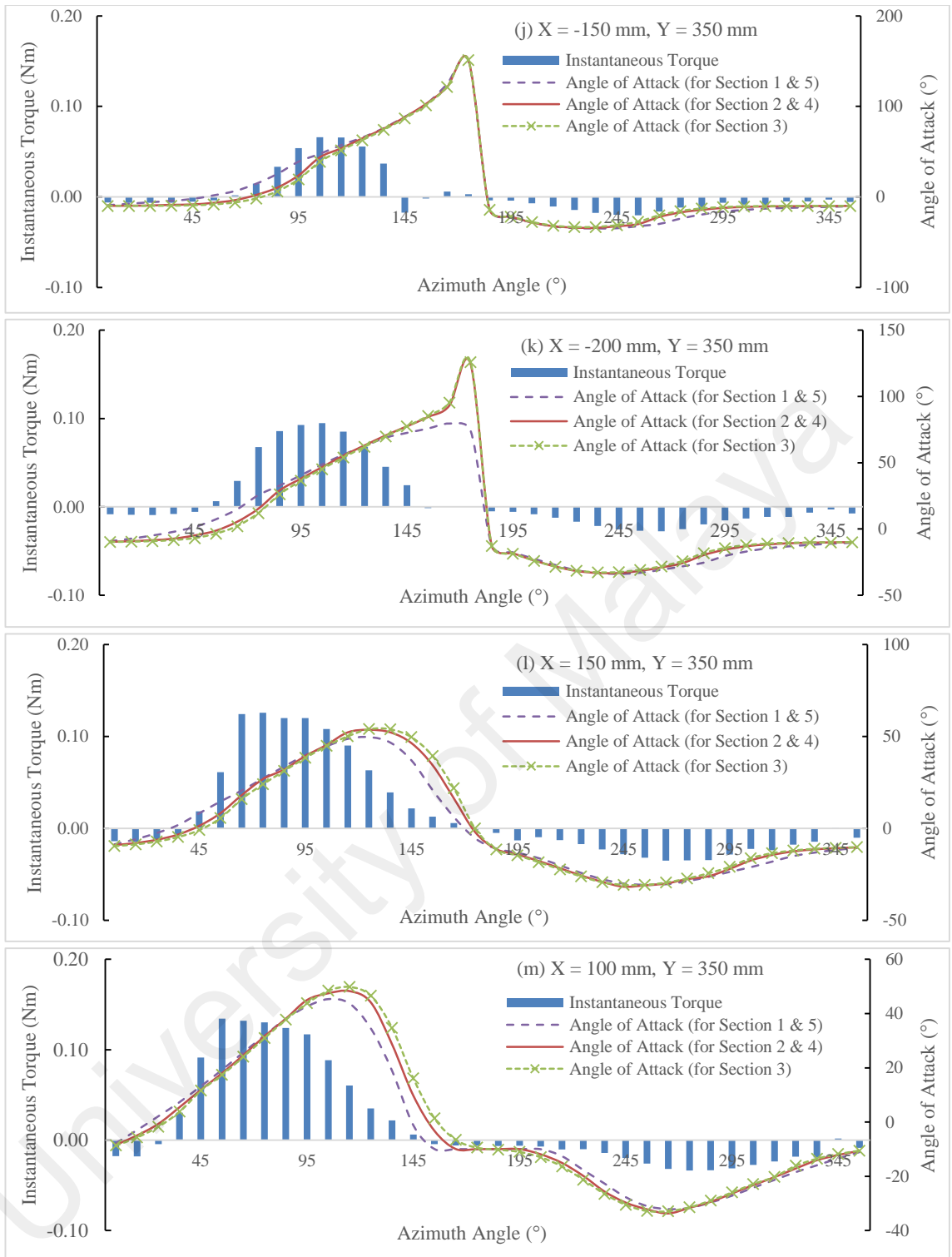




**Appendix D4: Instantaneous torque against azimuth angle and angle of attack versus azimuth angle at vertical position of  $Y = 350$  mm for the fan speed of 708 rpm.**

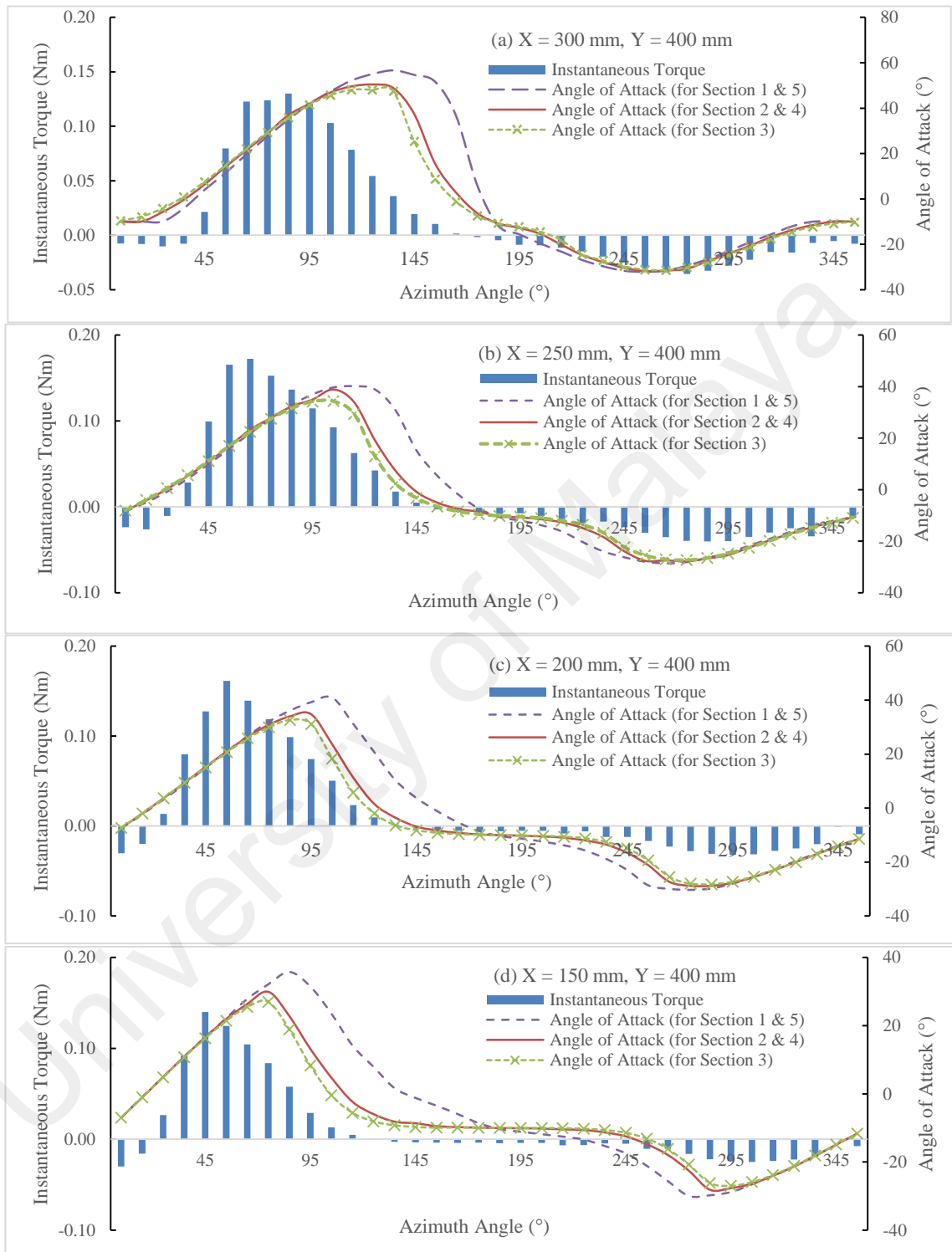


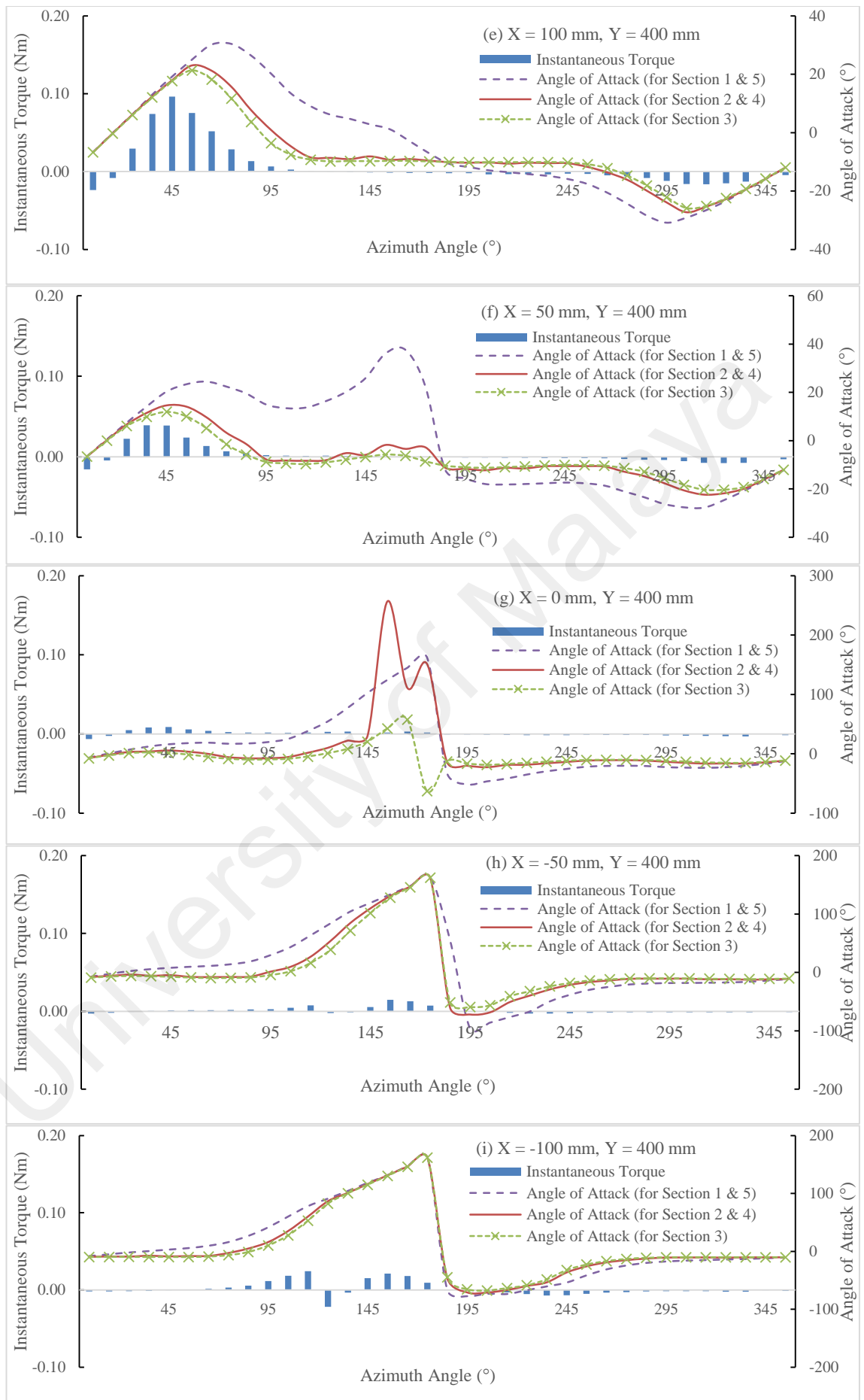


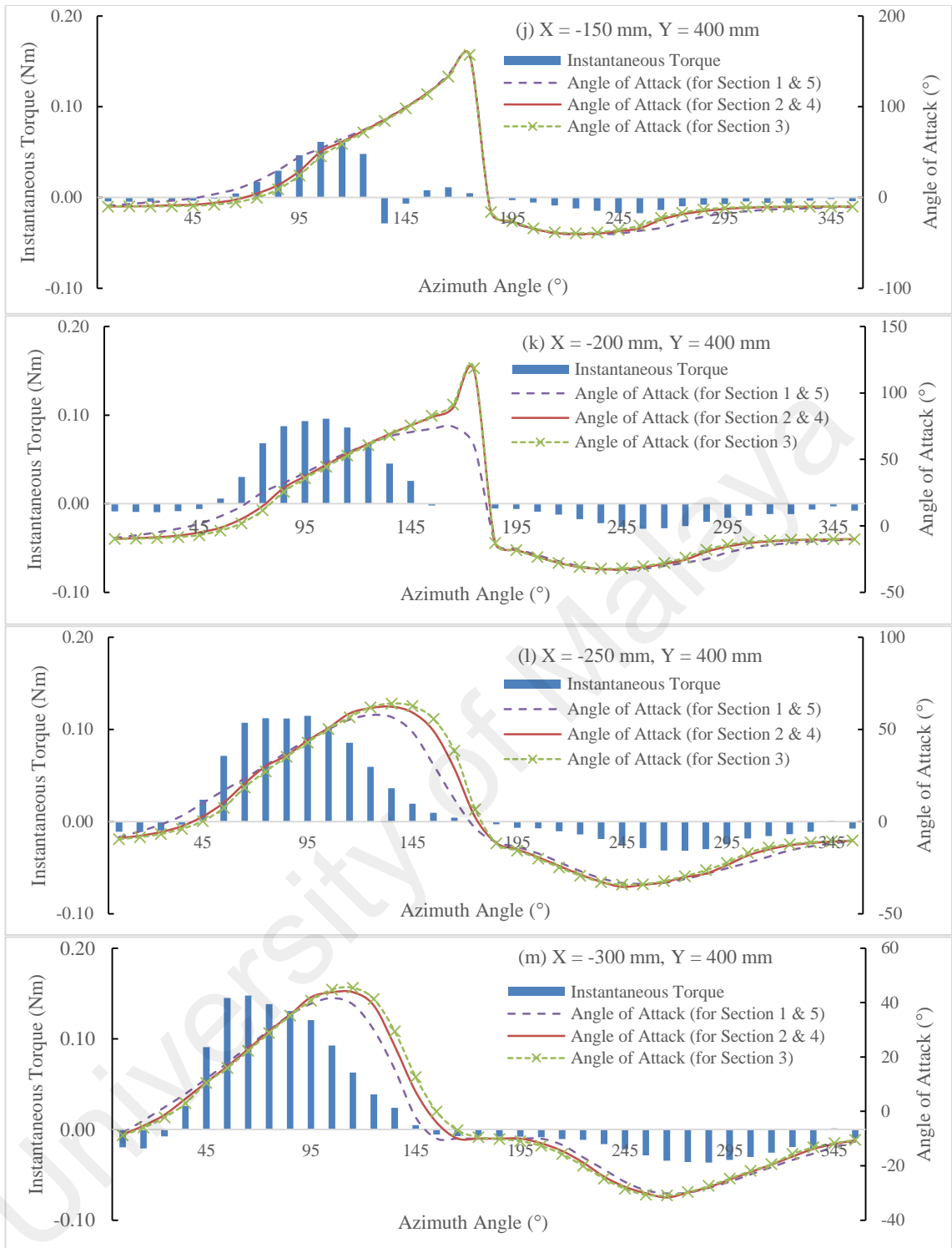




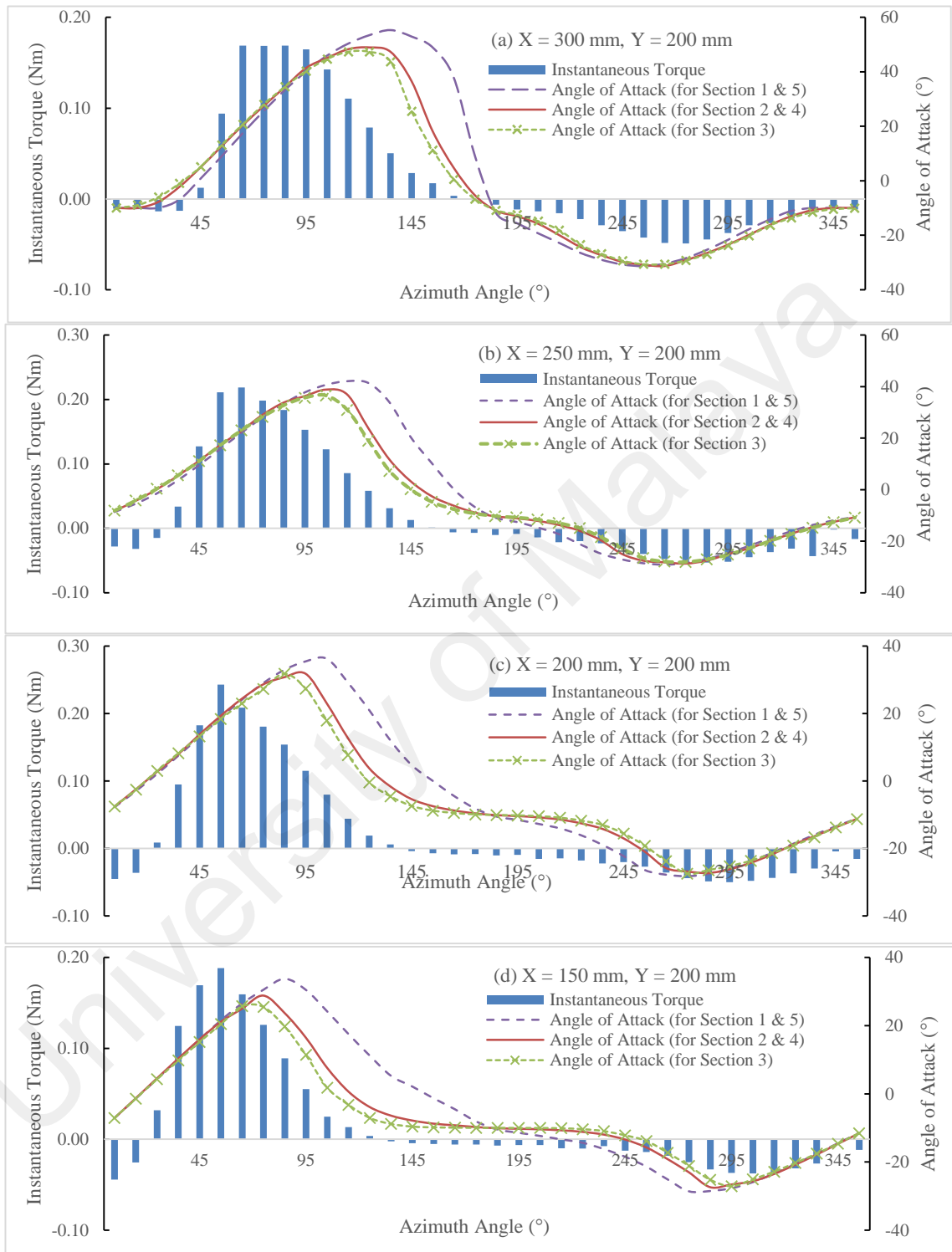
**Appendix D5: Instantaneous torque against azimuth angle and angle of attack versus azimuth angle at vertical position of  $Y = 400$  mm for the fan speed of 708 rpm.**

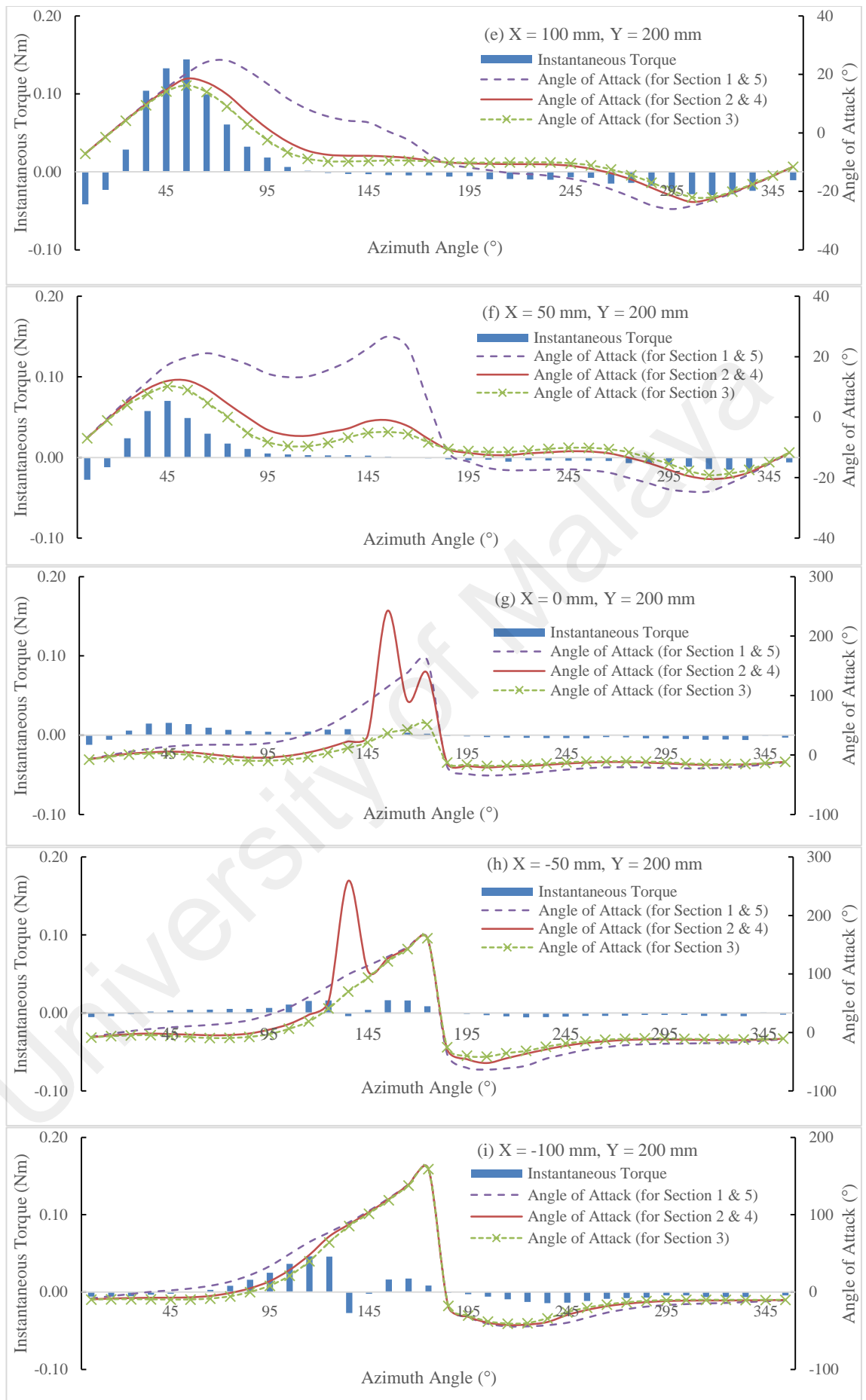


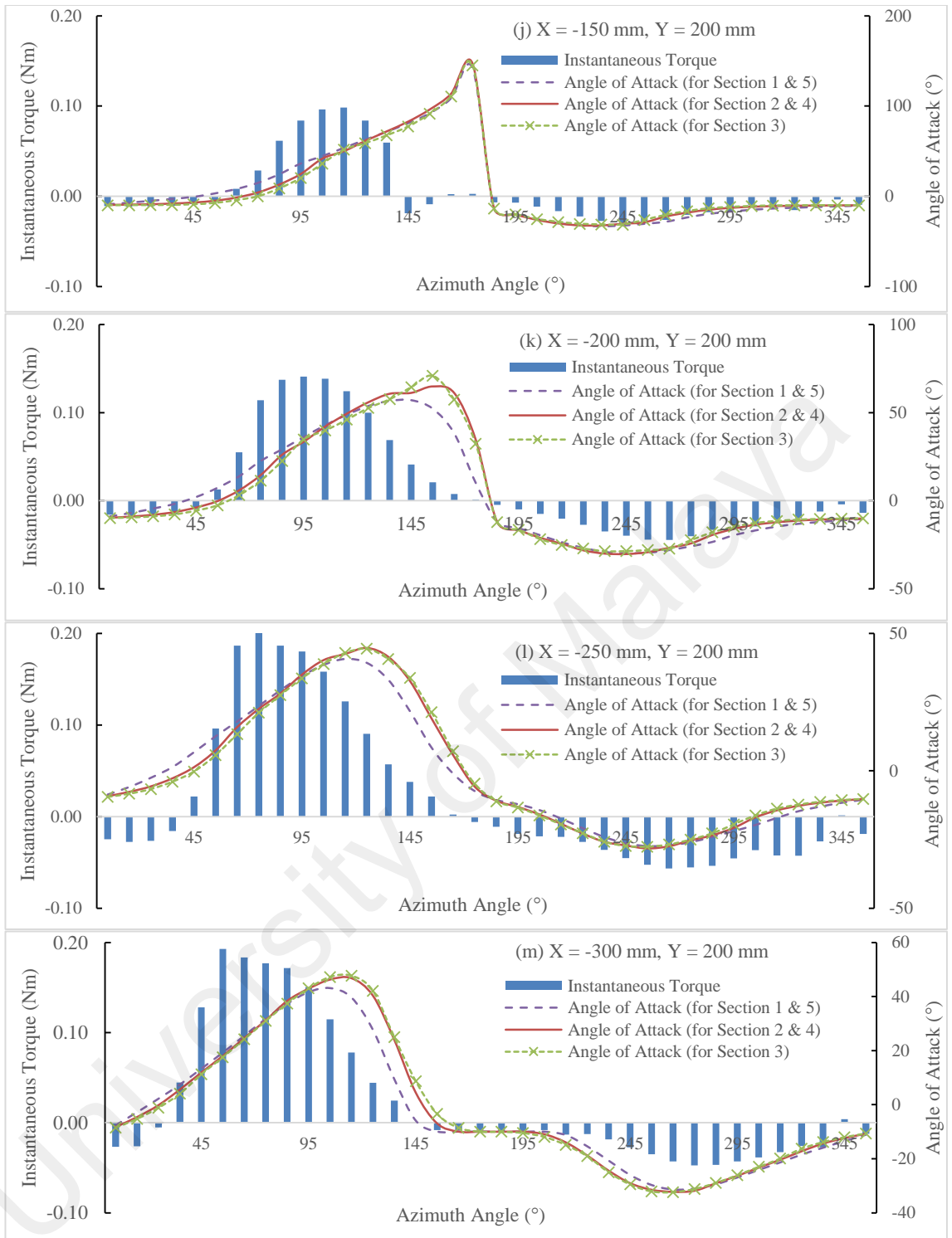




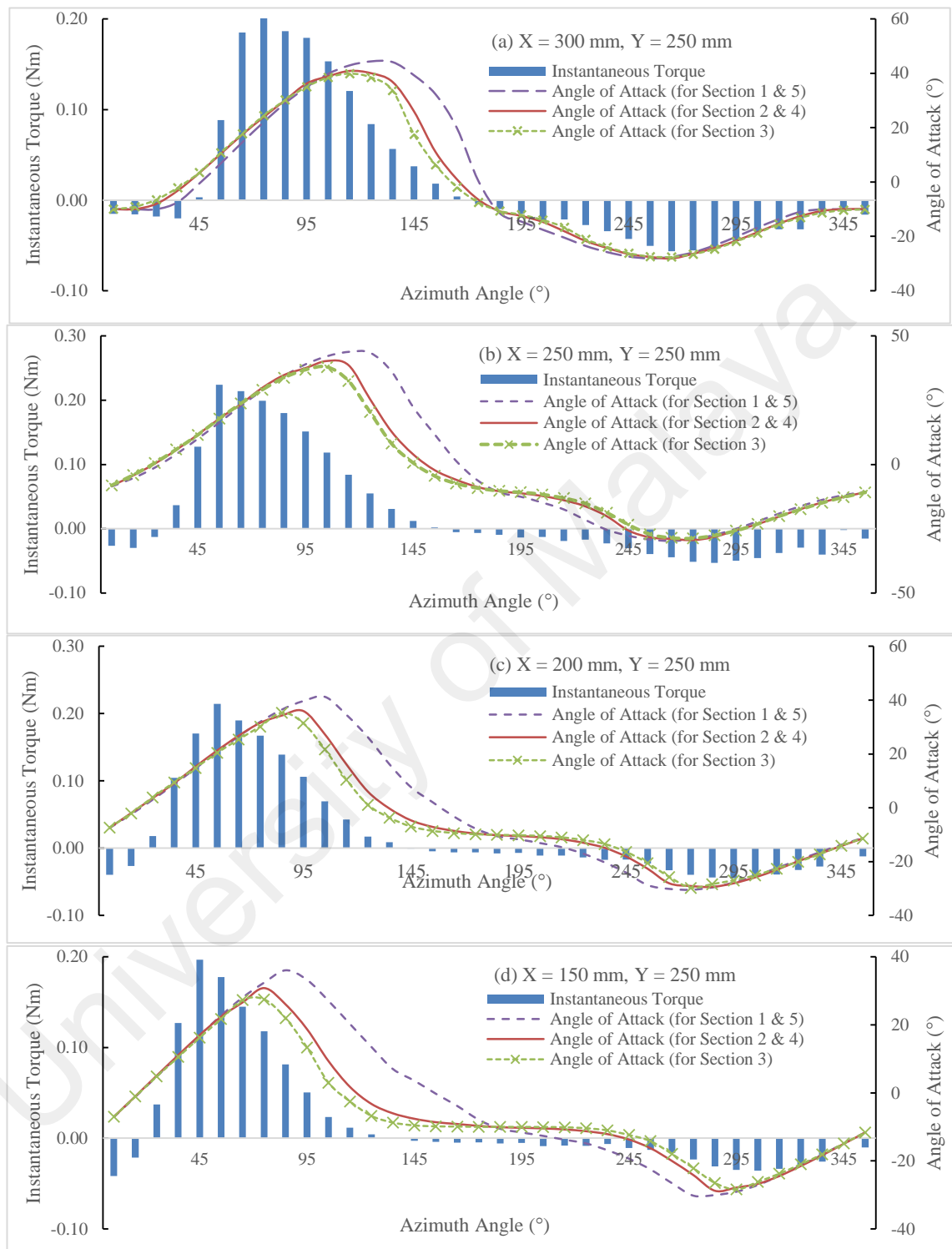
**Appendix D6: Instantaneous torque against azimuth angle and angle of attack versus azimuth angle at vertical position of  $Y = 200$  mm for the fan speed of 910 rpm.**

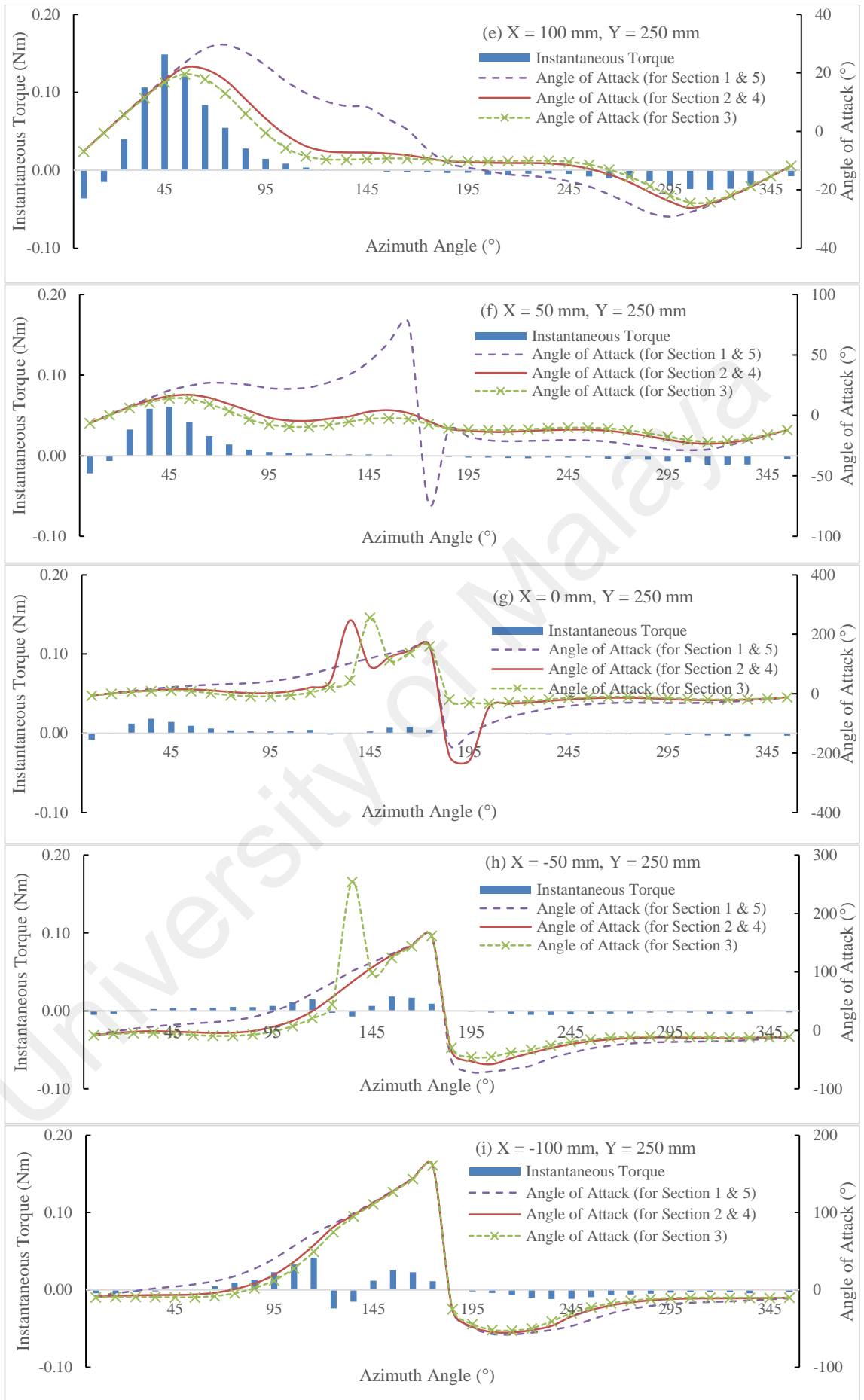




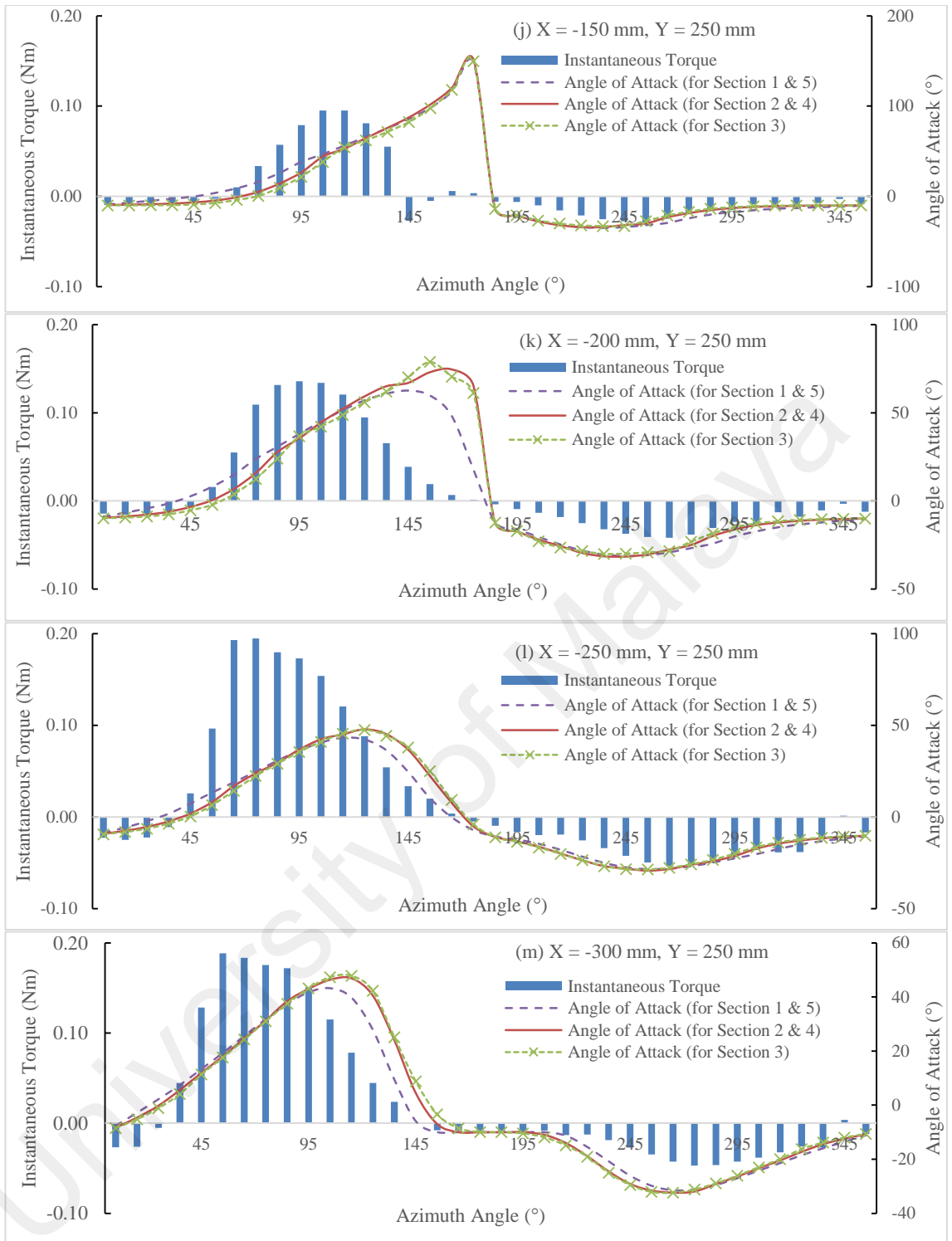


**Appendix D7: Instantaneous torque against azimuth angle and angle of attack versus azimuth angle at vertical position of  $Y = 250$  mm for the fan speed of 910 rpm.**

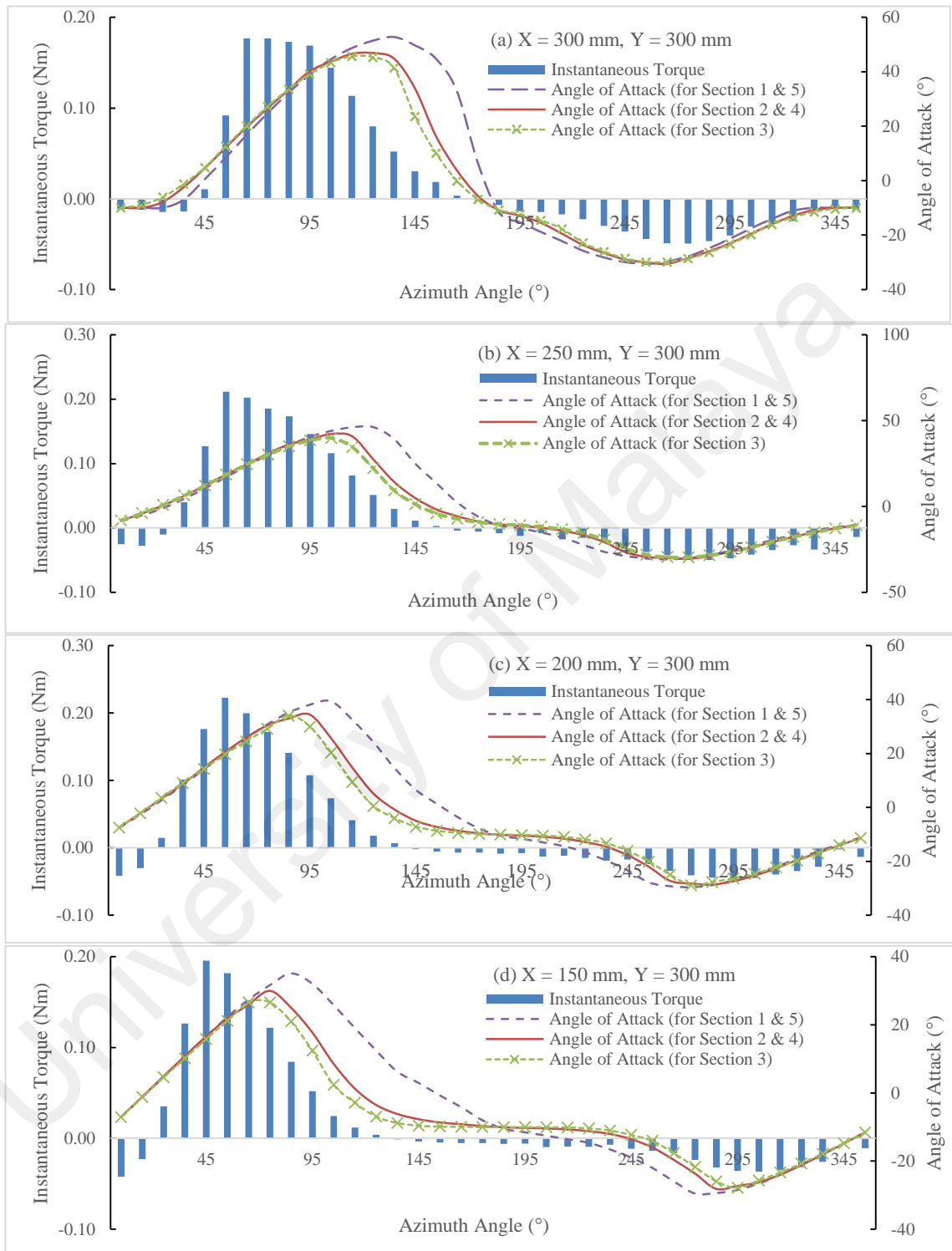


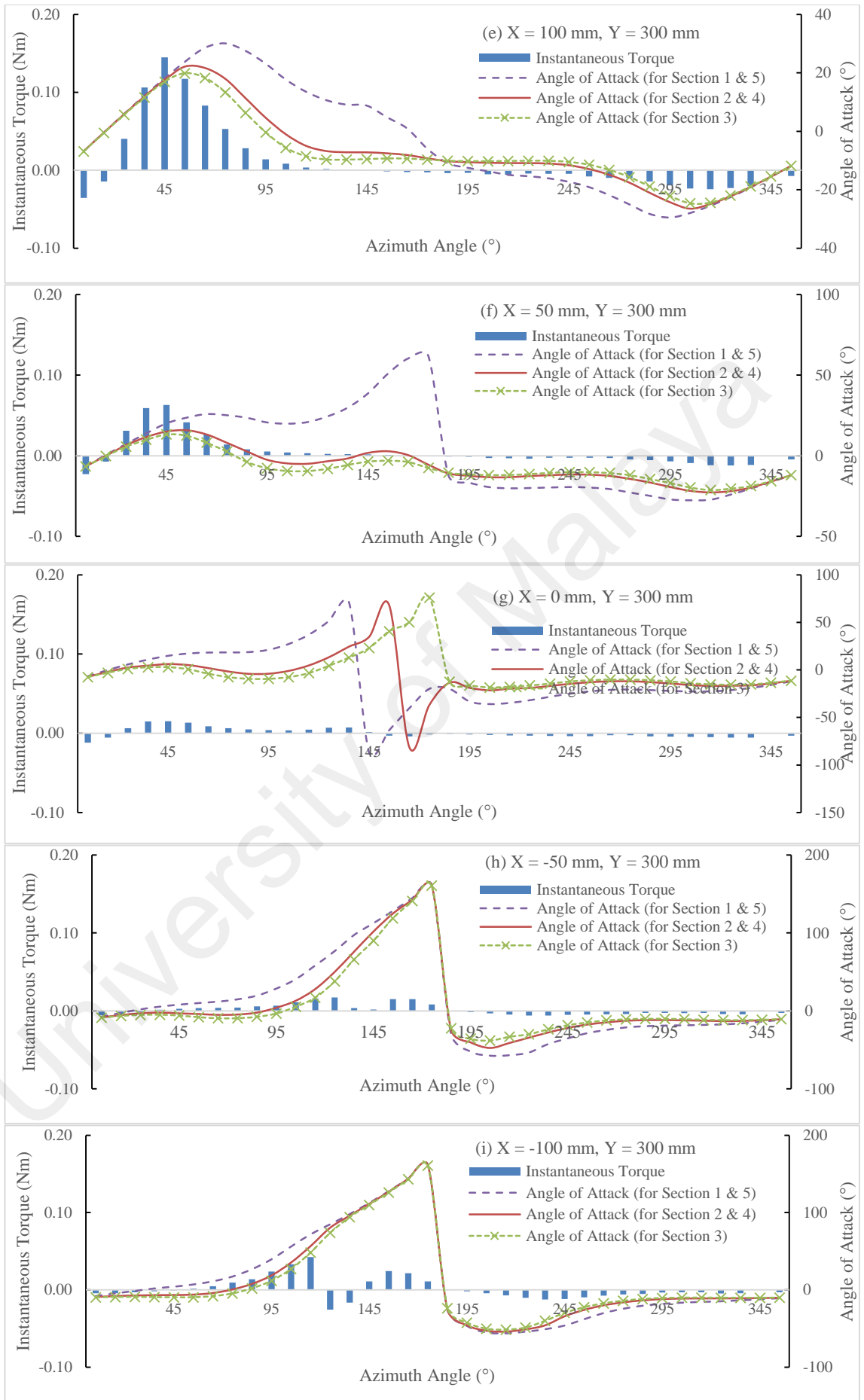


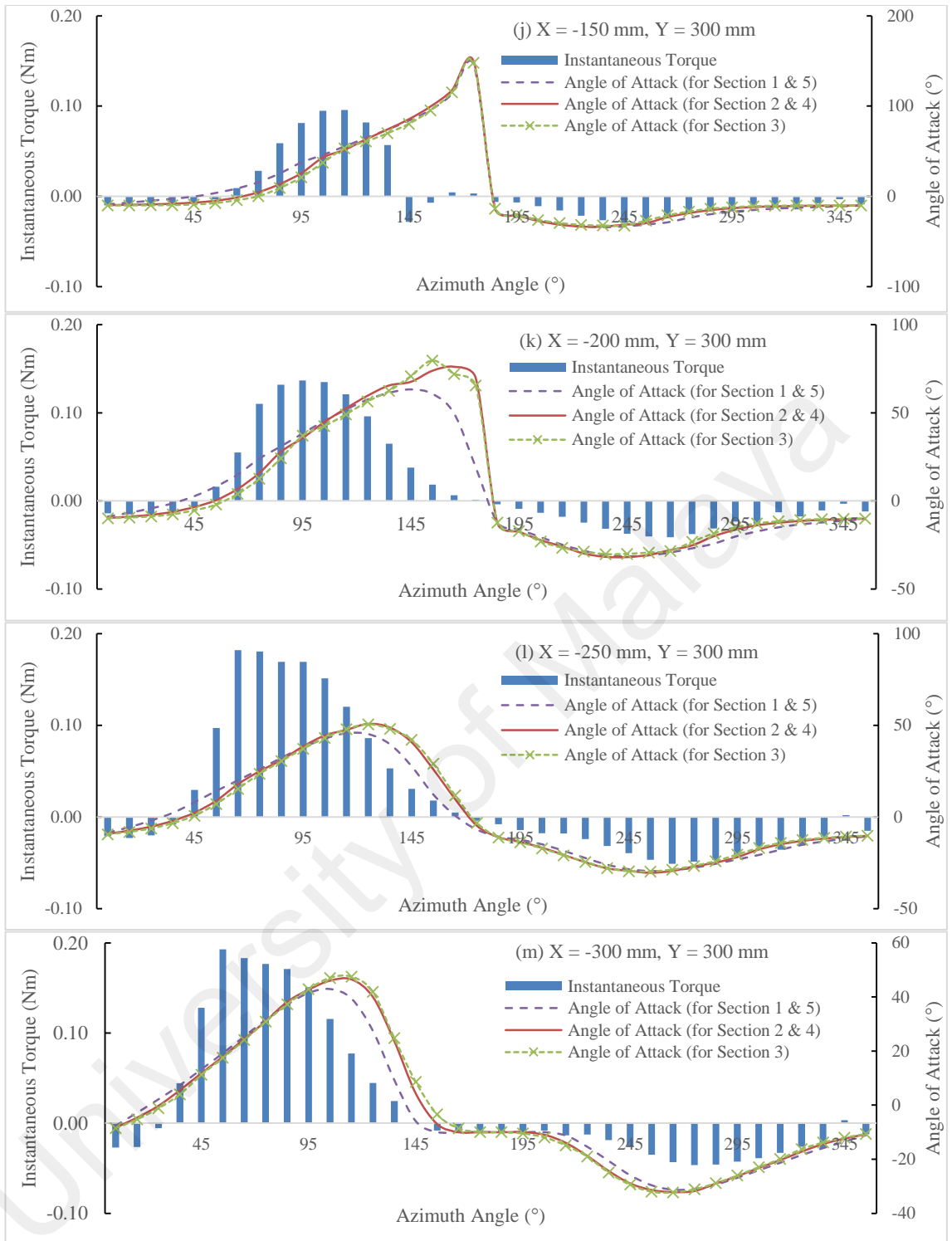




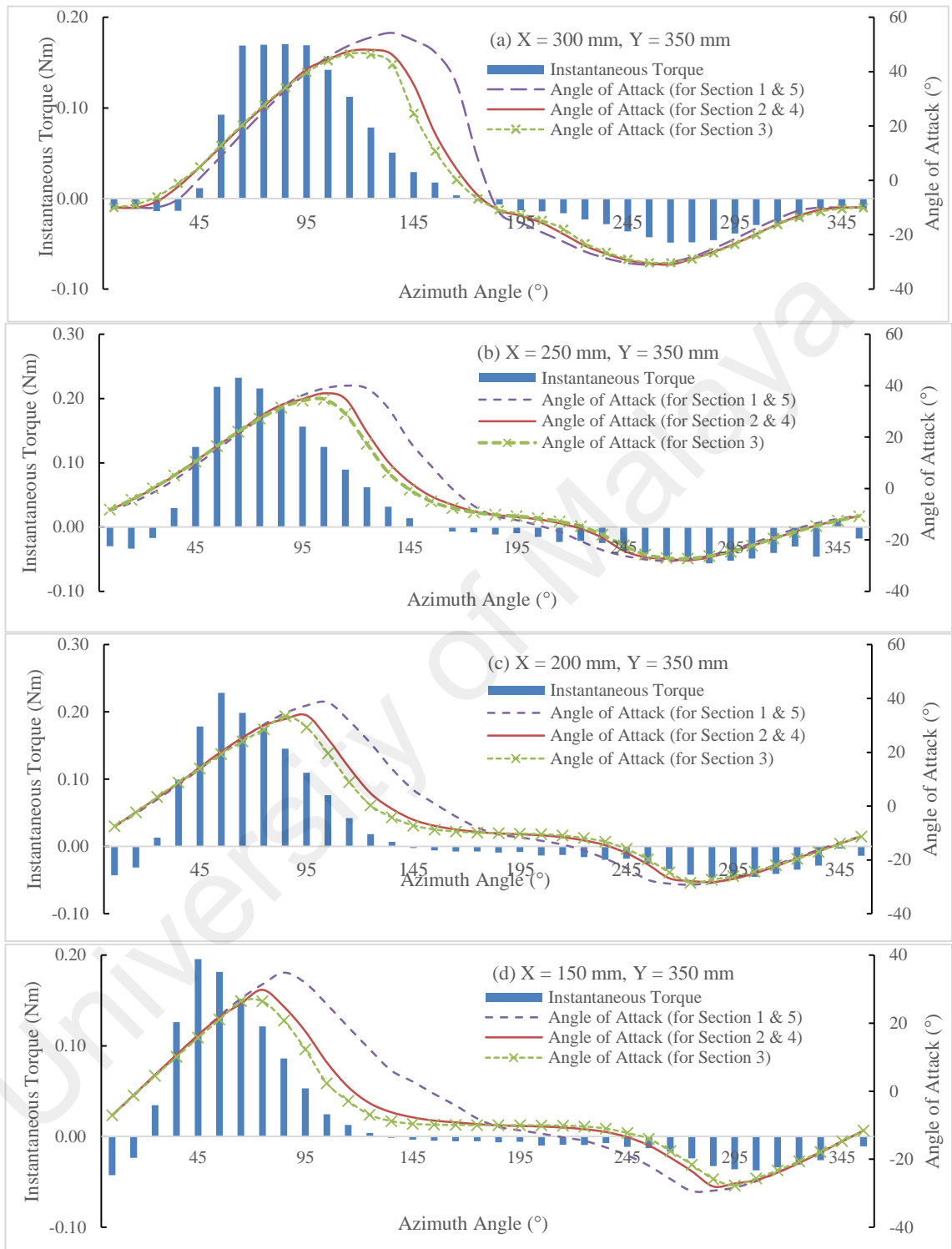
**Appendix D8: Instantaneous torque against azimuth angle and angle of attack versus azimuth angle at vertical position of  $Y = 300$  mm for the fan speed of 910 rpm.**

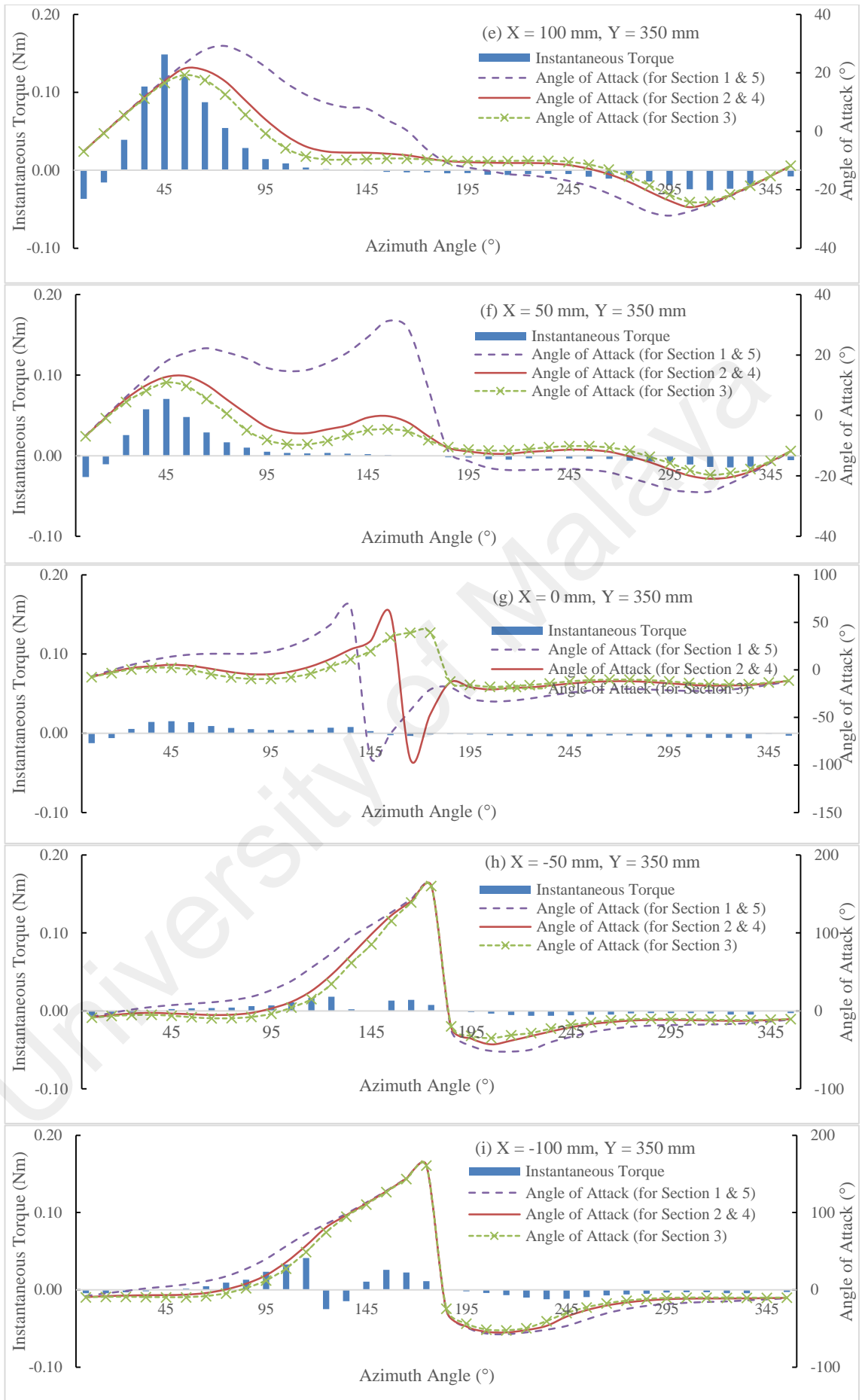


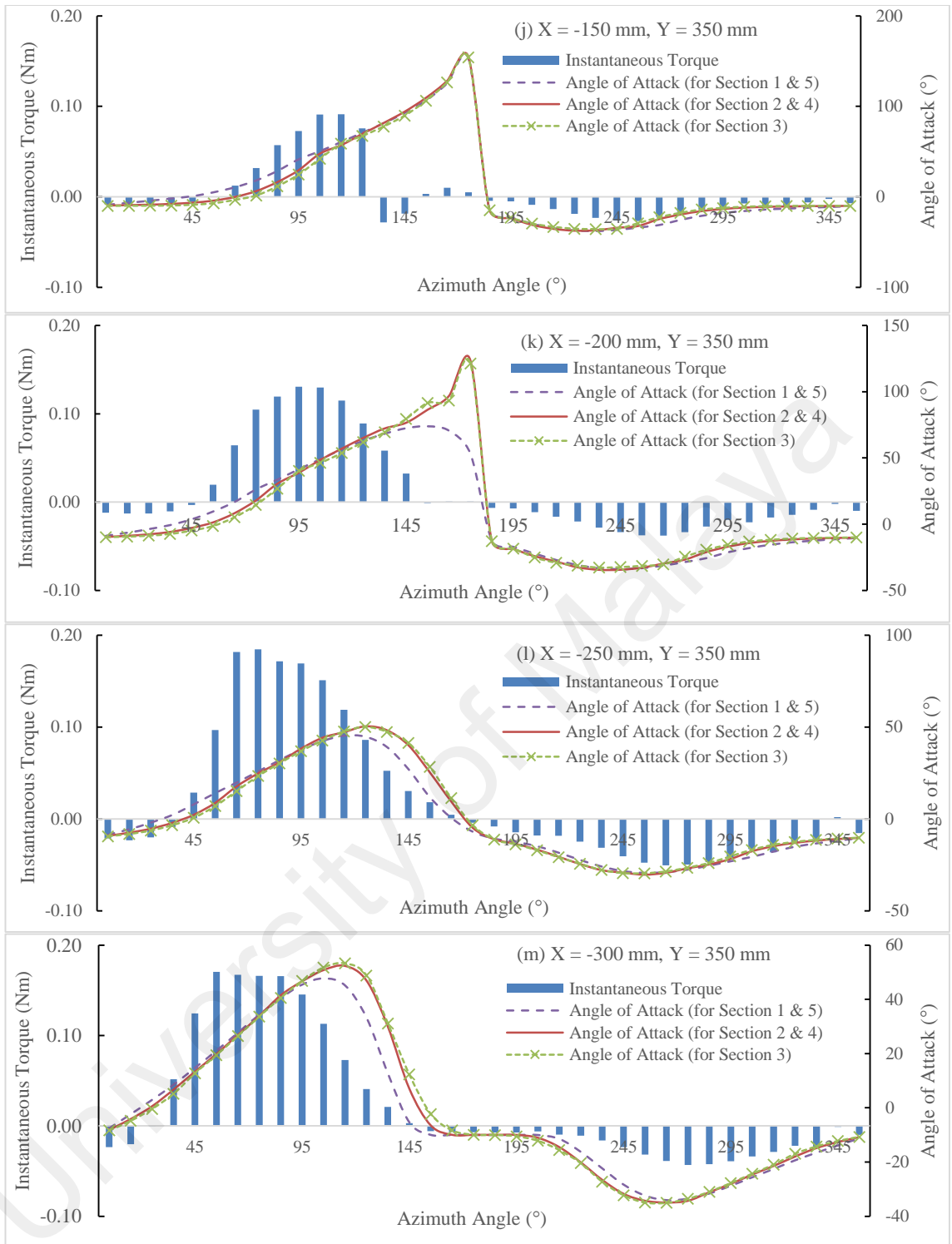




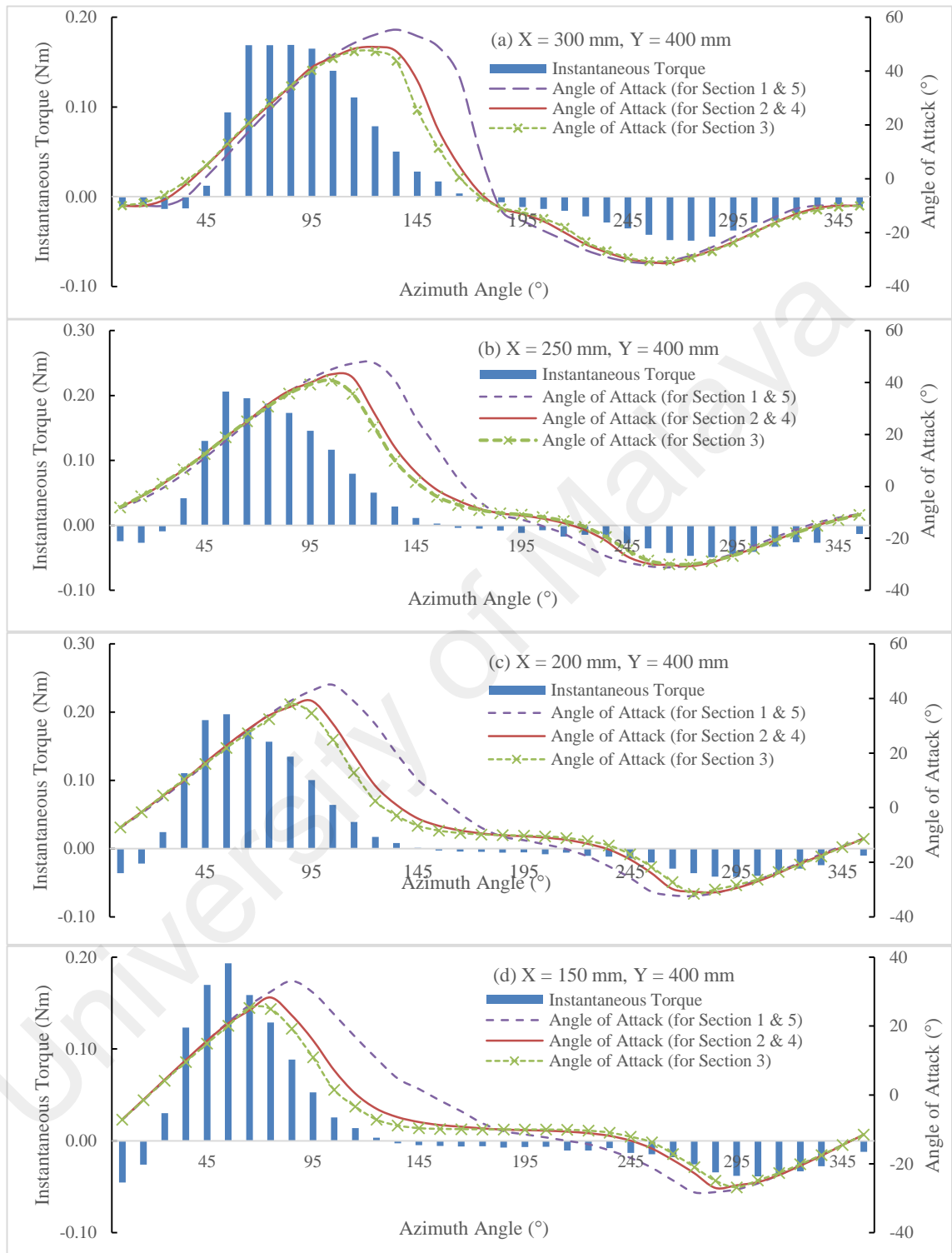
**Appendix D9: Instantaneous torque against azimuth angle and angle of attack versus azimuth angle at vertical position of  $Y = 350$  mm for the fan speed of 910 rpm.**



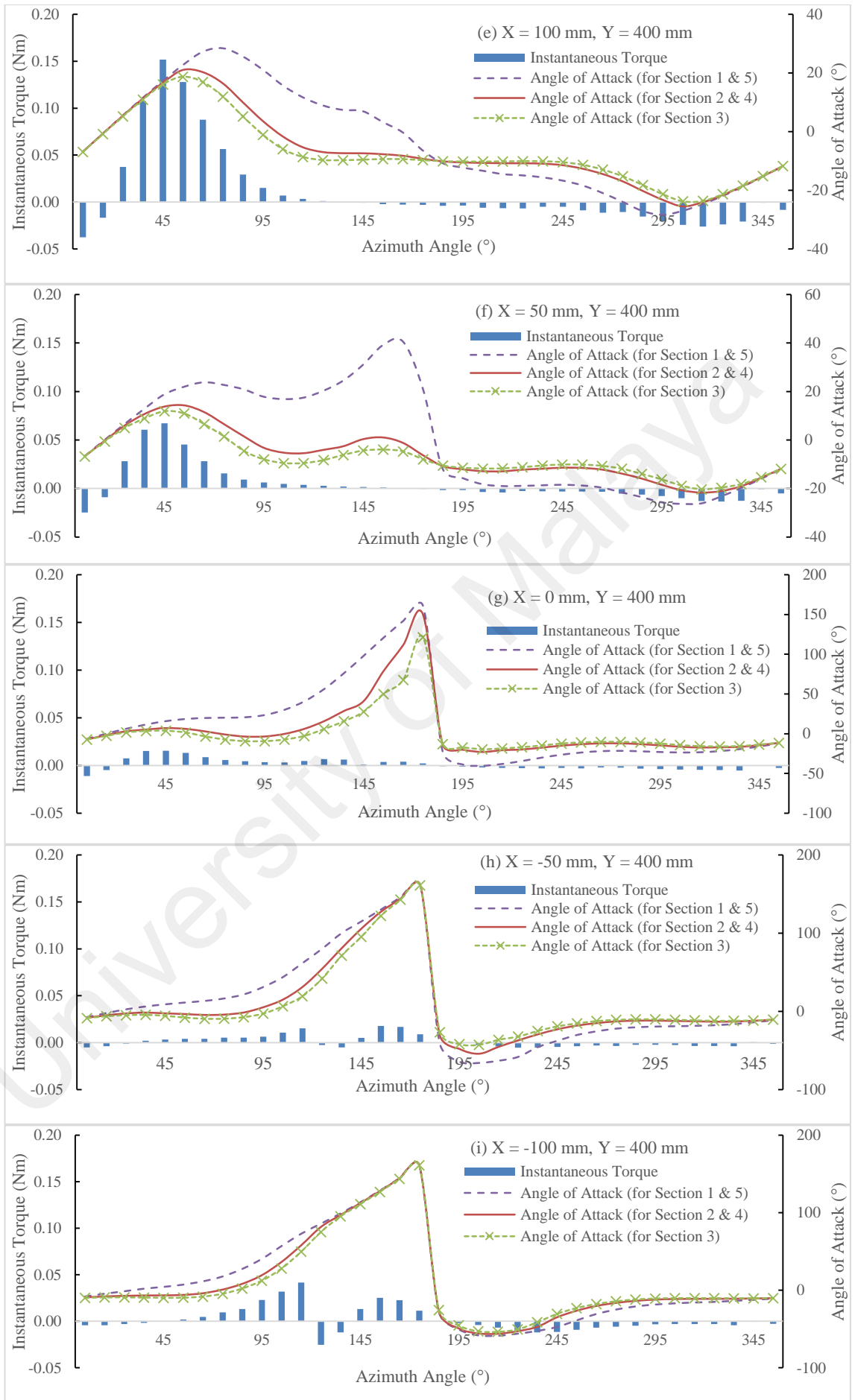


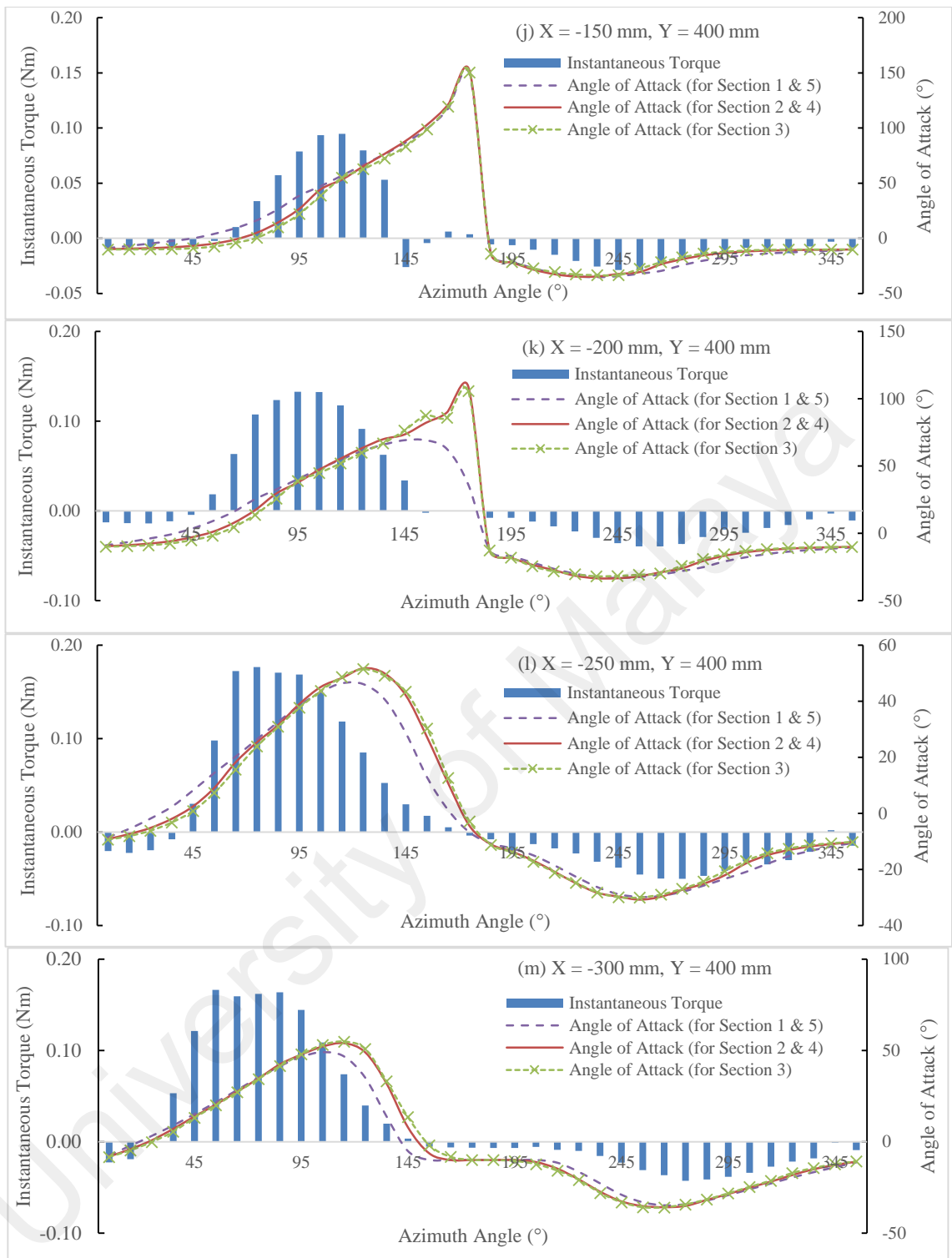


**Appendix D10: Turbine position against wind stream, torque against azimuth angle and angle of attack versus azimuth angle at vertical position of  $Y = 350$  mm for the fan speed of 910 rpm.**









## APPENDIX E

**Appendix E1: Wind turbine manufacturer's price (Source: [www.hi-vawt.com.tw](http://www.hi-vawt.com.tw),  
[sales@hi-vawt.com.tw](mailto:sales@hi-vawt.com.tw), October 2015)**



No.168, Jhulin 1<sup>st</sup> Rd., Linkou Township, Taipei County, 244 Taiwan

Tel: +886-2-86014373      Fax: +886-2-86011263

Website: <http://www.hi-vawt.com.tw>

### DISTRIBUTOR PRICE LIST

\*\*\*\*\*

Part No.	Description of Goods	Order Q'TY (SET)	Package	Unit Price (USD/SET)
DS-300	Hi Energy VASWT at rated power 300W including wind rotor, generator and controller, but excluding battery nor pole	1 set	Standard	1,800
		10 sets		1,500
		Container base		1,200
DS-700	Hi Energy VASWT at rated power 700W including wind rotor, generator and controller, but excluding battery nor pole	1 set	Standard	4,200
		10 sets		3,700
		Container base		3,200
DS-1500	Hi Energy VASWT at rated power 1.5KW including wind rotor, generator and controller, but excluding battery nor pole	1 set	Standard	11,000
		4 sets		10,000
		Container base	Container	8,500
DS-3000	Hi Energy VASWT at rated power 3KW including wind rotor, generator and controller, but excluding battery nor pole	1 sets	Standard	15,000
		4 sets		13,000
		Container base	Container	11,000
SL04-13024C-00-5	Hybrid street lamp <Fashion design>	1 sets	Standard	5,500
		10 sets		5,000
		Container base		4,500
SL03-2P13060D-00-1	Hybrid street lamp <Economic design>	1 sets	Standard	5,500
		10 sets		5,000
		Container base		4,500

**REMARKS:**

1. Payment term: 30% downpayment and the balanced 70% by T/T before shipment.
2. Delivery term: FOB Taiwan or Shanghai.
3. Lead time: 30~45 days after receiving the downpayment
4. Validity: 30 days

**Appendix E2: Maintenance free battery price from supplier (Source: Prodigy Integration, September 2015)**

**Prodigy Integration** (002104272-A)

No.129, Jalan BK 5/6, Bandar Kinrara, 47180 Puchong, Selangor. Tel/Fax: 03-80766809  
Email: prodigyintegration@gmail.com

Attention: Jabatan Kejuruteraan Mekanik  
Fakulti Kejuruteraan  
Universiti Malaya  
50603 Kuala Lumpur  
Attn: Dr Chong Wen Tong

Date: 29, Sept ,2015  
Tel: 03-79577351  
Fax:  
Re: 290920150001

**Quotation**

With reference to the above, we are pleased to quote you as follows:-

Item	Product Description	Qty	Price/Unit(RM)	Total Price(RM)
1	YUASA NP65-12 Maintenance-Free Lead-Acid Battery (65AH Capacity)	3	962.00	2,886.00
	GST	1	0.00	0.00
	<b>Grand Total</b>			<b>2,886.00</b>

**TERMS AND CONDITIONS:**

Price: Quoted in Ringgit Malaysia  
Validity: 30 days  
Delivery: 2-6 weeks subject to Manufacturer's final confirmation  
Payment: 30 days

Prodigy Integration



Fu Chee Ket (Marketing Manager)  
Mobile: 019-2108646

**Appendix E3: Controller price from supplier (Source: Prodigy Integration,  
January 2016)**

**Prodigy Integration** (002104273-A)

No.129, Jalan BK 5/6, Bandar Kinrara, 47180 Puchong, Selangor. Tel/Fax: 03-80766809  
Email: prodigyintegration@gmail.com

Attention: Jabatan Kejuruteraan Mekanik  
Fakulti Kejuruteraan  
Universiti Malaya  
50603 Kuala Lumpur  
Attn: Dr Chong Wen Tong

Date: 7, Jan ,2016  
Tel: 03-79577351  
Fax:  
Re: 070120160001

**Quotation**

With reference to the above, we are pleased to quote you as follows:-

Item	Product Description	Qty	Price/Unit(RM)	Total Price(RM)
1	Fabrication of Custom made size Wind & Solar Hybrid Controller Case size : Length 125/175* width 151 * high 66(mm) System rated voltage :12V/24V	2	1,456.00	2,912.00
<b>Grand Total</b>				<b>2,912.00</b>

**TERMS AND CONDITIONS:**

Price: Quoted in Ringgit Malaysia  
Validity: 30 days  
Delivery: 2-6 weeks subject to Manufacturer's final confirmation  
Payment: 30 days

Prodigy Integration



Fu Chee Ket (Marketing Manager)  
Mobile: 019-2108646

## LIST OF PUBLICATIONS: JOURNAL PAPERS

- i) Fazlizan, A., Chong, W. T., Yip, S. Y., Hew, W. P., & Poh, S. C. (2015). Design and Experimental Analysis of an Exhaust Air Energy Recovery Wind Turbine Generator. *Energies*, 8(7), 6566-6584.

*Energies* **2015**, 8, 6566-6584; doi:10.3390/en8076566

OPEN ACCESS

**energies**

ISSN 1996-1073

www.mdpi.com/journal/energies

Article

### Design and Experimental Analysis of an Exhaust Air Energy Recovery Wind Turbine Generator

Ahmad Fazlizan <sup>1</sup>, Wen Tong Chong <sup>1,\*</sup>, Sook Yee Yip <sup>2</sup>, Wooi Ping Hew <sup>2</sup> and Sin Chew Poh <sup>1</sup>

<sup>1</sup> Department of Mechanical Engineering, Faculty of Engineering, University of Malaya, 50603 Kuala Lumpur, Malaysia; E-Mails: a.fazlizan@siswa.um.edu.my (A.F.); pohsc@um.edu.my (S.C.P.)

<sup>2</sup> UM Power Energy Dedicated Advanced Centre, University of Malaya, Level 4, Wisma R&D, Jalan Pantai Baharu, 59990 Kuala Lumpur, Malaysia; E-Mails: sookyee.yip@siswa.um.edu.my (S.Y.Y.); wphew@um.edu.my (W.P.H.)

\* Author to whom correspondence should be addressed; E-Mail: chong\_wentong@um.edu.my; Tel.: +60-12-7235038; Fax: +60-3-79675317.

Academic Editor: Hossam A. Gabbar

Received: 5 May 2015 / Accepted: 17 June 2015 / Published: 30 June 2015

**Abstract:** A vertical axis wind turbine (VAWT) was positioned at the discharge outlet of a cooling tower electricity generator. To avoid a negative impact on the performance of the cooling tower and to optimize the turbine performance, the determination of the VAWT position in the discharge wind stream was conducted by experiment. The preferable VAWT position is where the higher wind velocity matches the positive torque area of the turbine rotation. With the proper matching among the VAWT configurations (blade number, airfoil type, operating tip-speed-ratio, etc.) and exhaust air profile, the turbine system was not only able to recover the wasted kinetic energy, it also reduced the fan motor power consumption by 4.5% and increased the cooling tower intake air flow-rate by 11%. The VAWT had a free running rotational speed of 479 rpm, power coefficient of 10.6%, and tip-speed-ratio of 1.88. The double multiple stream tube theory was used to explain the VAWT behavior in the non-uniform wind stream. For the actual size of a cooling tower with a 2.4 m outlet diameter and powered by a 7.5 kW fan motor, it was estimated that a system with two VAWTs (side-by-side) can generate 1 kW of power which is equivalent to 13% of energy recovery.

- ii) Chong, W. T., Fazlizan, A., Poh, S. C., Pan, K. C., Hew, W. P., & Hsiao, F. B. (2013). The design, simulation and testing of an urban vertical axis wind turbine with the omni-direction-guide-vane. *Applied Energy*, 112(0), 601-609.

Applied Energy 112 (2013) 601–609



Contents lists available at SciVerse ScienceDirect

## Applied Energy

journal homepage: [www.elsevier.com/locate/apenergy](http://www.elsevier.com/locate/apenergy)



---

### The design, simulation and testing of an urban vertical axis wind turbine with the omni-direction-guide-vane <sup>☆</sup>

W.T. Chong <sup>a,\*</sup>, A. Fazlizan <sup>a,b</sup>, S.C. Poh <sup>a</sup>, K.C. Pan <sup>a</sup>, W.P. Hew <sup>b</sup>, F.B. Hsiao <sup>c</sup>

<sup>a</sup> Department of Mechanical Engineering, Faculty of Engineering, University of Malaya, 50603 Kuala Lumpur, Malaysia  
<sup>b</sup> UMPEDAC, Level 4, Wisma R&D, University of Malaya, Jalan Pantai Baharu, 59990 Kuala Lumpur, Malaysia  
<sup>c</sup> Institute of Aeronautics and Astronautics, National Cheng Kung University, Tainan 70101, Taiwan, ROC



---

#### HIGHLIGHTS

- ▶ A system for on-site wind-solar hybrid power generation and rain water collection.
- ▶ The omni-direction-guide-vane (ODGV) overcomes the weak wind and turbulence conditions in urban areas.
- ▶ The ODGV improves the wind turbine performance by speeding-up and guiding the wind.
- ▶ The ODGV is designed to blend into the building architecture with safety enhancement.
- ▶ The wind tunnel test and CFD simulation results are presented.

#### GRAPHICAL ABSTRACT

Solar energy, renewable energy, urban wind energy, environment, augmented wind turbine.



---

#### ARTICLE INFO

*Article history:*  
Received 25 September 2012  
Received in revised form 26 December 2012  
Accepted 26 December 2012  
Available online 28 January 2013

*Keywords:*  
Guide vane  
Wind-solar energy system  
Wind turbine  
Computational fluid dynamics  
Building integrated renewable energy system  
Environment friendly

#### ABSTRACT

A novel omni-direction-guide-vane (ODGV) that surrounds a vertical axis wind turbine (VAWT) is designed to improve the wind turbine performance. Wind tunnel testing was performed to evaluate the performance of a 5-bladed (Wortmann FX63-137 airfoil) H-rotor wind turbine, with and without the integration of the ODGV. The test was conducted using a scaled model turbine which was constructed to simulate the VAWT enclosed by the ODGV placed on a building. The VAWT shows an improvement on its self-starting behavior where the cut-in speed was reduced with the integration of the ODGV. Since the VAWT is able to self-start at a lower wind speed, the working hour of the wind turbine would increase. At a wind speed of 6 m/s and under free-running condition (only rotor inertia and bearing friction were applied), the ODGV helps to increase the rotor rotational speed by 182%. With extra load application at the same wind speed (6 m/s), the wind turbine power output was increased by 3.48 times at its peak torque with the aid of the ODGV. The working concept of the ODGV is to minimize the negative torque zone of a lift-type VAWT and to reduce turbulence and rotational speed fluctuation. It was verified by re-simulating the torque coefficient data of a single bladed (NACA 0015 airfoil) VAWT published by the Sandia National Laboratories. From the simulation results, with the presence of the ODGV, it was shown that the torque output of the NACA 0015 airfoil, single bladed VAWT has been increased by 58% and 39% at TSR = 2.5 and TSR = 5.1 respectively. The negative torque zone has been minimized thus the positive torque that provides higher power can be obtained. As a conclusion, the ODGV integrated wind power

---

<sup>☆</sup> This paper is a revised article presented at the 4th International Conference on Applied Energy (ICAE 2012), 5–8 July, 2012, Suzhou, China.  
\* Corresponding author. Tel.: +60 12 7235038.  
E-mail addresses: [chong\\_wentong@um.edu.my](mailto:chong_wentong@um.edu.my), [chong\\_wentong@yahoo.com](mailto:chong_wentong@yahoo.com) (W.T. Chong).

0306-2619/\$ - see front matter © 2012 Elsevier Ltd. All rights reserved.  
<http://dx.doi.org/10.1016/j.apenergy.2012.12.064>

- iii) Chong, W. T., Yip, S. Y., Fazlizan, A., Poh, S. C., Hew, W. P., Tan, E. P., & Lim, T. S. (2014). Design of an exhaust air energy recovery wind turbine generator for energy conservation in commercial buildings. *Renewable Energy*, 67(0), 252-256.

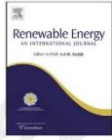
Renewable Energy 67 (2014) 252–256



Contents lists available at [ScienceDirect](#)

## Renewable Energy

journal homepage: [www.elsevier.com/locate/renene](http://www.elsevier.com/locate/renene)



---

### Design of an exhaust air energy recovery wind turbine generator for energy conservation in commercial buildings<sup>☆</sup>



W.T. Chong<sup>a,\*</sup>, S.Y. Yip<sup>b</sup>, A. Fazlizan<sup>a,b</sup>, S.C. Poh<sup>a</sup>, W.P. Hew<sup>b</sup>, E.P. Tan<sup>c</sup>, T.S. Lim<sup>c</sup>

<sup>a</sup>Department of Mechanical Engineering, Faculty of Engineering, University of Malaya, 50603 Kuala Lumpur, Malaysia  
<sup>b</sup>UMPEDEC, Level 4, Wisma R&D, University of Malaya, Jalan Pantai Baharu, 59990 Kuala Lumpur, Malaysia  
<sup>c</sup>Truwater Cooling Towers Sdn. Bhd., Executive Suite 702, Block B, Kelana Business Centre, No 97, Jalan SS 7/2, Kelana Jaya, 47301 Petaling Jaya, Selangor, Malaysia

---

**ARTICLE INFO**

*Article history:*  
Received 10 October 2013  
Accepted 14 November 2013  
Available online 13 December 2013

*Keywords:*  
Building integrated wind turbine  
Exhaust air system  
Energy recovery  
Power augmentation  
Urban wind energy  
Decarbonization

**ABSTRACT**

The exhaust air energy recovery wind turbine generator is an on-site clean energy generator that utilizes the advantages of discharged air which is strong, consistent and predictable. Two vertical axis wind turbines (VAWTs) in cross-wind orientation which are integrated with an enclosure are installed above a cooling tower to harness the discharged wind for electricity generation. It is mounted at a specific distance and position above the cooling tower outlet. The enclosure (consisting of several guide-vanes and diffuser-plates) acts as a wind power-augmentation device to improve the performance of the VAWTs. The guide-vanes are placed in between the discharged air outlet and the wind turbine. They are designed to guide the on-coming wind stream to an optimum flow angle before it interacts with the rotor blades. The diffuser-plates are built extended from the outlet duct of the exhaust air system. They are tilted at an optimum angle to draw more wind and accelerate the discharged air flow. A particular concern related to public safety which may be due to blade failure is minimized since the VAWTs are contained inside the enclosure. The performance of the VAWTs and its effects on the cooling tower's air intake speed and current consumption of the power-driven fan were investigated. A laboratory test was conducted to evaluate the effectiveness of the energy recovery wind turbine (5-bladed H-rotor with 0.3 m diameter) generator on a cooling tower model. The results showed a reduction in the power consumption of the fan motor for cooling tower with energy recovery turbine compared to the normal cooling tower while the intake air speed increased. Meanwhile, the VAWT's performance was improved by a 7% increase in rotational speed and 41% reduction in response time (time needed for the turbine to reach maximum rotational speed) with the integration of the enclosure. This system can be used as a supplementary power for building lighting or fed into electricity grid for energy demand in urban building. The energy output is predictable and consistent, allowing simpler design of the downstream system. The fact that there is an abundance of cooling tower applications and unnatural exhaust air resources globally causes this to have great market potential.

© 2013 Elsevier Ltd. All rights reserved.

---

### 1. Introduction

Dependency on fossil based energy resources leads to the energy crisis due to depletion of these resources. Increase of population and economic growth contribute to higher demands of energy that only worsens the situation. Therefore, one of the most important concerns globally is the need of energy security. Energy generation from renewable resources

such as wind, solar, tidal and biomass is one of the options to reduce the dependency on fossil resources. The idea of on-site renewable energy generation is another great approach where the energy is extracted from renewable sources close to the populated area where the energy is required. However, renewable energy generations are highly dependent on geographical conditions.

Urban areas are the places where energy is needed most. In Malaysia, at an urban area, the wind speed is less than 4 m/s for more than 90% of the total hours in a year [1]. This value is not conducive for on-site energy generation from wind. However, in this paper, an innovative idea to generate clean energy from alternative wind resources in urban areas is presented. The alternative source of wind is from the exhaust air systems.

---

<sup>☆</sup> This paper is an improved article presented at the World Renewable Energy Congress – Australia (WREC 2013), 14–18th July 2013.

\* Corresponding author. Tel.: +60 12 7235038; fax: +60 37 9675317.  
E-mail addresses: [chong\\_wentong@um.edu.my](mailto:chong_wentong@um.edu.my), [chong\\_wentong@yahoo.com](mailto:chong_wentong@yahoo.com) (W.T. Chong).

0960-1481/\$ – see front matter © 2013 Elsevier Ltd. All rights reserved.  
<http://dx.doi.org/10.1016/j.renene.2013.11.028>



- iv) Chong, W. T., Hew, W. P., Yip, S. Y., Fazlizan, A., Poh, S. C., Tan, C. J., & Ong, H. C. (2014). The experimental study on the wind turbine's guide-vanes and diffuser of an exhaust air energy recovery system integrated with the cooling tower. *Energy Conversion and Management*, 87(0), 145-155.



## The experimental study on the wind turbine's guide-vanes and diffuser of an exhaust air energy recovery system integrated with the cooling tower



W.T. Chong<sup>a,\*</sup>, W.P. Hew<sup>b</sup>, S.Y. Yip<sup>b</sup>, A. Fazlizan<sup>a,b</sup>, S.C. Poh<sup>a</sup>, C.J. Tan<sup>a</sup>, H.C. Ong<sup>a</sup>

<sup>a</sup>Department of Mechanical Engineering, Faculty of Engineering, University of Malaya, 50603 Kuala Lumpur, Malaysia

<sup>b</sup>UMPEDAC, Level 4, Wisma R&D, University of Malaya, Jalan Pantai Baharu, 59990 Kuala Lumpur, Malaysia

### ARTICLE INFO

**Article history:**  
Received 23 December 2013  
Accepted 1 July 2014  
Available online 26 July 2014

**Keywords:**  
Cooling tower  
Energy recovery  
De-carbonization  
Wind turbine  
On-site energy generation  
Renewable energy

### ABSTRACT

An assembly of two vertical axis wind turbines (VAWTs) and an enclosure is installed above a cooling tower to harness the discharged wind for electricity generation. The enclosure consists of guide-vanes and diffuser-plates, is used to enhance the rotational speed of the turbines for power augmentation. The angle of the guide-vanes is optimized to ensure the oncoming wind stream impinges the rotor blades of the turbine at an optimum angle. The diffuser-plates are tilted at an optimum angle to increase the discharged airflow rate. The performance of the system is tested in the laboratory followed by a field test on an actual size cooling tower. The VAWT performance is increased in the range of 7–8% with the integration of enclosure. There is no significant difference in the current consumption of the fan motor between the bare cooling tower and the one with installed VAWTs. With the presence of this system, approximately 17.5 GW h/year is expected to be recovered from 3000 units of cooling towers at commercial areas, assuming the cooling tower is driven by a 7.5 kW fan motor and operates 16 h/day. This amount of recovered energy can also be translated into 13% reduction in CO<sub>2</sub> emission.

© 2014 Elsevier Ltd. All rights reserved.

### 1. Introduction

World energy demand has shown a remarkable increase over the past century due to population growth and economic development. Currently, there are 7.1 billion people in the world [1]. In 2008, world primary energy consumption from all sources was recorded at 514 EJ (EJ is exajoule = 10<sup>18</sup> J) and 80% of it was generated from fossil fuels. It is projected to increase to 1000 EJ or more by the year 2050 [2]. Due to the uncontrolled population growth, the increase in fossil fuel consumption for energy generation is inevitable. However, the overconsumption of fossil fuel brings harmful impacts on the world's climate due to greenhouse gas (GHG) emissions. GHGs are the main contributor to anthropogenic climate change and it poses significant risks for human health, welfare and natural ecosystems. Two thirds of the anthropogenic GHGs emission is accounted by the energy related emission since all energy systems emit GHGs [3]. Taseska et al. have reported that the GHGs emission associated with energy demand is tabulated with the value of 6406 kilotonnes CO<sub>2</sub> equivalent in the year 2025 (which is an additional compared to year 2008) [3].

In order to reduce the dependence on fossil fuels for energy generation, renewable energy (RE) plays a critical role in reducing the GHGs emission leading the world toward fossil fuel independence. RE is important for sustainable development since it is natural, replenishable and has great potential for cost reduction, as opposed to the rise in fossil fuel prices. Recently, intensive researches have been done on improving the efficiency of the RE resources with the aim of converting the present energy systems into 100% RE electricity systems. Wind energy is the second biggest source of RE after solar energy. It is the fastest growing RE source in the world with an annual growth rate of 30% [4]. The share of wind energy is 14% at the global scale on the total mid-term RE resources potential and this value reflects its maturity in technology [5]. However, the uncertainty in wind energy is the main problem in matching the increasing demand for RE. The operation of wind power is susceptible to changing wind patterns resulting from climate change [6]. Thus, an efficient method is strongly demanded to harness the uncertain wind energy.

### 2. Concerns for installation of an on-site energy generation system

On-site renewable energy generation is useful for sustainable electrical power generation leading toward CO<sub>2</sub> abatement [7].

\* Corresponding author. Tel.: +60 12 7235038; fax: +60 3 79675317.

E-mail addresses: [chong\\_wentong@um.edu.my](mailto:chong_wentong@um.edu.my), [chong\\_wentong@yahoo.com](mailto:chong_wentong@yahoo.com) (W.T. Chong).

<http://dx.doi.org/10.1016/j.enconman.2014.07.009>  
0196-8904/© 2014 Elsevier Ltd. All rights reserved.

- v) Chong, W. T., Poh, S. C., Fazlizan, A., Yip, S. Y., Koay, M. H., & Hew, W. P. (2013). Exhaust Air Energy Recovery System for Electrical Power Generation in Future Green Cities. *International Journal of Precision Engineering and Manufacturing*, 14(6), 1029-1035.

## Exhaust Air Energy Recovery System for Electrical Power Generation in Future Green Cities

Wen Tong Chong<sup>1\*</sup>, Sin Chew Poh<sup>1</sup>, Ahmad Fazlizan<sup>1</sup>, Sook Yee Yip<sup>2</sup>, Mei Hyie Koay<sup>3</sup>, and Wooi Ping Hew<sup>4</sup>

<sup>1</sup> Department of Mechanical Engineering, Faculty of Engineering, University of Malaya, 50603 Kuala Lumpur, Malaysia  
<sup>2</sup> UMPEDAC, Level 4, Wisma R & D, University Malaya, Jalan Pantai Baharu, 59900 Kuala Lumpur, Malaysia  
<sup>3</sup> Faculty of Mechanical Engineering, Universiti Teknologi MARA, 40450 Shah Alam, Selangor, Malaysia  
\* Corresponding Author / E-mail: chong\_wentong@um.edu.my; chong\_wentong@yahoo.com, TEL: +60-127235038, FAX: +60-379675317

KEYWORDS: Cooling tower, Energy recovery, Green technology, Renewable energy, Urban wind energy, Wind turbine

*This paper investigates a technology-driven solution to supply a portion of energy demand in future green cities. An idea on harnessing unnatural wind resources for electricity is presented. Two vertical axis wind turbines with an enclosure are mounted above a cooling tower to recover part of the energy from the exhaust air. Guide-vanes are designed to create a venturi effect and guide the wind before it interacts with the turbine blades. Diffuser-plates help to draw more wind and accelerate the exhaust airflow. Safety concerns that may result from blade failure are minimized by the design of the enclosure. From the laboratory test and field test results, there is no significant difference in the current consumption of the fan motor with the installation of the wind turbines. The integration of the enclosure has shown an improvement on the turbine's rotational speed which is 30.4% higher. The electricity generated from this system can be fed into the electricity grid. For 3000 units of cooling tower (2 m outlet diameter powered by a 7.5 kW fan motor and operated for 16 hours/day), 13% of the energy to power the fan motor is expected to be recovered from this system which equals 17.5 GWh/year.*

Manuscript received: June 21, 2012 / Accepted: October 10, 2012

### NOMENCLATURE

GHG = Greenhouse Gas  
TNB = Tenaga Nasional Berhad  
VAWT = Vertical Axis Wind Turbine  
RE = Renewable energy  
DAWT = Diffuser Augmented Wind Turbine

### 1. Introduction

Nowadays, global energy consumption in both developed and developing countries has increased rapidly due to population growth and it is expected to double or more by the year 2040.<sup>1</sup> In Malaysia alone, total energy demand is growing at 5.4% per annum with 1.8% average annual population growth rate. Eventually, the energy demand in the year 2020 will be approximately 971 TWh with 33.4 million populations. As a consequence, Malaysia is predicted to become a net energy importer by 2020.<sup>2</sup> This energy consumption growth is

contributed by both industrial and residential sectors. The existing energy resources for electricity generation in Malaysia mainly depend on fossil fuels (oil, coal and natural gas) which contribute 94.5% of the electricity generation while only a small portion of energy supplies comes from hydroelectricity or others (solar, biomass, etc.). However, the usage of fossil fuels brings negative impacts to the environment such as greenhouse gases (GHG) emission. According to Ahmad et al., more than 90% of the energy related GHG emission is a result of the CO<sub>2</sub> emissions from fuel combustion globally.<sup>3</sup> Currently, the increase in the concentration of GHG emission has caused a notable rise of temperature in the earth's atmosphere (global warming) and thus widespread melting of snow and ice at the polar ice caps. The melting of ice causes the rise of sea level and lesser land can be used for an increasing world population, along with the changes in climate.<sup>4</sup>

In terms of the economic aspect, the deployment of fossil fuels for electricity generation will become more and more costly as these resources are limited in supply and will be exhausted one day. Based on the commercial tariff of electricity in Malaysia provided by Tenaga Nasional Berhad (TNB), energy cost is USD 0.113/kWh and it is predicted to increase by 10% annually.<sup>5</sup> In parallel with a country

- vi) Chong, W. T., Poh, S. C., Fazlizan, A., Yip, S. Y., Chang, C. K., & Hew, W. P. (2013). Early development of an energy recovery wind turbine generator for exhaust air system. *Applied Energy*, 112(0), 568-575.

Applied Energy 112 (2013) 568–575

Contents lists available at SciVerse ScienceDirect

**Applied Energy**


journal homepage: [www.elsevier.com/locate/apenergy](http://www.elsevier.com/locate/apenergy)

---

**Early development of an energy recovery wind turbine generator for exhaust air system**<sup>☆</sup>

W.T. Chong<sup>a,\*</sup>, S.C. Poh<sup>a</sup>, A. Fazlizan<sup>a,b</sup>, S.Y. Yip<sup>b</sup>, C.K. Chang<sup>c</sup>, W.P. Hew<sup>b</sup>

<sup>a</sup> Department of Mechanical Engineering, Faculty of Engineering, University of Malaya, 50603 Kuala Lumpur, Malaysia  
<sup>b</sup> UMPEDEC, Level 4, Wisma R&D, University of Malaya, Jalan Pantai Baharu, 50900 Kuala Lumpur, Malaysia  
<sup>c</sup> Heating, Ventilation, Air Conditioning and Refrigerating Section, Universiti Teknikal Malaysia Trusmi, Section 14, Jalan Temu Jonang, Bandar Baru Bangi, 43630 Selangor, Malaysia

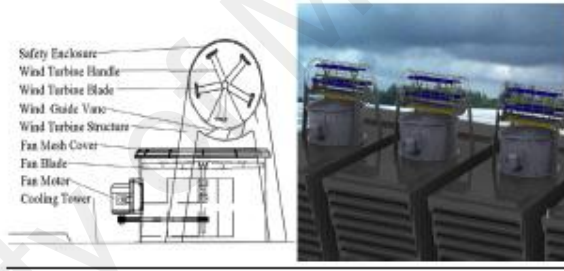


---

**HIGHLIGHTS**

- ▶ Exhaust air energy recovery system to recover part of the energy in discharged air.
- ▶ An innovative way to generate electricity and reduce CO<sub>2</sub> emission.
- ▶ Equipped with diffuser-plates and guide-vanes to improve wind turbine performance.
- ▶ Enclosure solves conventional wind turbine problems in urban areas.
- ▶ 13% of the energy consumed by the fan motor is expected to be recovered.

**GRAPHICAL ABSTRACT**



---

**ARTICLE INFO**

*Article history:*  
 Received 25 September 2012  
 Received in revised form 6 December 2012  
 Accepted 14 January 2013  
 Available online 20 February 2013

*Keywords:*  
 Building integrated wind turbine  
 Exhaust air system  
 Energy savings  
 Clean energy  
 Power augmentation  
 Urban wind energy

**ABSTRACT**

An innovative idea on extracting clean energy from man-made wind resources with micro wind turbine system for power generation is introduced in this paper. This system generates on-site clean energy using a micro wind generation system. A vertical axis wind turbine (VAWT) with an enclosure is mounted above a cooling tower's exhaust fan to harness the wind energy for producing electricity. The VAWT is positioned at a specific position at the cooling tower outlet to avoid a negative impact on the performance of the cooling tower. The enclosure can act as a safety cover and also enhance the performance of the VAWT. It is designed with several guide-vanes positioned at the up-stream side of the wind turbine to create a venturi effect and guide the wind before it interacts with the turbine blades. Moreover, the enclosure design is comprised of diffuser-plates that can draw more wind and accelerate the flow. Laboratory test conducted on a scaled model shows no measurable difference in the air intake speed and current consumption of the power-driven fan when the turbine was spinning above the cooling tower. Field test on an actual induced draft cooling tower shows no significant difference on the outlet air speed of the cooling tower. A small difference was observed on the power consumption by the fan motor which is 0.39% higher with the presence of the VAWT. This system is retrofit-able to existing cooling towers and has very high market potential due to abundant cooling towers and other unnatural exhaust air resources globally.

© 2013 Elsevier Ltd. All rights reserved.

---

<sup>☆</sup> This paper is a revised article presented at the International Conference on Applied Energy (ICAE 2012), 5–8 July 2012, Suzhou, China (Early development of an energy recovery wind turbine generator for exhaust air system).

\* Corresponding author. Tel.: +60 12 7235038; fax: +60 3 79675317.  
 E-mail addresses: [chong\\_wentong@um.edu.my](mailto:chong_wentong@um.edu.my), [chong\\_wentong@yahoo.com](mailto:chong_wentong@yahoo.com) (W.T. Chong).

0306-2619/\$ - see front matter © 2013 Elsevier Ltd. All rights reserved.  
<http://dx.doi.org/10.1016/j.apenergy.2013.01.042>

## LIST OF PUBLICATIONS: CONFERENCE PAPERS

- i) Performance and Environmental Evaluation of an On-site Waste-to-energy Conversion System by Using Exhaust Air Energy Recovery Turbine Generator. Paper presented at the International Green Energy Conference (IGEC-IX), Tianjin, China. 25-28th May 2014.

International Green Energy Conference (IGEC-IX), Tianjin, China. 25-28th May 2014.

### PERFORMANCE AND ENVIRONMENTAL EVALUATION OF AN ON-SITE WASTE-TO-ENERGY CONVERSION SYSTEM BY USING EXHAUST AIR ENERGY RECOVERY TURBINE GENERATOR

*W.T. Chong<sup>a,\*</sup>, A. Fazlizan<sup>a</sup>, S.Y. Yip<sup>b</sup>, S.C. Poh<sup>c</sup>, W.Z.W. Omar<sup>c,d</sup> and W.P. Hew<sup>b</sup>*

<sup>a</sup> Department of Mechanical Engineering, Faculty of Engineering, University of Malaya, 50603 Kuala Lumpur, Malaysia

<sup>b</sup> UMPEDEC, Level 4, Wisma R&D, University of Malaya, Jalan Pantai Baharu, 59990 Kuala Lumpur, Malaysia

<sup>c</sup> Centre of Electrical Energy Systems, Universiti Teknologi Malaysia, 81310 UTM, Johor Bahru, Malaysia

<sup>d</sup> Aeronautical, Automotive and Offshore Engineering Department, Faculty of Mechanical Engineering, Universiti Teknologi Malaysia, 81310 UTM, Johor Bahru, Malaysia

\*Corresponding author: [chong\\_wentong@um.edu.my](mailto:chong_wentong@um.edu.my)

#### ABSTRACT

An assembly of two vertical axis wind turbines (VAWTs) and an enclosure is installed above a cooling tower to harness the discharged wind for electricity generation. The enclosure consists of guide-vanes and diffuser-plates, is used to enhance the rotational speed of the turbines for power augmentation. The angle of the guide-vanes is optimized to ensure the oncoming wind stream impinges the rotor blades of the turbine at an optimum angle. The diffuser-plates are tilted at an optimum angle to increase the discharged airflow rate. The performance of the system is tested in the laboratory followed by a field test on an actual size cooling tower. The VAWT performance is increased in the range of 7 - 8% with the integration of enclosure. There is no significant difference in the current consumption of the fan motor between the bare cooling tower and the one with installed VAWTs. With the presence of this system, approximately 17.5 GWh/year is expected to be recovered from 3000 units of cooling towers at commercial areas, assuming the cooling tower is driven by a 7.5 kW fan motor and operates 16 hours/day. This amount of recovered energy can also be translated into 13% reduction in CO<sub>2</sub> emission.

**Keywords:** Cooling tower, Energy recovery, De-carbonization, Wind turbine, On-site energy generation, Renewable energy.

#### INTRODUCTION

Energy security is a major challenge in relation to achieving environmental goals and in striving for sustainable development. Global energy consumption has nearly doubled during the past 30 years and is projected to keep increasing. In 2008, world primary energy consumption from all sources was recorded at 514 EJ (EJ is exajoule =10<sup>18</sup> J) and 80% of it was generated from fossil fuels. It is projected to increase to 1000 EJ or more by the year 2050 (Moriarty & Honnery, 2012). This trend is significant in developing countries and effective measures are necessary to reduce energy consumption while maintaining economic growth. Committee on Energy and Global Warming, Science Council of Japan has pointed two major areas need to be focused which are energy supply and energy utilization ("Energy and Global Warming: Equitable Allocation of Efforts for Sustainable Society," 2007).

On the supply side of energy, an internationally coordinated framework is indispensable to ensure worldwide supply of various energy sources while dealing with global warming issues. More aggressive introduction of renewable energy sources, such as photovoltaic, wind, and biomass, is encouraged in order to counter global warming, ensure energy security, and improve energy accessibility. With respect to utilization of energy, energy-efficiency efforts should be reinforced to contribute further to mitigation of global warming and improvement of energy security. As one of the answer to these issues, this article presents an innovative way of to recover energy from a system which promotes energy efficiency.

- ii) Performance Evaluation of a Wind Power-Augmented Device on an Onsite Exhaust Air Energy Recovery Wind Turbine. Paper presented at the 3rd International Conference on Green Buildings Technologies and Materials (GBTM 2013), Kuala Lumpur, Malaysia. 21st- 22nd December 2013.

### Performance evaluation of a wind power-augmented device on an onsite exhaust Air energy recovery wind turbine

Wen Tong Chong<sup>1,a</sup>, Ahmad Fazlizan<sup>1,2,b</sup>, Sook Yee Yip<sup>2,c</sup>, Micheal K. H. Leung<sup>3,d</sup> and Sin Chew Poh<sup>1,e</sup>

<sup>1</sup>Department of Mechanical Engineering, Faculty of Engineering, University of Malaya, 50603 Kuala Lumpur, Malaysia

<sup>2</sup>UMPEDAC, Level 4, Wisma R&D, University of Malaya, Jalan Pantai Baharu, 59990 Kuala Lumpur, Malaysia

<sup>3</sup>School of Energy and Environment, City University of Hong Kong, Hong Kong, China

<sup>a</sup>chong\_wentong@um.edu.my, <sup>b</sup>a.fazlizan@siswa.um.edu.my, <sup>c</sup>sookyee.yip@siswa.um.edu.my, <sup>d</sup>mkh.leung@cityu.edu.hk, <sup>e</sup>pohsc@um.edu.my

**Keywords:** Energy Recovery, Wind Turbine, Onsite Green Energy, Wind Power-Augmentation Device, Renewable Energy, Decarbonisation.

**Abstract.** This paper presents an idea on generating green energy by extracting discharged wind energy from a cooling tower. Two vertical axis wind turbines (VAWTs) integrated with a wind power-augmentation device are installed above a cooling tower to harness unnatural wind for electricity generation. The wind power-augmentation device is built with several guide-vanes and diffuser-plates to improve the performance of the VAWTs. Guide-vanes are designed to create a venturi effect and guide the on-coming wind stream to an optimum flow angle which is matched to the optimum angle of attack of the VAWTs. Diffuser-plates are tilted at an optimum angle to draw more wind and accelerate the discharged airflow. From the laboratory test, the VAWTs performance was increased by 7 – 8 % when guide-vanes and diffuser-plates are installed at their optimum angle. The correct matching of VAWTs for this system is expected to generate electricity at their rated power constantly when the cooling tower is in operation. This system can contribute to the reduction of greenhouse gases emission and conservation of the environment for a healthier life since fossil fuel consumption for energy generation is reduced as well as efficient use of energy.

#### Introduction

Land availability for the on-site RE generation is becoming limited with the increase in urban density and an unprecedented world population growth [1]. Many research works have been done on enhancing the efficiency and increasing the total output power generation using an onsite renewable energy generation system built in a limited area. Shrouded diffuser has been used to improve the output power of a wind turbine. Abe et al. had reported that shrouded diffuser is capable of improving wind turbine power coefficient by 4 times [2]. Based on the test results analyzed by M. Kardous et al., the increased rate of wind velocity for diffuser without flange is about 58% while for the flanged diffuser, the rate is extended at the range of 64% – 81%. The effect of adding the flange is tabulated to be in between 13% and 23% since vortex formation increased at the exit path of wind flow, thus more mass flow was drawn to the wind turbine [3].

Taking into account the safety and reliability of the system, the authors have developed a 3-in-1 wind-solar hybrid renewable energy and rainwater harvester for urban high rise application with a wind turbine covered within an omni-direction-guide-vane (ODGV). The system is able to increase the power generation by VAWT up to 3.48 times compared to the bare VAWT [4, 5]. The variation of the RE resources, i.e. the insufficient natural wind speed for power generation is another problem faced by the system. In Malaysia, the wind speed is relatively low and fluctuating most of the hours all over the year (annual wind speed is in the range of 0 – 3 m/s) [6]. Hence, it is not realistic to harness the natural wind in Malaysia.

- iii) Wind tunnel testing of a Savonius wind turbine with the integration of the omni-direction-guide-vane. Paper presented at the New Energy and Sustainable Development, Beijing, China. 14-16<sup>th</sup> June 2013.

*International Conference on New Energy and Sustainable Development (NESD2013). Jun. 14-16 2013. Beijing, China.*

## **Wind tunnel testing of a Savonius wind turbine with the integration of the omni-direction-guide-vane**

**A. Fazlizan<sup>a,b,\*</sup>, W. T. Chong<sup>a,\*</sup>, W. P. Hew<sup>b</sup>, S. C. Poh<sup>a</sup> and K. C. Pan<sup>a</sup>,**

<sup>a</sup>Department of Mechanical Engineering, Faculty of Engineering, University of Malaya, 50603 Kuala Lumpur, Malaysia

<sup>b</sup>UMPEDAC, Level 4, Wisma R&D, University of Malaya, Jalan Pantai Baharu, 59990 Kuala Lumpur, Malaysia

\*Corresponding author. Email: [afazlizan@yahoo.com](mailto:afazlizan@yahoo.com) (A. Fazlizan)  
[chong\\_wentong@um.edu.my](mailto:chong_wentong@um.edu.my) (W. T. Chong)

### **Abstract**

Deploying a wind energy generation system in an urban population would raise concerns on its capability of generating energy and public issues. Urban areas generally have weak and turbulent wind conditions due to the presence of high rise buildings. For the public, issues such as visual impact, acoustic pollution and safety problems would be the concerns. A novel omni-direction-guide-vane (ODGV) that surrounds a vertical axis wind turbine (VAWT) is one that answers these concerns. The ODGV is designed to improve the wind turbine performance by increasing the oncoming wind speed and guiding the wind-stream to the optimum flow angles before impinging onto the turbine blades. Wind tunnel testing was performed to measure the performance of a Savonius VAWT, with and without the integration of the ODGV. Torque, rotational speed and power output were measured using a torque transducer with hysteresis brake applied to the rotor shaft. The presence of the ODGV led to the increment of rotor rotational speed where the highest increment in rotational speed (11.4%) was achieved at a wind speed of 3 m/s (at free-running condition). The ODGV also increased the power coefficient,  $C_p$  of the VAWT at all tested wind speeds and the maximum ( $C_p = 0.26$ ) was achieved at the tip speed ratio,  $TSR = 0.95$  for a wind speed of 3 m/s. The highest increment of  $C_p$  (56.9%) was obtained at the same  $TSR$  and wind speed. These results prove that the ODGV is capable of improving the VAWT performance. In addition, the safety issues are solved and the public concerns are minimized since the ODGV encloses the turbine.

**Keywords:** Guide vane, Wind-solar energy system, Wind turbine, Computational fluid dynamics, Building integrated renewable energy system, environment friendly

- iv) Design of an exhaust air energy recovery wind turbine generator for energy conservation in commercial buildings. Paper presented at the World Renewable Energy Congress - Australia (WREC 2013), Murdoch University, Western Australia. 14-18th July 2013. *(This conference paper accepted for publication in RENEWABLE ENERGY journal after minor revision).*

World Renewable Energy Congress - Australia 2013. Murdoch University, Western Australia, 14 - 18 July 2013.

### **Design of an exhaust air energy recovery wind turbine generator for energy conservation in commercial buildings**

W.T. Chong <sup>a,\*</sup>, A. Fazlizan <sup>a,b</sup>, S.Y. Yip <sup>b</sup>, S.C. Poh <sup>a</sup>, W.P. Hew <sup>b</sup>, E.P. Tan <sup>c</sup> and T.S. Lim <sup>c</sup>

<sup>a</sup> Department of Mechanical Engineering, Faculty of Engineering, University of Malaya,  
50603 Kuala Lumpur, Malaysia

<sup>b</sup> UMPEDAC, Level 4, Wisma R&D, University of Malaya, Jalan Pantai Baharu,  
59990 Kuala Lumpur, Malaysia

<sup>c</sup> Truwater Cooling Towers Sdn. Bhd., Executive Suite 702, Block B, Kelana Business Centre,  
No 97, Jalan SS 7/2, Kelana Jaya, 47301, Petaling Jaya, Selangor, Malaysia

#### **Abstract**

The exhaust air energy recovery wind turbine generator is an on-site clean energy generator that utilizes the advantages of discharged air which is strong, consistent and predictable. Two vertical axis wind turbines (VAWTs) in cross-wind orientation which are integrated with an enclosure are installed above a cooling tower to harness the discharged wind for electricity generation. It is mounted at a specific distance and position above the cooling tower outlet. The enclosure (consisting of several guide-vanes and diffuser-plates) acts as a wind power-augmentation device to improve the performance of the VAWTs. The guide-vanes are placed in between the discharged air outlet and the wind turbine. They are designed to guide the on-coming wind stream to an optimum flow angle before it interacts with the rotor blades. The diffuser-plates are built extended from the outlet duct of the exhaust air system. They are tilted at an optimum angle to draw more wind and accelerate the discharged airflow. A particular concern related to public safety which may be due to blade failure is minimized since the VAWTs are contained inside the enclosure. The performance of the VAWTs and its effects on the cooling tower's air intake speed and current consumption of the power-driven fan were investigated. A laboratory test was conducted to evaluate the effectiveness of the energy recovery wind turbine (5-bladed H-rotor with 0.3 m diameter) generator on a cooling tower model. The results showed a reduction in the power consumption of the fan motor for cooling tower with energy recovery turbine compared to the normal cooling tower. Meanwhile, the VAWT's performance was improved by a 7% increase in rotational speed and 41% reduction in response time (time needed for the turbine to reach maximum rotational speed) with the integration of the enclosure. This system can be used as a supplementary power for building lighting or fed into electricity grid for energy demand in urban building. The energy output is predictable and consistent, allowing simpler design of the downstream system. The fact that there are an abundance of cooling tower applications and unnatural exhaust air resources globally causes this to have great market potential.

**Keywords:** Building integrated wind turbine; Exhaust air system; Energy Recovery; Power augmentation; Urban wind energy

\* Corresponding author. Tel.: +6012-7235038. Fax: +603-79675317.

E-mail: chong\_wentong@um.edu.my (W.T. Chong)  
chong\_wentong@yahoo.com

- v) Exhaust air energy recovery system for electrical power generation in future green cities. International Symposium on Green Manufacturing and Applications 2012 (ISGMA 2012). Jeju Island, Korea, 27~29 October 2012. *(This conference paper is awarded as the BEST PAPER AWARD in the conference. It is also accepted for publication in INTERNATIONAL JOURNAL OF PRECISION ENGINEERING AND MANUFACTURING after minor revision).*

## Exhaust Air Energy Recovery System for Electrical Power Generation in Future Green Cities

Wen Tong Chong<sup>#</sup>, Sin Chew Poh<sup>1</sup>, Ahmad Fazlizan<sup>1</sup>, Sook Yee Yip<sup>2</sup>, Mei Hyie Koay<sup>3</sup> and Wooi Ping Hew<sup>2</sup>

<sup>1</sup> Department of Mechanical Engineering, Faculty of Engineering, University of Malaya, 50603 Kuala Lumpur, Malaysia.  
<sup>2</sup> UMPEDEC, Level 4, Wisma R & D, University Malaya, Jalan Pantai Baharu, 59990 Kuala Lumpur, Malaysia.  
<sup>3</sup> Faculty of Mechanical Engineering, Universiti Teknologi MARA, 40450 Shah Alam, Selangor, Malaysia.  
<sup>#</sup> Corresponding Author / E-mail: chong\_wentong@um.edu.my chong\_wentong@yahoo.com, TEL: +60127235038

KEYWORDS : Cooling Tower, Energy Recovery, Green Technology, Renewable Energy, Urban Wind Energy, Wind Turbine

*This paper investigates a technology-driven solution to supply a portion of energy demand in future green cities. An idea on harnessing unnatural wind resources for electricity is presented. Two vertical axis wind turbines with an enclosure are mounted above a cooling tower to recover part of the energy from the exhaust air. Guide-vanes are designed to create a venturi effect and guide the wind before it interacts with the turbine blades. Diffuser-plates help to draw more wind and accelerate the exhaust airflow. Safety concerns that may result from blade failure are minimized by the design of the enclosure. From the laboratory test and field test results, there is no significant difference in the current consumption of the fan motor with the installation of the wind turbines. The integration of the enclosure has shown an improvement on the turbine's rotational speed which is 30.4% higher. The electricity generated from this system can be fed into the electricity grid. For 3000 units of cooling tower (2 meters outlet diameter powered by a 7.5 kW fan motor and operated for 16 hours/day), 13% of the energy to power the fan motor is expected to be recovered from this system which equals 17.5 GWh/year.*

Manuscript received: August XX, 201X / Accepted: August XX, 201X

### NOMENCLATURE

GHG	= Greenhouse Gas
TNB	= Tenaga Nasional Berhad
VAWT	= Vertical Axis Wind Turbine
RE	= Renewable energy
DAWT	= Diffuser Augmented Wind Turbine

### 1. Introduction

Nowadays, global energy consumption in both developed and developing countries has increased rapidly due to population growth and it is expected to double or more by the year 2040 [1]. In Malaysia, total energy demand would be growing at 5.4% per annum with 1.8% average annual population growth rate. Eventually, the energy demand in the year 2020 would be approximately 971 TWh with 33.4 million population. As a consequence, Malaysia is predicted to become a net energy importer in 2020 [2]. This energy consumption

growth is contributed by both industrial and residential sectors. The existing energy resources for electricity generation in Malaysia mainly depends on fossil fuels which contribute 94.5% of the electricity generation while only a small portion of energy supplies comes from hydroelectricity or others (solar, biomass, etc.). However, the usage of fossil fuels brings negative impacts to the environment such as greenhouse gases (GHG) emission. According to Ahmad et al., more than 90% of the energy related GHG emission is resulted from the CO<sub>2</sub> emissions from fuel combustion globally [3]. Currently, the increase in the concentration of GHG emission has caused a notable rise of temperature in the earth's atmosphere and thus widespread melting of snow and ice at the polar ice caps. The melting of ice causes the rise of sea level and lesser land can be used for the increasing world population, along with the changes in climate [4].

In terms of the economic aspect, the deployment of fossil fuels for electricity generation will become more and more costly as these resources are limited in supply and will be exhausted one day. Based on the commercial tariff of electricity in Malaysia provided by Tenaga Nasional Berhad (TNB), energy cost is USD 0.113/kWh and it is predicted to increase by 10% annually [5]. In parallel with a country experiencing rapid growing energy demand and economic



- vi) Early development of an energy recovery wind turbine generator for exhaust air system. International Conference on Applied Energy 2012 (ICAE 2012). Suzhou, China. 5~8 Jul 2012. (*This conference paper is accepted for publication in APPLIED ENERGY journal after minor revision*).

International Conference on Applied Energy  
ICAE 2012, Jul 5-8, 2012, Suzhou, China  
Paper ID: ICAE2012-A10229

## EARLY DEVELOPMENT OF AN ENERGY RECOVERY WIND TURBINE GENERATOR FOR EXHAUST AIR SYSTEM

W.T. Chong<sup>1,\*</sup>, A.Fazlizan<sup>1</sup>, S.C. Poh<sup>1</sup>, S.Y. Yip<sup>2</sup>, W.P. Hew<sup>2</sup>, C.K.Chang<sup>3</sup>

<sup>1</sup>Department of Mechanical Engineering, University of Malaya, 50603 Kuala Lumpur, Malaysia.

<sup>2</sup>UMPEDAC, Level 4, Wisma R & D, University Malaya, Jalan Pantai Baharu, 59990 Kuala Lumpur, Malaysia.

<sup>3</sup> Heating, Ventilating, Air Conditioning and Refrigerating Section, Universiti Kuala Lumpur Malaysia France Institute Section 14, Jalan Teras Jernang, Bandar Baru Bangi, 43650, Selangor, Malaysia.

\* Corresponding author. E-mail address: chong\_wentong@yahoo.com  
Tel: +60 12 7235038

### ABSTRACT

An innovative idea on extracting clean energy from man-made wind resources is introduced. The system is designed to recover part of the energy from the exhaust air resources and improve the exhaust air system discharge. It generates on-site clean energy using a micro wind generation system and is suitable for application in urban areas. A vertical axis wind turbine (VAWT) in cross-wind orientation, with a safety enclosure was mounted above a cooling tower's exhaust fan to harness the wind energy for producing electricity. The performance of the VAWT and its effects on the cooling tower's air intake speed, air discharge speed, and current consumption of the power-driven fan were investigated. The VAWT is positioned at a specific area and distance at the outlet of the cooling tower to avoid a negative impact on the performance of the cooling tower and at the same time to recover more energy. The enclosure can act as a safety cover and also enhance the performance of the VAWT. It is designed with several guide-vanes positioned at the up-stream side of the wind turbine to create a venturi effect (to increase the wind speed) and guide the wind before it interacts with the turbine blades. Moreover, the enclosure design is also comprised of diffuser-plates that are mounted at specific angles so that it can draw more wind and accelerate the flow. In addition to performance enhancement, safety concerns due to blade failure or maintenance activities are tackled by the design of the enclosure. Laboratory test conducted on a scaled model shows no measureable difference in the air intake speed and current consumption of the power-driven fan when the turbine is spinning on top of the scaled model of the cooling tower. Field test on an actual induced-draft cooling tower with 2 meters outlet diameter which was powered by a 7.5 kW motor was performed using a 3-bladed Darrieus wind turbine with 1.24 meter rotor diameter. There was no significant

difference on the outlet air speed of the cooling tower, i.e. 10.545 m/s for cooling tower without wind turbine and 10.363 m/s for the cooling tower with the presence of the wind turbine (rotational speed = 875 rpm). A small difference was observed on the power consumption by the fan motor which is 0.39% higher with the presence of the VAWT. The electricity generated from this system can be for commercial usage or fed into the electricity grid. This system is retrofit-able to existing cooling towers and has very high market potential due to abundant cooling towers and other unnatural exhaust air resources globally.

**Keywords:** Wind Turbine, Cooling Tower, Energy Recovery, Clean Energy, Urban Wind Energy

### NOMENCLATURE

#### Abbreviation

VAWT	Vertical Axis Wind Turbine
BIWT	Building Integrated Wind Turbine
RPM	Revolution Per Minute/ Rotational Speed
CTI	Cooling Tower Institute

#### Symbols

$Q$	Volume flow rate
$V_{outlet}$	Discharge air speed at outlet
$A_{outlet}$	Outlet area
$P_{in}$	Input power
$V$	Voltage
$I$	Electric current
$pf$	Power factor

### 1. INTRODUCTION

The massive growing rate of fossil fuel consumption and nuclear waste generation with their negative impacts of pollution has attracted worldwide attention to invest in researches and development in renewable energy as an alternative energy source. The most environment-friendly


# PATENT FILING


Chong, Wen Tong, Kong, Y. Y., & Fazlizan, A. Wind and Exhaust Air Energy Recovery System. *Intellectual Property Corporation of Malaysia*. Application no.: PI 2011700168 & PCT/MY2012/000274. International publication no.: WO2013073930-A1.

(12) INTERNATIONAL APPLICATION PUBLISHED UNDER THE PATENT COOPERATION TREATY (PCT)

(19) World Intellectual Property Organization  
International Bureau

(43) International Publication Date  
23 May 2013 (23.05.2013)





(10) International Publication Number  
**WO 2013/073930 A1**

---

(51) International Patent Classification:  
*F01N 5/04* (2006.01)    *F03D 9/00* (2006.01)  
*F03D 3/00* (2006.01)    *F03D 11/00* (2006.01)  
*F03D 3/04* (2006.01)    *F24F 12/00* (2006.01)

(21) International Application Number:  
PCT/MY2012/000274

(22) International Filing Date:  
16 November 2012 (16.11.2012)

(25) Filing Language: English

(26) Publication Language: English

(30) Priority Data:  
PI2011700168 17 November 2011 (17.11.2011) MY

(71) Applicant: UNIVERSITI MALAYA [MY/MY]; 50603 W.P. Kuala Lumpur (MY).

(72) Inventors: **CHONG Wen Tong**; Department Of Mechanical Engineering, Faculty Of Engineering, University Of Malaya 50603 W.P., Kuala Lumpur (MY). **KONG, Yuen Yoke**; Department Of Mechanical Engineering, Faculty Of Engineering, University Of Malaya 50603 W.P., Kuala Lumpur (MY). **AHMAD, Fazlizan Abdullah**; Department of Mechanical Engineering, Faculty of Engineering, University of Malaya 50603 W.P., Kuala Lumpur (MY).

(74) Agent: **LOK, Choon Hong**; Suite 6.03, 6th Floor, Wisma Mirama, Jalan Wisma Putra, 50460 Kuala Lumpur (MY).

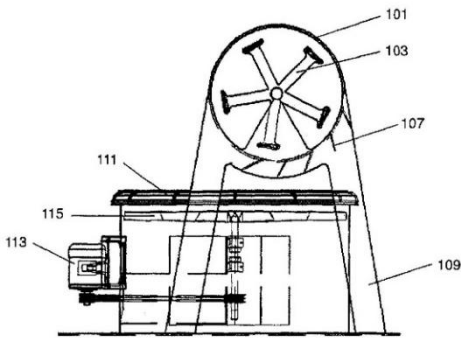
(81) Designated States (unless otherwise indicated, for every kind of national protection available): AE, AG, AL, AM, AO, AT, AU, AZ, BA, BB, BG, BI, BN, BR, BW, BY, BZ, CA, CH, CL, CN, CO, CR, CU, CZ, DE, DK, DM, DO, DZ, EC, EE, EG, ES, FI, GB, GD, GE, GH, GM, GT, HN, HR, HU, ID, IL, IN, IS, JP, KE, KG, KM, KN, KP, KR, KZ, LA, LC, LK, LR, LS, LT, LU, LY, MA, MD, ME, MG, MK, MN, MW, MX, MY, MZ, NA, NG, NI, NO, NZ, OM, PA, PE, PG, PH, PL, PT, QA, RO, RS, RU, RW, SC, SD, SE, SG, SK, SL, SM, ST, SV, SY, TH, TJ, TM, TN, TR, TT, TZ, UA, UG, US, UZ, VC, VN, ZA, ZM, ZW.

(84) Designated States (unless otherwise indicated, for every kind of regional protection available): ARIPO (BW, GH, GM, KE, LR, LS, MW, MZ, NA, RW, SD, SL, SZ, TZ, UG, ZM, ZW), Eurasian (AM, AZ, BY, KG, KZ, RU, TJ, TM), European (AL, AT, BE, BG, CH, CY, CZ, DE, DK, EE, ES, FI, FR, GB, GR, HR, HU, IE, IS, IT, LT, LU, LV, MC, MK, MT, NL, NO, PL, PT, RO, RS, SE, SI, SK, SM, TR), OAPI (BF, BJ, CF, CG, CI, CM, GA, GN, GQ, GW, ML, MR, NE, SN, TD, TG).

Published:  
— with international search report (Art. 21(3))

---

(54) Title: WIND AND EXHAUST AIR ENERGY RECOVERY SYSTEM



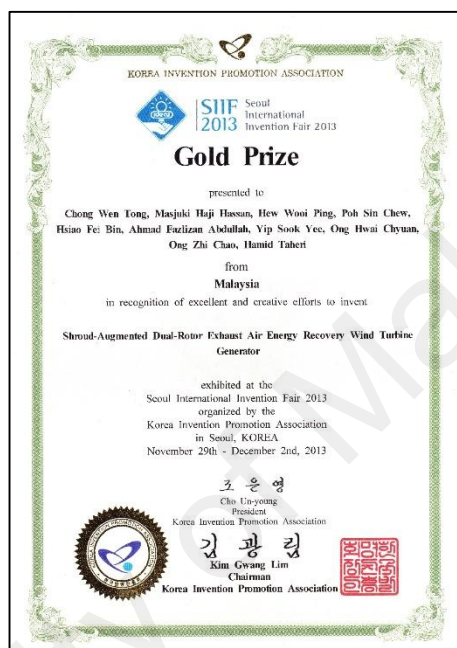
(57) Abstract: This invention is a wind and exhaust air energy recovery system comprising a supportive frame (101); a turbine rotor assembly (103) mounted on the supportive frame (101) and being able to rotate about a horizontal axis; wherein the turbine rotor assembly (103) are positioned neighbouring an exhaust outlet (111) that exhaust air flow from the outlet (111) in which the exhaust air flow drives the turbine rotor assembly (103) to rotate; and at least one electric generator connected to the turbine rotor assembly (103) for converting kinetic energy caused by movement of the turbine rotor assembly (103) to electrical or mechanical energy; characterized in that at least one guide vane (107) is arranged in between the outlet (111) and the turbine rotor assembly (103) to direct the air flow towards the turbine rotor assembly (103) at a predetermined angle. The supportive frame (101) and safety enclosure (102) can be supported with additional holding structures (109) so as to be firmly secured to the exterior of the exhaust outlet (111) without obstructing the exhaust air flow.

WO 2013/073930 A1

187

## LIST OF AWARDS

- i) **Gold Medal Award:** Seoul International Invention Fair 2013 (SIIF 2013), Seoul, Korea. Korea Invention Promotion Association (KIPA). December 2013.



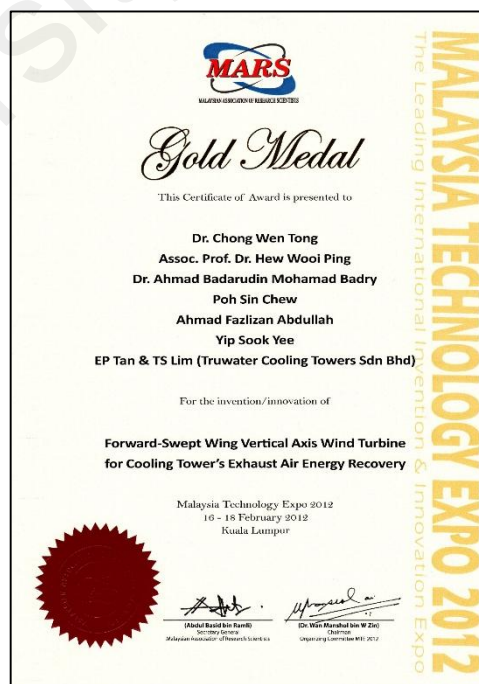
- ii) **Diploma:** International Trade Fair 2012 (iENA 2012), Germany.



- iii) **Best Paper Award:** International Symposium on Green Manufacturing and Applications 2012 (ISGMA 2012), Korea Society for Precision Engineering (KSPE) and Institute of Advanced Machinery and Design, Seoul National University (SNU) and Manufacturing Institute for Research on Advanced Initiative (Pan-Pacific MIRAI). August 2012.



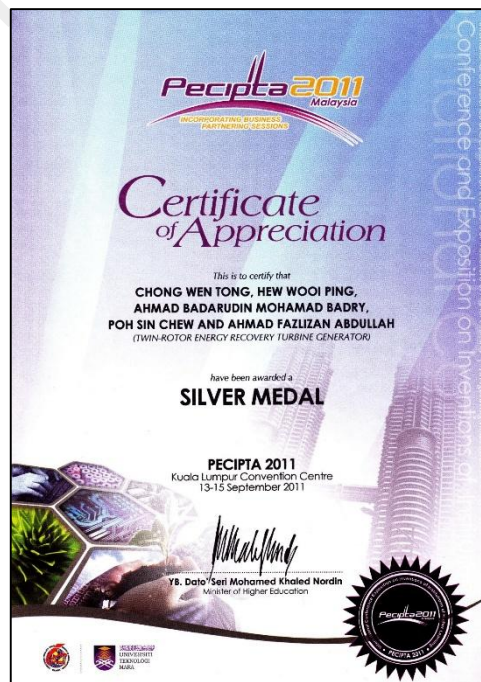
- iv) **Gold Medal Award:** Malaysia Technology Expo 2012 (MTE 2012), Malaysia Association of Research Scientists (MARS).



- v) **Special Prize from Korean Invention Promotion Association (KIPA):** Malaysia Technology Expo 2012 (MTE 2012), Malaysia Association of Research Scientists (MARS).



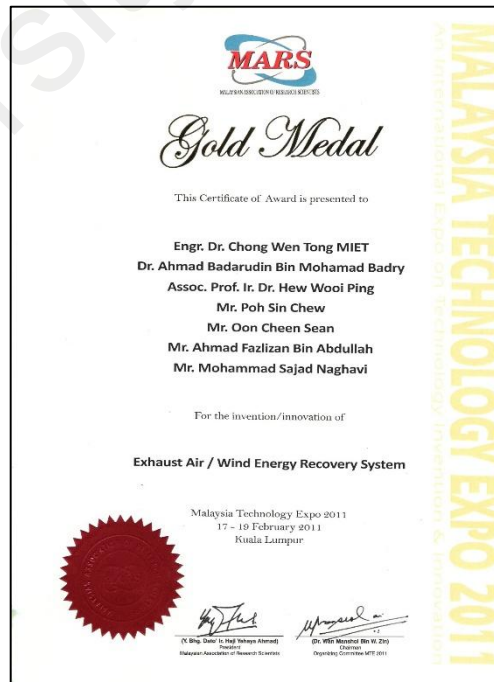
- vi) **Silver Medal Award:** International Conference and Exposition on Invention of Institutions of Higher Learning 2011 (PECIPTA 2011), Minister of Higher Education (MOHE).



- vii) **Gold Medal Award:** Invention, Innovation and Technology Exhibition 2011 (ITEX '11), Malaysia Invention and Design Society (MINDS).



- viii) **Gold Medal Award:** Malaysia Technology Expo 2011 (MTE 2011), Malaysia Association of Research Scientists (MARS). February 2011.



- ix) Finalist: Patent Competition-Solution for Everyday Life, Joint organized by Malaysia Intellectual Property office (MyIPO), Korean Intellectual Property Office (KIPO) and World Intellectual Property office (WIPO).



- x) **The Outstanding Technopreneur Award (Young Intellectual Category):** 5th Technopreneurship & Innovation Symposium & Exhibition (TISE) 2013, Malaysian Scientific Association (MSA) and WENCOM Career Consultancy (WENCOM).

